Life finds a way: The recovery of frog populations from a chytridiomycosis outbreak

Donald T. McKnight, BSc, MSc

A thesis submitted for the degree of Doctor of Philosophy

College of Science and Engineering

James Cook University

September 2019

ACKNOWLEDGMENTS

This thesis has been a huge effort by numerous people, and I am deeply grateful to everyone for their help. First and foremost, I would like to thank my amazing supervisors Kyall Zenger, Lin Schwarzkopf, Ross Alford, and Deborah Bower. They entrusted me with this project despite my total lack of experience in genetics and molecular ecology, and they provided constant help, advice, and feedback throughout my research. They also mentored me more generally and provided teaching opportunities, gave me invaluable career advice, and prepared me for the next steps in my research career. I truly appreciate everything that they have done for me. I am also extremely grateful to Roger Huerlimann and Monal Lal for their constant help both in the lab and with analysing molecular data. They both invested a lot of time in training me on laboratory techniques and helping me troubleshoot problems.

Additionally, I would like to thank everyone who assisted me with the field work for this project. Collecting the samples was truly insane and involved many long, cold, wet nights scrambling up impossible creek beds looking for frogs, and I appreciate the help of all my volunteers: Lorenzo Bertola, Leah Carr, Bartek Ćwikliński, Jeremy Day, Kimberley Day, Lexie Edwards, Connor Kaplan, Jen McKnight, Juan Mula, Eric Nordberg, Donna Simmons, Chi Wei, and Madeline Wuth. I would especially like to thank Leah, Bartek, and Donna who accompanied me on the majority of my expeditions, often with very short notice.

In addition to the people I have thanked specifically, I would like to say a general thank you to everyone in the Molecular Ecology and Evolution Lab (MEEL) as well as everyone in the Lizard Lunch group for their friendship, comradery, and always being there to help me with anything I needed. They have done everything from helping me figure out how to order supplies to troubleshooting PCRs and giving me feedback on presentations and research ideas. I would also like to specifically thank Carolyn Smith-Keune for her amazing work keeping MEEL running smoothly. Having a well-stocked and well-maintained laboratory space to work in has been extremely helpful.

I am also grateful to the various organizations that provided funding for this research, including the Australian Research Council, James Cook University Graduate Research School, Ecological Society of Australia (Holsworth Wildlife Research Endowment), Skyrail Rainforest Foundation, Wet Tropics Management Authority, Australian Society of

Herpetologists, and Australian Wildlife Society. I also appreciate the GIS layers that were kindly provided by the Wet Tropics Management Authority. Additionally, I am indebted to the Nywaigi people for working with me and allowing me to conduct research on their land.

Finally, I am, of course, extremely thankful for my wife, Jen McKnight, who has made a lot of sacrifices so that I could pursue my PhD and agreed to literally move to the other side of the planet with me (as well as tolerating all manner of insanity from me).

STATEMENT OF CONTRIBUTIONS AND ETHICS DECLARATION

Many people have assisted me with me thesis. All four of my supervisors (Kyall Zenger, Lin Schwarzkopf, Ross Alford, and Deborah Bower) provided advice on experimental design, analysis, and writing throughout my project and are co-authors on all my chapters. Kyall's expertise is in genetics and molecular ecology, and he provided a lot of input for designing and analysing the molecular components of the project (particularly chapters 2–4). Lin, Ross, and Deborah all have a background in ecology and extensive experience working with chytridiomycosis in the Wet Tropics, and they provided advice and help for the ecological aspects of the project. Ross was also particularly involved with the statistical analyses (especially chapters 7–8) as well as lending his extensive knowledge of this disease system. Lin and Deborah provided additional knowledge and input on the study system, experimental design, and analyses, and they were generally the first people to read and edit drafts of my papers. Additionally, Roger Huerlimann assisted with the laboratory work and analyses of the microbial data sets and is a co-author on chapters 5–8. Similarly, Monal Lal trained me on laboratory procedures and population genetics analyses, and he is a co-author on chapter 3.

Throughout my PhD, I received financial support from an International Postgraduate Student Fellowship from the Australian Government. My research was funded by Australian Research Council Discovery Grant (#DP130101635), as well as grants from the James Cook University Graduate Research School, Holsworth Wildlife Research Endowment (via the Ecological Society of Australia), Skyrail Rainforest Foundation, Wet Tropics Management Authority, Australian Society of Herpetologists, and Australian Wildlife Society. GIS layers were provided by the Wet Tropics Management Authority.

All research was conducted under Department of Environment and Heritage Protection permit #WITK16243115 and with the approval of James Cook University's animal ethics committee (#A2209). Every reasonable effort has been made to gain permission and acknowledge the owners of copyright material. I would be pleased to hear from any copyright owner who has been omitted or incorrectly acknowledged.

Publications and author roles

My PhD research has resulted in the following publications and planned publications which have been incorporated as chapters or appendices.

Chapter #	Publication	Author roles
2	**(Published)** McKnight, DT, L Schwarzkopf, RA Alford, DS Bower, KR Zenger. 2017. Effects of emerging infectious diseases on host population genetics: a review. *Conservation Genetics* 18:1235–1245.	All authors developed the topic for the review. DTW reviewed the literature and led the writing. All authors edited the paper.
3	**(Published)** McKnight, DT, MM Lal, DB Bower, L Schwarzkopf, RA Alford, KR Zenger. 2019. The return of the frogs: The importance of habitat refugia in maintaining diversity during a disease outbreak. *Molecular Ecology* 28:2731–2745.	DTM, DSB, LS, RAA, and KRZ designed the study. DSB, LS, RAA, and KRZ supervised the research. DTM collected the samples. DTM and MML did the lab work and analyses. DTM led the writing, and all authors edited the paper.
4	**(In preparation)** McKnight DT, DS Bower, L Schwarzkopf, RA Alford, KR Zenger. Population genetics of a remnant frog population following a disease outbreak. *Conservation Genetics*	All authors developed the project. DTM conducted the field work, laboratory work, and data analysis. DTM led the writing, and all authors edited the paper.
5	**(Published)** McKnight, DT, R Huerlimann, DS Bower, L Schwarzkopf, RA Alford, KR Zenger. 2019. Methods for normalizing microbiome data: an ecological perspective. *Methods in Ecology and Evolution* 10:389–400.	DTM wrote the simulations and led the project design, analysis, and writing. RH, RAA, LS, DSB, and KRZ supervised the research, assisted with project design and analysis, and edited the manuscript.
6	**(Published)** McKnight, DT, R Huerlimann, DS Bower, L Schwarzkopf, RA Alford, KR Zenger. 2019. microDecon: A highly accurate read-subtraction tool for the post-sequencing removal of contamination in metabarcoding studies. *Environmental DNA* 1:14–25.	DTM designed and wrote the R package and scripts and led the analyses and writing. DTM and RH conducted the sequencing experiment. RH, DSB, LS, RAA, and KRZ supervised the project, including providing input and advice for the design of the project and analysis of the data. All authors edited, read, and approved the final manuscript.
7	**(In preparation)** McKnight, DT, R Huerlimann, DS Bower, L	DTM and DSB collected the samples. DTM and RH performed the laboratory

	Schwarzkopf, RA Alford, KR Zenger. More is better: Microbiome richness is associated with frog population recovery following a disease outbreak. *Microbial Ecology*	work and bioinformatics. RH, DSB, LS, RAA, and KRZ supervised the project, including providing input and advice for the design of the project and analysis of the data. DTM led the writing. All authors edited, read, and approved the final manuscript.
8	**(In preparation)** McKnight, DT, R Huerlimann, DS Bower, L Schwarzkopf, RA Alford, KR Zenger. The interplay of fungal and bacterial microbiomes in rainforest frogs following a disease outbreak. *Science.*	DTM and DSB collected the samples. DTM and RH performed the laboratory work and bioinformatics. RH, DSB, LS, RAA, and KRZ supervised the project, including providing input and advice for the design of the project and analysis of the data. DTM led the writing. All authors edited, read, and approved the final manuscript.
Appendix 1	**(Published)** McKnight, DT, RA Alford, CJ Hoskin, L Schwarzkopf, SA Greenspan, KR Zenger, DS Bower. 2017. Fighting an uphill battle: The recovery of frogs in Australia's Wet Tropics. *Ecology* 98:3221–3223	DSB and DTM planned the paper. DTM led the writing. All authors contributed input and edited the paper.

ABSTRACT

Emerging infectious diseases are a serious threat to wildlife, but not all populations or species have the same response to outbreaks. In some cases, diseases shift from being epizootic to enzootic, allowing populations to recover, but both the causes of recoveries and the long-term consequences of disease outbreaks remain poorly understood. My PhD aimed to further our knowledge of these important topics by using a frog assemblage in the Australian Wet Tropics as a model system for understanding recoveries from disease outbreaks.

This region was impacted by an outbreak of the fungal disease chytridiomycosis (caused by the pathogen *Batrachochytrium dendrobatidis* [*Bd*]) in the late 1980s and early 1990s, during which high elevation populations of several frog species declined or disappeared, while low elevation populations remained stable. Following the outbreak, some species recovered at upland sites, but the patterns of both declines and recoveries vary among species. *Litoria dayi* disappeared from upland sites and has never recovered. *Litoria nannotis* disappeared from upland sites and has largely recovered. *Litoria serrata* declined at upland sites and has recovered, and *Litoria wilcoxii* did not decline substantially at any elevation. These different histories with the disease presented a great opportunity for studying the factors that allowed some species to recover, while apparently precluding recovery in others, and my thesis examined both population genetics and microbiomes of frogs in this system. My primary goals were to examine the long-term consequences of the outbreak (e.g., fragmentation, inbreeding, loss of diversity) and test several hypotheses for the differences in the history of declines and recoveries among species (e.g., differences in dispersal abilities, a lack of adaptive potential due to lost diversity, differences in microbiomes).

I used single nucleotide polymorphisms to examine connectivity patterns, test for a loss of diversity, and test for *Bd*-driven selection. I examined low elevation populations of *L. nannotis*, *L. serrata*, and *L. dayi* that survived the outbreak, and compared them to recovered upland populations of *L. nannotis* and *L. serrata*. I sampled *L. dayi* at three national parks and *L. nannotis* and *L. serrata* at two national parks. All three species showed high levels of connectivity within a given park, and there was no structuring along streams,

suggesting that all three species have good dispersal abilities. No inbreeding was present in any species, and all species showed high genetic diversity levels north of Paluma Range National Park. At Paluma, however, both *L. nannotis* and *L. serrata* had reduced genetic diversity, and diversity levels followed a west–east pattern, with higher diversity on the western half of the park (*L. dayi* does not occur at Paluma). These diversity patterns matched habitat patterns, with higher diversity in wetter areas with larger sections of rainforest, suggesting that the size and quality of refuge habitat may play an important role in the retention of genetic diversity during a disease outbreak. I did not find consistent evidence of selection in *L. nannotis*, but there was consistency among outlier testes for *L. dayi*. These tests could not conclusively demonstrate that *L. dayi* was undergoing disease-induced selection, but they were suggestive.

Prior to analysing the microbiomes of the frog species, it was necessary to test or develop several microbiome methodologies. First, microbiome data often need to be normalized prior to analysis, and many methods are available, but several of the most popular methods use variance standardizing techniques that can distort ecological data. Therefore, I compared six methods (rarefaction, proportions, upper quartile, CSS, edgeR-TMM, and DESeq-VS) using both a published data set and simulations. My results showed that upper quartile, CSS, edgeR-TMM, and DESeq-VS failed to fully standardize reads, and inflated minor differences among rare micro-organisms while suppressing large differences among common micro-organisms, thus distorting community comparisons. In contrast, using proportions or rarefaction produced accurate results, with proportions outperforming rarefaction.

Another common issue with microbiome studies is the ubiquitous presence of bacterial contamination. This problem has been widely documented, but no method of accurately removing contaminate reads exists. Therefore, I developed an algorithm for identifying and removing contaminate reads, wrote an R package (microDecon) to implement it, and tested it using two large simulations, a published data set, and a sequencing experiment. All tests showed that microDecon was highly accurate and improved the results in 98.1% of cases.

Having tested and developed these methods, I was able to apply them to the microbiomes of frog populations. Multiple laboratory studies have documented beneficial effects of bacteria for amphibian hosts during *Bd* infections, and several field studies have

suggested that microbiomes may play important roles in infection dynamics. Nearly all of this research has focused on bacteria, while the fungal microbiomes of amphibians remain largely unexplored. Therefore, I examined both the fungal and bacterial microbiomes of *L. dayi*, *L. nannotis*, *L. serrata*, and *L. wilcoxii* to make one of the first comparisons of bacteria and fungi in frog populations and test the hypothesis that differences in microbiomes could explain the differences in patterns of declines and recoveries in the Wet Tropics frog assemblage. I also used qPCR to examine *Bd* infection prevalence and intensity.

Bacterial microbiomes generally had higher operational taxonomic unit (OTU) richness but lower evenness than the fungal microbiomes. Bacterial microbiomes also tended to be less variable within groups of samples (e.g., frog species), resulting in stronger clustering in ordination plots. Nevertheless, fungal and bacterial Bray-Curtis dissimilarities were positively correlated within frog species (i.e., two individuals with similar fungal microbiomes tended to also have similar bacterial microbiomes). Fungal and bacterial richness were also correlated. This is a somewhat novel result that suggests that either one microbiome is driving the other, or both are being affected similarly by environmental variables.

Results for associations with *Bd* were mixed. I did not find associations between *Bd* and beta-diversity for fungi or bacteria. Also, the relative abundance of bacteria that are inhibitory to *Bd* (based on previous culturing studies) did not follow the expected patterns of association with *Bd*. *Litoria dayi* had the highest relative abundance of inhibitory bacteria despite having never recovered from the outbreak, while *L. wilcoxii* (which never declined) had a low relative abundance of inhibitory bacteria. Additionally, for *L. dayi* and *L. wilcoxii* there were significant positive associations between the relative abundance of inhibitory bacteria and *Bd* infection intensity. In contrast, OTU richness showed negative associations with *Bd* infection intensity for both fungi and bacteria. Additionally, for both fungi and bacteria, *L. dayi* had the lowest OTU richness of any frog species. These results are consistent with a protective effect of OTU richness and suggest that a lack of richness in *L. dayi* has played a role in its inability to recover from the outbreak.

In summary, I found that having large areas of high-quality lowland habitat is likely important for allowing populations to retain genetic diversity during an outbreak, and they should be a focus of conservation efforts. Additionally, neither differences in genetic diversity nor differences in dispersal abilities could explain why *L. dayi* has been unable to

recover from population declines. There was some evidence that *L. dayi* is in the process of adapting, but this was not conclusive. The microbiome data did not show significant associations between *Bd* and either total community composition or the relative abundance of inhibitory bacteria, but there were associations with the OTU richness of both fungal and bacterial microbiomes, suggesting that richness may be an important factor in infection dynamics.

TABLE OF CONTENTS

LIST OF TABLES

results for the full models that included all data but no interactions. Grey shading = significant at $\alpha = 0.05$.

Appendix 2 Table 2 — P values for the tests examining total bacterial richness, richness of the inhibitory community, and the relative abundance of inhibitory community. Comparisons were made among species, elevations, and parks. This table shows the results from a data set containing only Paluma and Kirrama and no *L. dayi*. This was done to allow all interactions (*) between species, park, and elevation. The interactions and main effects in the full models determined how post hoc comparisons were conducted (e.g., the *L. nannotis – L. serrata* relative abundance comparison at Kirrama was not subset by elevation due to a lack of significance in the main model). Grey shading = significant at $\alpha = 0.05$.

Appendix 2 Table 3 — P values for the tests examining total bacterial richness, richness of the inhibitory community, and the relative abundance of inhibitory community. Comparisons were made among species, elevations, and parks. This table shows a data set that only included Tully and Kirrama lowlands, without *L. serrata*. This was done so that *L. dayi* comparisons cold be made, as well as comparisons between Tully and Kirrama. The interactions and main effects in the full models determined how post hoc comparisons were conducted (e.g., the *L. dayi - L. nannotis* comparison for total richness was not run separately on each park because there was not a significant main effect or interaction for Park in the full model). Grey shading = significant at $\alpha = 0.05$.

Appendix 2 Table 4 — Bacterial OTUs that were differentially abundant between infected and uninfected frogs. Each species was tested separately, and within species, FDR = 0.01 was applied. Numbers are log-fold changes. Only significant results are shown. Yellow (positive) indicates that an OTU was more abundant in infected individuals, and blue (negative) indicates that it was less abundant in infected individuals. The "Inhibitory" shows whether an OTU was inhibitory in the Woodhams et al. 2015 database.

Appendix 3 Table 1 — P values from correlations between richness and evenness. The panel letters correspond to the panels in Appendix 3 Figure 1.

Appendix 3 Table 2 — Fungal OTUs that were differentially abundant between infected and uninfected frogs. Each species was tested separately, and within species, FDR = 0.01

was applied. Numbers are log-fold changes. Only significant results are shown. Yellow (positive) indicates that an OTU was more abundant in infected individuals, and blue (negative) indicates that it was less abundant in infected individuals.

LIST OF FIGURES

compared to S1. BC = Bray-Curtis dissimilarity between S1 and the sample in a given column.

Figure 5.2 — Samples (S5–S7) from three hypothetical communities illustrating the potential problems that arise from log transforming community data. The samples are shown with and without a log2(x+1) transformation, and the data are shown both as a table of raw read counts and a stacked bar plot. The bar plot illustrates the fact that the log transformation increases the importance of rare OTUs which decreasing the importance of common OTUs, ultimately suppressing the differences between S5 and S7 and exaggerating the differences between S5 and S6. BC = Bray-Curtis dissimilarity between S5 and the sample in a given column (for the log-transformed data, the comparisons were made with the log-transformed S5).

Figure 5.3 — Correlations between the Bray-Curtis dissimilarities for the original (non-normalized [true]) data and the Bray-Curtis dissimilarities following normalization. Black lines show a slope of one and intercept of zero. These data are from the mouse gut microbiome data set, and only the 81 pairs of samples where the percent difference between read depths was <0.5% for the original data are shown (all data were used during the normalization step). It should be noted that DESeq-VS has the option of doing transformations "blind" (i.e., without incorporating *a priori* knowledge about groups) or with *a priori* knowledge. For this data set, the results were highly inaccurate if *a priori* information was used. Therefore, I presented the results without *a priori* information here, and the results with *a priori* information are available in Supporting information 1.

Figure 5.4 — Simulation results. (rows a–c) The percent of iterations (out of 200) where a PERMANOVA returned a significant difference ($\alpha = 0.05$) between the populations. (row d) The percent of iterations (out of 200) where there was a significant correlation ($\alpha = 0.05$) between read depth and mean Bray-Curtis dissimilarity (mean per individual). These are spurious correlations that indicate a failure of the normalization method. Mean dissimilarity = the setting for the difference between the distributions from which the populations were constructed (0 = identical distributions, 0.8 is highly dissimilar), All = all OTUs were allowed to vary between the two distributions on which the populations were based, Top 10% = only the OTUs in the 90th percentile and above (based on DNA yield for population 1's

distribution) varied between distributions, Bottom 30% = only the OTUs in the 30th percentile and below varied. The thick black "Original" line shows the results for the real communities without a log transformation (even in the log2(x+1) columns, where is serves as a point of comparison); whereas the green "Original log" line shows those data following a log2(x+1) transformation.

Figure 5.5 — Correlations between the Bray-Curtis (BC) dissimilarities for the original communities ("Actual BC") and the BC dissimilarities following normalization. Black lines show a slope of one and intercept of zero. Data are from 200 iterations of the simulator (per column). All = all OTUs were allowed to vary between the two distributions on which the populations were based, Top 10% = only the OTUs in the 90th percentile and above (based on DNA yield for population 1's distribution) varied between distributions, Bottom 30% = only the OTUs in the 30th percentile and below varied, log = the data were transformed with a log2(x+1) transformation.

Figure 6.1 — The basic steps used by microDecon to decontaminate samples. The process is iterative, and each sample is treated completely independently. The constant is an OTU that is entirely contamination (i.e., should not be present in an uncontaminated sample). Because the constant is entirely contamination, it can be used as a point of comparison to determine how many reads in the sample are from contamination. Percent differences are calculated as: ([blank proportion – sample proportion]/ blank proportion) *100. Some numbers reported in the 4th table appear to be slight deviations of the expected values based on the 3rd table. This is simply an artefact of rounding the values in the 3rd table to four decimal places. *Full details on the algorithms are available in the microDecon user's guide.

Figure 6.2 — Simulation 1 results showing the ability of microDecon ("Decontaminated") to corrected contaminated samples. Data (Bray-Curtis dissimilarity between the sample and uncontaminated copy of the sample) were grouped based on the proportion of contamination. The simulation control box is based on subsetting the data to only the OTUs that did not amplify in the blank. Whiskers represent the 90th and 10th percentile. For readability, outliers represent the 95th and 5th percentile. A total of 100,000 iterations were run, but 2,395 had contamination levels higher than 1 and are excluded (all iterations and outliers are visible in Appendix 3).

Figure 6.3 — A). Distributions of Bray-Curtis dissimilarities (BC) from 100,000 iterations of simulating individual samples. For readability, the X axis stops at 0.5, but there were 1,756 contaminated points and 20 decontaminated points greater than that (max = 0.906 and 0.712 respectively). The simulation control distribution is from the OTUs in the decontaminated sample that did not amplify in the blank. B). Relationship between the number OTUs and the BC for the simulation controls (i.e., stochastic variation). Increasing numbers of OTUs resulted in greater dissimilarities, which were partially responsible for the slight shift in the decontaminated distribution in Figure 6.3A. Whiskers represent the 90^{th} and 10^{th} percentile, and outliers are shown as the 95^{th} and 5^{th} percentile.

Figure 6.4 — A comparison of the effectiveness of microDecon versus removing all contaminant OTUs for simulated data. Using microDecon ("Decontaminated") was superior to either removing contaminant OTUs ("Contaminated OTUs removed") or making no adjustments for contamination ("contamination"). Whiskers represent the 90^{th} and 10^{th} percentile. For readability, outliers are shown as the 95^{th} and 5^{th} percentile (full data in Appendix 3).

Figure 6.5 — Results of simulations on entire groups (Simulation 2), showing the ability of microDecon ("Decontaminated") to correct contaminated samples. Means are per group per iteration. For the simulation controls, comparisons were made between the decontaminated and uncontaminated samples using only the OTUs that were not in the blank (i.e., the ones unaffected by contamination and decontamination). Controls were expected to be slightly lower than decontaminated samples because they contained fewer OTUs (see Figure 6.3). Whiskers represent the 90^{th} and 10^{th} percentile, and all outliers are shown.

Figure 6.6 — Mean Bray-Curtis dissimilarities for comparisons between groups (groups consisted of 5, 10, or 20 samples). For each iteration (100 per panel), comparisons were made between groups for the uncontaminated, decontaminated (with microDecon), and contaminated samples. Whiskers represent the 90^{th} and 10^{th} percentile, and all outliers are shown.

Figure 6.7 — PCoAs (based on square root transformed Bray-Curtis dissimilarities [BC]) comparing groups ("g1" and "g2") for uncontaminated, decontaminated, and contaminated samples. The data were subset to the OTUs that amplified in the blank

so that the effects of contamination and microDecon ("Decontaminated") could be seen more clearly. A–C). Best, median, and worst results out of 100 iterations (judged based on mean BC between the uncontaminated and decontaminated samples for group 2). Group 2 had lower DNA yield and, therefore, was more affected by contamination. D). Results from the sequencing experiment, showing that microDecon effectively removed the contamination.

Figure 6.8 — Results from simulation 1, showing the best, median, and worst iteration (out of 100 iterations). The stacked bars show the percent of each sample that was comprised by each OTU (each colour/section is an OTU). Each cluster of three samples is a sample. The best, median, and worst were determined by mean Bray-Curtis dissimilarities between the decontaminated and uncontaminated samples, and they were extracted separately per group (e.g., the best for group 1 and for group 2 are not from the same iteration).

Figure 6.9 — Comparison of uncontaminated (U), decontaminated (D), and contaminated (C) samples for the sequencing test. Stacked bars show the percent of each sample that was comprised by each OTU (each colour/section is an OTU). Each group of 3–4 bars is a sample. The last sample in each group has a replicate uncontaminated sample. Data were subset to the OTUs that amplified in the blank (contaminant OTUs) so that trends could easily be seen. There were several prominent OTUs in the contaminated samples that were removed or greatly reduced by microDecon.

Figure 7.1 — OTU richness for all individuals, regardless of park or elevation. (A) Richness of entire community. (B) Richness of inhibitory bacteria. Letters indicate species that were not significantly different from each other. Whiskers represent the 10^{th} and 90^{th} percentile (calculated via the "standard" formula in SigmaPlot 11.0) and all outliers are shown.

Figure 7.2 — OTU richness split by species, park, and elevation. (A) Richness of entire community (B) Richness of inhibitory bacteria. P values for tests are shown below, with "A" and "B" corresponding to the panels. Results are shown for the post hoc tests on data that were subset based on interactions. Some comparisons were made without subsetting by park or elevation if no relevant interactions were present. Capital letters before species names indicate park (P = Paluma, K = Kirrama, T = Tully, K-T = Kirrama and Tully [when no interaction was present]) and elevation (L =

lowland, U = upland). Only significant and nearly significant (P < 0.1) results are shown, but full results are presented in Appendix 2. Whiskers represent the 10th and 90th percentile (calculated via the "standard" formula in SigmaPlot 11.0) and all outliers are shown.

Figure 7.3 — Relative abundance (proportion) of inhibitory bacteria. (A) All inhibitory bacteria ("prop. Inhib."). (B) Members of the genus *Pseudomonas* ("prop. *Pseudo*"). Dashed horizontal lines separate parks (data for both elevations are included in each box). Tables to the right show the P values for statistical comparisons. For readability, only comparisons that were significant in at least one park are shown (- = no test conducted, NS = not significant). Full results of all statistical tests are available in Appendix 2. Whiskers represent the 10th and 90th percentile (calculated via the "standard" formula in SigmaPlot 11.0) and all outliers are shown.

Figure 7.4 — Association between *Bd* infection intensity (for *Bd*+ individuals) and richness. Total OTU richness (row 1), inhibitory richness (row 2), and the relative abundance of inhibitory bacteria (Prop. inhibitory; row 3) are shown. Some *Bd* values are negative because I did not use a pseudocount for the log transformation. The positive trend for *L. serrata* inhibitory richness is largely driven by park effects, and the result is not significant when park is taken into account.

Figure 7.5 — Richness for infected and uninfected frogs. (A) Total OTU richness. (B) Richness of inhibitory OTUs (B) for uninfected and infected frogs. Whiskers represent the 10th and 90th percentile (calculated via the "standard" formula in SigmaPlot 11.0) and all outliers are shown.

Figure 7.6 — NMDS plots based on Bray-Curtis dissimilarities for frog species, elevation, and infection intensity. A and C show the results for the entire community, and B and D are for just the inhibitory portion of the community. The shading on plots C and D shows the infection intensity based on a log10 transformation of the qPCR results (I added a pseudocount of one to avoid negative values for this visualization). The partial association with *Bd* is driven largely by elevational differences in bacterial communities (*Bd* is more abundant in the uplands), and the patterns are not significant after accounting for elevation. Data were normalized to proportions prior to calculations (B and D, they were normalized after restricting the data to the

inhibitory community). The horseshoe affect in B and D is a result of having few overlapping OTUs for many individuals (Morton et al. 2017).

Figure 7.7 — Composition of the inhibitory portion of the bacterial community. (A) Order. (B) Family. Each bar is the mean per collection site. L = lowland, U = upland, T = Tully Gorge National Park. P = Paluma Range National Park, K = Kirrama Range National Park. The "low abundance" category in plot B is the sum of seven families that each comprised an average of less than 0.1% of the communities (Streptococcaceae, Sphingomonadaceae, Sphingobacteriaceae, Burkholderiaceae, Bradyrhizobiaceae, Streptomycetaceae, Micrococcaceae).

Figure 8.1 — Richness and evenness of the fungal and bacterial communities. Letters indicated groups (within panels) that were not significantly different form each other. For panel C, *Bd* was removed from the community prior to calculations. For panels C–E, 1 = a totally even community. All data per species were combined (data split by park and elevation are available in Appendix 3). Whiskers represent the 10^{th} and 90^{th} percentile and all outliers are shown.

Figure 8.2 — Distributions of OTUs across species. The first row shows the results from all samples, and the second row shows the results for frogs at the Kirrama lowlands only, to control the number of samples per species and park and elevation effects (ten samples per species; one sample was randomly removed for *L. nannotis*).

Figure 8.3 — Bray-Curtis dissimilarities for all comparisons (1 = totally dissimilar, 0 = identical). The scatterplot shows the relationship between the bacterial and fungal dissimilarities, with points falling above the line indicating that the bacterial communities were more similar (less dissimilar) than the fungal communities. The histograms show the distribution of dissimilarities for bacteria and fungi. Fungal communities tended to be more dissimilar than bacterial communities.

Figure 8.4 — nMDS plots (based on Bray-Curtis dissimilarities) of fungal and bacterial communities split by park and showing clustering of elevations and species. Both fungi and bacteria clustered by elevation, but the clustering by species was not as strong for fungi as it was for bacteria. *Bd* was removed from the fungal community prior to normalizing and calculations.

Figure 8.5 — nMDS plots (based on Bray-Curtis dissimilarities) for the fungal communities with and without *Bd* (i.e., for panels B and D, *Bd* was removed from the community

prior to normalization and calculations). Panels C and D are shaded by *Bd* infection intensity based on qPCR results. When *Bd* was included in the community, it was the dominant factor explaining the ordination (C) because it was often highly abundant; however, it had no discernible impact on the rest of the community (B and D).

Figure 5.6 — Example simulation results of PCoAs comparing population 1 (yellow circles) with population 2 (dark squares) using different normalization methods. Original = the real communities prior to sequencing. Proportions and rarefying generally produced results that were very similar to the original data. Following a log transformation, all methods often produced clusters that were not present in the original data (when all OTUs or only the bottom 30% varied between the initial distributions) or failed to produce clusters that were present in the original data (when only the top 10% of OTUs varied between the initial distributions). For log-transformed data, only CSS is presented here because of that method's popularity, but other methods involving a log transformation produced similar results (full results are available in Supporting information 1). 1000–20000 and 5000–15000 = the range from which the numbers of reads per sample were randomly selected for each sample, All = all OTUs were allowed to vary between the two distributions on which the populations were based, Top 10% = only the OTUs in the 90th percentile and above (based on DNA yield for population 1's distribution) varied between distributions, Bottom 30% = only the OTUs in the 30th percentile and below varied. For rows 1 and 2, the mean dissimilarity was set to 0.2, for row 3 it was 0.3, and for row 4 it was 0.8.

Appendix 1 Figure 1 — Recent survey data for four species of Australian frog that were affected by an amphibian chytridiomycosis outbreak. Frogs were present in the bright green highlighted sections at each survey date, and they were never present in the non-highlighted sections. Waterfall frogs and green-eyed tree frogs have recovered at upland locations (photographed at recovered upland sites at Paluma Range National Park, 2015). Mist frogs and lace-lids are no longer present at Paluma (photographed at lowland sites at Girringun Range National Park, 2015). At Kirrama/Girringun, lace-lids are essentially restricted to low elevation sites (≤330 m elevation; the highlights at 350 m and 410 m represent one frog each). Mist frogs have established slightly further up the streams, but they are still not found above

roughly 400 m elevation (the two points on survey site seven represented fewer than 10 recorded individuals each).

Appendix 2 Figure 1 — A). Calculated yield of inhibitory bacteria. B). Calculated yield of inhibitory bacteria divided by snout-urostyle length (SUL). C). Calculated yield of all bacteria. D). Calculated yield of all bacteria divided by SUL.

Appendix 2 Figure 2 — OTU evenness for all individuals of each species. Whiskers represent the 10th and 90th percentile (calculated via the "standard" formula in SigmaPlot 11.0) and all outliers are shown.

Appendix 2 Figure 3 — OTU evenness split by species, parks, and elevations. Whiskers represent the 10^{th} and 90^{th} percentile (calculated via the "standard" formula in SigmaPlot 11.0) and all outliers are shown.

Appendix 3 Figure 1 — Scatter plots comparing richness and evenness within and among bacterial and fungal communities. P values are provided in table, and full model details and outputs are available in supplemental information.

Appendix 3 Figure 2 — Bacterial and fungal richness and evenness split by species, park, and elevation. Fungal results were calculated after removing *Bd*. Bacterial results were previously reported in Chapter 7 and are shown again here for sake of easy comparisons. Whiskers represent the 10^{th} and 90^{th} percentile and all outliers are shown.

LIST OF ONLINE ADDITIONAL FILES AND DATA

This list is for supplementary information for chapters that have already been published. Supplementary information for unpublished chapters is included at the end of the thesis as appendices.

Additional file 3.1 — Additional tables and figures for Chapter 3 mec15108-sup-0001-SupInfo.pdf

Additional file 3.2 — Filtered and unfiltered SNP data sets for Chapter 3 https://doi.org/10.5061/dryad.7c0h1sb

Additional file 5.1 — Additional tables and figures for Chapter 5 mee313115-sup-0001-Supinfo.docx

Additional file 5.2 — Input distributions and R scripts for simulations for Chapter 5 https://doi.org/10.5061/dryad.tn8qs35

Additional file 6.1 — microDecon user's guide edn311-sup-0001-AppendixS1.pdf

Additional file 6.2 — Simulation 1 R script edn311-sup-0002-AppendixS2.R

Additional file 6.3 — Methods details and additional results for Chapter 6 edn311-sup-0003-AppendixS3.pdf

Additional file 6.4 — Distribution for simulation 1 edn311-sup-0004-AppendixS4.csv

Additional file 6.5 — Simulation 2 R script edn311-sup-0005-AppendixS5.R

Additional file 6.6 — Distribution for simulation 2 edn311-sup-0006-AppendixS6.csv

Additional file 6.7 — FASTA file of results from sequencing experiment edn311-sup-0007-AppendixS7.fasta

Additional file 6.8 — OTU table and metadata edn311-sup-0008-AppendixS8.xlsx

Additional file 6.9 — Simulation 3 R script edn311-sup-0009-AppendixS9.R

CHAPTER 1: INTRODUCTION

Emerging infectious diseases are an increasingly important topic for wildlife conservation (Daszak et al. 2000; Smith et al. 2006). These diseases are taxonomically diverse and afflict a wide range of organisms. In recent decades, many species of amphibian (Daszak et al. 1999; Green et al. 2002; Scheele et al. 2019), reptile (Johnson et al. 2008; Grisnik et al. 2018), bird (van Riper III et al. 1986), mammal (Miller et al. 2000; Harding et al. 2002; Frick et al. 2010), fish (Langdon and Humphrey 1987; Whittington et al. 1997), and various invertebrates (Harvell et al. 1999) have been affected, sometimes with devastating consequences. Nevertheless, even within a taxonomic group, not all species respond to diseases in the same way. Some experience massive declines while others demonstrate considerable resistance or tolerance to infection. Further, in many species that experience declines, the disease eventually shifts from being epizootic to enzootic, allowing populations to persist with it and even recover (Briggs et al. 2010; Catenazzi et al. 2017; Jani et al. 2017; Scheele et al. 2017). These differential responses hold important clues for designing appropriate conservation measures to both facilitate recoveries in populations that have already declined and prevent future declines. However, there is still much that we do not understand about these infection dynamics, and the causes of many population recoveries remain a mystery.

One obvious explanation for why some populations recover from outbreaks is adaptation to the pathogen (Dybdahl and Lively 1998; Foster et al. 2007; Elderd et al. 2008; Robinson et al. 2012). This is not, however, a guaranteed outcome, and other factors like a lack of diversity, high levels of gene flow, or genetic drift can prevent populations from adapting (Lacy 1987; Gandon et al. 1996; Lenormand 2002; Morgan et al. 2005; Foster et al. 2007; Strand et al. 2012). Further, even if adaptation takes place, it may not be strong enough to drive changes that are meaningful for managing diseased populations (Robinson et al. 2012).

Another possible mechanism for population recoveries is a shift in the hosts' microbiomes. There is growing recognition that microbiomes play critical roles in host health and ecology, and they have been implicated in the infection dynamics of multiple diseases (Harris et al. 2009a; Mao-Jones et al. 2010; Mattoso et al. 2011). For example,

some studies have suggested that microbial communities with high diversity can resist the invasion and proliferation of pathogens (Dillon et al. 2005; Matos et al. 2005; Eisenhauer et al. 2013; Fraune et al. 2015; Harrison et al. 2017). Other studies have identified bacterial species that are inhibitory to particular pathogens (Harris et al. 2006; Lauer et al. 2007, 2008; Becker and Harris 2010; Bell et al. 2013), and, in laboratory trials, these bacteria can help their hosts survive infections (Becker et al. 2009; Harris et al. 2009b, a; Muletz et al. 2012). Similarly, some field-based studies have found associations between microbial communities and population recovery or persistence (Woodhams et al. 2007; Lam et al. 2010; Flechas et al. 2012; Kueneman et al. 2016; Burkart et al. 2017; Jani et al. 2017; Bates et al. 2018; Bell et al. 2018; Catenazzi et al. 2018). These observations have led to the proposal of using probiotics on wild populations to facilitate recoveries, but a more complete understanding of the role of microbiomes in infection dynamics is needed before those strategies can be carried out effectively.

Additionally, the research on wildlife microbiomes to date has focused almost exclusively on bacterial microbiomes, and our current knowledge of fungal microbiomes comes largely from studies on humans (Wargo and Hogan 2006; Findley et al. 2013; Hoffmann et al. 2013; Huffnagle and Noverr 2013), laboratory rodents (Scupham et al. 2006), domesticated ruminants (Kittelmann et al. 2013), and soil communities (especially mycorrhizal communities; Bonfante and Anca 2009; Ma et al. 2016). Relatively few studies have examined the fungal microbiomes of non-domesticated vertebrates (Kueneman et al. 2016, 2017; Kearns et al. 2017; Allender et al. 2018; Chen et al. 2018; Medina et al. 2019), and of those few, many had limitations such as using captive animals (Kearns et al. 2017; Chen et al. 2018) or primers that were not specific for fungi (Kueneman et al. 2016, 2017). Nevertheless, fungal microbiomes are likely important, especially given the prevalence of fungal pathogens (Fisher et al. 2012), and this is a topic that merits further study.

In addition to the poorly understood causes of recoveries, little is known about the long-term consequences of disease outbreaks for populations that recover from them. For example, some populations lose genetic diversity during a decline (Trudeau et al. 2004; Schoville et al. 2011; Albert et al. 2014; Serieys et al. 2015), which could make them susceptible to future disease outbreaks even if they return to pre-decline numbers (Spielman et al. 2004; Pearman and Garner 2005; Whiteman et al. 2006; Hughes et al. 2008). However, many populations experience large, disease-induced declines without losing

genetic diversity (Queney et al. 2000; Eggert et al. 2008; Lachish et al. 2011; Brüniche-Olsen et al. 2013). The duration of the decline and the total number of individuals who survive likely affect the amount of genetic diversity that is lost (Zenger et al. 2003; Yuan et al. 2015), but more research is needed to properly understand these dynamics, and gaining that understanding is necessary for adequately managing disease afflicted populations.

The goal of my PhD research is to help fill these gaps in our knowledge by using amphibian chytridiomycosis as a model system for understanding why and how populations recover from disease outbreaks, as well as examining the long-term consequences of those outbreaks. Chytridiomycosis is caused by the fungal pathogen *Batrachochytrium dendrobatidis* (hereafter referred to as *Bd*; Berger et al. 1998), and it affects amphibians by growing in keratinized surfaces, such as skin and mouthparts, at high infection loads that impede osmoregulation (Voyles et al. 2007, 2011). The ensuing electrolyte imbalance often culminates in cardiac arrest and death (Voyles et al. 2009). The exact origin(s) of this fungus has been widely debated, but the most recent evidence suggests that it originated in Asia (Hanlon et al. 2018) and was recently spread around the world by human activities (Rachowicz et al. 2005; Fisher and Garner 2007; Fisher et al. 2009; Rosenblum et al. 2010). Regardless of its point of origin, *Bd* can now be found on every continent except Antarctica, and it has been responsible for declines or even extinctions in over 500 species of frogs (Lips et al. 2006; Pounds et al. 2006; Skerratt et al. 2007; Fisher et al. 2009; Alford 2010; Scheele et al. 2019).

The Wet Tropics of northeastern Australia is among the regions that have been heavily impacted by *Bd*. A large outbreak occurred there in the late 1980s and early 1990s and caused declines or extinctions in at least eight species of frog (Richards et al. 1993; Laurance et al. 1996; McDonald and Alford 1999). The waterfall frog (*Litoria nannotis*), green-eyed treefrog (*Litoria serrata*), and Australian lace-lid frog (*Litoria dayi*) were among the affected species; however, the extent of the declines differed among species and locations. *Batrachochytrium dendrobatidis* does not grow well at temperatures above 26–28°C (Piotrowski et al. 2004; Stevenson et al. 2013), and frogs that can increase their body temperatures can often clear infections (Woodhams et al. 2003; Rowley and Alford 2007a; Richards-Zawacki 2010; Forrest and Schlaepfer 2011). As a result, *Bd*-induced declines often follow an elevational gradient, with the highest infection rates and most severe declines occurring at the cooler, high elevation sites (Retallick 2002; Lips et al. 2008; Sapsford et al.

2013; Stevenson et al. 2014). This was the case for *L. nannotis, L. serrata*, and *L. dayi* (McDonald and Alford 1999). During the outbreak, populations of *L. nannotis* and *L. dayi* above 400 m elevation (often above 300 m) disappeared, but low elevation populations persisted and remained relatively stable (Ingram and McDonald 1993; Richards et al. 1993; Trenerry et al. 1994; Laurance et al. 1996; McDonald and Alford 1999). *Litoria serrata* experienced a similar elevational pattern, but upland populations simply declined, rather than fully disappearing (McDonald and Alford 1999; Richards and Alford 2005).

In the years following the outbreak, upland populations of both *L. nannotis* and *L. serrata* have largely recovered and are persisting despite the fact that *Bd* is still present (Richards and Alford 2005; McKnight et al. 2017a). In contrast, *L. dayi* continues to be restricted to low elevations and has not recovered (McKnight et al. 2017a). Additionally, a fourth sympatric species, the Stoney Creek frog (*Litoria wilcoxii*), has remained stable at all elevations throughout the outbreak.

Because of these different histories with *Bd*, this system presents an excellent natural laboratory for studying infection dynamics and elucidating the factors that confer resistance or tolerance in some species, while precluding recoveries in others. Similarly, it offers a rare opportunity to examine the long-term consequences of a disease outbreak on species that have recovered from the initial decline. I took advantage of those opportunities by using next generation sequencing technologies to examine the population genetics, bacterial microbiomes, and fungal microbiomes of these species, both at recovered populations and populations that remained stable during the outbreak.

Thesis chapter outline

The primary goals of my thesis were first, to examine the long-term genetic consequences of the *Bd* outbreak on the population genetics of several frog species, and second, to examine the factors allowing some species to recover, while precluding recovery in others. I specifically wanted to test the hypotheses that species had adapted to *Bd* and that the frogs' microbiomes (both bacterial and fungal) had played a role in recoveries. Addressing these goals resulted in five data chapters and a literature review, as well as a short note that is included as an appendix.

- Chapter 2 — I conducted a review of the literature on our current knowledge of the effects of disease outbreaks on host population genetics, with the goals of

summarizing our current knowledge and identifying knowledge gaps that require further study. This chapter was published in *Conservation Genetics* (McKnight et al. 2017b).

- Chapter 3 — I examined the population genetics of *L. nannotis* and *L. serrata* at both upland populations that recovered from the outbreak and lowland populations that did not decline during the outbreak. I checked for long-term consequences of the outbreak (loss of diversity, inbreeding, fragmentation, etc.), examined factors, such as habitat quality, that could help populations survive an outbreak without experiencing a loss of diversity, and looked for evidence of adaptation to *Bd*. I made comparisons both within and between species to see if both species responded in the same way. This chapter has been published in *Molecular Ecology* (McKnight et al. 2019b).
- Chapter 4 — Following Chapter 3, I wanted to flip my questions about recovery and ask, "why has this species not recovered?" rather than "why has this species recovered?" To do this, I examined the population genetics of *L. dayi* at three parks. I tested the hypotheses that low dispersal rates have prevented recovery, that a lack of diversity has prevented recovery, and that the species is slowly adapting to *Bd.*
- Chapter 5 — As I began examining host microbiomes, it quickly became clear that there was little agreement about the best way to normalize microbiome sequence data, and many studies were using methods that did not seem appropriate. Therefore, I conducted a large simulation study to test normalization methods so I could use the most appropriate method in my analyses. This chapter was published in *Methods in Ecology and Evolution* (McKnight et al. 2019a).
- Chapter 6 — Bacterial contamination is a critical issue in microbiome research and impacted my data. However, adequate methods for removing contamination from sequence data were lacking. Therefore, I developed the R package "microDecon" to remove contaminant reads, and I tested it both with computer simulations and a sequencing experiment. This chapter has been published in *Environmental DNA* (McKnight et al. 2019c).
- Chapter 7 — I examined the bacterial microbiomes of *L. dayi*, *L. nannotis*, *L. serrata*, and *L. wilcoxii* at both upland and lowland sites to test the hypothesis that

microbiomes had played a role in recoveries. I was specifically interested in the effects of species richness, bacterial community structure, and the abundance of known inhibitory bacteria. I made comparisons within and among species, including looking for associations with *Bd* infection status.

- Chapter 8 — I examined the frogs' fungal microbiomes using the same samples and design as Chapter 7. I conducted the same comparisons as Chapter 7, but I also made comparisons between the bacterial and fungal communities.
- Chapter 9 — Finally, I brought all my chapters together to discuss the factors affecting population recovery and persistence following a disease outbreak.

CHAPTER 2: EFFECTS OF EMERGING INFECTIOUS DISEASES ON HOST POPULATION GENETICS: A REVIEW

Published as: McKnight, DT, L Schwarzkopf, RA Alford, DS Bower, KR Zenger. 2017. Effects of emerging infectious diseases on host population genetics: a review. *Conservation Genetics* 18:1235–1245.

Abstract

Emerging infectious diseases threaten the survival of many species and populations by causing large declines and altering life history traits and population demographics. Therefore, it is imperative to understand how diseases impact wildlife populations so that effective management strategies can be planned. Many studies have focused on understanding the ecology of host/pathogen interactions, but it is equally important to understand the effects on host population genetic structure. In this review, I examined the literature on how infectious diseases influence host population genetic makeup, with a particular focus on whether or not they alter gene flow patterns, reduce genetic variability, and drive selection. Although the results were mixed, there was evidence for all of these outcomes. Diseases often fragmented populations into small, genetically distinct units with limited gene flow among them. In some cases, these isolated populations showed the genetic hallmarks of bottlenecks and inbreeding, but in other populations, there was sufficient gene flow or enough survivors to prevent genetic drift and inbreeding. Direct evidence of diseases acting as selective pressures in wild populations is somewhat limited, but there are several clear examples of it occurring. Also, several studies found that gene flow can impact the evolution of small populations either beneficially, by providing them with variation, or detrimentally, by swamping them with alleles that are not locally adaptive. Thus, differences in gene flow levels may explain why some species adapt while others do not. There are also intermediate cases, whereby some species may adapt to disease, but not at a rate that is meaningful for conservation purposes.

Introduction

Recent decades have seen the emergence and spread of multiple infectious wildlife diseases, often with devastating consequences for biodiversity (Daszak et al. 2000; Smith et al. 2006). It appears that this has often been caused or exacerbated by anthropogenic activities (Daszak et al. 2001; Anderson et al. 2004; Tompkins et al. 2015). For example, increased use of land for raising livestock and anthropogenic encroachment on wildlife habitats have greatly increased rates of contact between domestic animals and wildlife, facilitating pathogen spill over to novel hosts (Bengis et al. 2002; Gortazar et al. 2007). Similarly, in our highly connected world, both wild and domestic animals are frequently transported over long distances, and they often carry diseases with them (Karesh et al. 2005; Fèvre et al. 2006; Talbi et al. 2010; Fisher et al. 2013). Finally, anthropogenic climate change has been implicated in the emergence, spread, and severity of multiple diseases (Harvell et al. 1999, 2002; Benning et al. 2002; Pounds et al. 2006; Alford et al. 2007).

These emerging diseases are taxonomically diverse and have afflicted a wide range of animals. Well known examples include diseases such as the fungal infection chytridiomycosis, which has severely affected amphibian populations around the world (Daszak et al. 1999; Lips et al. 2006) and avian malaria, which has caused many bird populations to decline sharply (van Riper III et al. 1986). Many other emerging diseases have also been documented, such as devil facial tumour disease in Tasmanian devils (*Sarcophilus harrisii*; Hawkins et al. 2006), chronic wasting disease in cervids (Miller et al. 2000), canine and phocine distemper viruses in seals (Mamaev et al. 1995; Kennedy et al. 2000; Harding et al. 2002), white-nose syndrome in bats (Frick et al. 2010), herpesvirus in pilchards (Whittington et al. 1997), ranaviruses in fish (Langdon and Humphrey 1987), amphibians (Daszak et al. 1999; Green et al. 2002) and chelonians (Johnson et al. 2008), and a multitude of diseases in marine invertebrates (Harvell et al. 1999).

Because of their diversity, rapid spread, and high virulence, these diseases present an unprecedented threat to many wildlife species and are of growing concern for conservationists (Scott 1988; Smith et al. 2006). It is, therefore, imperative to understand the responses of host populations to these diseases so we can prevent future declines and facilitate population recoveries. Modern molecular techniques provide powerful tools for examining both the influence of genetic variation on disease outbreaks and the impact of

epizootics on host populations. Recent advances, such as the advent of next generation sequencing, have opened the door for more extensive studies and, importantly, studies of non-model organisms.

One useful avenue of research is to examine the genetic variation of the pathogens themselves. Research in this area has revealed the importance of landscapes, pathogen genetic diversity, and species interactions in the emergence and spread of diseases, and these topics have been reviewed by several authors (McDonald and Linde 2002; Archie et al. 2009; Biek and Real 2010). Another approach is to study the effect of the hosts' genes on their susceptibility to disease. Research in this area is more limited, but several studies have documented that genetic diversity in host populations is an important determinant of a host population's ability to survive infectious diseases, and that low diversity within a population often corresponds to increased susceptibility to diseases (Spielman et al. 2004; Pearman and Garner 2005; Whiteman et al. 2006). A final area of consideration is the effect of diseases on host population genetic diversity and structure. It has been predicted that large disease outbreaks should reduce the level of population genetic diversity through population genetic bottlenecks and/or by strong selective pressures that favour a subset of individuals in the population (O'Brien and Everamnn 1988). However, it has only relatively recently been possible to properly test these predictions on non-model organisms. Nevertheless, understanding the response of wildlife populations to diseases is clearly of paramount importance for conservation efforts; therefore, in this review I examine the evidence for and against the hypotheses that disease outbreaks alter gene flow patterns, reduce diversity, and drive local adaptation.

Natural selection

When novel pathogens enter a naïve host population, they often cause epizootics that result in mass mortality (Berger et al. 1998; Daszak et al. 1999; Frick et al. 2010). In some cases, this initial wave of infection may cause host population extirpation or even species extinction, especially if the population was small to begin with or if there are multiple host species (De Castro and Bolker 2005). However, in most cases there are survivors, and in those situations, a disease can act as a selective pressure that drives the evolution of tolerance or resistance and causes the disease to switch from being epizootic to

being enzootic (Karlsson et al. 2014; see Boots et al. 2009 for a review of the theory behind how and why populations adapt to diseases). Indeed, disease-driven selection has been documented in several taxa, including insects (Elderd et al. 2008), snails (Dybdahl and Lively 1998), cervids (Robinson et al. 2012), and birds (Foster et al. 2007; Eggert et al. 2008).

In some cases, however, selection may occur, but still be too weak to have a significant impact on management (Robinson et al. 2012). That is, in situations where the disease is killing individuals at a low rate that is unlikely to cause rapid population declines, the population may eventually adapt to the disease, but it may take too long to be meaningful for short-term conservation and management efforts. In these situations, it may be tempting to simply let nature take its course. However, even if the disease is unlikely to directly cause population extinction, it can act as a stressor which may interact with other stressors (such as habitat loss) and predispose a population to extinction (Traill et al. 2010).

Much of the literature on disease-induced selection has focused on the evolution of the major histocompatibility complex (MHC), and it has been documented that diseases can drive the evolution and maintenance of MHC diversity (Jeffery and Bangham 2000; Teacher et al. 2009; Spurgin and Richardson 2010; but see Zeisset and Beebee 2014). There is also some evidence that high MHC diversity corresponds to increased resistance to diseases, but more research is needed (reviewed in Radwan et al. 2010 and Blanchong et al. 2016). Other studies have provided evidence that diseases can drive selection for specific MHC alleles. For example, several studies on amphibian populations have found evidence that the fungal disease chytridiomycosis causes directional selection for the region of the MHC genes containing the Q and ST4 alleles, and that populations that contain these alleles are less susceptible to chytridiomycosis than populations that lack them (Savage and Zamudio 2011; Bataille et al. 2015; Savage and Zamudio 2016).

Some studies have also looked at genes other than the MHC. A remarkable example of this comes from research on white-tailed deer (*Odocoileus virginianus*) affected by chronic wasting disease. Researchers have documented that the 96GS genotype for the prion protein gene is associated with both resistance to chronic wasting disease and slowed progression of the disease (Johnson et al. 2006; Keane et al. 2008). Also, a large study that combined genotyping and modelling documented a selection pressure for the 96GS genotype in a wild population (Robinson et al. 2012). However, the authors estimated that it

would take several hundred years for the resistance allele to rise to prominence in the population, and this allele does not appear to completely preclude infections.

A similar study examined the rates of occurrence of the Toll-like receptor 2 variant *TLR2* c_2 across European populations of the bank vole (*Myodes glareolus*; Tschirren 2015). *TLR2* c_2 is associated with resistance to infections from the tick-borne pathogen *Borrelia burgdorferi* (Tschirren et al. 2013), and Tschirren (2015) found a positive correlation between *TLR2* c_2 frequencies in voles and rates of human Lyme borreliosis (human Lyme borreliosis is also caused by *B. burgdorferi* so it was used as a proxy for infection risk). This result suggests that *B. burgdorferi* is driving selection, ultimately producing increased frequencies of *TLR2* c_2 in the populations that are under the greatest selection pressure.

The studies mentioned so far have focused on particular genes or gene regions (e.g., the MHC); but advances in next generation sequencing technologies have also allowed researchers to expand beyond a handful of genes and look at reduced representations of entire genomes (e.g., by using single nucleotide polymorphisms [SNPs]). Linkage disequilibrium, allele frequency, and F_{ST}-based methods can then be used to identify major loci that are under selection (Vitalis et al. 2014; Hoban et al. 2016). This is potentially a very useful approach, because it does not require *a priori* knowledge about the region of the genome that is undergoing selection. However, to date, few researchers have taken advantage of these tools in the context of adaptation to diseases, and some of the existing studies have not yielded promising results. For example, two recent studies used genome-wide loci to test whether Tasmanian devils are adapting to devil facial tumour disease, and they reached opposite conclusions. Epstein et al. (2016) identified seven candidate genes that appeared to be under selection, whereas Brüniche-Olsen et al. (2016) failed to find a consistent pattern that would indicate adaptation to the disease. Similarly, Shultz et al. (2016) used SNPs to test for selection in house finch populations that had been affected by epizootics of *Mycoplasma gallisepticum*, but they did not find evidence of selection using the genome-wide markers, despite results from transcriptome studies that indicate that the finches have adapted (Bonneaud et al. 2011; Bonneaud et al. 2012). The lack of evidence for selection in these genome-wide studies likely results from insufficient genome coverage (Lowry et al. 2016; Shultz et al. 2016), or a lack of power to detect the additive effects of many genes regulating the traits, or both. Further improvements in genome-wide genetic

resources and quantitative trait experimental designs will be necessary for these methods to have wide applicability in the context of disease ecology.

A final approach has been to compare genetic patterns among populations with different infection histories (e.g., never infected, infected and recovered, infected and not recovered) to gain insight into observed demographic patterns. A good example of this type of research comes from a group of Hawaiian honeycreepers that have experienced declines from the introduction of avian malaria (Warner 1968). Historically, the Amakihi (*Hemignathus virens*), Apapane (*Himatione sanguinea*), and ‘I’iwi (*Drepanis* [*Vestiaria*] *coccinea*) were all found at various elevations ranging from coastland to mountain forests, but avian malaria (which is most prevalent in lowlands) greatly reduced their populations in areas below 900 m (Eggert et al. 2008). Following the initial declines, however, *H. virens* were found in surprisingly large numbers in low elevation forests (Woodworth et al. 2005; Spiegel et al. 2006). Further, these populations were breeding and growing despite the fact that most individuals had been infected with malaria (Woodworth et al. 2005), which suggests that low-elevation populations of *H. virens* had adapted and become tolerant to avian malaria. In contrast, *H. sanguinea* and *D. coccinea* populations had not recovered at low elevations.

Research on the population genetics of these three species found no evidence of genetic structuring across elevations for *H. sanguinea* or *D. coccinea*, but there was significant structuring for *H. virens*, and low-elevation populations were distinct from mid and high-elevation populations (Foster et al. 2007; Eggert et al. 2008). Mid and high-elevation populations of *H. virens* were also different from each other, but they were more similar to each other than to low-elevation populations (Eggert et al. 2008). Further, the low-elevation populations contained alleles that were not found in the other populations (private alleles), suggesting that the current populations descended from a few surviving lowland birds, rather than from immigration from mid or high-elevation populations (Foster et al. 2007; Eggert et al. 2008).

Given the large declines that the *H. virens* experienced, the size of its current low-elevation populations suggests that the disease acted as a strong selective pressure, which selected for alleles that conferred tolerance to the pathogen. The idea that avian malaria could exert a strong selective force is also supported by high mortality rates among experimentally infected birds (Atkinson et al. 1995; Atkinson et al. 2000). Further, research

on house sparrows (*Passer domesticus*) has identified specific MHC alleles associated with resistance to avian malaria (Bonneaud et al. 2006). Finally, recent experimental results showed that both high and low-elevation populations of *H. virens* were equally susceptible to becoming infected, but low elevation populations had significantly lower mortalities and weight loss after the parasite entered their bodies (Atkinson et al. 2013).

Fragmentation, gene flow, and genetic drift

Even for populations that survive the initial disease outbreak and evolve to coexist with the pathogen, there are often further effects mediated by the fragmentation of previously connected populations and subsequent reductions in gene flow. It is well established that habitat fragmentation is harmful to many species, and, as a result, many conservation efforts place a priority on maintaining habitat connectivity (Harrison and Bruna 1999; Crooks and Sanjayan 2006; Minor and Urban 2008). One of the primary reasons that fragmentation can be harmful is that it can break up large, contiguous populations into multiple disjointed populations with limited gene flow among them (Hitchings and Beebee 1997; Couvet 2002).

Infectious diseases can act like fragmentation, by isolating populations even when there is suitable habitat connecting them (Addison and Hart 2004). Two studies on the effects of chytridiomycosis on anuran populations illustrate this well. Morgan et al. (2008) documented this in northern and southern corroboree frogs (*Pseudophryne pengilleyi* and *P. corroboree*, respectively), and Albert et al. (2014) found this pattern in midwife toads (*Alytes obstetricans*). All three species were heavily impacted by chytridiomycosis and were reduced to a few disconnected populations. The molecular data confirmed the presence of strong genetic structuring, with large genetic differences among the populations and no evidence of gene flow. Albert et al. (2014) found low levels of genetic diversity at all scales; whereas Morgan et al. (2008) found that individual populations had little diversity, but the species as a whole (all populations combined) still retained a high level of diversity. It should be noted, however, that it is difficult to disentangle historic patterns from recent disease-induced patterns unless pre-decline samples are available (Zellmer and Knowles 2009; Hudson et al. 2016).

These results mirror the genetic patterns seen in populations divided by habitat fragmentation (Allentoft and O'Brien 2010). Multiple studies have, for example, shown that roads can act as significant barriers to dispersal, and populations that are separated by roads often show strong genetic structuring with large differences among populations and little gene flow (Seitz 1990; Keller and Largiader 2003; Lesbarrères et al. 2006; Holderegger and Giulio 2010). Indeed, Serieys et al. (2015) found that a three-year outbreak of notoedric mange in bobcats (*Lynx rufus*) had a greater isolating effect than large freeways that had been in place for over 60 years. Further, fragmentation by disease may be a particularly significant problem for species with low dispersal rates, because they may be unlikely to move among populations even if the habitat is still suitable (Bowne and Bowers 2004; Allentoft and O'Brien 2010).

Fragmentation of previously connected populations can also act as a source of microevolution by altering patterns of gene flow in a way that predisposes population fragments to genetic drift. Genetic drift is simply a random change in a population's allele frequencies, often as a result of the stochastic nature of independent assortment (Wright 1931). Stochastic loss of alleles is problematic because it constitutes a loss of population genetic diversity, and, unlike natural selection, the alleles that are lost are random. It is well understood that small populations are more prone to the effects of genetic drift than are large populations (Crow and Kimura 1970; Nei et al. 1975), and in very small populations, genetic drift can actually have a greater influence on a population's evolution than natural selection does (Lacy 1987; Whitlock 2000). This is especially problematic for very small populations because genes that would confer resistance or tolerance to a disease may be lost by genetic drift before selection can act on them (Lacy 1987; Strand et al. 2012). Gene flow can, however, prevent or reduce genetic drift by restocking a populations' gene pool, thus maintaining high genetic diversity (Wright 1931; Slatkin 1985; Slatkin 1987; Whiteley et al. 2015).

The benefits of increased genetic diversity *via* gene flow may be particularly important in the context of diseases. Studies on the coevolution of pathogens (and parasites more generally) and their hosts have shown that host gene flow is an important factor in determining whether the host will adapt, because gene flow supplies it with the diversity necessary for selection to act (Gandon et al. 1996; Gandon and Michalakis 2002). This also applies to adaptation of the pathogen, and in the evolutionary arms race between

pathogens and their hosts, it is predicted that, all else being equal, the group with greater gene flow will have greater potential for adaptation (Morgan et al. 2005).

Conversely, under certain circumstances isolation may actually be beneficial because gene flow can counteract natural selection by flooding populations with alleles that are not locally adaptive (García-Ramos and Kirkpatrick 1997; Lenormand 2002; Kawecki and Ebert 2004; Foster et al. 2007; Funk et al. 2012). However, in situations where there is a strong selection pressure, adaptation can still occur, even with high levels of gene flow (Limborg et al. 2012; Nayfa and Zenger 2016). Thus, whether isolation benefits disease-afflicted populations is context dependent. Gene flow helps to avoid genetic drift and inbreeding, and it can furnish populations with additional diversity for selection to act on (Gandon et al. 1996; Gandon and Michalakis 2002). However, if there is too much gene flow (especially gene flow from populations that are not infected) and weak selection, it may not be possible for populations to adapt to pathogens.

The literature on gene flow versus local adaption in the context of disease outbreaks in wild populations is scarce, but *H. virens* may represent a case where isolation was beneficial. One obvious difference between *H. virens* (which adapted to be tolerant to avian malaria) and its conspecifics, *H. sanguinea* and *D. coccinea* (which did not adapt), is that *H. virens* is largely sedentary and does not disperse as far as *H. sanguinea* or *D. coccinea* (Foster et al. 2007). This is consistent with the observation that there was elevational genetic structuring for *H. virens* but not *H. sanguinea* or *D. coccinea* (Foster et al. 2007; Eggert et al. 2008), and it suggests that a lack of movement among *H. virens* populations may have allowed the low-elevation populations to evolve resistance to malaria without having the effects of selection diluted by gene flow from the mid- and high-elevation populations, which were not under strong selection.

Finally, it is important to note that not all diseases affect gene flow in the same way. Some simply alter gene flow patterns by modifying behaviour and dispersal patterns (Hurtado 2008; Jones et al. 2008; Lachish et al. 2008; Teacher et al. 2009b). For example, a study on the effects of devil facial tumour disease showed that female Tasmanian devils in post-disease populations do not disperse as far as females from pre-disease populations (Lachish et al. 2011). Presumably, this is because resources were abundant following large population declines, and, therefore, females did not need to disperse far to find enough resources to reproduce and rear their young. Nevertheless, this altered dispersal still had

the effect of reducing gene flow among populations and increasing genetic structuring (Lachish et al. 2011). In contrast to Lachish et al. (2011), Brüniche-Olsen et al. (2013) failed to find evidence of sex-specific changes in the dispersal rates of disease afflicted populations of devils. However, they did detect increases in gene flow from non-affected populations into declining populations, and they attributed this to source-sink dynamics. They also questioned the results of Lachish et al. (2011) and suggested that genetic changes among populations were better explanations for differences in allelic frequencies among populations than were changes within populations.

Bottlenecks and inbreeding

Because disease outbreaks cause a loss of many individuals, they can cause population bottlenecks, and several studies have revealed that these population bottlenecks can lead to significant reductions in genetic diversity (i.e., genetic bottlenecks) in disease afflicted populations. For example, Trudeau et al. (2004) found genetic diversity reductions in black-tailed prairie dog (*Cynomys ludovicianus*) colonies affected by the sylvatic plague, and Schoville et al. (2011) uncovered genetic bottlenecks in populations of mountain yellow-legged frogs (*Rana muscosa*), a species that has been heavily impacted by chytridiomycosis (Rachowicz et al. 2006). Similarly, genetic bottlenecks were found in remnant populations of the common midwife toad following infection with chytridiomycosis (Albert et al. 2014), as well as in populations of bobcats (*Lynx rufus*) that had been depleted by notoedric mange (Serieys et al. 2015). However, several other studies have either failed to find the signatures of a genetic bottleneck, or only found genetic bottlenecks in a few infected populations. For example, a study on the impacts of chytridiomycosis on *P. pengilleyi* and *P. corroboree* revealed genetic diversity reductions in only seven out of 24 populations (Morgan et al. 2008). Similarly, no genetic bottlenecks were detected in populations of Tasmanian devils (Lachish et al. 2011; Brüniche-Olsen et al. 2013), European rabbits (*Oryctolagus cuniculus*; Queney et al. 2000), western lowland gorillas (*Gorilla gorilla gorilla*; le Gouar et al. 2009), common frogs (*Rana temporaria*; Teacher et al. 2009b), mountain chickens (*Leptodactylus fallax*; a frog species; Hudson et al. 2016) or *H. virens* (Foster et al. 2007; Eggert et al. 2008), even though all of those populations had experienced steep, disease-induced declines.

There are several possible explanations for the result that so many populations seem to be declining without experiencing genetic bottlenecks. First, tests for a reduction in genetic diversity are often unreliable and fail to detect genetic bottlenecks even after very steep declines (Peery et al. 2012). This is especially true when only a few markers or few individuals are used (see Hoban and Gaggiotti [2013] and Hoban et al. [2013] for marker and sample size recommendations). Nevertheless, most authors proposed alternative interpretations. The effect that declines have on population genetic diversity depends on both the number of survivors and the duration of the bottleneck. This is the case because initial declines tend to eliminate rare alleles, but much of the decrease in diversity during a genetic bottleneck results from persistently small population sizes that reduce diversity through genetic drift (Nei et al. 1975; Allendorf 1986). Thus, some populations may not experience a large loss of diversity during a bottleneck because they retain a genetically representative number of individuals through the initial decline, expand quickly after the decline, or both (Zenger et al. 2003). Indeed, several authors proposed a large number of survivors (Queney et al. 2000; Lachish et al. 2011; Longo et al. 2015) or rapid post-epizootic expansion (Savage et al. 2015) as the reason that they failed to detect a bottleneck. However, gene flow can also be significant in avoiding a loss of diversity, because gene flow from neighbouring populations can rescue a population from a genetic bottleneck by restocking its gene pool (Keller et al. 2001; Tallmon et al. 2004; Teacher et al. 2009b; Whiteley et al. 2015). Finally, several authors acknowledged the fact that because it often takes genetic drift several generations to reduce diversity during a bottleneck, studies that are done shortly after a decline may fail to find genetic evidence of a bottleneck simply because not enough time has passed (Queney et al. 2000; le Gouar et al. 2009; Brüniche-Olsen et al. 2013).

The fact that it often takes populations several generations to lose diversity following a decline has important implications for disease ecology. In some cases, selection may cause pathogens to become less virulent (May and Anderson 1983; Boots et al. 2004), which can result in brief epizootics followed by rapid population recovery, and in those situations, populations may avoid a loss of diversity despite experiencing large numerical declines. Conversely, if a disease persists in an epizootic state for a prolonged period of time, the host population may undergo genetic drift and a subsequent loss of diversity. Therefore, I expect there to be a correlation between the rate at which a pathogen

attenuates and the probability of an afflicted population experiencing a large loss of diversity. To date, no authors of whom I am are aware have examined that hypothesis, but understanding the relationship between pathogen attenuation and the loss of host diversity is important for conservation.

Although many studies of disease-afflicted populations have failed to find the hallmarks of a genetic bottleneck, several have found evidence of inbreeding in populations for which there was no genetic evidence of a bottleneck. For example, Lachish et al. (2011), failed to find bottlenecks in devil populations devastated by devil facial tumours, but they did find that inbreeding was higher in post-disease populations than it was in pre-disease populations. Teacher et al. (2009b) reported an analogous situation in European common frogs. Similar to Lachish et al. (2011), they did not detect any bottlenecks, but they did find evidence of inbreeding. Interestingly, in their case, inbreeding seemed to be caused by a behavioural change in the frogs, wherein the ranavirus infection caused assortative mating, illustrating the complexity of the relationship between disease outbreaks and genetic diversity. Even in populations that remain large enough that inbreeding is not expected, it may still occur if the disease modifies the host's behaviour.

Finally, it should be noted that most of these studies (with a few exceptions such as Lachish et al. [2011] and Hudson et al. [2016]) relied entirely on post-decline samples, which can result in falsely ascribing historical trends to recent disease outbreaks. For example, one of the few studies that used pre-decline samples (Hudson et al. 2016) found low levels of heterozygosity and allelic richness in both pre- and post-decline samples of mountain chickens (*Leptodactylus fallax*; a frog that has been impacted by chytridiomycosis), and although the post-decline samples were less diverse, the difference between pre- and post-decline samples was not statistically significant. Thus, although the disease may have reduced genetic diversity, there is also a clear historic pattern of low diversity which, in the absence of pre-decline samples, could easily have been viewed entirely as a result of the disease outbreak.

Feedback loops and conservation

Because infectious diseases can reduce both population size and genetic diversity, they present serious conservation concerns, even for populations that have survived an

outbreak. It is well established that small populations have a higher probability of extinction from stochastic events (Shaffer 1981; Gilpin and Soule 1986; Melbourne and Hastings 2008). Thus, a reduction in population size alone is a cause for concern. Further, both low genetic diversity and inbreeding can reduce fitness, decrease survival rates, compromise a population's ability to adapt to changes in the environment, and, most germane to the current discussion, increase a population's susceptibility to disease (Hedrick and Kalinowski 2000; Keller and Waller 2002; Reed and Frankham 2003; Spielman et al. 2004; Whiteman et al. 2006; Hughes et al. 2008). For example, during a morbillivirus outbreak in Mediterranean striped dolphins (*Stenella coeruleoalba*), inbred individuals experienced higher mortality rates than individuals who were not inbred (Valsecchi et al. 2004). Similarly, a study on California sea lions (*Zalopus californianus*) found that sick animals were often inbred (Acevedo-Whitehouse et al. 2003). They also found that the degree of inbreeding was different for different diseases; animals that were affected by carcinomas (which are often associated with herpesvirus; Lipscomb et al. 2000) had the highest level of inbreeding, whereas animals suffering from algal toxins had the lowest level (excluding animals injured by traumas). Animals with helminth infections, non-specific illnesses, and bacterial infections also showed genetic evidence of inbreeding, and inbred animals had significantly slower recovery rates than non-inbred animals. Similarly, a study of Soay sheep (*Ovis aries*) found that they were more susceptible to diseases when inbred (Coltman et al. 1999), and research on the New Zealand robin (*Petroica australis*) found that individuals from a bottlenecked population had a reduced immune response (Hale and Briskie 2007). Finally, there are often, but not always, positive relationships between high genetic diversity and disease resistance in many species (Meagher 1999; Spielman et al. 2004; Pearman and Garner 2005; King and Lively 2012; Savage et al. 2015).

The fact that inbred and genetically bottlenecked populations are more susceptible to diseases raises the disturbing possibility of a feedback loop, wherein a population survives a disease outbreak, but becomes inbred or genetically bottlenecked and, as a result, becomes more susceptible to future outbreaks of that disease or other diseases. Restoring connectivity may help to ameliorate this problem (Tallmon et al. 2004; Hogg et al. 2006), and encouraging gene flow is often part of the conservation plan for small populations (Bennett 1998), but the conservation of populations that have been affected by diseases has several complex issues that have to be considered. First, restoring connectivity

may be very difficult if the populations have been isolated by disease rather than by a lack of suitable habitat corridors (Morgan et al. 2008). This may require the translocation of individuals among populations, which is a controversial strategy that must be carried out cautiously (Moritz 1999; Murphy et al. 2010; Frankham 2015; Kelly and Phillips 2015). Second, in some populations, isolation may actually serve a beneficial role by allowing the population to evolve resistance to disease without diluting the resistance alleles with new alleles brought in by gene flow (García-Ramos and Kirkpatrick 1997; Storfer 1999; Lenormand 2002; Foster et al. 2007). Conversely, if the population is too small, then the lack of gene flow may result in genetic drift reducing or even counteracting the effects of natural selection (Lacy 1987; Strand et al. 2012), and there may be insufficient genetic variation for selection to act on (Gandon et al. 1996; Morgan et al. 2005). Therefore, great care and a detailed knowledge of the population genetics of the species in question is needed when designing conservation plans for populations that have been reduced by diseases (see, for example, the decision tree in Frankham et al. 2011).

Kelly and Phillips (2015) suggest that we should mange disease afflicted populations by using "targeted gene flow." This strategy is an extension of assisted gene flow, and it involves translocating individuals from populations that have adapted to the disease into populations that have not adapted, which, in concept could restore gene flow without swamping local adaption and could encourage local adaptation by providing declining populations with alleles that are tolerant or resistant to the disease. However, it assumes that the gene complexes associated with resistance are simple and easily transferred to the target population. However, if the mechanisms of resistance are complex, for example if many subtle changes in behaviour are involved, adding new individuals could swamp non-target adaptive gene complexes, with unexpected or unintended consequences.

Conclusions and future directions

There is ample evidence that large disease outbreaks can alter population genetic structure and drive adaptation; however, different populations and species appear to respond differently to them. Some species adapt to disease, but other species either do not adapt, or adapt too slowly for management purposes. Similarly, some disease-afflicted populations undergo extreme genetic bottlenecks, while others maintain a high level of

diversity. Gene flow seems to be one of the key factors in determining a population's response to disease, but it is a double-edged sword. In some cases, a high level of gene flow rescues a declining population, provides diversity upon which selection can act, and precludes inbreeding and the detrimental effects of genetic drift, but in others, it prevents local adaptation by swamping the population with alleles that are not locally advantageous, especially when selection pressures are relatively low. Additionally, the rate at which pathogens attenuate likely plays a role in determining whether genetic bottlenecks occur. Future research should attempt to further elucidate the relationship between gene flow, pathogen attenuation, and local adaptation, and conservation efforts should carefully consider the costs and benefits of maintaining high levels of gene flow.

This field would also benefit from more studies that compare populations before and after epizootics. Most of the literature to date has only looked at populations following a disease outbreak (with a few exceptions such as Lachish et al. [2011], Epstein et al. [2016], Hudson et al. [2016], and Shultz et al. [2016]), but without information on a population's pre-decline genetic structure, it can be difficult to disentangle historic and disease-induced effects. In many cases, this study design is unavoidable, but researchers should make use of pre-epizootic museum specimens whenever possible. Similarly, in some cases disease outbreaks spread in a predictable pattern, and in those cases, it would be useful for researchers to collect tissue samples from areas predicted to become infected, so that comparisons can be made following the outbreak

Finally, most of the current studies were conducted only a few generations after an outbreak occurred, but it often takes many generations for diversity to be lost or for selection to shift allele frequencies enough that its signature can be isolated from background noise. Therefore, more long-term studies that look at populations many generations after the introduction of a disease would be beneficial.

CHAPTER 3: THE RETURN OF THE FROGS: THE IMPORTANCE OF HABITAT REFUGIA IN MAINTAINING DIVERSITY DURING A DISEASE OUTBREAK

Published as: McKnight, DT, MM Lal, DB Bower, L Schwarzkopf, RA Alford, KR Zenger. 2019. The return of the frogs: The importance of habitat refugia in maintaining diversity during a disease outbreak. *Molecular Ecology* 28:2731–2745.

Abstract

Recent decades have seen the emergence and spread of numerous infectious diseases, often with severe negative consequences for wildlife populations. Nevertheless, many populations survive the initial outbreaks, and even undergo recoveries. Unfortunately, the long-term effects of these outbreaks on host population genetics are poorly understood; to increase this understanding, I examined the population genetics of two species of rainforest frogs (*Litoria nannotis* and *Litoria serrata*) that have largely recovered from a chytridiomycosis outbreak at two national parks in the Wet Tropics of northern Australia. At the wetter, northern park there was little evidence of decreased genetic diversity in either species, and all of the sampled sites had high minor allele frequencies (mean MAF = 0.230–0.235), high heterozygosity (0.318–0.325), and few monomorphic markers (1.4–4.0%); however, some recovered *L. nannotis* populations had low N_e values (59.3–683.8) compared to populations that did not decline during the outbreak (1537.4–1756.5). At the drier, southern park, both species exhibited lower diversity (mean MAF = 0.084–0.180; heterozygosity = 0.126–0.257; monomorphic markers = 3.7–43.5%; N_e = 18.4–676.1). The diversity patterns in this park matched habitat patterns, with both species having higher diversity levels and fewer closely related individuals at sites with higher quality habitat. These patterns were more pronounced for *L. nannotis,* which has lower dispersal rates than *L. serrata*. These results suggest that refugia with high quality habitat are important for retaining genetic diversity during disease outbreaks, and that gene flow following disease outbreaks is important for restabilising diversity in populations where it was reduced.

Introduction

Emerging infectious diseases present a great threat to the conservation of many species, and there are still many unknowns regarding their long-term consequences for host population genetics. Indeed, while a substantial amount of effort has been invested in understanding infection dynamics and demographic declines, comparatively few studies have looked at the genetic consequences of those declines. Further, a recent review of the current literature on the effects of emerging infectious diseases on host population genetics revealed that these effects vary widely (McKnight et al. 2017b). Large disease outbreaks are, intuitively, expected to reduce diversity and connectivity, as well as potentially driving adaptation, and several studies have found evidence of fragmentation in post-disease populations (Addison and Hart 2004; Albert et al. 2014; Serieys et al. 2015). However, while some studies have found evidence of genetic bottlenecks, inbreeding, or both (Trudeau et al. 2004; Rachowicz et al. 2006; Albert et al. 2014; Serieys et al. 2015), others have found no evidence of substantial losses of diversity (Queney et al. 2000; Eggert et al. 2008; Morgan et al. 2008; le Gouar et al. 2009; Lachish et al. 2011). Understanding why some populations undergo large losses of diversity while others retain their genetic diversity is critical for conservation and management efforts, as well as for enhancing our understanding of disease ecology and the influence of diseases on host population genetics.

Multiple factors can affect retention of diversity in a population during a disease outbreak, and more research is needed to understand the interactions of these factors in natural populations. For example, for many declining populations, conservationists focus on maintaining gene flow with neighbouring populations, because gene flow enhances diversity by restocking a population's gene pool (Wright 1931; Slatkin 1985, 1987; Whiteley et al. 2015). In disease-afflicted populations, the situation is more complicated, because long-term persistence may depend on the population's ability to adapt to the pathogen, and high levels of gene flow from disease-free populations can swamp selection (García-Ramos and Kirkpatrick 1997; Kawecki and Ebert 2004; Foster et al. 2007; Funk et al. 2012). Conversely, gene flow may benefit affected populations by providing them with the genetic material needed to adapt to the disease (Gandon et al. 1996; Gandon and Michalakis 2002). Additionally, other factors, such as the length and severity of the disease outbreak (i.e., the extent of the genetic bottleneck), may be important in determining whether a population

retains sufficient genetic variation to persist and respond to future threats (Zenger et al. 2003; McKnight et al. 2017b).

Rainforest frogs in Australia's Wet Tropics offer an excellent study system for examining population genetics following a disease outbreak and elucidating the factors that affect the retention of genetic diversity. During the late 1980s and early 1990s, frogs in this region experienced an outbreak of the emerging infectious disease chytridiomycosis (McDonald and Alford 1999). This disease is caused primarily by the fungal pathogen *Batrachochytrium dendrobatidis* (*Bd*) and has caused wide-spread declines and extinctions around the world (Berger et al. 1998; Daszak et al. 1999; Lips et al. 2006; Scheele et al. 2019). In Australia, green-eyed treefrogs (*Litoria serrata* [*genimaculata*]) and waterfall frogs (*Litoria nannotis*) were among the affected species. Historically, both species occurred sympatrically at most elevations along rainforest streams in the Wet Tropics, however, *L. serrata* were generally less common at lowland sites. During the outbreak, *L. nannotis* disappeared from high elevation sites (i.e., sites above 300–400 m elevation) and high-elevation *L. serrata* populations declined sharply (Ingram and McDonald 1993; Richards et al. 1993; Laurance et al. 1996; McDonald and Alford 1999). Nevertheless, both species persisted at low elevation sites (Richards et al. 1993; Laurance et al. 1996; McDonald and Alford 1999; Daskin et al. 2011), likely due to warmer temperatures that were sub-optimal for *Bd* and allowed frogs to clear infections (Piotrowski et al. 2004; Sapsford et al. 2013; Rowley and Alford 2013).

Following the initial epidemic, both species have largely recovered at upland sites, although *Bd* is still present and continues to be detected on the frogs at all elevations (Additional file 3.1). *Litoria serrata* recovered more rapidly and has returned to roughly its pre-decline abundance; whereas *L. nannotis* recovered more slowly, first re-appearing at upland sites in the late 1990s and early 2000s, and has not returned to its pre-decline abundance in many areas (Richards and Alford 2005). Nevertheless, breeding populations of *L. nannotis* are present at the headwaters of many of the streams from which they had been extirpated (McKnight et al. 2017a).

These populations and species are ideal for examining the genetic consequences of disease outbreaks and understanding the factors influencing the retention of genetic diversity, and I used them to achieve several important goals. First, for *L. nannotis* I aimed to determine if the recovered populations had experienced a loss of diversity. Second, I aimed

to compare populations both within and between parks to see if patterns of diversity loss were consistent across populations and, if differences were evident, I made comparisons among habitats to determine whether high quality refugia facilitated the retention of genetic diversity. Third, I aimed to test whether populations had become fragmented and to determine the role of gene flow in the recovery of these populations. Fourth, I aimed to compare *L. nannotis* and *L. serrata*. Given that *L. serrata* has greater dispersal than *L. nannotis* and only declined at upland sites rather than being extirpated, I expected *L. serrata* to have retained greater amounts of genetic diversity. To achieve the first four aims, I looked at family groupings as well as standard diversity metrics, with the expectation that reduced population sizes due to the disease and low dispersal rates should have produced tighter family groups. Finally, for *L. nannotis*, I wanted to test the hypothesis that upland populations had recovered by adapting to the disease.

Materials and Methods

Study Sites, Habitat, and Tissue Collection

Frogs were sampled at Paluma Range National Park, Girramay National Park, and Kirrama Range National Park in North Queensland from October 2015 to January 2016 (Figure 3.1; Table 3.1). Girramay and Kirrama are adjacent and have contiguous forests and streams; therefore, they will be treated as a single park (referred to as Girramay-Kirrama).

These sites were chosen because my research group has been monitoring these populations for several decades and their history with *Bd* is documented (declines and disappearances were observed in 1989, with initial evidence of recovery observed in 1999–2001; Alford et al. pers. obs.; Richards et al. 1993; McDonald and Alford 1999; Richards and Alford 2005; Woodhams and Alford 2005; McKnight et al. 2017a). *Litoria nannotis* disappeared from the uplands followed by recolonization, while *L. serrata* declined at upland sites followed by population recoveries (Trenerry et al. 1994; Woodhams and Alford 2005). Despite recoveries, both species continue to be infected with *Bd* at both upland and lowland sites. I have included infection data for these populations from a recent survey in Additional file 3.1; however, I do not have infection data for the individuals used in this study because the tissue samples were collected at a time of year when infection prevalence and intensity are low (Woodhams and Alford 2005). Therefore, infection

prevalence and intensity from this sampling period would have been uninformative. Nevertheless, because *Bd* infection occurs at all elevations and the histories of declines and recoveries are well documented (Trenerry et al. 1994; McDonald and Alford 1999; Woodhams and Alford 2005; McKnight et al. 2017a), a lack of specific infection data for the individuals in this study did not hinder my ability to address the study aims.

Paluma is the southern extent of the species' range for both *L. nannotis* and *L. serrata*, and Girramay-Kirrama is roughly 100 km north of this location. Previous studies have demonstrated that both species exhibit an ancient North/South split that divides them into two clades; however, both Paluma and Kirrama are in the southern clade (Schneider et al. 1998; Cunningham 2001). Nevertheless, the sites were separated during the Pleistocene, as rainforests contracted (Schneider et al., 1998). Both species may have disappeared from Paluma at this time, but the rainforests expanded, re-establishing connectivity ~8,000 years ago, at which point *L. nannotis* and *L. serrata* dispersed from Girramay-Kirrama to Paluma (Schneider et al. 1998). Subsequently, the rainforests contracted again, once more isolating the parks. Currently, Girramay-Kirrama is wetter than Paluma and has a larger section of lowland rainforest (Stanton and Stanton 2005). Additionally, within Paluma, the western half of the park is wetter and contains more rainforest than the eastern half (Stanton and Stanton 2005). Maps showing the vegetation and rainfall patterns of both sites are available in the Additional file 3.1.

At each site, an area containing several streams was selected, and tissue samples were collected from both the upland (defined as > 300 m elevation) and lowland (defined as < 300 m elevation) sections of each major stream within each study area (Figure 3.1). Upland samples were collected from the highest elevation at which both species were present. In contrast, low elevation samples were collected just below 300 m elevation. This elevation was chosen because, during the initial *Bd* outbreak, stable populations occurred only below 300–400 m (Richards et al. 1993; Laurance et al. 1996; McDonald and Alford 1999).

Frogs were captured at night while I walked transects (~100–500 m) along the streams. Each frog was captured in a clean plastic bag and handled using a new pair of nitrile gloves. Tissue samples were collected by using surgical scissors to take toe tips from two toes (one on each rear foot). This procedure is minimally invasive and does not result in bleeding. Scissors were dipped in ethanol and flame sterilized between each frog. Frogs

were released at their capture locations shortly after capture. Samples were immediately placed in 70% ethanol and were stored at 4°C within 12 hours of collection. They were kept at 4°C for up to two months prior to DNA extraction. At each collection site, tissue samples were obtained from 16–31 individuals (median = 27; Table 3.1).

Where possible, both species were collected from the same location; however, at two sites, only *L. nannotis* was present in the lowlands, and at two sites, only *L. serrata* was present in the uplands (both cases for *L. nannotis* were streams that did not flow into a lowland rainforest refugium). At Paluma, *L. nannotis* samples were collected from four upland sites and three lowland sites, and *L. serrata* were collected from six upland sites and two lowland sites (Figure 3.1; Table 3.1). At Girramay-Kirrama, *L. nannotis* samples were collected from three upland sites and two lowland sites, and *L. serrata* were collected from three upland sites and one lowland site (Figure 3.1; Table 3.1). Throughout this paper, each site will be referred to by the acronyms in Table 3.1, where the uppercase letters are the stream name, followed by a lowercase "l" for "lowland" or "u" for "upland."

To quantify the lowland habitat, vegetation survey layers were obtained from the Wet Tropics Management Authority, and ArcGIS 10.4 was used to clip the habitat layers for each stream to the lowland area (< 300 m) currently occupied by *L. nannotis*. Occupancy area was defined as the length of lowland stream where *L. nannotis* have been documented in my surveys (McKnight et al. 2017a; McKnight pers. obs.) with a 35-m buffer on either side of the stream. Thirty-five meters was chosen as the buffer distance because it is the maximum distance away from a stream that *L. nannotis* moved in a telemetry study (Rowley and Alford 2007b). For each stream, I calculated the total area, the total amount of rainforest, and percent of habitat area that consisted of rainforest (Figure 3.2).

DNA extraction, sequencing, and SNP assembly

Genomic DNA was extracted using the cetyl trimethyl ammonium bromide (CTAB) protocol (Doyle and Doyle 1987). Sequencing and single nucleotide polymorphism (SNP) detection were carried out by Diversity Arrays Technology (DArT PL) using their proprietary genotyping by sequence protocol. Briefly, this method employed a double restriction digest using methylation-sensitive restriction enzymes (RE) in a joint digestion-ligation reaction at 37 °C for 2 hr with 150-200ng gDNA. The PstI and SphI enzymes were used. Custom proprietary barcoded adapters (6-9 bp) were then ligated to RE cut-site overhangs with

adapters designed to modify RE cut sites following ligation to prevent insert fragment re-digestion. Fragments were selectively PCR amplified using custom designed primers for each sample, and the samples were sequenced on an Illumina HiSeq 2500. The DArT pipeline is described in detail in Sansaloni et al. (2011), Kilian et al. (2012), and Lal et al. (2017).

Filtering and quality control

Sequencing by DArT produced 34,531 SNPs for *L. nannotis* and 37,031 SNPs for *L. serrata*. The SNPs for each species were filtered separately, but the same criteria were used. Initially, the data from both parks were kept together as a single set, but large differences in polymorphisms between Paluma and Girramay-Kirrama biased intra-population SNP selection. Therefore, the two parks were separated and filtered independently for each species. All filtering steps were applied to entire parks (Paluma or Girramay-Kirrama) unless otherwise noted.

To filter each data set, first duplicate SNPs and SNP clusters (assigned with a 95% probability) were removed (Lal et al. 2017). Next, the following criteria were applied: average number of reads ≥ 7, minor allele frequency (MAF) ≥ 0.02, call rate ≥ 0.7, and reproducibility ≥ 0.9. BayeScan v.2.1, (Foll and Gaggiotti 2008; Foll 2012) and LOSITAN (Antao et al. 2008) were then used to identify possible outlier loci. The data were entered with each collection site as a population, and a false discovery rate (FDR) of 0.1 was applied. To produce a conservative set of neutral loci, any SNPs that were identified as outliers by either BayeScan or a consensus of three runs of LOSITAN were removed.

PLINK (v1.9; Purcell et al., 2007) was used to identify SNPs that were in strong linkage disequilibrium (LD), and any loci with an $R^2 \geq 0.6$ were removed. This was done iteratively by first identifying the SNP with the greatest number of significant links and removing it, then repeating the process until no significant links remained (e.g., if SNP1 and SNP2 were linked to SNP3 but not to each other, only SNP3 would be removed). This retained the maximum number of SNPs while still removing all tightly linked markers.

To identify loci that were out of Hardy-Weinberg Equilibrium (HWE; potentially as a result of null alleles), an exact test in Arlequin (v3.5.2.2; Excoffier et al. 2005) with 100,000 Markov chain steps was used. The markers at each population were tested for HWE, and any markers that differed from HWE with $P < 0.01$ at all populations were removed. Population identity for this test was defined based on the clusters produced by NetView R

via the R package “netview” (v1.0; Steinig et al. 2015) and discriminant analysis of principal components (DAPC) via the R package “adegenet” (v2.0.1; Jombart, 2008; Figure 3.1). This was done because identifying accurate population composition improves power for detecting null alleles. Therefore, populations were pooled based on NetView and DAPC groupings to provide a more liberal method of identifying markers that were out of HWE.

To produce a data set including both parks, the filtered datasets for each park were combined (i.e., any SNPs that passed filtering at either park were included). There were, however, some markers that had high call rates in one park, but low call rates at the other, suggesting the presence of null alleles. These were assessed by using chi-square tests to compare the call rates at the two parks for each SNP. An FDR of 0.01 was applied to the results of the chi-square tests via the "p.adjust" function in R, and any SNPs with significantly different call rates were removed.

After all filtering and quality control steps, the following six neutral data sets were retained and used for analyses: all *L. nannotis* (Paluma and Girramay-Kirrama; 9,091 SNPs), Paluma *L. nannotis* (4,161 SNPs), Girramay-Kirrama *L. nannotis* (8,458 SNPs), all *L. serrata* (Paluma and Girramay-Kirrama; 8,810 SNPs), Paluma *L. serrata* (5,977 SNPs), and Girramay-Kirrama *L. serrata* (8,268 SNPs; Additional file 3.2).

Between and within park genetic diversity

To compare the connectivity and diversity measures between parks, the data sets combining SNPs across both parks were used, and all individuals within a park were clustered as a single group. Arlequin was used to generate pairwise *Fst* values between the parks, and Genetix (v4.05.2; Belkhir 2004) was used to calculate the expected and observed heterozygosities (adjusted for population size) within each park. Additionally, the MAF and level of polymorphism were compared between the parks. Finally, an analysis of molecular variance (AMOVA) in Arlequin was used to determine the amount of variance that was attributable to differences between parks, and differences within parks (each park was entered as a group, with collection sites as populations within the groups).

To assess diversity within each park, the data sets that were filtered separately for each park were used. Each collection site was treated as a separate sample population for all analyses unless otherwise noted. Heterozygosity, MAF, and the number of polymorphic SNPs were calculated and compared for each park as described above. Additionally, *Fis*

values and 95% confidence intervals were calculated using the R package diveRsity (v1.9.90; Keenan et al. 2013).

To estimate effective population sizes, the LD method in NeEstimator v2.01 (Do et al. 2014) was used. Within each population, only SNPs with an MAF ≥ 0.05 were selected. Because NeEstimator assumes that all markers are unlinked, it was run both on the full data sets, and on data sets where a more stringent LD filtering was applied to evaluate any possible biases (SNPs that were linked with an $R^2 \geq 0.15$ were removed using the procedure described previously). The results of both sets of analyses were similar (< 9 % difference; median % difference = 1.5); therefore, only the results where LD < 0.6 are presented (LD < 0.15 are available in Additional file 3.1).

Fine-scale structure and connectivity within each park

Population structure was visualized using NetView (Steinig et al. 2015) and DAPC (Jombart 2008), and pairwise *Fst* values were calculated in Arlequin (Excoffier et al. 2005). Family groups were assessed using COLONY (Jones and Wang 2010). Because no relationships were known *a priori*, every individual was entered as a potential offspring, all males were entered as potential fathers, and all females were entered as potential mothers. Additionally, all collection sites at a park were entered simultaneously so that potential relationships among sites could be calculated. Because of the long run times involved with COLONY, the data were subset to 500 high quality markers. This was accomplished by removing any SNPs with missing data or a MAF < 0.05, then randomly selecting 500 SNPs from the remaining markers. Some of the family groups produced by COLONY contained individuals with a low probability of assignment; therefore, new family groups were generated by taking the pairwise relationship results (for any first or second order relationship), filtering them to only include relationships with a probability ≥ 0.9, then making new family groups by matching individuals from pairwise relationships (e.g., if individual A and B were siblings, and individuals B and C were half-siblings, then individuals A, B, and C formed one family group). Average population relatedness was assessed *via* the Queller and Goodnight method (Queller and Goodnight 1989) implemented in the R package related (v1.0; Pew et al. 2015); both sexes were analysed together). Additionally, to test for isolation by distance among individuals within parks, the autocorrelation test in GenAlEx (v6.503) was used with 999 permutations for calculating 95% confidence intervals

(Peakall and Smouse 2012). Autocorrelation was assessed at 0.5 km intervals using pairwise relatedness distances.

Signatures of selection

Several methods were used to examine the possibility that adaptation to *Bd* was responsible for the recoveries of upland populations. These analyses focussed on *L. nannotis* which are a better model than *L. serrata*, because *L. nannotis* fully disappeared from the uplands while lowland populations remained largely unaffected. This means they can be clearly demarcated as either "disappeared and recovered" or "non-decline". Conversely, *L. serrata* populations only briefly declined at upland sites, and they are uncommon in the lowlands. For these analyses, the data sets that were filtered separately for each park were used, but they were only filtered by average number of reads, MAF, call rate, and reproducibility. They were not filtered by neutral markers, LD, or HWE. Thus, low quality SNPs were removed, but SNPs that could be under selection were retained.

At each park, the data sets were separated into pairwise comparisons between the upland and lowland collection sites along each stream (e.g., one set included only ECu and ECl). This was done to provide replicate biological comparisons between recovered upland populations and their nearest non-decline lowland counterparts. YCu did not have a direct water connection to a lowland site, therefore it was paired with the closest lowland site (MRl). Additionally, at each site, a data set was constructed with all lowland sites combined and all upland sites combined. All data sets were examined using BayeScan (FDR = 0.1), LOSITAN (FDR = 0.1), and HacDivSel (Antao et al. 2008; Foll and Gaggiotti 2008; Foll 2012; Carvajal-Rodriguez 2017). If local adaption was occurring and supported the recovery of upland populations, then the expectation was that there should be agreement among the methods, as well as among the pairwise comparisons within a site (i.e., the same SNPs should be identified as outliers by multiple methods and at multiple sites). Any SNP that was identified as an outlier by at least two methods in each of at least two pairwise comparisons was assessed further by attempting to align it to the following genomes using NCBI BLAST (blastn): African clawed frog (*Xenopus laevis*; taxid: 8355), western clawed frog (*Xenopus tropicalis*; taxid: 8364), and Tibetan frog (*Nanorana parkeri*; taxid: 125878)(Altschul et al. 1997). BLAST was also used to examine any SNPs that were identified as outliers in at least

two methods for the upland vs. lowland comparison. Results were limited to matches with an e-value < 1 and a query coverage > 75%.

Results

Between and within park genetic diversity

Large differences were observed between Paluma and Girramay-Kirrama for both species (using the combined *L. nannotis* and combined *L. serrata* data sets). For *L. nannotis* the between park *Fst* was 0.58 and for *L. serrata* the *Fst* was 0.39 (P values for both *Fst* calculations were < 0.00001, indicating that the *Fst* values were reliable). Additionally, Girramay-Kirrama had higher heterozygosity and a higher mean MAF for both species, but the differences were greatest for *L. nannotis* (Table 3.2). Similarly, there were multiple SNPs that were polymorphic at one park, but monomorphic at the other (indicating a loss of diversity), but for both species, Paluma contained fewer polymorphic loci than Girramay-Kirrama, and for both parks *L. nannotis* contained fewer polymorphic loci than *L. serrata* (Table 3.2). The AMOVA revealed similar patterns. For *L. nannotis*, 58.3% of the variation was explained by differences between the parks, and 39.1% was explained by variation within individuals (Additional file 3.1). For *L. serrata*, 39.3% of the variation was explained by differences between the parks, and 56.7% was explained by variation within individuals (Additional file 3.1).

Similar patterns were observed within each park using the data sets that were filtered separately for each park. At Paluma, both species had low levels of polymorphic markers. This was particularly pronounced for *L. nannotis*, which exhibited both a west- east pattern of diversity and a lowland-upland pattern (i.e., some markers that were polymorphic when looking at the entire park were monomorphic at particular collection sites, and the number of polymorphic markers per site decreased from the west to the east side of the park and were lowest at the upland sites; Figures 3.2 and 3.3). Other diversity metrics, such as MAF, heterozygosity, and N_e, were also low and followed similar patterns (Table 3.3; Figure 3.2). *Litoria serrata* at Paluma had higher diversity indices (e.g., heterozygosity, N_e, MAF) than *L. nannotis*, and only a west-east pattern was apparent, with higher levels of diversity and the largest effective population size occurring in the west half of the park (Figure 3.3, Table 3.3).

At Girramay-Kirrama, both species had higher diversity scores than at Paluma. For *Litoria nannotis*, the lowland sites had higher N_e values than the upland sites, but no other patterns were apparent (Table 3.3). Based on *Fis* values, inbreeding was not evident in either park or species. Similarly, the observed heterozygosity closely matched the expected heterozygosity for all collection sites (Table 3.3)

The lowland habitat data showed similar patterns (Figure 3.2; Additional file 3.1) and correlated with diversity metrics. Girramay-Kirrama had larger sections of rainforest than were found at Paluma, and within Paluma, the availability of lowland rainforest decreased from west to east. Thus, areas with large amounts of high-quality lowland habitat where, presumably, many *L. nannotis* could have survived the outbreak, had high levels of diversity, whereas areas with low-quality lowland habitat had low diversity.

Fine-scale structure and connectivity within each park

For the Paluma *L. nannotis* dataset, NetView and DAPC identified four clusters (Figure 3.1). Three clusters corresponded to upland/lowland pairs of sites that were connected along a stream, and the remaining cluster contained a single upland stream (CCu), despite the fact that there was a direct water connection from CCu to a lowland stream (ECl). These visualizations revealed a high level of connectivity along each stream, with a lower level of connectivity between streams. These observations were corroborated by the pairwise *Fst* values (Additional file 3.1), which were lowest between uplands and lowlands along a stream (0.019–0.076), but still low for most comparisons across streams (0.035–0.137; only comparisons involving one site [CCu] had *Fst* values > 0.1).

NetView and DAPC revealed two clusters for the Paluma *L. serrata* dataset (Figure 3.1). One cluster included the four westernmost sites, and the other included the four easternmost sites. *Fst* values were low for all comparisons (0.012–0.049), but the highest values occurred for comparisons between the two clusters (Additional file 3.1).

At Girramay-Kirrama, neither species had obvious structuring, and all populations appeared to be highly connected (Figure 3.1). Similarly, the *Fst* values were low for all pairwise comparisons (*L. nannotis* = 0.005–0.0236; *L. serrata* = 0.003–0.007; Additional file 3.1). All *Fst* values were significant ($P < 0.05$ after accounting for multiple comparisons) indicating that they are reliable (see Additional file 3.1).

The autocorrelation analysis revealed similar patterns to the other clustering analyses (Additional file 3.1). For *L. nannotis* at Paluma, significant correlations were detected up to 1 km and again at 2 km, but not at greater distances. This indicates genetically similar individuals within collection sites (0.5 km) and along streams (1 km and 2 km), but no pattern of isolation by distance among streams, which is consistent with the NetView and DAPC clusters. *Litoria serrata* at Paluma had significant autocorrelation up to a distance of 3.5 km but did not show a pattern of isolation by distance beyond that. This is consistent with the distance between sites within the clusters identified by NetView and DAPC. Finally, for both species at Girramay-Kirrama, autocorrelation was only detected at 0.5 km, suggesting increased similarity within a collection site, but no isolation by distance among sites. This is consistent with the high levels of connectivity in NetView and DAPC.

COLONY identified first and second order relationships for both species at both parks, but the majority were half-sibling relationships, with only a few full-sibling relationships, and a total of four parent/offspring relationships (Table 3.4). At both sites, *L. nannotis* had more relationships and a higher percentage of individuals were related to at least one individual (Table 3.4; Figure 3.4). Also, for both species, there were more relationships at Paluma than at Girramay-Kirrama. At Paluma, 88.6% of *L. nannotis* were related to at least one other individual, but all the relationships occurred within sites or between the paired upland and lowland sites within a stream (Figure 3.4). In contrast, for *L. serrata* at Paluma, only 58.5% of individuals were related to at least one other individual, and there were 16 relationships involving two separate streams, including a relationship spanning the two most widely-separated sites. The average population relatedness results were similar and illustrated the same patterns as COLONY, NetView, and DAPC (Additional file 3.1).

Selection

At Paluma, there was little agreement among the methods for identifying outlier loci (Additional file 3.1). BayeScan did not detect any outliers for any of the pairwise comparisons, and although LOSITAN and HacDivSel both identified multiple outliers for each comparison (132–348 and 11–115 respectively), only 4–48 of them were identified by both methods for a given pairwise comparison, and only one SNP was identified by both methods in two comparisons. Additionally, only four of the HacDivSel outliers were “extremely

positive" (all from the CCu vs. ECl comparison). Similarly, all three methods identified outliers (83 total) for the upland vs. lowland comparison at Paluma, but only one SNP was identified by more than one method (it was not identified by LOSITAN).

At Girramay-Kirrama, there was greater agreement among the three methods. For the pairwise comparisons, a total of 32 SNPs were identified as outliers by all three methods, but only one of those SNPs was identified by all three methods in more than one pairwise comparison. Similarly, for the upland vs. lowland comparison, 15 SNPs were identified by more than one method, but none were identified by all three methods.

The BLAST searches did not associate any of the outlier loci to known *Bd* resistance genes. Out of the 40 SNPs from the pairwise comparisons for which BLAST alignment was attempted, only 21 found a match with an e-value < 1, and only one of those had a query coverage > 75% (SNP sequences were 69 base pairs long). It matched a tubulin alpha-1A chain-like gene in *X. laevis* (GeneBank accession #BC041195.1). Similarly, of the 16 SNPs that were identified by more than one method for the upland vs lowland comparisons, 13 had an e-value < 1 (only two < 0.1) and only one of them had a query coverage > 75%. It was the same tubulin alpha-1A sequence identified previously. Additionally, none of the SNPs that were used in either BLAST search met my inclusion criteria at both parks.

Discussion

Effects of disease and habitat

The patterns of diversity in *L. serrata* and *L. nannotis* suggest that the recent chytridiomycosis outbreak interacted with habitat features to shape the species' current population genetics. For both species, the diversity patterns within and between sites matched the habitat patterns of the sites, suggesting that habitat quality may have had an important influence on the ability of populations to retain genetic diversity during the disease outbreak. Populations in areas with more extensive rainforest (i.e., Girramay-Kirrama and the western half of Paluma), tended to have higher effective population sizes, higher MAFs, and more polymorphic markers than populations in drier areas.

The effects of the chytridiomycosis outbreak are seen most clearly in the comparisons of upland and lowland sites for *L. nannotis*, particularly at Paluma, where the upland populations consistently had lower MAFs, fewer polymorphic markers, and lower

effective population sizes than the lowland populations. At Girramay-Kirrama, the MAFs and numbers of polymorphic markers were similar between upland and lowland populations, but the effective population sizes were substantially lower in the uplands. These results are consistent with the fact that *L. nannotis* disappeared from the uplands, followed by recolonization from the surviving lowland populations. These patterns also highlight the importance of environmental refugia for populations that are afflicted by disease (Puschendorf et al. 2011), as well as the role of gene flow in enabling population recovery.

In contrast to *L. nannotis*, *L. serrata* did not show an upland-lowland pattern of decreasing genetic diversity. This lack of pattern is consistent with the history of *L. serrata*, which only declined in the uplands, rather than fully disappearing (McDonald and Alford 1999) and with the distribution of *L. serrata*, which only has small lowland populations that do not extend as far downstream as the populations of *L. nannotis* (McKnight pers. obs.; McKnight et al. 2017a).

For both *L. nannotis* and *L. serrata*, there were large differences between Paluma and Girramay-Kirrama (based on the data sets that included both sites), with higher diversity levels at Girramay-Kirrama. This differs from the results of previous studies that reported few differences between these regions (Schneider et al. 1998; Cunningham 2001). This disparity is likely at least partially because previous studies used only a few mitochondrial genes rather than several thousand genome-wide SNPs. The differences I observed in diversity levels between parks may be partially a historic founder effect resulting from the dispersal of frogs from Girramay-Kirrama ~8,000 years ago (Schneider et al. 1998), but an examination of the fine-scale patterns within each park suggests that the chytridiomycosis outbreak also played a role in the loss of diversity at Paluma.

Girramay-Kirrama is wetter than Paluma and, importantly, has a more extensive stretch of lowland rainforest, resulting in a larger area where *L. nannotis* could have survived the *Bd* outbreak (Figure 3.2; Additional file 3.1; McKnight et al. 2017a). As a result, Girramay-Kirrama should have retained larger resulting in a larger area where *L. nannotis* could have survived the *Bd* outbreak (Figure 3.2; Additional file 3.1; McKnight et al. 2017a). As a result, Girramay-Kirrama should have retained larger surviving lowland populations of *L. nannotis*, and, by virtue of having larger numbers of surviving individuals, Girramay-Kirrama is likely to have retained higher levels of genetic diversity (Nei et al. 1975; Allendorf 1986). This is consistent with relatively large lowland N_e estimates for *L. nannotis* at

Girramay-Kirrama (1756.5 and 1537.4), compared to Paluma (173.3, 89.8, and 40.5), and the denser rainforest at Girramay-Kirrama is consistent with the higher diversity levels for both species at Girramay-Kirrama compared to Paluma.

Differences in habitat quality may also explain the patterns that were observed within Paluma. Both species, but especially *L. nannotis*, exhibited a west-east pattern, with higher diversity levels and larger effective population sizes in the more heavily rainforested western half of the park. This pattern appears to be recent, rather than the result of a historical founder event, because while the *Fst* values among sites were low (suggesting substantial gene flow), there were large differences in the percentages of polymorphic markers (Figure 3.4). For example, for *L. nannotis*, the pairwise *Fst* between the two most distant lowland populations (ECl and LCCl) was 0.044, suggesting an exchange of ≈5.4 individuals per generation (based on Wright's formula for *Nm*; Wright 1931; Slatkin and Barton 1989). Nevertheless, 93.7% of all markers were polymorphic at ECl compared to 60.8% at LCCl (i.e., ECl has many private alleles that are not present at LCCl). Gene flow would be expected to quickly homogenize those populations (Wright 1931; Slatkin 1985), making it highly unlikely that such a large difference in polymorphisms could have persisted for ~8,000 years following the founding of the Paluma populations.

A similar pattern was apparent for the family groups. At the eastern-most stream (LCC), 98.0% of *L. nannotis* were related to at least one other individual (as a first or second order relationship), and at the stream in the middle (UC1), 88.9% of individuals were related to at least one other individual. In contrast, in the western-most stream (EC), only 70.4% of individuals were related to at least one other individual. Similarly, in the east, the relationships clustered into a few (generally large) family groups (two in LCC and four in UC1), suggesting that few family groups had survived the initial outbreak. In the western-most stream (EC), however, the relationships were broken into seven smaller groups.

It should be noted that my conclusion that high quality habitat refugia are important for retaining diversity during outbreaks initially appears to differ from previous work that suggested that disturbed habitats were actually beneficial, in the context of *Bd* infections, because they had lower *Bd* prevalence and intensity than did pristine sites (Becker and Zamudio 2011). However, there are two important distinctions that need to be clarified. First, as Becker and Zamudio (2011) acknowledged, habit disturbances will only be beneficial for the subset of species that can tolerate such disturbances (i.e., habitat generalists);

whereas my research looked at rainforest specialist. Second, my conclusion is predicated on having high quality habitat in areas that provide refuge from the disease (e.g., through climates that are sub-optimal for the pathogen, such as those found at my lowland sites; Piotrowski et al. 2004; Sapsford et al. 2013; Rowley and Alford 2013). In other words, I agree with Becker and Zamudio (2011) that disturbances may be beneficial (particularly for generalists) at sites within the optimal climatic conditions for *Bd*, but in areas where climatic conditions are already unfavourable for *Bd*, high quality habitat is likely beneficial, particularly for specialists, and maintaining those refugia may be critical for retaining genetic diversity during outbreaks.

Substructure and gene flow

At both sites, *L. serrata* appeared to have greater dispersal abilities. This was suggested by visualizations such as NetView and DAPC, lower *Fst* values, and the presence of first and second order relationships among individuals at distant streams. Greater dispersal in *L. serrata* is consistent with telemetry data showing that they are not as restricted to streams as are *L. nannotis* (Rowley and Alford 2007b).

Both species exhibited more structuring at Paluma than at Girramay-Kirrama. At Paluma, *L. nannotis* clustered into four groups (usually consisting of the upland and lowland collection sites on a given stream), while *L. serrata* clustered into two large groups (a western group and eastern group). In contrast, at Girramay-Kirrama, no sub-structuring was evident for either species. This may be because the wetter environment allowed the frogs to disperse more easily.

The notion of higher dispersal abilities at Girramay-Kirrama is also supported by examining the upland portions of streams that do not have a lowland *L. nannotis* population (YCu at Girramay-Kirrama and BCu and UC2u at Paluma). These streams are interesting, because *L. nannotis* would have to migrate overland (rather than upstream) to recolonize them. Currently, a *L. nannotis* population is present at YCu, but not BCu or UC2, again potentially suggesting that *L. nannotis* can disperse more easily at Girramay-Kirrama than at Paluma.

These differences in dispersal rates and subsequent structuring between sites have important implications for disease management. One of the concerns with infectious diseases is that they will fragment populations, even when suitable habitat remains (Serieys

et al. 2015; McKnight et al. 2017b). Further, fragmentation may be particularly harmful for disease-afflicted populations, because gene flow can enhance organisms' ability to adapt to diseases by supplying them with additional genetic variation (Gandon et al. 1996; Gandon and Michalakis 2002; Morgan et al. 2005) . Conversely, high levels of gene flow from populations that are not under the same selective pressures can swamp selection, by flooding populations with alleles that are not locally adaptive (García-Ramos and Kirkpatrick 1997; Kawecki and Ebert 2004; Funk et al. 2012). Therefore, gene flow is an important consideration for managing disease-afflicted populations, and my results highlight both the necessity of gene flow for restocking the gene pools of declined populations, and the interactions that can occur between gene flow and habitat.

Selection

A heritable component of *Bd* infection risk has been detected in other species (Palomar et al. 2016), suggesting that at least some species have the adaptive potential to evolve in response to *Bd* (Voyles et al. 2018). However, I did not find any consistent evidence suggesting that *L. nannotis* had adapted to *Bd*. There was little agreement between methods, sites, and parks. There are several possible explanations for this lack of evidence. First, adaptation to the disease may not have been responsible for the recoveries of upland *L. nannotis* populations, and other factors, such as changes in microbiomes, climate, behaviour, or disease virulence may be at play (Refsnider et al. 2015; Scheele et al. 2015, 2017; McKnight et al. 2017a). Second, the lack of evidence for adaptation may simply be an artefact of methodological limitations, rather than an indication that frogs have not adapted.

Conclusions and implications for disease management

I found important differences between species and locations in the effects of a chytridiomycosis outbreak on the population genetics of *L. nannotis* and *L. serrata*. In all cases, the observed differences in diversity were consistent with differences in habitat quality, which is expected to correspond to differences in the number of individuals that survived the outbreak. Therefore, I suggest that lowland sites with large amounts of high-quality habitat provided important refugia during the outbreak that allowed populations to

retain high levels of genetic diversity compared to populations that were restricted to lower quality habitat. This explanation is admittedly *ad hoc* and correlative, and it would be useful for future work to examine many populations with varying levels of lowland rainforest to explicitly test my hypothesis. Nevertheless, several lines of reasoning support my explanation.

First, the low diversity levels for upland *L. nannotis* cannot be historical, because we know that those populations disappeared and were recolonized by the surviving lowland populations (Ingram and McDonald 1993; Richards et al. 1993; Laurance et al. 1996; McDonald and Alford 1999). Therefore, the most reasonable explanation is that the low diversity in the uplands is a result of recent founder events following the disappearance of the original populations. Similarly, I argue that the low *Fst* values and high gene flow levels make it unlikely that west-east pattern of diversity at Paluma is historical. The large differences in polymorphisms and frequent presence of numerous private alleles should not be sustainable under high levels of gene flow. Even a single migrant per generation would be expected to have a homogenising effect. Therefore, the current pattern suggests a recent decline rather than a historical pattern. The difference between Girramay-Kirrama and Paluma is harder to definitively explain because it is likely that there were historical differences in diversity pre-outbreak. Nevertheless, the observed differences are consistent with the patterns within Paluma. Therefore, I think it is probable that the *Bd* outbreak reduced the diversity at Paluma and played a role in shaping the current differences between the parks. Finally, the differences in dispersal ability correspond well with my explanation, because species and sites with higher dispersal abilities would be able to more quickly homogenise their populations and dilute the patterns of a recent disease outbreak, which is consistent with the patterns I observed.

My study also highlighted the importance of gene flow. First, because *L. nannotis* disappeared from the uplands, immigration was clearly necessary to re-establish those populations. However, the diversity levels for this species were still lower in the uplands than in the lowlands, and additional gene flow will be necessary to fully restock those gene pools. Additionally, although some migration was evident for *L. nannotis* at Paluma, they exhibited greater structuring than *L. serrata*, which has higher dispersal abilities. Therefore, species conservation and management plans should account for differences in dispersal ability to ensure that adequate gene flow is being maintained.

My results also apply more broadly to other species and populations that are affected by emerging infectious diseases. They suggest that maintaining refugia with high quality habitat may be critical for allowing populations to retain a high level of genetic diversity and hence adaptive potential during a disease outbreak. Additionally, gene flow is likely important for restocking the gene pools of declined populations and facilitating their recovery.

Tables

Table 3.1 — Sampling locations and sample sizes. Samples were collected along ~100–500 m transects. The elevations and coordinates are for the midpoints of those transects. P = Paluma, G-K = Girramay-Kirrama.

Site name	ID	Park	Elevation	Latitude	Longitude	# of *L. serrata* samples	# of *L. nannotis* samples
Birthday Creek (upland)	BCu	P	800	-18.98071	146.16800	27	0
Cloudy Creek (upland)	CCu	P	830	-19.00008	146.20097	26	27
Ethel Creek (lowland)	ECl	P	240	-18.98630	146.20810	16	27
Ethel Creek (upland)	ECu	P	700	-18.99219	146.19232	26	27
Little Crystal Creek (lowland)	LCCl	P	274	-19.01286	146.26971	26	27
Little Crystal Creek (upland)	LCCu	P	530	-19.01851	146.25250	26	22
Unnamed Creek 1 (lowland)	UC1l	P	265	-18.99750	146.22870	0	27
Unnamed Creek 1 (upland)	UC1u	P	525	-19.00400	146.23500	27	27
Unnamed Creek 2 (upland)	UC2u	P	644	-19.01990	146.21788	26	0
Douglas Creek (lowland)	DCl	G-K	260	-18.17171	145.82864	30	31
Douglas Creek (upland)	DCu	G-K	700	-18.21040	145.80688	30	31
Murray River (lowland)	MRl	G-K	265	-18.17960	145.81130	0	28
Murray River (upland)	MRu	G-K	715	-18.20927	145.79079	30	31
Yuccabine Creek (upland)	YCu	G-K	675	-18.18297	145.77817	27	27

Table 3.2 — Diversity measures for data sets including both parks (i.e., within each species, the same SNPs were used for each park). H n.b. = expected heterozygosity (corrected), H obs. = observed heterozygosity corrected for population size, Mean MAF = the minor allele frequency averaged across all markers in a population, % polymorphic = percent of markers that were polymorphic in a given population, % with MAF < 0.05 = the percent of markers in a given population that had a minor allele frequency less than 0.05. P = Paluma, G-K = Girramay-Kirrama.

	L. nannotis		*L. serrata*	
	P	G-K	P	G-K
H n.b.	0.061	0.308	0.131	0.335
H obs.	0.057	0.287	0.125	0.302
Mean MAF	0.038	0.227	0.090	0.247
% polymorphic	55.5	95.1	73.9	99.7
% with MAF < 0.05	79.7	14.8	60.0	6.2

Table 3.3 — Diversity metrics for data sets where each site was filtered separately for each species. H n.b. = expected heterozygosity (corrected for population size), H obs. = observed heterozygosity, Ne = effective population size, Mean MAF = the minor allele frequency averaged across all markers in a population, % poly = percent of markers (out of all markers at a park) that are polymorphic at a particular collection site.

	H n.b.	H obs.	*Fis* (95% CI)	Ne (95% CI)	Mean MAF	% poly
Litoria nannotis: Paluma						
ECu	0.206	0.201	0.002 (-0.026–0.03)	36.2 (35.9–36.6)	0.135	89.9
ECl	0.199	0.192	0.016 (-0.004–0.035)	173.3 (167.9–179.1)	0.126	93.7
CCu	0.173	0.174	-0.024 (-0.059–0.01)	18.4 (18.2–18.5)	0.119	69.4
UC1l	0.166	0.157	0.031 (0.000–0.06)	89.8 (87.8–91.8)	0.107	78.2
UC1u	0.162	0.154	0.032 (0.000–0.057)	35.2 (34.8–35.6)	0.107	70.6
LCCl	0.134	0.132	-0.006 (-0.036–0.022)	40.5 (39.9–41.2)	0.089	60.8
LCCu	0.128	0.118	0.061 (0.024–0.091)	39.6 (38.8–40.5)	0.084	56.5
Litoria nannotis: Girramay-Kirrama						
DCl	0.324	0.305	0.042 (0.03–0.052)	1756.5 (1595.4–1953.4)	0.235	97.7
DCu	0.319	0.304	0.031 (0.015–0.045)	66.5 (66.2–66.8)	0.232	97.0
MRl	0.324	0.306	0.038 (0.020–0.049)	1537.4 (1392.1–1716.5)	0.234	97.8
MRu	0.322	0.307	0.030 (0.017–0.040)	683.8 (657.6–712.1)	0.234	97.9
YCu	0.318	0.304	0.026 (-0.001–0.048)	59.3 (59.0–59.6)	0.230	96.0
Litoria serrata: Paluma						
BCu	0.262	0.249	0.032 (0.017–0.042)	676.1 (629.1–730.5)	0.180	96.3
ECu	0.250	0.237	0.033 (0.014–0.047)	160.3 (157.1–163.6)	0.171	94.1
ECl	0.247	0.236	0.014 (-0.053–0.071)	10.3 (10.2–10.3)	0.169	84.8
CCu	0.237	0.226	0.029 (0.008–0.043)	141.6 (139.0–144.3)	0.161	92.8
UC1u	0.212	0.203	0.024 (0.003–0.041)	136.5 (133.9–139.3)	0.145	84.8
UC2u	0.215	0.206	0.026 (0.01–0.038)	219 (212.3–226.1)	0.146	89.7
LCCl	0.205	0.195	0.031 (0.006–0.054)	136.5 (133.6–139.6)	0.139	84.1
LCCu	0.208	0.197	0.035 (0.015–0.053)	237.5 (229.2–246.3)	0.141	85.9
Litoria serrata: Girramay-Kirrama						
DCl	0.324	0.300	0.056 (0.043–0.067)	206.8 (204.0–209.7)	0.234	98.4
DCu	0.323	0.300	0.057 (0.043–0.068)	362.3 (353.9–371.1)	0.233	98.5
MRu	0.325	0.298	0.065 (0.051–0.075)	248.1 (244.1–252.2)	0.234	98.6
YCu	0.325	0.297	0.067 (0.053–0.077)	345.6 (336.8–354.7)	0.233	98.3

Table 3.4 — Relationship results from COLONY. Only relationships with a probability ≥ 0.9 were included. Family groups were defined by matching individuals from pairwise relationships (e.g., if individual A and B were siblings, and individuals B and C were half-siblings, then individuals A, B, and C formed one family group). % of individuals related to another = the percent of individuals that are related to at least one other individual.

	L. nannotis Paluma	*L. nannotis* Girramay-Kirrama	*L. serrata* Paluma	*L. serrata* Girramay-Kirrama
Total # of individuals	184	147	200	117
% of individuals related to another	88.6	36.1	58.5	26.5
Total # of relationships	344	37	80	20
# of half-sibling relationships	324	28	67	16
# of full-sibling relationships	17	9	12	4
# of parent/offspring relationships	3	0	1	0
# of family groups	13	21	44	13
Max group size (# of relationships)	97	5	8	3
Max group size (# of individuals)	42	4	7	4

Figures

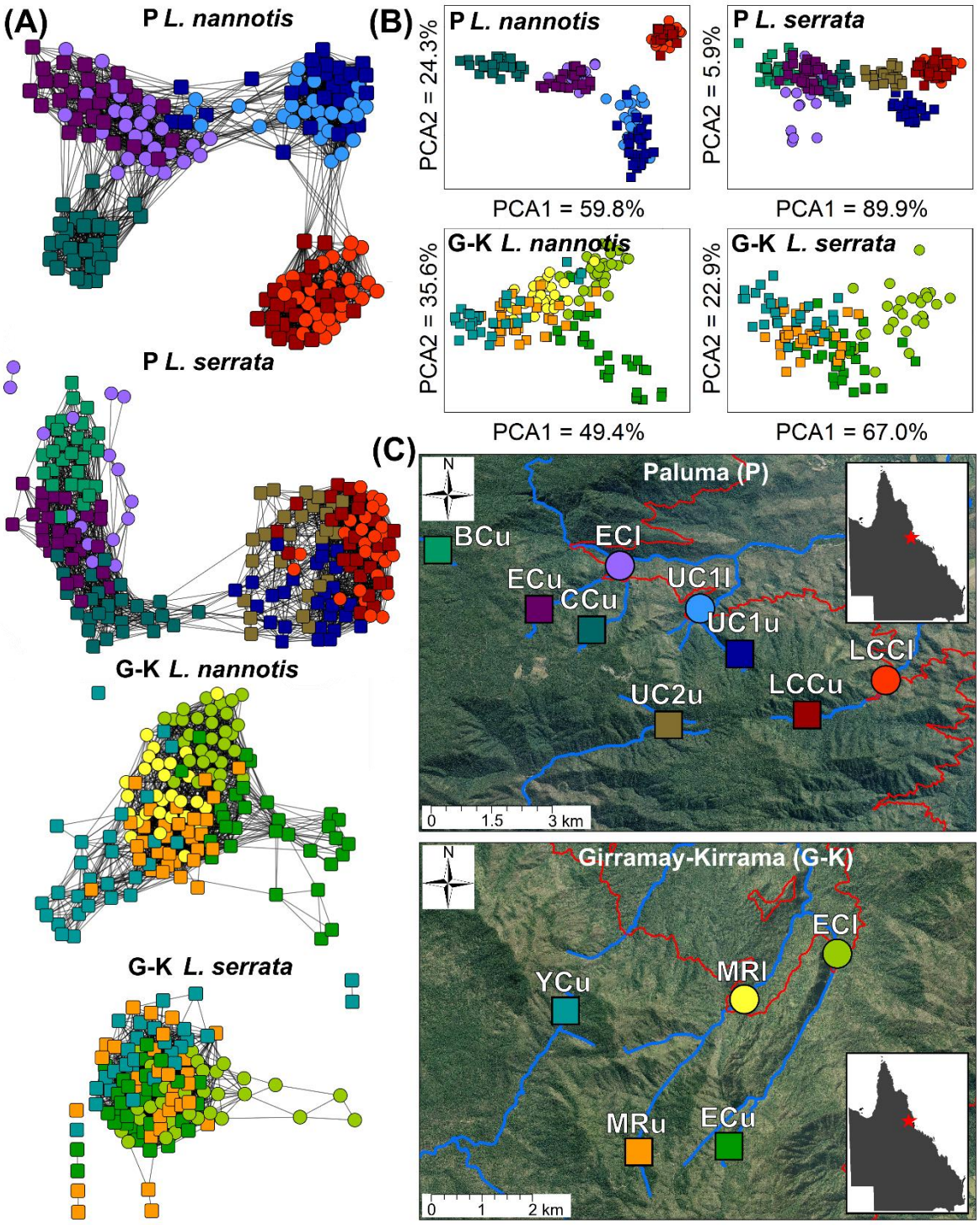

Figure 3.1 — Substructure and study sites (colours and shapes are consistent across panels and Panel C provides a key to sites and geographic relationships for the other panels; squares = upland, circles = lowland). These results were based on the fully filtered data sets (filtered separately for each park), but they show the same clusters that were used for HWE testing. (A) NetView images for the individual data sets for each species/park with lines

connecting up to 40 nearest neighbours. These plots should be read by looking at clustering, rather than the length of the lines. (B) DAPC results for the individual data sets for each species/park (for ease of reading, the y-axis of G-K *L. nannotis* and x-axis of G-K *L. serrata* were flipped). (C) Maps of the study sites. The squares and circles show the middle of the collection sites, blue lines = streams, red lines = 300 m elevation (lowland [l] populations of *L. nannotis* below this line survived the *Bd* outbreak, but upland [u] populations above it did not). *Litoria nannotis* were not sampled at BCu or UC2u, and *L. serrata* were not sampled at UC1l or MRl.

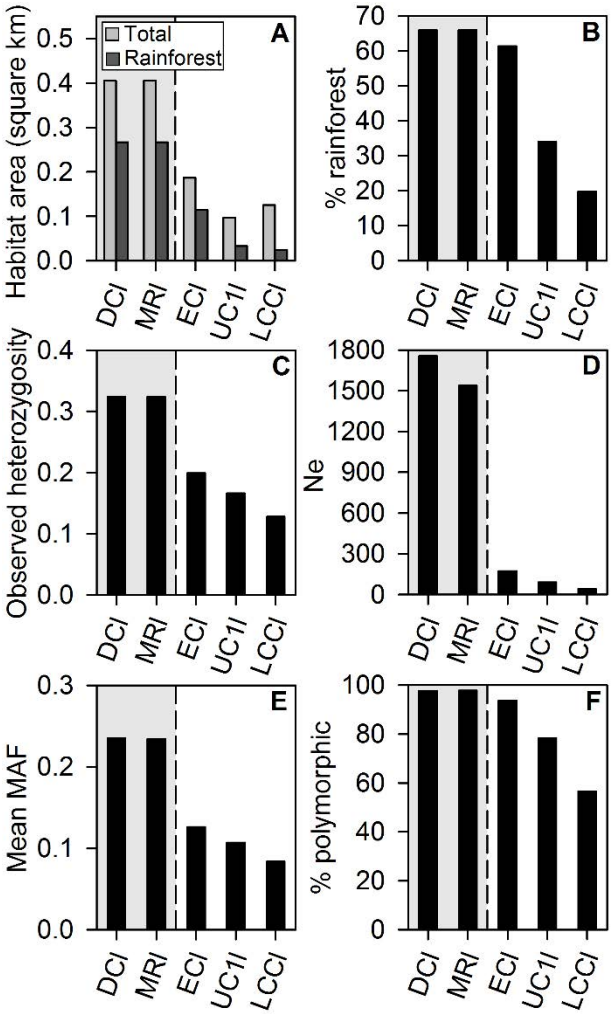

Figure 3.2 — Habitat and diversity results for each lowland stream (grey background shading indicates Girramay-Kirrama streams; Paluma streams are ordered from west to east). (A–B) Total habitat area, rainforest area, and percent of area occupied by rainforest. The "rainforest" category includes both rainforests and rainforest transitions (see Additional file 3.1). The lowland habitat was the same for both Girramay-Kirrama streams because they join downstream of the sampling sites. (C) Observed heterozygosity. (D) Effective population size. (E) Mean minor allele frequency (averaged across loci). (F) Percent of markers that were polymorphic. All diversity metrics correlated with both the total amount lowland rainforest and the percent of lowland area that consisted of rainforest.

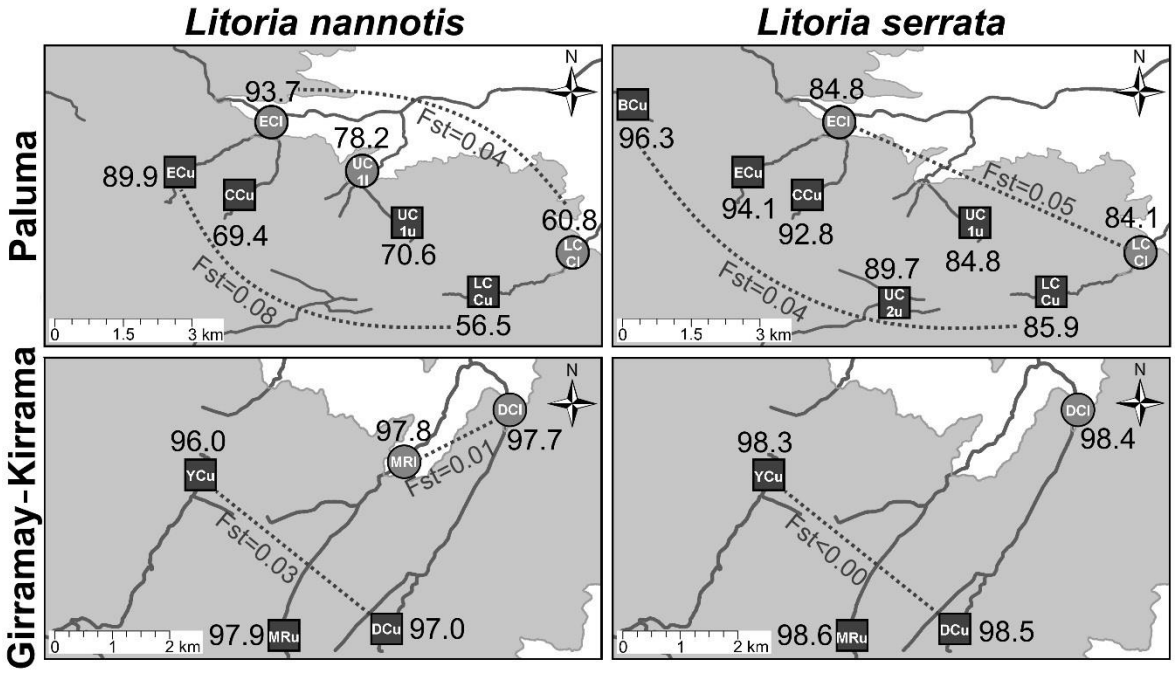

Figure 3.3 — Percent of markers that were polymorphic at each collection site (i.e., all SNPs were polymorphic when looking at an entire park, but some were monomorphic at particular collection sites). Results are from the data sets that were filtered independently for each species/park. Grey shading indicates uplands (>300 m elevation). Solid lines are streams. *Fst* values are shown between the furthest lowland and furthest upland sites for each species (connected by dotted lines). The low *Fst* values combined with large differences in polymorphisms suggest recent declines.

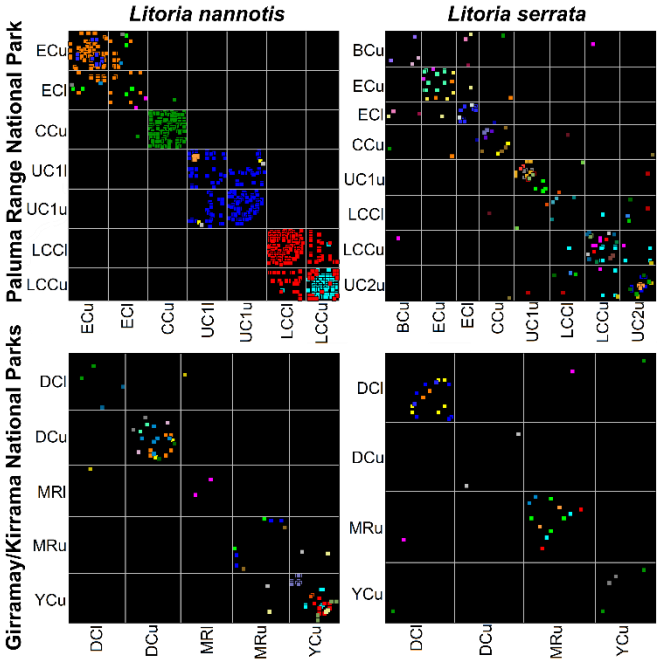

Figure 3.4 — Family groups constructed with COLONY using the separate datasets for each species/park. Within each panel, each point shows a first or second order relationship between two individuals and each colour is a family group. Data are arranged as in a heatmap, where each individual has both a column and a row, and each point is the intersection of an individual on the x axis and an individual on the y axis. White lines separate collection sites. For readability, points were enlarged, sometimes resulting in overlap.

CHAPTER 4: POPULATION GENETICS OF A REMNANT FROG POPULATION FOLLOWING A DISEASE OUTBREAK

In preparation for submission as: McKnight DT, DS Bower, L Schwarzkopf, RA Alford, KR Zenger. Population genetics of a remnant frog population following a disease outbreak. *Conservation Genetics*

Abstract

Emerging infectious diseases have caused dramatic declines in wildlife populations. Nevertheless, some populations and species have recovered from declines, but the patterns of recoveries are often varied, with some members of a community experiencing recoveries while sympatric species continue to either decline or persist at low abundances. Studying these differential recovery patterns may yield important information for managing disease-afflicted populations and facilitating population recoveries. In the late 1980s, a chytridiomycosis outbreak caused multiple frog species in Australia's Wet Tropics to decline. Populations of some of those species (e.g., *Litoria nannotis*) have subsequently recovered, while others (e.g., *Litoria dayi*) have, apparently, been unable to recover. I examined the population genetics of *L. dayi* to test the hypotheses that 1) a lack of individual dispersal abilities has prevented recolonization of previously occupied locations, 2) a loss of genetic variation has resulted in limited adaptive potential, and 3) that *L. dayi* is currently in the process of adapting to chytridiomycosis. Genetic analyses results revealed moderate to high levels of gene flow and diversity among populations (Fst range = <0.01–0.15; minor allele frequency = 0.192–0.245) indicating that dispersal or genetic diversity would not limit the species ability to recover. Indeed, population connectivity and diversity for *L. dayi* were comparable to previously reported values for *L. nannotis* at locations where *L. nannotis* populations have recovered. I did find consistent evidence of selection occurring at all three parks I examined; however, I was unable to identify the regions of the genome that were under selection, so I cannot conclusively say that these populations are adapting to the disease. Nevertheless, my results are suggestive and merit further study.

Introduction

Recent decades have seen a dramatic increase in emerging infectious diseases in wildlife. These diseases are caused by a diverse range of pathogens (bacteria, fungi, viruses, etc.) and have afflicted most major animal taxa, often causing devastating declines or even extinctions (Daszak et al. 2000; Smith et al. 2006; Scheele et al. 2019). Nevertheless, diseases often shift from being epizootic to being enzootic, and, in some cases, populations may rebound following an initial outbreak (Woodworth et al. 2005; McKnight et al. 2017a; Scheele et al. 2017). These recoveries are not guaranteed, and in a single area, some species may recover while others continue to either decline or persist only in low numbers (McKnight et al. 2017a). These differential recovery patterns may hold important clues for understanding how wildlife populations respond to diseases. By understanding differential population responses, conservationists may better manage populations that have experienced declines, and prevent or limit declines in other populations and species.

Chytridiomycosis presents a useful model to study differential recoveries. This disease is caused primarily by the fungal pathogen *Batrachochytrium dendrobatidis* (*Bd*) and has caused declines and extinctions in hundreds of amphibian species around the world (Berger et al. 1998; Daszak et al. 1999; Lips et al. 2006; Scheele et al. 2019). The Wet Tropics of Queensland, Australia experienced a large outbreak in the late 80s and early 90s, during which several species declined, including green-eyed treefrogs (*Litoria serrata* [previously *genimaculata*]), waterfall frogs (*Litoria nannotis*), and Australian lace-lid frogs (*Litoria dayi*) (Ingram and McDonald 1993; Richards et al. 1993; Laurance et al. 1996; McDonald and Alford 1999). Historically, all three species occurred at most elevations along rainforest creeks; however, during an outbreak in the late 1980s, populations above 300–400 m elevation (hereafter referred to as "upland") either declined sharply (*L. serrata*) or disappeared (*L. nannotis* and *L. dayi*), while lowland populations (< 400–300 m) remained stable (Richards et al. 1993; Laurance et al. 1996; McDonald and Alford 1999). Following this initial decline, upland *L. serrata* populations quickly recovered, while *L. nannotis* gradually recolonised the upland sites, and both species now have breeding populations at the headwaters of many upland creeks, despite the fact that *Bd* is still present and continues to infect both species (Richards and Alford 2005; McKnight et al. 2017a). In contrast, *L. dayi* has

not recolonised upland sites and continues to be restricted to low elevations (McKnight et al. 2017a).

In a previous study (McKnight et al. 2019b), I examined the population genetics of *L. serrata* and *L. nannotis* and found that both species have high levels of gene flow among populations but recovered upland populations have reduced diversity. Additionally, large areas of high-quality lowland habitat appeared to be important refugia for maintaining diversity during the outbreak. In the current study, I aimed to build on those results by studying the population genetics of *L. dayi* and comparing those data to my previous results to further our understanding of both how diseases affect host population genetics, as well as why *L. dayi* has been unable to recover. I was specifically interested in testing three hypotheses: 1) *Litoria dayi* is restricted by low individual dispersal ability, which has prevented them from recolonising upland sites. 2) The chytridiomycosis outbreak resulted in a genetic bottleneck reducing the genetic diversity required for adapting to the disease. 3) *Litoria dayi* is currently in the process of adapting to *Bd.* These three hypotheses were tested by examining genetic diversity and connectivity patterns among regions, populations, and individuals in surviving lowland populations and comparing them to the genetic patterns observed in *L. serrata* and *L. nannotis* populations, as well as searching for signatures of selection across the genome.

Materials and Methods

Study sites and samples

Tissue samples were collected from *L. dayi* populations located at three regions: Wooroonooran National Park, Tully Gorge National Park (hereafter "Tully"), and Girramay Range/Kirrama Range National Parks (Figure 4.1). Girramay and Kirrama border each other and share contiguous forests and streams; therefore, they will be referred to as a single site: "Girramay-Kirrama." At each site, frogs were sampled at both the highest and lowest elevations that *L. dayi* currently occupies. At Wooroonooran, frogs were sampled at two points along Pugh Creek. At Tully, *L. dayi* individuals were obtained at Python creek and an unnamed creek. Both creeks feed into the Tully River. At Girramay-Kirrama, two creeks were sampled at the current highest elevation for *L. dayi* (these sites correspond to DCl and MRl in my previous study on *L. nannotis* and *L. serrata*; McKnight et al. 2019b). Both creeks

connect below those sampling sites, so a third site was sampled downstream, at the lowest elevation for *L. dayi* at Girramay-Kirrama. At all three parks, there was a direct water connection between the highest and lowest elevation sites. More details sampling sites are provided in Figure 4.1 and Table 4.1.

At each site, frogs were sampled at night by walking a transect starting at either the lowest or highest point where *L. dayi* could be found (depending on if it was a site at the low or high end of the current elevational range of *L. dayi*). Every *L. dayi* individual encountered was sampled until a minimum representative number (n~30) had been reached, or no more *L. dayi* could be found. At Girramay-Kirrama, *L. dayi* were rare, resulting in long transects, particularly at the lowest elevation; whereas at Tully, they were abundant, resulting in short transects (Table 4.1). Female *L. dayi* spend most of their time in the forest, and are seldom found along streams (Hodgkison and Hero 1999). As a result, all samples were collected from males, with the exception of one female at Girramay-Kirrama, and one juvenile at Tully. All sampling took place in September 2017.

Each frog was captured in a clean plastic bag, handled using a new pair of nitrile gloves, and released at its collection site within minutes of being captured. Tissue samples were collected via toe tips (one from each rear foot). This procedure is minimally invasive and does not typically result in bleeding. The scissors were dipped in ethanol and flame sterilized between each frog. Tissues were stored in vials of 70% ethanol. They were kept at room temperature for up to 48 hours, after which they were placed on ice for transport and stored at 4°C.

Extraction and sequencing

Genomic DNA was extracted from each sample using the cetyl trimethyl ammonium bromide (CTAB) procedure (with a chloroform precipitation; Doyle and Doyle 1987) , and the quality and quantity of DNA was checked using gel electrophoresis and a Nanodrop DNA/RNA spectrophotometer analyser. Genome-wide single nucleotide polymorphisms (SNPs) were generated by Diversity Arrays Technology (DArT PL) using their proprietary DArTSeq genotyping by sequence methodology (Sansaloni et al. 2011; Kilian et al. 2012; Lal et al. 2017). This same approach was previously used to generate SNP data for *L. serrata* and *L. nannotis* and is outlined in (McKnight et al. 2019b).

Filtering and quality control

DArTSeq sequencing and analysis pipelines delivered a total of 33,016 SNPs. To obtain the highest quality data, SNPs were further filtered by first removing duplicate SNPs within the same sequence read (69 base pairs) and sequences with a high degree of similarity (assigned with a 95% probability; Lal et al. 2017) . Next, the following criteria were applied: average number of reads (averaged between the two alleles) ≥ 7, minor allele frequency (MAF) ≥ 0.02, call rate = 1.0 (i.e., no missing data), and reproducibility ≥ 0.9. A very stringent call rate was used because of the possible presence of null alleles at some parks (McKnight et al. 2019b).

To identify potential outlier loci under selection, BayeScan v.2.1, (false discovery rate [FDR] = 0.1; Foll and Gaggiotti 2008; Foll 2012) , HacDivSel (Carvajal-Rodriguez 2017), and FstHet (Flanagan and Jones 2017) were used both on the entire dataset (with each collection site as a population) and on each park separately (at Girramay-Kirrama, both higher elevation sites [G1 and G2] were entered as a single population; HacDivSel was not used for the entire dataset because it requires datasets within only two populations). This produced four sets of tests (one for the entire dataset and one for each park). Any markers that were identified as outliers in at least two programs for any of the four sets of tests were removed, producing two separate datasets (i.e., outlier and neutral loci).

PLINK (v1.9 Purcell et al. 2007) was used to test for linkage disequilibrium (LD; all individuals were included in the analysis). Any links with an R2 ≥ 0.6 were removed. To minimize the loss of data, this was done by iteratively removing the SNPs with the greatest number of significant links until no links ≥ 0.6 remained.

The GWASExactHW package in R (v1.01; Painter and Washington 2013) was used to identify markers that were out of Hardy-Weinberg equilibrium (HWE). This test was performed with all the sites within each park combined into a single population. Any markers that were significantly out of HWE ($P < 0.01$) at all populations were removed (P values were not adjusted for multiple comparisons, resulting in the retention of a conservative set of markers).

These filtering steps resulted in a final dataset of 8,304 high quality, neutral SNPs. With the exception of the call rate threshold and the filtering criteria for neutral markers, these were the same filtering steps used in (McKnight et al. 2019b) for *L. serrata* and *L. nannotis*.

Population structure and connectivity

Several methods were used to examine population structure and connectivity and, in so doing, test the hypothesis that *L. dayi* has low physical dispersal abilities which are preventing it from recolonising the uplands. First, the genetic distances among populations were calculated as *Fst* values in Arlequin (v3.5.2.2; Excoffier et al. 2005) . Second, the divMigrate function in the R package diveRsity (v1.9.90; Keenan et al. 2013) was used to examine differential migration rates.

Population structure was visualized using both NetView R (v1.0; Steinig et al. 2015) and a discriminant analysis of principal components (DAPC) via the R package "adegenet" (v2.0.1; Jombart, 2008; Figure 4.1). Additionally, an analysis of molecular variance (AMOVA) in Arelquin was used to examine how the variance was partitioned among parks and within parks (parks were included as the groups, with sampling sites within parks included as the populations).

Family genetic structure was assessed by using the program COLONY to identify relationships among individuals (Jones and Wang 2010). For this test, each park as analysed separately, and all sites within a population were included together so that relationships among individuals at different sampling sites within a park could be detected. All individuals were entered as both potential offspring and potential parents and no prior probabilities were used. Because of the high computational requirements of COLONY, a random subset of 1000 markers were used.

Genetic diversity

Genetic diversity was examined both within each sampling site and within each park (all sampling sites combined). The following metrics were calculated: minor allele frequencies (MAF), percent of markers that were polymorphic within a given site or park (both with and without rarefying), expected and observed heterozygosities (Genetix v4.05.2; Belkhir 2004), and *Fis* (Genetix). Additionally, the effective population size (Ne) was calculated using the LD method in NeEstimator, with only alleles with an MAF > 0.05 (v2.01; Do et al. 2014). The Ne for each park was also calculated in COLONY using the relationships among individuals.

Selection

To examine the possibility that *L. dayi* is in the process of adapting to *Bd*, I examined the results of the BayeScan, HacDivSel, and FstHet outlier tests comparing the two elevation extremes within each park. A recent disease survey of these sites (Carr unpublished data) confirmed that both infection prevalence (i.e., percent of frogs that are infected) and intensity (i.e., zoospore load per frog) increased with elevation, with the majority of frogs at the highest elevation (300–400 m) being infected. Thus, the selection pressure from *Bd* should be greater at the highest elevations than at the lowest elevations.

The results of the outlier tests were examined for consistency both within and among parks. Within each park, any SNPs that were identified as outliers by all three methods were extracted and a NCBI BLAST (blastn) search was performed to align them with the following genomes: African clawed frog (*Xenopus laevis*; taxid: 8355), western clawed frog (*Xenopus tropicalis*; taxid: 8364), and Tibetan frog (*Nanorana parkeri*; taxid: 125878). Results were filtered at an e-value < 1 and percent query coverage > 75%.

Results

There was no evidence of genetic subdivision within parks ($Fst \leq 0.04$) and only moderate differences among parks ($Fst \leq 0.15$; Figure 4.1). Similarly, both NetView and DAPC showed that each park clustered separately from the others, but there was little evidence of sub-structure within parks (nearly all of the variation in the DAPC was explained by differences among parks; Figure 4.1). Further, the AMOVA found that differences among parks accounted for 9.05% of the variation in the data, whereas differences among sampling sites within parks only explained 1.55% of the variation (differences among individuals within sites = 2.11%; variation within individuals = 87.3%). At Girramay-Kirrama, COLONY identified six half-sibling pairs where one member was at site G1 and the other was at site G3 (no relationships that crossed sampling sites were detected at the other parks). The divMigrate results suggested that geneflow was bi-directional along the streams.

Diversity analyses generally did not suggest a large loss of diversity or inbreeding (Table 4.2; Figure 4.2). Girramay-Kirrama had slightly reduced diversity compared to the other parks, but expected and observed heterozygosities were similar at all sites, and *Fis* values did not deviate substantially from zero. Similarly, average MAFs per site ranged from 0.192–

0.243 and the percentage of polymorphic markers within each site ranged from 79.0–97.8. Nevertheless, Ne estimates were low at Girramay-Kirrama (7.9–40.3 per site) and Wooroonooran (38.0–63.3 per site). Relationship results from COLONY largely agreed with the Ne patterns, with Wooroonooran and Girramay-Kirrama both having low Ne values and numerous relationships (Table 4.3). Indeed, at Girramay-Kirrama at site G2, which had the lowest Ne, all 19 individuals were related to at least one other individual.

Outlier tests indicated that a small number of loci were possibly under selection at each park. BayeScan was generally the most conservative method, but most of the outliers it detected were also detected by FstHet or HacDivSel (Table 4.4). Thus, there was a consensus among programs for 31 markers at Wooroonooran, 16 at Tully, and three at Girramay-Kirrama. Additionally, there were four markers that were identified as outliers by all three programs at both Wooroonooran and Tully. However, BLAST produced low quality matches that I did not consider reliable (no sequences had a query coverage > 75%).

Discussion

My results suggest that *L. dayi* has both high population connectivity (suggesting good dispersal abilities) and high levels of genetic diversity (comparable to *L. nannotis* and *L. serrata*). These results are not consistent with either the hypotheses that *L. dayi* has low dispersal abilities, or that it has undergone a recent genetic bottleneck. There were, however, consistent patterns of outlier loci, likely indicating selection, which may be the result of ongoing adaptation to *Bd*, but that possibility could not be confirmed.

Low dispersal hypothesis

My results are not consistent with the hypothesis that low dispersal abilities have prevented *L. dayi* from recolonising upland sites. Because frogs are not broadcast spawners, gene flow requires the physical movement of individuals; therefore, population connectivity provides a useful proxy for dispersal ability, and I observed high levels of connectivity within each park. Within each park, the *Fst* values were low, and both NetView and the DAPC showed little evidence of structuring. Also, half siblings were found several kilometres apart at Girramay-Kirrama. Additionally, divMigrate did not detect asymmetry in the gene flow patterns, suggesting that frogs were moving both upstream and downstream. Although a

downstream bias in gene flow is common in some stream-dwelling species (Bolnick et al. 2008; Guarnizo and Cannatella 2013), its absence in *L. dayi* makes sense, because their eggs are attached to rocks, and their tadpoles possess adaptations to fast-flowing water, such as suctorial mouth discs and specialized tails, to prevent them from being washed downstream (Davies and Richards 1990).

The *Fst* values for *L. dayi* were similar to the previously reported values for *L. nannotis* (which went through the same pattern of declines but has recolonised the upland sites). Indeed, at Girramay-Kirrama, where my G1 and G2 sites correspond to *L. nannotis* sampling sites in (McKnight et al. 2019b), *L. dayi* only had a slightly higher *Fst* than *L. nannotis* (0.04 compared to 0.01), and when looking across similar sites for each study, the ranges of *Fst* values were similar for both species (*L. dayi*: <0.01–0.04; *L. nannotis*: 0.01–0.08; only sites with direct water connections were included in these ranges). These results are also consistent with the fact that *L. dayi* move away from streams, with females spending most of the year in the forest (Hodgkison and Hero 1999). It is not known if females make long-distance migrations while away from the stream bed.

Taken together, these results do not suggest a low dispersal ability in *L. dayi*. Indeed, the similarities to previously reported values and patterns for *L. nannotis* suggest that both species have similar dispersal abilities. Therefore, given that *L. nannotis* experienced the same declines at the same sites as *L. dayi,* but has recolonised the upland sites, a lack of dispersal ability in *L. dayi* does not appear to explain its lack of recovery.

Loss of diversity hypothesis

Litoria dayi had high levels of genetic diversity, and my results do not suggest that a lack of diversity has prevented them from adapting and recovering from the disease outbreak. Although the diversity was slightly lower at Girramay-Kirrama than at Wooroonooran or Tully, possibly as a result of *Bd* (McKnight et al. 2019b), none of the parks showed obvious signs of inbreeding or low diversity. Several factors affect a population's ability to retain diversity during an outbreak, including the duration of the decline, the number of individuals that survived the decline, and gene flow from neighbouring populations (McKnight et al. 2017b). Thus, although diseases do have the potential to cause a large loss of diversity (Trudeau et al. 2004; Schoville et al. 2011; Albert et al. 2014; Serieys et al. 2015), many populations can endure a large loss of individuals without experiencing

bottlenecks or inbreeding (Morgan et al. 2008; le Gouar et al. 2009; Teacher et al. 2009a; Lachish et al. 2011; Brüniche-Olsen et al. 2013). In the case of *L. dayi*, the populations at Wooroonooran and Tully appear to be robust with high densities of *L. dayi* occurring over large areas (McKnight, pers. obs.). They were less dense at Girramay-Kirrama, but still occurred over a large area. Additionally, based on the high levels of connectivity I observed, it is likely that my study populations benefitted from gene flow from populations I did not sample. This large number of individuals surviving in the lowlands, combined with geneflow, would allow the retention of high levels of genetic diversity, despite the loss of all populations at sites above 300–400 m elevation (Lachish et al. 2011; Whiteley et al. 2015; McKnight et al. 2017b, 2019b).

The observed diversity values were similar to the previously reported values for *L. serrata* and *L. nannotis* (McKnight et al. 2019b). At Girramay-Kirrama, *L. dayi* had slightly lower genetic diversity values than *L. nannotis* and *L. serrata*, but when comparing the species across all sites, *L. dayi* at Wooroonooran and Tully generally had slightly higher genetic diversity than was reported for *L. serrata* or *L. nannotis* at Girramay-Kirrama (Figure 4.2). Further, at all three sites, *L. dayi* generally had higher diversity than was reported for either *L. serrata* or *L. nannotis* at Paluma Range National Park. Although these comparisons are admittedly strained due to the fact that, in some cases, different parks were sampled for different species, the fact that *L. dayi* showed no signs of inbreeding and has not been able to recover even at parks with high diversity, while *L. serrata* and *L. nannotis* both recovered even at sites with low diversity, suggests that a lack of genetic diversity is not precluding *L. dayi* from adapting to coexist with *Bd* at upland sites.

Effective population sizes for *L. dayi* at Wooroonooran and Girramay-Kirrama were generally low, but they were higher at Tully, particularly at site T2, which had the highest density of *L. dayi* (based on the transect distance required to sample 30 frogs: 150 m as opposed to 350–1540 m; median = 560 m) and is close to numerous other small creeks populated by *L. dayi*. The other sampling sites were comparatively more isolated. Additionally, the generally low Ne values may also be partially a sampling artefact resulting from the fact that female *L. dayi* live in the forests, and not along the streams, and therefore I was unable to sample them (Hodgkison and Hero 1999).

Adaptation hypothesis

At each park, several markers were consistently identified as outlier loci by each program, and four of those loci were identified at two parks. This potentially suggests that adaptation is occurring, and alleles are being selected at one of the elevation extremes. These results are consistent with the hypothesis that *L. dayi* is in the process of adapting to *Bd*, but they are not conclusive. Unfortunately, I was unable to reliably identify the regions of the genome under selection *via* a BLAST search. The inability to identify regions is likely due to a combination of short sequence lengths (~69 bp) and a lack of genetic resources for *Litoria*. The currently available amphibian genomes are highly divergent from *Litoria,* and future genomes of more closely related species might improve results.

Interestingly, unlike my *L. dayi* results, previous research on *L. nannotis* that used similar methods for identifying outlier loci failed to find consistent patterns either within or between parks, despite the fact that *L. nannotis* has undergone upland recoveries (McKnight et al. 2019b). An intriguing, but admittedly speculative, explanation is that *L. nannotis* adapted quickly, and the beneficial alleles spread rapidly through populations, rendering us unable to detect outliers when comparing high and low elevations. In contrast, if adaptation in *L. dayi* is occurring more slowly, I may have sampled the populations before the alleles became homogenised, thus allowing us to detect signatures of selection.

Previous research in other systems has documented that there is a heritable component to *Bd* infection risk (Palomar et al. 2016), and several studies have found evidence of *Bd* driving selection (Grogan et al. 2018; Voyles et al. 2018; Kosch et al. 2019). However, more work on *L. dayi* is needed before I can confirm that they are adapting to *Bd*. It would be particularly useful to employ techniques such as controlled heritability trials and transcriptomics. Additionally, these efforts are currently hindered by a shortage of genetic resources for frogs in the family Hylidae, and a Hylid reference genome would greatly enhance my ability to test for adaptation to *Bd*.

Conclusion

I tested three hypotheses for the lack of population recovery in *L. dayi*, and my results suggest that neither low dispersal abilities nor a lack of genetic diversity can explain the absence of population recoveries. I did find consistent evidence that some loci are undergoing selection, but I was unable to confirm that *Bd* is driving the selection. Thus, it is

possible that *L. dayi* is currently in the process of adapting to *Bd*, but more research is needed to address this, ideally including controlled heritability trials.

Additionally, there are several other potential explanations for the differential recovery patterns of Australia's rainforest frogs that were beyond the scope of this paper. For example, differences in microbial communities or anti-microbial peptides may have played a role in the differential recovery patterns (Kueneman et al. 2016; Jani et al. 2017; Bates et al. 2018; Bell et al. 2018). Additionally, in other systems, a shift in the timing of reproduction has allowed populations to recover from *Bd* (Scheele et al. 2015). This has not been tested for my system, but it is possible that *L. nannotis* and *L. serrata* underwent such a shift, while *L. dayi* did not. Future studies should continue to examine this system to test these possibilities and further our understanding of the factors that allow some populations to recover while precluding recovery in others.

Tables

Table 4.1 — Study sites and sample sizes. The coordinates represent the approximate midpoints of each transect. *Litoria dayi* were not abundant at Girramay-Kirrama, resulting in long transect distances, particularly at the lowest elevations where they were clustered around small creeks that fed into the main channel. G1 and G2 correspond roughly to DCl and MRl (respectively) in (McKnight et al. 2019b).

Park	Site	N	Latitude	Longitude	Elevation midpoint (m)	Elevation range (m)	Transect length (m)
Wooroonooran	W1	29	-17.38523	145.86868	320	296–356[a]	560[a]
Wooroonooran	W2	28	-17.39803	145.89468	58	47–64	450[b]
Tully	T1	28	-17.77420	145.59390	386	359–424[b]	350
Tully	T2	28	-17.77607	145.66484	95	91–99	150
Girramay-Kirrama	G1	28	-18.17451	145.82828	300	283–327	610
Girramay-Kirrama	G2	19	-18.18250	145.80926	302	286–338	560
Girramay-Kirrama	G3	23	-18.15697	145.82381	177	160–212	1540

[a]Only one frog was found above 334 m (363 m Transect length excluding that frog)
[b]Only one frog was found above 398 m (210 m Transect length excluding that frog)

Table 4.2 — Diversity results for each site and for each park (i.e., all sites within a park combined). MAF = minor allele frequency, % poly. = percent of markers that were polymorphic at a given site, % poly. rare = percent of markers that were polymorphic at a given site after rarefying the data to the lowest sample size, H n.b. = expected heterozygosity (corrected), Het. obs. = observed heterozygosity, *Fis* (SD) = mean inbreeding coefficient and SD of the mean (median values ranged from -0.008–0.000). Ne estimates are shown from both NeEstimator and COLONY.

	Mean MAF (SD)	% poly.	% poly. rare	H n.b.	Het. obs.	*Fis* (SD)	Ne (jackknife CI) [NeEstimator]	Ne (CI) [COLONY]
W1	0.236 (0.146)	95.6	94.1	0.324	0.315	0.028 (0.206)	63.3 (34.6–211.6)	-
W2	0.237 (0.146)	95.6	93.9	0.324	0.315	0.028 (0.210)	38.0 (19.1–150.2)	-
T1	0.243 (0.143)	97.5	96.3	0.333	0.323	0.033 (0.208)	67.7 (25.9–∞)	-
T2	0.243 (0.141)	97.8	96.3	0.334	0.321	0.044 (0.207)	7499.3 (3086.5–∞)	-
G1	0.204 (0.158)	86.4	84.4	0.280	0.270	0.034 (0.200)	40.3 (22.2–114.7)	-
G2	0.192 (0.162)	79.0	79.0	0.265	0.272	-0.021 (0.246)	7.9 (4.8–12.5)	-
G3	0.204 (0.158)	85.1	84.0	0.281	0.282	-0.002 (0.218)	22.1 (9.9–98.5)	-
W	0.241 (0.143)	97.6	97.6	0.327	0.315	0.039 (0.158)	87.3 (53.5–187)	147 (22–104)
T	0.245 (0.140)	98.9	98.9	0.334	0.322	0.042 (0.157)	307.4 (124.8–∞)	743 (429–2878)
G	0.207 (0.157)	90.5	89.8	0.282	0.274	0.027 (0.143)	57.0 (40.7–86.1)	96 (68–135)

Table 4.3 — Relationship results from COLONY, showing the number of individuals that were related to at least one other individual at each park, the number of half sibling, full sibling, and parent/offspring relationships, and the number and sizes of family clusters. Clusters were defined as groups where each individual was related to at least one other individual in a cluster such that a chain of relationships could be made from any individual to any other individual in a cluster.

	N	# of related individuals	# of half sibling pairs	# of full sibling pairs	# of parent offspring pairs	# of clusters	Max cluster size	Median cluster size
Wooroonooran	57	32	17	13	4	9	8	2
Tully	56	11	6	1	1	4	4	1.5
Girramay-Kirrama	70	56	30	31	9	17	8	2.5

Table 4.4 — Number of outliers detected by each method and combination of methods (combinations show the number of outliers that were found by all of the methods). All = all parks were used with each sampling site as a population. Wooroonooran, Tully, and Girramay-Kirrama show the results when a given park was tested independently (i.e., comparisons were made between the highest and lowest elevation sites in each park).

	BayeScan	FstHet	HacDivSel	BayeScan+ FstHet	BayeScan+ HacDivSel	FstHet+ HacDivSel	BayeScan+ FstHet+ HacDivSel
All	1292	978	-	494	-	-	-
Wooroonooran	44	528	447	44	31	292	31
Tully	17	510	561	16	17	326	16
Girramay-Kirrama	5	481	320	5	3	100	3

Figures

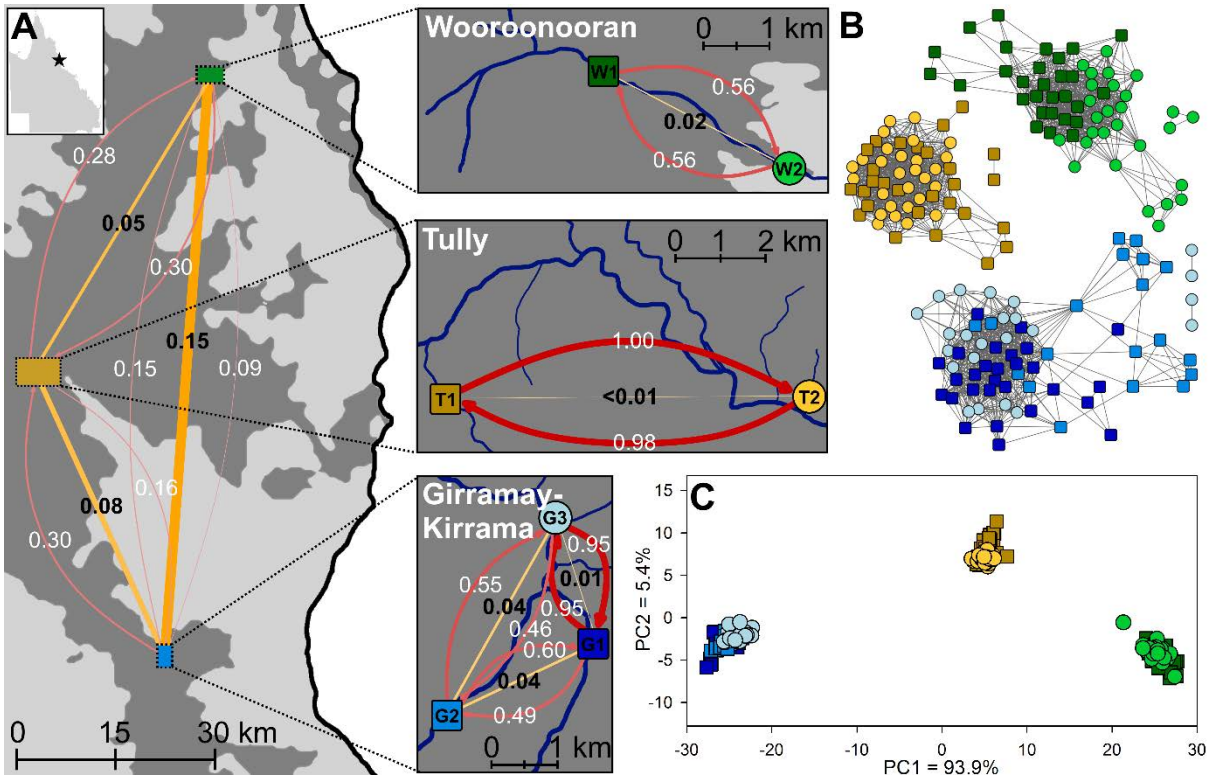

Figure 4.1 — Study sites and connectivity. (A) Maps of study sites. Dark grey areas = rainforest, blue lines = streams, bold black numbers and orange lines = *Fst* values (the thickness and darkness of the lines are scaled with the *Fst*), white numbers and red lines = relative migration rates from divMigrate (arrows indicate the direction of gene flow; all values are relative to each other with 1 being the highest level of migration observed; the darkness and thickness of the lines scale with the migration rates). (B) Results from NetView (k30) showing population structuring (all parks and populations were analysed together; lines = connections to up to 30 nearest neighbours; branch lengths are irrelevant, and this should be read by looking at the number and density of connections, rather than the exact placement of points). (C) DAPC results.

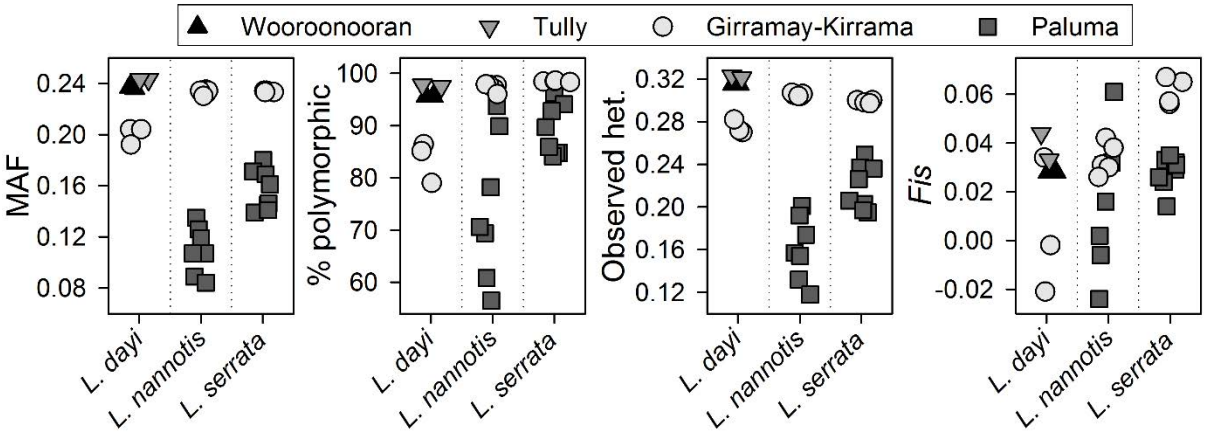

Figure 4.2 — Genetic diversity metrics from this study (*L. dayi*) compared to the previously reported results for *L. serrata* and *L. nannotis* (McKnight et al. 2019b). Each point is a sampling site. MAF = minor allele frequency, % polymorphic = percent of markers that were polymorphic in a given population, Observed het. = observed heterozygosity.

CHAPTER 5: METHODS FOR NORMALIZING MICROBIOME DATA: AN ECOLOGICAL PERSPECTIVE

Published as: McKnight, DT, R Huerlimann, DS Bower, L Schwarzkopf, RA Alford, KR Zenger. 2019. Methods for normalizing microbiome data: an ecological perspective. *Methods in Ecology and Evolution* 10:389–400.

Abstract

Microbiome sequencing data often need to be normalized due to differences in read depths, and recommendations for microbiome analyses generally warn against using proportions or rarefying to normalize data and instead advocate alternatives, such as upper quartile, CSS, edgeR-TMM, or DESeq-VS. Those recommendations are, however, based on studies that focused on differential abundance testing and variance standardization, rather than community-level comparisons (i.e., beta diversity), Also, standardizing the within-sample variance across samples may suppress differences in species evenness, potentially distorting community-level patterns. Furthermore, the recommended methods use log transformations, which I expect to exaggerate the importance of differences among rare OTUs, while suppressing the importance of differences among common OTUs. I tested these theoretical predictions *via* simulations and a real-world data set. Proportions and rarefying produced more accurate comparisons among communities and were the only methods that fully normalized read depths across samples. Additionally, upper quartile, CSS, edgeR-TMM, and DESeq-VS often masked differences among communities when common OTUs differed, and they produced false positives when rare OTUs differed. Based on my simulations, normalizing via proportions may be superior to other commonly used methods for comparing ecological communities.

Introduction

Using high-throughput sequencing to examine microbial communities has become a common practice. These techniques are, however, not without their pitfalls, and it is important for researchers to use the most appropriate analytical methods for answering the ecological questions at hand. One common pitfall stems from the fact that sequencing results in variable numbers of reads per sample. These differences in read depth often need to be corrected prior to analyses, and many methods have been proposed for normalizing data.

Two of the oldest and most intuitive methods are (1) transforming the data to proportions by dividing the reads for each operational taxonomic unit (OTU) in a sample by the total number of reads in that sample (also known as Total Sum Normalization [TSS]) and (2) rarefying the data by randomly subsampling each sample to the lowest read depth of any sample. In recent years, however, both methods have been heavily criticized. Proportions are criticized because they do not account for heteroskedasticity (Weiss et al. 2017) and result in spurious correlations when comparing the abundance of specific OTUs relative to other OTUs (Jackson 1997). Rarefying is criticized because it discards potentially useful data (McMurdie & Holmes, 2014; but see Weiss et al., 2017). Further, several studies have documented that proportions and rarefied data perform poorly in differential abundance testing and often have high type I error rates (Bullard et al. 2009; Dillies et al. 2013; McMurdie and Holmes 2014; Weiss et al. 2017). As a result, other methods have been proposed and have rapidly gained popularity. These methods include, upper quantile normalization (UQ; Bullard et al., 2009), CSS normalization implemented in the R package metagenomeSeq (Paulson, Stine, Bravo, & Pop, 2013), a variance stabilizing transformation implemented in the R package DESeq2 (hereafter referred to as DESeq-VS; Love, Huber, & Anders, 2014), and a trimmed mean of M-values normalization implemented in the R package edgeR (hereafter referred to as edgeR-TMM; Robinson, McCarthy, & Smyth, 2010; McCarthy, Chen, & Smyth, 2012).

Several studies have contrasted the effectiveness of these normalization methods, generally favouring CSS, DESeq-VS, and edgeR-TMM; however, they have usually judged the methods based on how well they standardized the within-sample variance across samples, whether they allowed data to cluster in ordination plots, and how well they performed in

differential abundance testing (Bullard et al. 2009; Dillies et al. 2013; Paulson et al. 2013; McMurdie and Holmes 2014; Lin et al. 2016; Weiss et al. 2017). By those metrics, proportions and rarefying perform poorly, which has often led to blanket recommendations against using them. From an ecological perspective, however, there are additional performance measures that are important to consider. Specifically, it is valuable to determine whether these methods produce accurate comparisons among entire communities (i.e., beta-diversity), rather than simply whether specific OTUs differ.

The Bray-Curtis dissimilarity metric (BC) is one of the most easily interpreted and widely used methods for comparing communities, particularly in microbiome analyses. It can be used as a stand-alone measure of dissimilarity, as well as providing dissimilarity matrices that are used for constructing ordination plots and making statistical comparisons among sets of communities (e.g. PERMANOVAs). Bray-Curtis dissimilarities, and most other distance and dissimilarity measures, do not require equal variances, and there is good reason to think that standardizing the variance prior to calculating BC would distort patterns, rather than clarifying them. Therefore, this paper will first discuss the ecological reasons why transforming to proportions or rarefying may be the most suitable methods for transforming ecological data prior to calculating distance or dissimilarity measures, then it will provide both real and simulated data to illustrate the concepts. It is important to note that while I will focus on BC scores throughout this paper, my arguments and conclusions also apply to other community comparison metrics that incorporate abundance.

The importance of fully standardizing reads

The first potential pitfall of transformation methods such as UQ, CSS, edgeR-TMM, and DESeq-VS is that, unlike proportions and rarefying, they do not guarantee that the number of reads will be equal across samples. This is problematic, because measures like BC are affected by differences in read depths, sometimes in unintuitive ways. For example, consider the four hypothetical samples in Fig. 1. S1 and S2 are samples from the same community, but S2 has twice the read depth of S1. As a result, the BC between them is 0.333, even though they are from the same community and should have a BC of zero. Furthermore, the community from which S3 was sampled is only slightly different from that of S1, whereas S4's community differs strongly from S1's. Nevertheless, because S3 and S4 both have twice the read depth of S1, the BC for both samples is 0.333 when compared to

S1. Indeed, when comparing two samples where the read depth of one sample is twice that of the other, the BC will always be a minimum of 0.333 (it will be exactly 0.333 if the number of reads for each individual OTU is also equal to or greater than the number of reads for that OTU in the other sample). Thus, the differences in read depths have rendered the community-level comparisons among these samples meaningless, and even misleading. Therefore, the fact that many normalization methods do not guarantee standardized read depths raises serious concerns about their applicability for community-level comparisons.

The importance of species evenness

The diversity of a community can be partitioned into species richness (i.e., the number of species present) and species evenness (i.e., the relative abundance of the species present). Evenness (and its inverse, dominance) is an important aspect of diversity (Stirling and Wilsey 2001; Wilsey et al. 2005; Hillebrand et al. 2008) that has strong effects on community function and stability (Hillebrand and Cardinale 2004; Ghazoul 2006; Wittebolle et al. 2009), resistance to invasion (Wilsey and Polley 2002), and the influence of species richness on community functions (Hillebrand et al. 2007). Therefore, species evenness is an important consideration when comparing communities.

Nevertheless, many normalization methods (e.g., UQ, CSS, edgeR-TMM, and DESeq-VS) focus on standardizing the within-sample variance across samples (i.e., forcing each sample to have the same distribution of reads; Dillies et al., 2013; Lin et al., 2016). For some statistical tests, such as most methods for differential abundance testing, having the same variance in each sample is important, but it is potentially problematic when comparing entire communities, because variance and evenness are tightly linked. A highly even community (i.e., a community where all members are roughly equally abundant) will also have a low variance (i.e., there will be a low variance within the community because all the OTUs will be present in similar numbers); whereas a community with low evenness (i.e., a community where a few members dominate) will have a high variance. Therefore, by standardizing the variance across samples, these methods suppress differences in species evenness.

Consider, for example, two communities, each of which consist of the same 100 OTUs, but one has high evenness and the other has very low evenness. These communities will differ greatly in their variances, but that difference in variances is not only important, it

is the critical distinction between those communities, and standardizing the variance would mask that crucial difference.

Dominant species vs rare species

The next potential problem is that methods like UQ, CSS, edgeR-TMM, and DESeq-VS employ log transformations as part of their mechanism for standardizing variances (generally a log base 2 with a plus one pseudocount). The purpose behind this is to reduce the effect of highly abundant OTUs so that the effects of rare OTUs can be seen. With the exception of CSS, these methods originated for RNA-seq data where reducing the effect of dominant genes is vital to detect differences among rare genes; however, its utility for community data is less clear. Although rare members of an ecological community often perform important functions (Pedrós-Alió 2006; Fuhrman 2009), the dominant members tend to drive the bulk of community functionality (Cottrell and Kirchman 2003; Zhang et al. 2006; Fuhrman 2009). Therefore, reducing the importance of dominant OTUs and amplifying the importance of rare OTUs may give a misleading picture of the differences among communities.

Consider, for example, the hypothetical communities in Figure 5.2. S5 and S6 are nearly identical, whereas S7 clearly differs from S5, and those similarities and differences are conveyed by the BC values in the raw data. After log transforming the data, however, the difference between S5 and S6 (based on BC) increases, while the difference between S5 and S7 is greatly reduced. Indeed, based on the log-transformed data, one would incorrectly conclude that S7 is the community that is most similar to S5. This erroneous result arises from the fact that the log transformation amplified the slight differences between S5 and S6 for OTU3, while suppressing the large differences between S5 and S7 for OTU1 and OTU2.

Materials and Methods

Mouse gut microbiomes

To examine the potential problems with normalization methods, I applied several different transformations to a mouse gut microbiome dataset (Turnbaugh et al. 2009), previously used in the paper proposing CSS (Paulson et al., 2013; available in the metagenomeSeq package). I normalized the data using proportions, rarefying (performed in the phyloseq package; McMurdie & Holmes, 2013), UQ (performed in the edgeR package),

CSS (performed in the metagenomeSeq package), edgeR-TMM, and DESeq-VS (with "blind" set to False). UQ, CSS, edgeR-TMM, and DESeq-VS generally apply a log2 transformation with a pseudocount of one as the final step, but because I was also interested in the effects of log transformations, I normalized the data with and without the log transformation for each method (including proportions, rarefied data, and the original [true] data). The choice of pseudocount affects the log-transformed results, and, for results to be comparable, it is important for the scale of the pseudocount relative to the total number of reads to be similar across normalization methods (Costea et al. 2014), Therefore, for proportions, UQ, and edgeR-TMM, the normalized results were multiplied by 10,000 prior to the log transformation, and for CSS the results were multiplied by 1,000 prior to log transformation (which is standard for CSS). Scaling the results by a constant value does not affect the BC results for the normalized data prior to the log transformation, but it does affect the BC value following the log transformation, and scaling by these values was necessary for the log-transformed data to be comparable across methods (Costea et al. 2014).

For each normalization method, I examined the spread of the data (i.e., maximum number of reads per sample, minimum numbers of reads, mean number of reads per sample, and percent difference between the maximum and minimum number of reads) to see how well the methods standardized the read depths across samples. Additionally, to test how accurately the methods performed for BC comparisons, I identified 81 pairs of samples in which the percent difference between the read depth for the original (non-normalized) data was <0.5%. Because those samples were extremely similar in read depth, they were comparable without normalizing. Therefore, I calculated BC dissimilarities within each pair of samples for the original data (without normalizing), and I considered those comparisons to be the true results. Then, I calculated BC dissimilarities for each pair using each normalization method and compared the results with the results from the original data. For each method, I normalized the entire data set prior to subsetting to these pairs, and each sample was compared to the sample with the closest read depth. The package vegan (Oksanen et al. 2017) was used for all BC calculations. Metadata for the pairs of samples I analysed, as well as additional analyses comparing samples of different diet types are available in Additional file 5.1.

Simulated data

To further compare the results of different normalization methods, I wrote a simulation in R (Additional file 5.2) to conduct a mock microbiome study involving two populations. Briefly, the simulation took a distribution of OTUs and randomly sampled from it to form an initial distribution for population 1 (consisting of an amount of DNA per OTU). Then, for each OTU in that distribution, it randomly selected a number from a normal distribution with a user-defined mean (hereafter called the mean dissimilarity) and a SD of 0.3 times that mean. It then multiplied the DNA yield for that OTU by that number and randomly added or subtracted the resulting amount of DNA. This produced a second initial distribution that was used to form population 2 (it could also be set so that only OTUs in a given percentile [based on the amount of DNA in the distribution for population 1] varied between the two distributions). A similar procedure was then used to generate ten individuals in each population, based on the two distributions (each individual was a microbiome sample). The amount of DNA was then standardized (as occurs in real studies) and each sample was "read" by randomly sampling from it (with replacement). The number of reads per sample were randomly selected from a user-defined range.

Next, the data were normalized using each method as described in the "Mouse gut microbiomes" section, and for each method, the simulation returned the maximum and minimum read depths for the 20 simulated samples, as well as the P-value and R^2 value for a linear regression between read depth and BC (mean per sample based on comparisons to all other samples). Additionally, it performed a PERMANOVA between the two populations *via* the package vegan (Oksanen et al. 2017). Finally, it returned the BC between the first individual in each population. All of these calculations were also performed on the original, standardized samples prior to sequencing. These standardized samples all had the same amount of DNA (with slight rounding errors) and represented the true communities (they will be referred to as "original" throughout). Thus, they provided a baseline for testing how well the methods performed. Although standardizing DNA yields prior to sequencing is a component of real studies, in simulations, it is mathematically equivalent to transforming to proportions; therefore, to ensure that this did not bias my results in favour of proportions, I also conducted several tests where the baseline points of comparison were the raw samples (prior to standardization for sequencing) with a UQ, CSS, edgeR-TMM, or DESeq-VS

normalization. These tests did not alter my results and are presented and discussed in Additional file 5.1.

I used this simulator to simulate 200 iterations each for all combinations of the following conditions: mean dissimilarity between populations = 0, 0.2, 0.4, 0.6, 0.8 (when mean dissimilarity = 0, the two populations were formed from the same distribution); range of possible read depths = 5,000–15,000 and 1,000–20,000; OTUs that varied between population starting distributions = all, top 10% [i.e., only the OTUs in the 90th percentile and above based on DNA yield in the population 1 distribution], and the bottom 30%.

I used a variation of that simulator (Additional file 5.2) to examine the effect of normalization methods on clustering in ordination plots. It constructed populations as above, but it simply returned PCoAs based on BC for each normalization method.

I used several metrics to judge the performance of the normalization methods. First, I compared their ability to standardize read depths by examining the percent difference in read depths between the sample with the highest read depth and the sample with the lowest read depth within each iteration. Next, I examined the accuracy of the BC estimates by constructing scatter plots comparing the BC estimates from normalized data to the BC estimates from the original communities. I expected normalization methods that accurately reflected the original communities to have little variation between the original and normalized BC values (i.e., a high R^2), slopes close to one, and intercepts close to zero. I also compared the results of the PERMANOVAs, correlations between read depth and BC, and PCoAs, with the expectation that methods appropriate for comparing communities should yield results that are similar to the results from the original communities.

Results

Mouse gut microbiomes

All normalization methods except for proportions and rarefying performed poorly in terms of their ability to standardize the read depth across samples (Table 5.1). In every case (except proportions and rarefied data), the sample with the deepest read depth had over twice the number of reads as the sample with the lowest read depth. Additionally, for the 81 pairs of samples that had similar read depths before standardization, all methods that did not involve a log transformation produced BC dissimilarities that correlated closely with

the BC estimates from the untransformed data, though rarefied data had a slightly inaccurate slope and the UQ data had more variation than the other methods (Figure 5.3). After applying the log transformation, however, the results for all methods had increased variation in the relationship between the original and normalized BC values, the slopes of the regressions deviated strongly from one, and the intercepts deviated from zero.

Simulated data

All normalization methods except proportions and rarefying performed poorly in terms of their ability to standardize the read depth across samples (Table 5.2). For the log-transformed data, when the read depths varied from 1,000–20,000, the mean percent differences between the sample with the deepest and shallowest read depth per iteration were 25.9, 49.9, 37.0, and 42.2 for UQ, CSS, edgeR-TMM, and DESeq-VS, respectively. Further, for every method except proportions and rarefying, there were frequently undesirable correlations between the number of reads and mean BC (Figure 5.4). This was particularly true for the log-transformed data and for simulations that had a wide range of read depths prior to normalizing.

Similarly, for the comparisons between the BC of the original communities and the BC of the normalized data, proportions had both the tightest correlation and the slope that most closely matched a slope of one (Figure 5.5). The other methods (particularly CSS) had increased levels of variation in the relationship between original and normalized data. All methods performed poorly following the log transformation, resulting in increased variation and slopes that deviated strongly from one, especially when only the bottom 30% of OTUs varied between the initial distributions.

The PERMANOVAs showed that when the variation in initial read depth was low (5,000–15,000) all methods were roughly equally powerful, prior to the log transformation (rarefied data had a slight loss of power), and their results closely matched the results of the original data (i.e., the real communities; Figure 5.4). This was true even when only the top 10% or bottom 30% of OTUs varied in the initial distributions. Results were similar when the variation in initial read depth was higher (1,000–20,000); however, there was a slight loss of power across methods (particularly for CSS); proportions, UQ, and edgeR-TMM performed the best.

In contrast, when the data were log transformed, they did not closely match the results of the original data (Figure 5.4). When the variation in read depth was low and all OTUs varied between starting communities, all log-transformed methods had a high rate of false positives compared to the original data (i.e., they detected differences in the communities that were not apparent in the original data). When the variation in read depth was higher, the results were varied and proportions, rarefied data, and UQ had false positives, while CSS, edgeR-TMM, and DESeq-VS had reduced power. When only the top 10% of OTUs varied in the initial distributions, all log-transformed methods had reduced power, and when only the bottom 30% of OTUs varied, all methods had high rates of false positives (except rarefied data when variability in read depth was high). For the top 10% data, the results were exaggerated when the variation in read depth was high, and for the bottom 30% data, the results were exaggerated when the variation in read depth was low. After log transforming the original data, they showed similar patterns to the normalization methods, but the patterns were often exaggerated.

The PCoAs revealed similar patterns (Figure 5.6; Additional file 5.1). All methods generally performed reasonably well prior to a log transformation (with proportions and rarefied data most closely matching the original communities). Once the data were log transformed, however, the results often differed strongly from the results of the original data. When all OTUs varied in the initial distributions and the mean dissimilarity between the populations was set to a low value (e.g., 0.2), log-transformed data frequently showed clusters that were not evident in the original data. This was particularly pronounced when only the bottom 30% of OTUs varied in the initial distributions. In contrast, when only the top 10% of OTUs varied in the initial distributions, log transforming the data often obscured clusters that were apparent in the original data. Additionally, log-transformed ordination plots generally explained less of the variance in the data and frequently clustered most individuals tightly, often with a few distant outliers.

Discussion

The results of both the mouse gut data and simulated data agreed strongly with my predictions, suggesting that methods other than proportions and rarefying distort community-level comparisons. First, with the exception of proportions and rarefying, none

of the methods successfully standardized read depth across samples, and those remaining differences in read depths influenced the results, often affecting the BC dissimilarities. This is discouraging, as standardizing read depths is the initial impetus for normalizing the data (i.e., if all samples had equal read depths after sequencing, there would be no need to normalize).

In all analyses, transforming the data to proportions without log transforming returned the most accurate BC dissimilarities compared to the original communities. This is in agreement with previous studies (McMurdie and Holmes 2014; Weiss et al. 2017) and suggests that, although proportions are not suitable for differential abundance testing (Bullard et al. 2009; Dillies et al. 2013; McMurdie and Holmes 2014; Weiss et al. 2017), they are the most suitable method for community-level comparisons using dissimilarity and distance measures. Furthermore, proportions produced PCoAs that most closely matched the original data. Rarefied data also performed well but tended to have more variation than data transformed to proportions. All other methods generally performed well prior to a log transformation, but they had more variation than proportions or rarefied data, suggesting they were still inferior.

Additionally, for all methods, applying a log transformation distorted the BC values, resulting in BC dissimilarities that poorly matched the original values. As a result, the subsequent analyses were strongly influenced by the log transformation. I expected the log transformation to decrease the importance of the most dominant members of the microbial community, while increasing the importance of differences in the rare members, and I observed this in both the PERMANOVAs and PCoAs. This was most clearly illustrated by the comparisons where either only the top 10% of OTUs (i.e., the most abundant OTUs) or the bottom 30% (i.e. the least abundant OTUs) differed between the initial distributions upon which the populations were based. When the initial distributions differed only in the most abundant OTUs, log transforming the data suppressed the differences between populations, resulting in a loss of power to both detect differences among populations and ordinate them into clusters. Conversely, when only the least abundant OTUs varied, the log transformation exaggerated those differences, and both the PERMANOVAs and PCoAs detected differences and clusters that were not apparent in the original data. Furthermore, because microbial communities typically consist of a few common, and many rare, OTUs, even when all OTUs varied between the initial distributions, log transforming the data often

ordinated the data into clusters and produced significant differences between the communities that were not evident in the original data. It should also be stressed that these patterns occurred across log-transformed normalization methods (including log transforming the original data), and the log transformation had a much greater impact on the results than did the choice of normalization method.

Although the loss of power when only common OTUs varied was clearly problematic, for most microbial communities, a log transformation should boost the statistical power, because most communities include many rare OTUs. Whether that boost in statistical power is desirable is, however, debatable. On one hand, because the log transformation detects differences that are not apparent in the original communities, it could be argued that the log transformation results in the detection of exceedingly minor differences that have little ecological relevance. This line of reasoning is especially relevant when you consider the small differences that were often statistically significant following a log transformation (Additional file 5.1). Indeed, in simulations where only the bottom 30% of OTUs varied in the initial distributions, the BC between the initial communities was only 0.005 on average, and the OTUs in the bottom 30% of initial distributions only varied from 0–5 reads, even when the mean dissimilarity was set to 0.8 (the highest setting I tested). Nevertheless, such slight differences were often statistically significant following the log transformations. On the other hand, because the initial distributions were different (albeit only slightly), it could be argued that the log transformation really is boosting statistical power and allowing the detection of previously obscured trends, rather than detecting inflated differences. My purpose in this paper was not to give a definitive resolution to the discussion of whether it is beneficial to differentiate communities based on slight differences in rare OTUs, but rather to encourage researchers to think carefully about the ecological questions they are asking when comparing microbial communities.

Nevertheless, some general recommendations are warranted. In most cases, I think that researchers should strive to obtain the most accurate possible representation of the original communities. Thus, given that methods involving a log transformation distort communities and alter species evenness, I argue that community-level comparisons should generally use proportions (preferably) or rarefied data. There are, however, situations in which other normalization methods may be preferable. For example, if the communities in question contain several dominant members (i.e., have low evenness) that are similar across

communities, researchers may want to use log-based methods, like CSS, so that differences in the rare members of the communities can be detected. The results should, however, be interpreted within that context, because any detected differences will reflect differences in the rare members of the community, rather than differences in the community as a whole. In other words, when using normalization methods that involve a log transformation, it would be incorrect to say that the communities as a whole differ, and it would be more accurate to state that uncommon members of the community differ after reducing the importance of the common members. Conversely, if a significant difference is not detected when using log-based methods, it would be misleading to say that the communities are not different, because log-based methods suppress differences in abundant OTUs and can mask differences between communities.

Conclusions and recommendations

Both rarefied data and, especially, proportions outperformed all other normalization methods for producing accurate Bray-Curtis dissimilarities and subsequent PCoAs and PERMANOVAs. They were the only methods that were capable of truly standardizing read depths, and they avoided the spurious correlations that were produced by the other methods. Therefore, although previous studies have raised serious concerns over their applicability for differential abundance testing, I do not think that they should be dismissed for community-level comparisons.

Further, although log transformations are a standard component of many normalization procedures, I showed that they can often distort comparisons of communities by suppressing large differences in common OTUs and amplifying slight differences in rare OTUs. In cases when populations of samples differ only in the most abundant OTUs, log transformations make the populations artificially similar and can mask differences. Conversely, when there are many rare OTUs, as is often the case in microbial communities, they can reveal differences that are not otherwise detectable. Whether that trait is a desirable boost in power or an undesirable false positive will depend on the specific ecological questions being asked. I am not, therefore, making blanket recommendations one way or the other, but simply want to encourage researchers and readers to carefully

consider the ecology of their communities, the specific questions they are asking, and whether a given normalization method is suitable for addressing those questions.

Tables

Table 5.1 — Read depths for the mouse gut microbiome data set based on different normalization methods.

	Original	Proportions	Rarefied	UQ	CSS	edgeR-TMM	DESeq-VS	Original log	Proportions log	Rarefied log	UQ log	CSS log	edgeR-TMM log	DESeq-VS log
Max	5808	10000	848	39352	22512	26408	5878	1081	1825	404	2504	1719	1843	1126
Min	848	10000	848	3535	4871	5644	882	342	891	192	511	825	842	359
Mean	2270	10000	848	11579	9340	10196	2332	647	1282	318	1313	1238	1285	675
SD	654	0	0	6662	2097	2254	662	129	170	39	411	154	189	134
% diff max-min	85.4	0.0	0.0	91.0	78.4	78.6	85.0	68.4	51.2	52.5	79.6	52.0	54.3	68.2
% diff pairs	0.2	0.0	0.0	69.8	16.0	16.2	0.4	12.4	12.6	12.5	35.1	7.1	12.8	12.4

% diff max-min = the percent difference between the maximum and minimum read depth, % diff pairs = the mean percent difference in read depth between the 81 pairs of samples where, prior to normalization, the percent difference in read depth was <0.5% (i.e., after normalization, the percent difference was calculated for each pair, then averaged across pairs). The “Original” column shows the data prior to any normalization. For the pairs of samples where read depths were similar beforehand, most normalization methods actually increased the differences between samples.

Table 5.2 — Mean (SD) percent differences between the maximum and minimum read depth per iteration for the simulated data.

	Original	Proportions	Rarefied	UQ	CSS	edgeR-TMM	DESeq-VS	Original log	Proportions log	Rarefied log	UQ log	CSS log	edgeR-TMM log	DESeq-VS log
5000–15000	0.0	0.0	0.0	44.8	47.8	36.9	36.7	18.4	21.3	22.3	12.7	26.7	20.3	22.1
	(0.0)	(0.0)	(0.0)	(11.5)	(6.6)	(7.5)	(7.0)	(7.2)	(7.1)	(7.4)	(2.8)	(4.7)	(6.9)	(5.8)
1000–20000	0.0	0.0	0.0	46.9	72.0	48.9	57.1	17.3	29.0	24.4	25.9	49.9	37.0	42.2
	(0.0)	(0.0)	(0.0)	(10.6)	(7.4)	(8.0)	(7.7)	(6.9)	(7.5)	(7.4)	(8.0)	(7.9)	(7.8)	(7.5)

For each iteration, the percent difference was calculated, and these are the means across iterations. 5000–15000 and 1000–20000 indicate the range of possible read depths prior to normalization.

Figures

	S1	S2	S3	S4
OTU1	1000	2000	2010	1000
OTU2	500	1000	1000	500
OTU3	100	200	200	720
OTU4	10	20	20	1000
# of reads	1610	3220	3230	3220
BC (vs. S1)	-	0.333	0.333	0.333

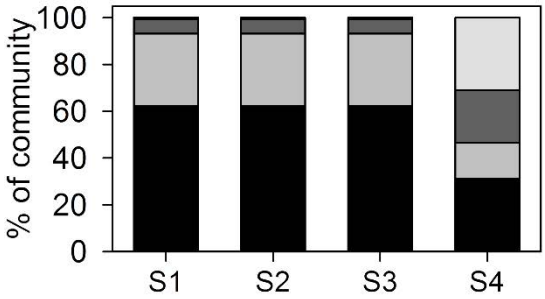

Figure 5.1 — Samples (S1–S4) from four hypothetical communities illustrating the potential problems that arise when samples have different numbers of reads. The data are shown both as a table of raw read counts and a stacked bar plot. The bar plot illustrates the fact that S1, S2, and S3 are nearly identical after accounting for read depth, whereas S4 is distinct. Nevertheless, all samples have the same BC when compared to S1. BC = Bray-Curtis dissimilarity between S1 and the sample in a given column.

	S5	S6	S7	log2(S5+1)	log2(S6+1)	log2(S7+1)
OTU1	1000	1009	750	9.97	9.98	9.55
OTU2	100	100	350	6.66	6.66	8.46
OTU3	10	1	10	3.46	1	3.46
# of reads	1110	1110	1110	20.08	17.64	21.47
BC (vs. S5)	-	0.008	0.225	-	0.066	0.053

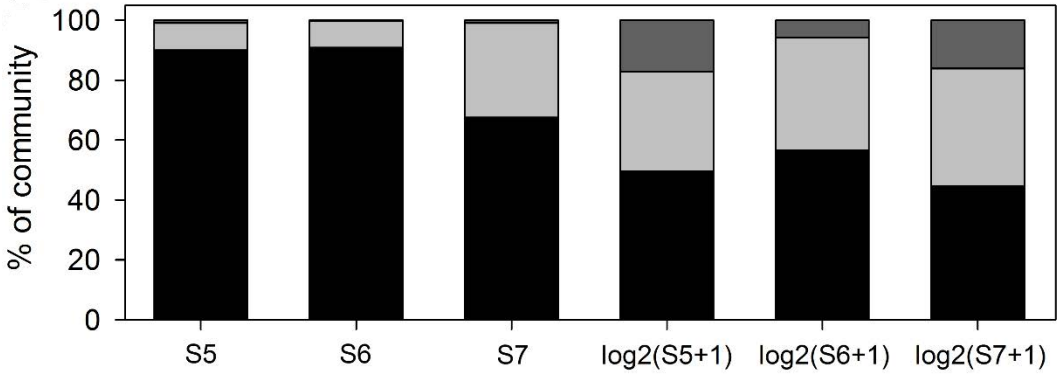

Figure 5.2 — Samples (S5–S7) from three hypothetical communities illustrating the potential problems that arise from log transforming community data. The samples are shown with and without a log2(x+1) transformation, and the data are shown both as a table of raw read counts and a stacked bar plot. The bar plot illustrates the fact that the log transformation increases the importance of rare OTUs which decreasing the importance of common OTUs, ultimately suppressing the differences between S5 and S7 and exaggerating the differences between S5 and S6. BC = Bray-Curtis dissimilarity between S5 and the sample in a given column (for the log-transformed data, the comparisons were made with the log-transformed S5).

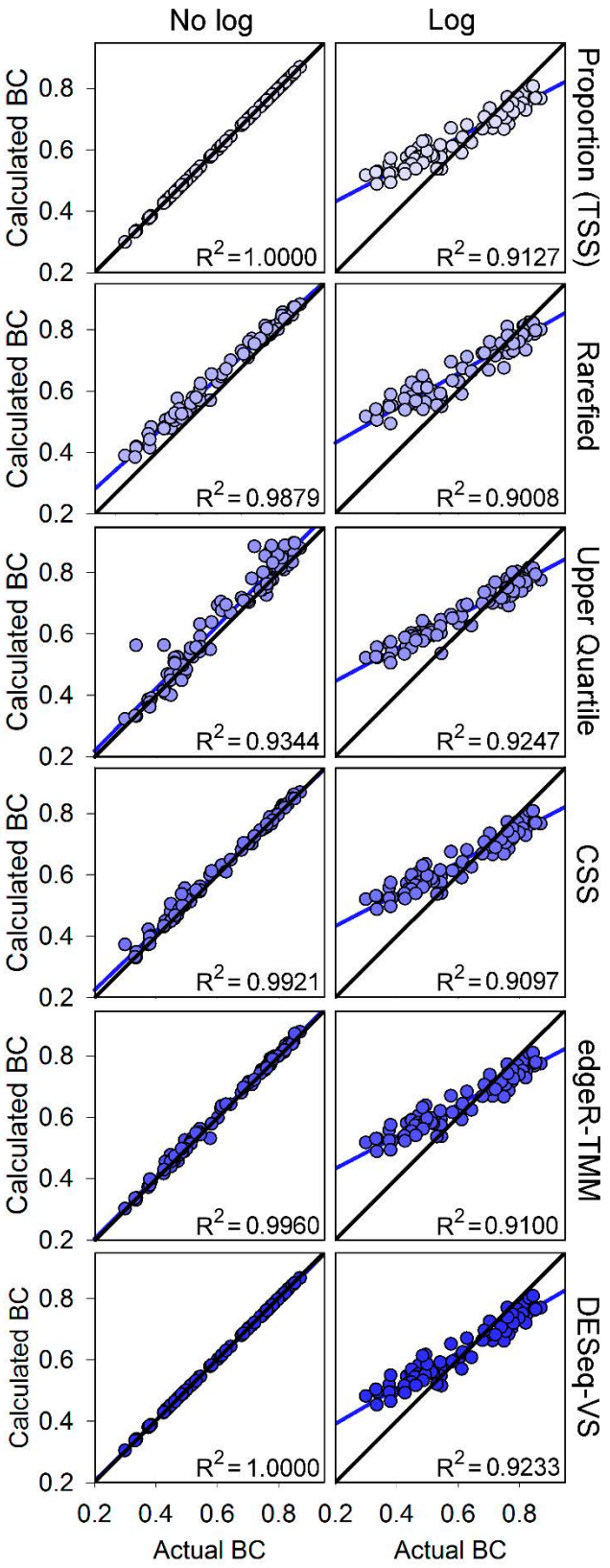

Figure 5.3 — Correlations between the Bray-Curtis dissimilarities for the original (non-normalized [true]) data and the Bray-Curtis dissimilarities following normalization. Black lines show a slope of one and intercept of zero. These data are from the mouse gut

microbiome data set, and only the 81 pairs of samples where the percent difference between read depths was <0.5% for the original data are shown (all data were used during the normalization step). It should be noted that DESeq-VS has the option of doing transformations “blind” (i.e., without incorporating *a priori* knowledge about groups) or with *a priori* knowledge. For this data set, the results were highly inaccurate if *a priori* information was used. Therefore, I presented the results without *a priori* information here, and the results with *a priori* information are available in Additional file 5.1.

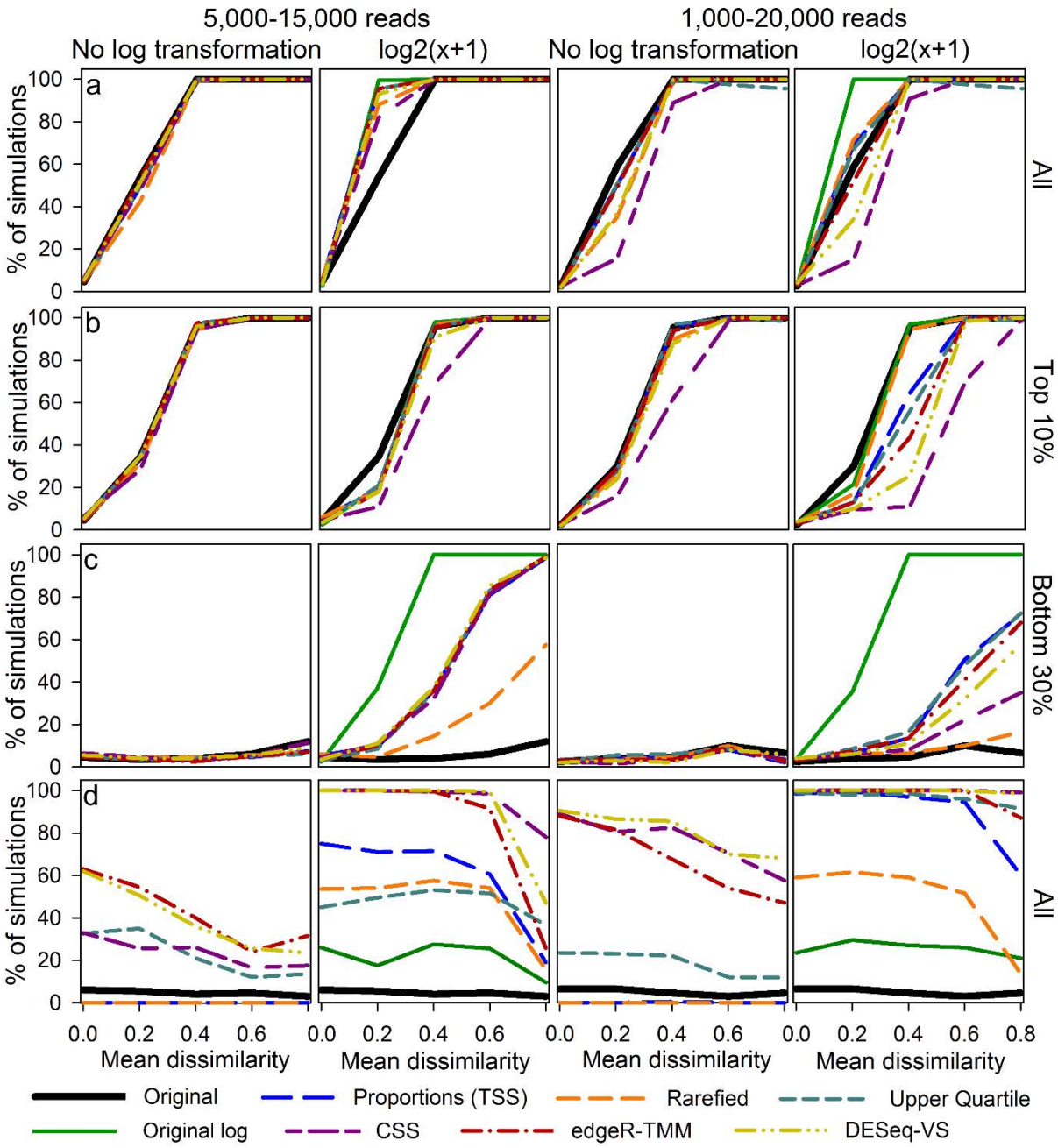

Figure 5.4 — Simulation results. (rows a–c) The percent of iterations (out of 200) where a PERMANOVA returned a significant difference (α = 0.05) between the populations. (row d) The percent of iterations (out of 200) where there was a significant correlation (α = 0.05) between read depth and mean Bray-Curtis dissimilarity (mean per individual). These are spurious correlations that indicate a failure of the normalization method. Mean dissimilarity = the setting for the difference between the distributions from which the populations were constructed (0 = identical distributions, 0.8 is highly dissimilar), All = all OTUs were allowed to vary between the two distributions on which the populations were based, Top 10% = only the OTUs in the 90th percentile and above (based on DNA yield for population 1's

distribution) varied between distributions, Bottom 30% = only the OTUs in the 30th percentile and below varied. The thick black “Original” line shows the results for the real communities without a log transformation (even in the log2(x+1) columns, where is serves as a point of comparison); whereas the green “Original log” line shows those data following a log2(x+1) transformation.

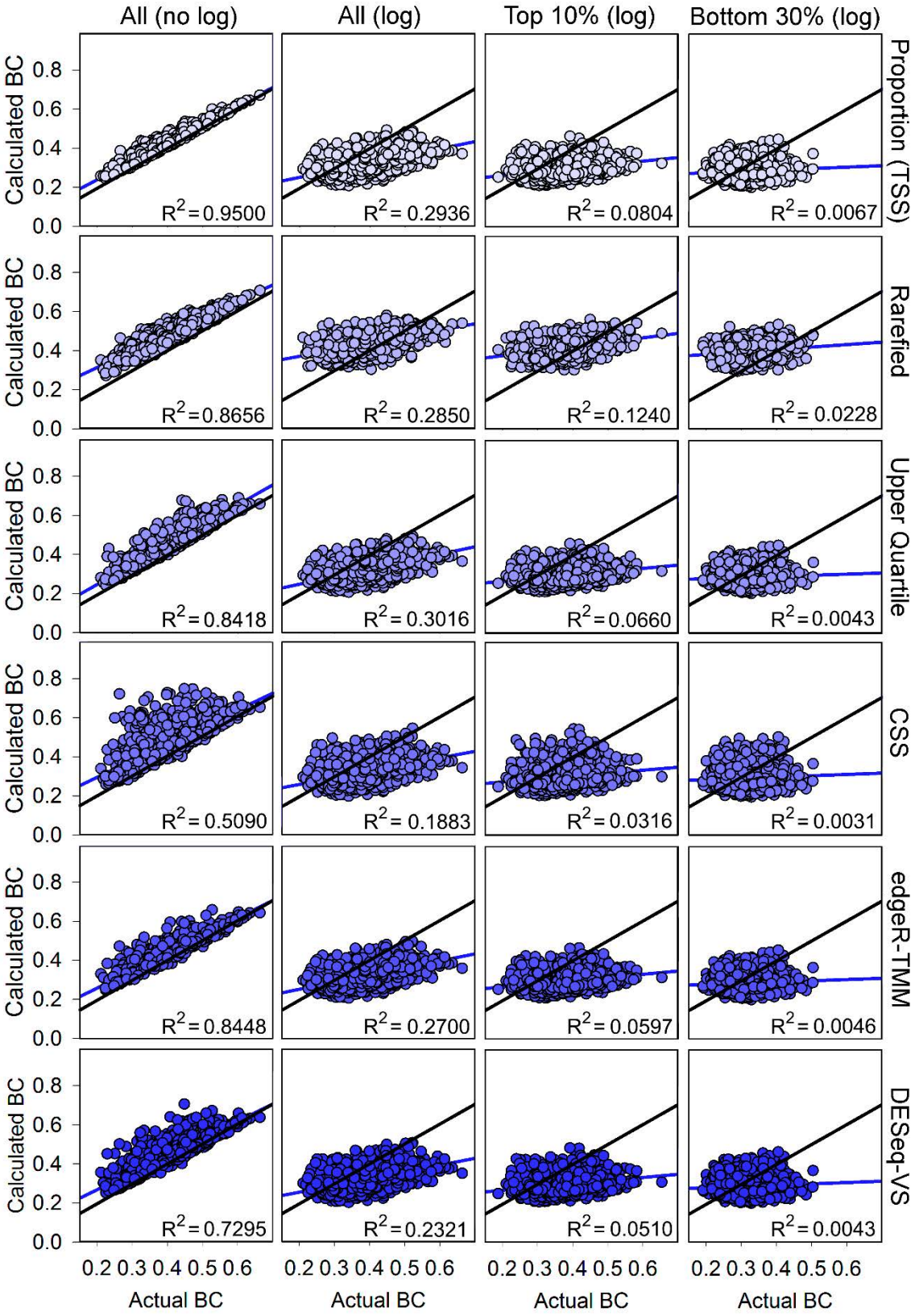

Figure 5.5 — Correlations between the Bray-Curtis (BC) dissimilarities for the original communities ("Actual BC") and the BC dissimilarities following normalization. Black lines show a slope of one and intercept of zero. Data are from 200 iterations of the simulator (per

column). All = all OTUs were allowed to vary between the two distributions on which the populations were based, Top 10% = only the OTUs in the 90th percentile and above (based on DNA yield for population 1's distribution) varied between distributions, Bottom 30% = only the OTUs in the 30th percentile and below varied, log = the data were transformed with a log2(x+1) transformation.

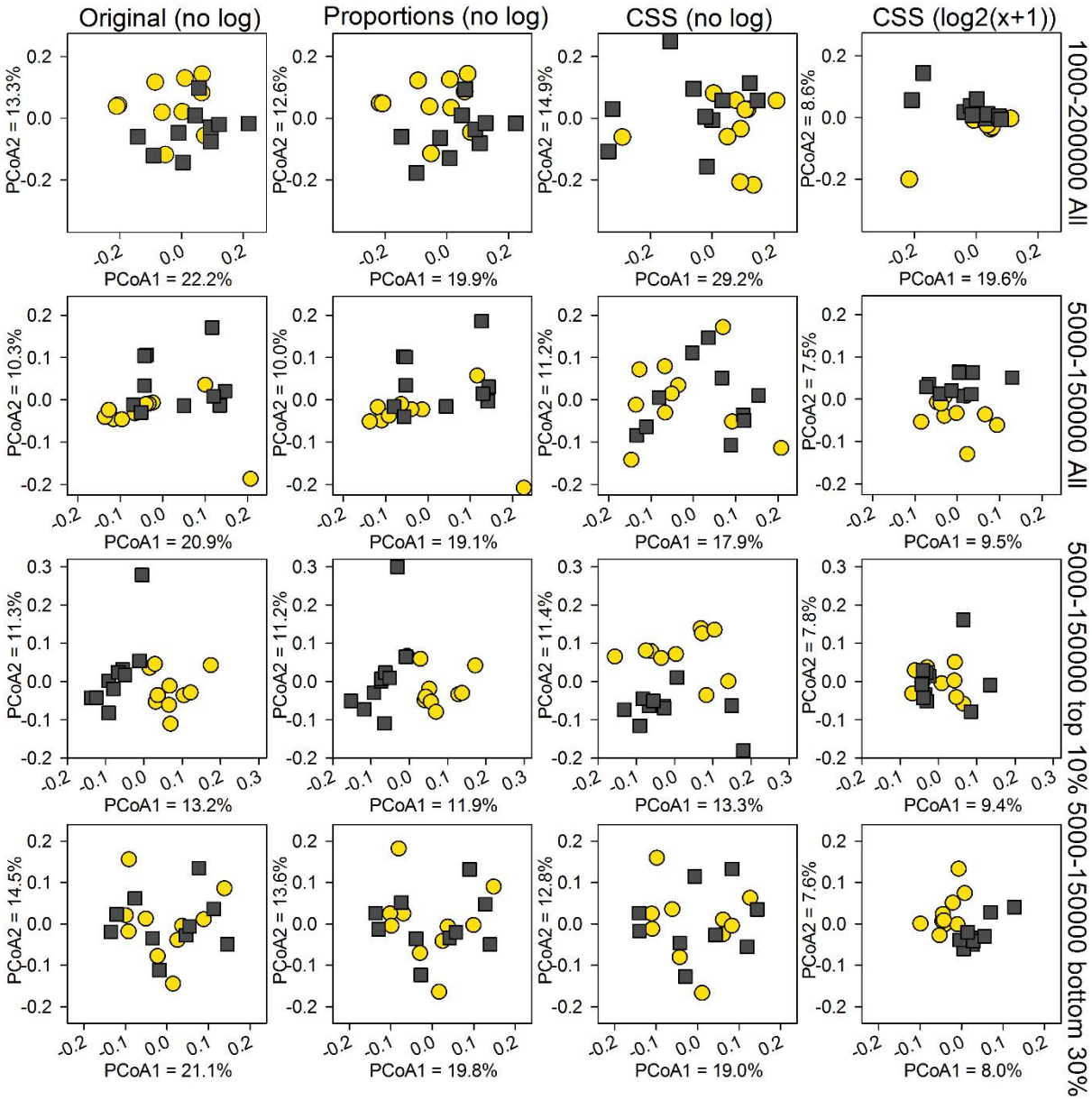

Figure 5.6 — Example simulation results of PCoAs comparing population 1 (yellow circles) with population 2 (dark squares) using different normalization methods. Original = the real communities prior to sequencing. Proportions and rarefying generally produced results that were very similar to the original data. Following a log transformation, all methods often produced clusters that were not present in the original data (when all OTUs or only the bottom 30% varied between the initial distributions) or failed to produce clusters that were present in the original data (when only the top 10% of OTUs varied between the initial distributions). For log-transformed data, only CSS is presented here because of that method's popularity, but other methods involving a log transformation produced similar results (full results are available in Additional file 5.1). 1000–20000 and 5000–15000 = the range from which the numbers of reads per sample were randomly selected for each

sample, All = all OTUs were allowed to vary between the two distributions on which the populations were based, Top 10% = only the OTUs in the 90th percentile and above (based on DNA yield for population 1's distribution) varied between distributions, Bottom 30% = only the OTUs in the 30th percentile and below varied. For rows 1 and 2, the mean dissimilarity was set to 0.2, for row 3 it was 0.3, and for row 4 it was 0.8.

CHAPTER 6: MICRODECON: A HIGHLY ACCURATE READ-SUBTRACTION TOOL FOR THE POST-SEQUENCING REMOVAL OF CONTAMINATION IN METABARCODING STUDIES

Published as: McKnight, DT, R Huerlimann, DS Bower, L Schwarzkopf, RA Alford, KR Zenger. 2019. microDecon: A highly accurate read-subtraction tool for the post-sequencing removal of contamination in metabarcoding studies. *Environmental DNA* 1:14–25.

Abstract

Contamination is a ubiquitous problem in microbiome research and can skew results, especially when small amounts of target DNA are available. Nevertheless, no clear solution has emerged for removing microbial contamination. To address this problem, I developed an R package (microDecon), which uses the proportions of contaminant operational taxonomic units (OTUs) in blank samples to systematically identify and remove contaminant reads from metabarcoding data sets. I rigorously tested microDecon using a series of computer simulations and a sequencing experiment using actual samples. I also compared it to the common practice of simply removing all contaminant OTUs. Both the computer simulations and my sequencing data confirmed the utility of microDecon. In my largest simulation (100,000 samples), using microDecon improved the results in 98.1% of samples. Additionally, in the sequencing data and in simulations involving groups, it enabled accurate clustering of groups as well as detection of previously obscured patterns. It also produced more accurate results than simply removing contaminant OTUs. These results demonstrate that microDecon effectively removes contamination across a broad range of situations. It should, therefore, be widely applicable to microbiome studies, as well as to metabarcoding studies in general.

Box 1. Definitions of Terms

- Blank = a negative control collected at the same time as the samples and carried through the entire extraction, amplification, and sequencing process
- Constant = an OTU that is entirely contamination and is used as the basis for decontaminating samples
- Contaminant OTUs = OTUs that amplified in the blank
- Entirely contamination = contaminant OTUs that would not be found on an uncontaminated sample (i.e., they occur on the species, substrate, etc. that is being studied)
- OTU = operational taxonomic unit
- OTUs not in the blank = OTUs that did not amplify in the blank
- Overlapping OTUs (overlap) = contaminant OTUs that would also be found on an uncontaminated sample (i.e., they occur on the species, substrate, etc. that is being studied as well as in the source of contamination; thus, some of their reads are real and some are from contamination)
- Simulation control = a comparison between uncontaminated and decontaminated/contaminated samples using only the OTUs that were not in the blank (subsetting is done before any transformations). Because those OTUs are unaffected by contamination, they act as a control for background heterogeneity.

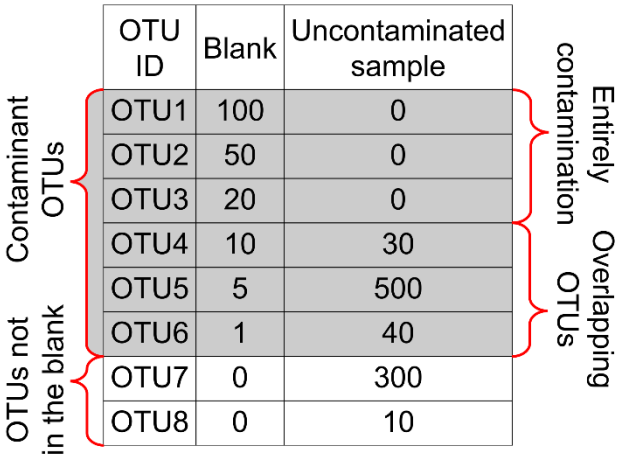

OTU ID	Blank	Uncontaminated sample
OTU1	100	0
OTU2	50	0
OTU3	20	0
OTU4	10	30
OTU5	5	500
OTU6	1	40
OTU7	0	300
OTU8	0	10

Box 6.1 Figure 1 — Hypothetical sequencing reads, illustrating the terms used in this paper (in an actual study, the uncontaminated sample would be unknown).

Introduction

Advances in sequencing technology have greatly expanded our ability to harness the power of metabarcoding for studying microbial communities, and it is now possible to sequence an entire community using a minuscule amount of starting material. However, our ability to detect organisms from just a few fragments of nucleic acid is both a blessing and a curse; while it greatly improves our detection of target species, it also carries the risk of sequence contamination. Indeed, there is growing recognition that contamination (especially bacterial contamination) is a serious hindrance in microbiome studies, and several studies have documented that contamination is ubiquitous, even in places that should be DNA/RNA free, such as molecular grade water, PCR polymerases, and DNA extraction kits (Corless et al. 2000; Kulakov et al. 2002; Peters et al. 2004; Shen et al. 2006; Hang et al. 2014; Weiss et al. 2014). Contamination is particularly problematic for studies using low-biomass samples, where even a small amount of contamination can severely affect the results (Salter et al. 2014).

Although this problem is widespread, no clear solution has emerged. Good laboratory techniques are important but cannot eliminate contamination, because many kits and PCR reagents are contaminated (Salter et al. 2014) and contamination can occur when the samples are being collected. To address these issues, strategies such as using a single kit for all extractions or randomizing samples across kits and PCR runs have been recommended (Salter et al. 2014; Weiss et al. 2014). Additionally, various methods have been proposed for removing contamination from kits and reagents, but mixed levels of success have been reported, and they often cause PCR inhibition (Mohammadi et al. 2005; Rueckert and Morgan 2007; Champlot et al. 2010).

None of the proposed methods are likely to eliminate contamination in all cases; therefore, there is still a need to identify and deal with contamination post-sequencing. Some researchers have advocated for a log-ratio test for identifying contamination (Robinson et al. 2017), while others have suggested that contaminants can be identified by looking for negative correlations between pre-standardization amplicon concentration and the relative abundance of operational taxonomic units (OTUs) post-sequencing (Jervis-Bardy et al. 2015). Perhaps the most effective and straightforward suggestion is simply to use negative controls (hereafter called “blanks”) that are carried through the entire collection,

extraction, amplification, and sequencing process (Barton et al. 2006; Salter et al. 2014). These blanks can then be used to quantify the levels of contamination present.

Regardless of the mechanism used to detect contamination, the problem of what to do once it has been detected remains. One option is to simply report the level of contamination, but this is unsatisfactory as it is difficult to know the influence of contamination on comparisons among groups. To solve this dilemma, some researchers have advocated the use of mock communities that are extracted, amplified, and sequenced alongside actual samples (Wilner et al. 2013; Brooks 2016). In some situations, this is likely to be a very useful approach, especially when working with low-diversity communities and in situations where a research group frequently works with similar communities. Indeed, in situations with little contamination, it may even be possible to use the mock community to establish an abundance threshold that can be used to filter out contamination (Wilner et al. 2013; Brooks 2016). For many applications, such as sequencing diverse communities and exploratory research, however, constructing a meaningful mock community is often not feasible, and thresholds will not be effective for communities with either many rare OTUs or high quantities of contamination.

One obvious solution is to simply remove any contaminant OTUs from all samples (Segal et al. 2013; Jervis-Bardy et al. 2015). In cases where there are very few contaminant OTUs, or there is a solid biological basis for thinking those OTUs should not be present, or both, that may be a good solution. In many cases, however, contaminant OTUs are likely to occur naturally on the host or in the environment being studied, as well as being present as contamination (hereafter these will be called “overlapping OTUs”). Simply removing any contaminant OTUs therefore removes potentially important data and can either artificially exaggerate or reduce any differences among groups (depending on whether those OTUs are equally abundant across groups). A final option is to simply subtract the contaminant reads from the reads in the samples; however, this is also problematic because read depth typically differs among samples. Further, because samples are standardized prior to sequencing, samples with few OTUs (such as contaminated blanks) will have more reads per OTU than diverse samples.

Because of the problems associated with the removal of contamination enumerated above, a better solution is clearly needed. Thus, I developed and rigorously tested the R package microDecon, which provides several easy-to-use tools for identifying and removing

contamination. microDecon uses information from blank samples to calculate and remove the contaminant reads for each OTU, rather than simply consigning an entire OTU to contamination. As such, it provides a substantial improvement over current methods, and importantly, avoids the loss of useful data.

Methods

microDecon

The package microDecon operates on the principle that all the samples will receive the same proportions of contamination from a common source. For example, if a contaminated reagent contains 100 ng/µL of OTU1 and 50 ng/µL of OTU2, then each sample should receive twice as much OTU1 contamination as OTU2 contamination. Thus, if I can identify an OTU that is entirely contamination (hereafter referred to as the "constant"), I can use it to calculate the number of reads in the actual sample that originate from contamination. microDecon does this in the following steps (illustrated in Figure 6.1). First, it subsets the data to include only the contaminant OTUs (i.e., OTUs that amplified in the blank). Second, it estimates the number of overlapping OTUs and uses that estimate to identify the best OTU to use as the constant (the algorithms it uses are based on regression equations that I developed through numerous simulations; details in Additional file 6.1). Third, it divides the reads for each OTU in the blank by the number of reads for the constant in the blank. Fourth, it multiplies those values by the number of reads for the constant in the actual sample. This produces the number of reads in the actual sample that are from contamination, and those reads are then subtracted. This entire process is done iteratively for each sample. Thus, each sample is treated completely independently.

As an example, consider a sample and blank with two OTUs that amplified in the blank. In the blank, OTU1 has 1000 reads, and OTU2 has 100 reads. Thus, the ratio for those OTUs in the blank is 10:1. If I also know that one of those OTUs is entirely contamination (i.e., a constant), I can use that to determine the number of reads in the sample that are from contamination for both OTUs. If, for example, I know that OTU1 is entirely contamination, and in the sample, OTU1 has 600 reads while OTU2 has 100 reads, I can deduce that all 600 reads for OTU1 are from contamination and, based on the 10:1 ratio in

the blank, 60 of the reads for OTU2 are from contamination. Therefore, a decontaminated sample would have zero reads for OTU1 and 40 reads for OTU2. Because this method relies on the proportions of OTUs in the blank relative to a constant, rather than the raw number of reads, it does not require samples to have consistent amounts of starting material or read depths. Thus, the results of the example with two OTUs above would be the same if the OTUs in the blank had one million reads and one hundred thousand reads (respectively) or ten reads and one read (respectively).

This method is clearly dependant on identifying an appropriate constant. The algorithms for doing this are described in detail in Additional file 6.1, but briefly, the percent difference between the proportions of reads in the blanks and portions of reads in the samples (i.e., the fourth table in Figure 6.1) are useful for determining if an OTU is entirely contamination. When the percent difference is positive, it suggests that an OTU is under-represented in the sample, likely indicating that it is entirely contamination; whereas when it is negative, it suggests that the OTU is over-represented in the sample, likely indicating that it is an overlapping OTU. Based on my simulations, most OTUs with a positive percent difference will perform well as a constant, but both very large and very small positive percent differences tend not to perform optimally. Therefore, I used extensive simulations to examine correlations between known parameters in a dataset and the rank of the best OTU to use as the constant. From those simulations, I developed several regression equations for identifying the constant, and microDecon automatically selects among those regressions based on the data set it is given (see Additional file 6.1 for details).

Due to the potential pitfalls of any novel method, I rigorously tested microDecon over a wide range of situations, including both simulated 16S data sets and a real, sequenced data set, to ensure that the method was robust. I also compared microDecon with the common strategy of simply removing all contaminant OTUs, as well as with the method of detecting and removing contaminant OTUs proposed in Jervis-Bardy et al. (2015). I used the primary function in the microDecon package (decon()) on its default values for all tests. The function, its input parameters, and the tests I used to identify the best default values are explained in the microDecon User's Guide.

Simulation 1: individual samples

I wrote a simulation in R (R Team, 2017) to test the utility of microDecon, (Additional file 6.2). For each iteration, this simulation creates an uncontaminated microbial sample, as well as an artificial contaminant community. It then uses the contaminant community to contaminate the sample (a copy of the contaminant community is saved as a blank). Next it processes and "sequences" the sample and the blank. Finally, it uses microDecon to decontaminate the contaminated sample.

Within each iteration, each OTU in the contaminant community is multiplied by a number that is randomly selected from a user-defined normal distribution before adding the contamination to the sample (a new number is selected for each OTU). This simulates heterogeneity from DNA extraction and library preparation. Additionally, the communities are *in-silico* "sequenced" by repeatedly randomly selecting DNA copies from the entire community (each OTU is coded as a number of DNA copies), which simulates heterogeneity from actual sequencing. Full details on the simulation and input OTU distribution are available in Appendices 3 and 4.

I ran 100,000 iterations of this simulation over a broad range of situations, including varying amounts of starting material and varying amounts of contamination (varied both in terms of numbers of OTUs and DNA yield for those OTUs). For each iteration, the input parameters were randomly selected from the following values: number of OTUs that were entirely contamination = 0–150, number of OTUs not in the blank = 50–1000, and number of overlapping OTUs = 0–150 (OTUs were randomly sampled from a supplied distribution, resulting in varying amounts of DNA per OTU). I created within-iteration heterogeneity in the contamination that was applied to the sample by multiplying each OTU by a number that was randomly selected from a normal distribution with a mean between 0.15–1.0 and SD that was the mean multiplied by 0.1–0.7 (a new number was randomly selected for each OTU, and a new mean and SD were randomly selected for each iteration). This produced a median contamination level of 0.12 (range = 0.0002–10.4; i.e., the amount of contaminant DNA that was applied to a sample divided by the amount of DNA in the uncontaminated sample). Finally, the number of sequencing reads for the blank and the sample were independently selected from a range of 18,000–20,000.

For each iteration, I calculated Bray-Curtis dissimilarities (BC) between the uncontaminated versus contaminated sample and uncontaminated versus decontaminated

sample and used those dissimilarities to judge the effectiveness of microDecon. Throughout this study, I calculated all BC by transforming the data to proportions (McKnight et al. 2019a) and using the vegan package in R (Oksanen et al. 2017). Additionally, I applied multiple linear regression to the results to see how different factors affected the effectiveness of microDecon (results are presented in Additional file 6.3).

Finally, I ran 10,000 iterations of a slightly modified version of simulation 1 that tested the effects of simply removing contaminant OTUs (i.e., all contaminant OTUs were set to zero in the final sample). It returned BC for the contaminated versus uncontaminated sample, decontaminated (with microDecon) versus uncontaminated sample, and sample with contaminant OTUs removed versus uncontaminated sample. I used the same settings as simulation 1.

Simulation 2: groups of samples

I used a second simulation to examine the effects of microDecon at a group level (i.e., the effects when examining multiple samples from different populations, species, environments, etc.; Additional file 6.5). The core code and functionality of this simulation is similar to simulation 1, but there are a few key differences. First, it simulates two groups with a user-defined number of samples per group (samples in each group are more similar to each other than to samples in the other group). Additionally, it creates variability in the amount of DNA present in each sample. The samples are then contaminated as in simulation 1, but the procedure for producing heterogeneity in the contaminated community is applied separately for each sample. Thus, there is variation in the proportions of OTUs in the contamination applied to each sample. Within each group, it returns mean BC for comparisons between the uncontaminated and contaminated samples as well as the uncontaminated and decontaminated samples. Additionally, it returns mean BC for comparisons between the groups for the uncontaminated, contaminated, and decontaminated samples. Full details on the simulation and input OTU distribution are available in Appendices 3 and 6.

I used this simulation to compare groups of 5, 10, and 20 samples each (100 iterations per group size). For each iteration, there were a total of ~500 OTUs, of which ~120 amplified in the blank (the exact numbers varied because of stochasticity in the simulation). Of the ~120 contaminant OTUs, ~30 were entirely contamination, ~30 overlapped with

group 1, but not group 2, ~30 overlapped with group 2 but not group 1, and ~30 overlapped with both groups. I varied the level of contamination between groups by giving samples in group 1 an average of 2.2 times the amount of starting material as samples in group 2. As a result, the level of contamination (DNA yield in contamination/DNA yield in sample) in group 1 had a mean of 0.05 (range = 0.02–0.13) and group 2 had a mean of 0.11 (range = 0.05–0.27).

Sequencing experiment

I constructed a sequencing experiment using fungal microbiota. I used fungal microbiomes because they are less prone to contamination than are bacterial microbiomes and eliminating unwanted background contamination was vital for this experiment. Therefore, conducting this experiment on bacteria was not possible because contamination-free bacterial samples are extremely difficult to achieve. Nevertheless, because microDecon simply uses ratios of OTUs, it is not taxa-specific, and there is no *a priori* reason to expect it to behave differently for different taxa. Indeed, this becomes obvious when one considers the fact that microbiome simulations do not specify the taxa, and simulated OTUs can be discussed as bacterial OTUs, fungal OTUs, protist OTUs, etc. Thus, given that the same methodologies are used to produce bacterial and fungal OTU tables, testing this method on fungi rather than bacteria is completely valid and does not affect the applicability of my results.

Briefly, I constructed a contaminant fungal community (consisting of cells, rather than DNA). I then collected eight soil samples: four from a dry stream bed (group 1) and four from a nearby forest (group 2) and added two fungal species that I included in my contaminant community. I did this to ensure that at least a few OTUs would be present among all samples, as well as in my contamination. Next, I homogenised the samples, split them in half, and added 90 µL of my contaminant community to one of the halves of each sample, producing both an uncontaminated and contaminated copy of each sample. For one sample from each group, I split it into thirds and only contaminated one third so that I would have replicate uncontaminated samples; unless otherwise noted, I only used the first of those two replicates in the analyses and summary statistics to avoid pseudo-replication. I also added 90 µL of contamination to each of four empty vials. These served as my blanks and allowed us to test the assumption that the contamination ratios would be

homogeneous across samples. To account for background contamination, I also analysed a control vial that did not receive my contaminant community. This produced a total of three reads from only two OTUs; therefore, given that the actual samples consisted of thousands of reads and had been diluted to a standard concentration prior to sequencing (whereas this control sample did not have detectable levels of DNA by either gel electrophoresis or Enspire quantification), I considered that level of background contamination to be inconsequential and do not discuss it further.

I extracted the DNA from all samples using a CTAB protocol (Doyle and Doyle 1987) modified to include a bead beating step, and, with a few exceptions, I followed the Illumina 16S Metagenomics Sequencing Library Preparation guide (Illumina 2017) to prepare my samples. I used the ITS3_KY02/ITS4 primer pair to amplify the ITS2 region of the fungal genome (Toju et al. 2012). Also, I used 10 µL reactions and 30 cycles for the amplification PCR, and 40 µL reactions for the indexing PCR. For clean-ups, I used Sera-mag SpeedBeads rather than AMPure beads. I sequenced the samples on an Illumina Miseq (Reagent kit V3 600 cycles PE, Illumina, USA). More details of my experimental design and methods are available in Additional file 6.3.

After sequencing, I used PIPITS (v1.4.5) (Gweon et al. 2015) to prepare a read pairs list (*pipits_getreadpairlist*), process the reads (*pipits_prep*) using PEAR (Zhang et al. 2013), and extract the ITS region (*pipits_funits*), according to the user manual. I followed this with chimera checking (*identify_chimeric_seqs.py*) using usearch61 (Edgar et al. 2011), and *de novo* OTU picking (*pick_de_novo_otus.py*) in QIIME (v1.9) (Caporaso et al. 2010), using the 97% sequence similarity UNITE database (12_11, alpha release) (Abarenkov et al. 2010). In some cases, multiple OTUs were identified as the same species; therefore, I combined those OTUs for each fungal species. Sequencing results are available in Appendices 7 and 8.

Following sequencing, filtering, and annotation, I applied microDecon to the contaminated samples, producing three data sets: uncontaminated, contaminated, and decontaminated. I used the data from all four blanks to decontaminate the samples (tests comparing the effects of using multiple blanks are available in Additional file 6.1).

I tested the utility of microDecon in several ways. First, I used PERMANOVAs via the adonis2() function in the vegan package to compare the uncontaminated and contaminated samples, as well as the uncontaminated and decontaminated samples (Oksanen et al. 2017) (contamination status and group were factors; sample was the strata; 5000 permutations).

To avoid spurious signals from heterogeneity in OTUs that were not present in the blanks, and more effectively test microDecon, I subset the data to include just the contaminant OTUs. . Additionally, I examined BC both within and among groups. Finally, I compared microDecon with the method of detecting and removing contaminant OTUs proposed in Jervis-Bardy et al. (2015). This test and its results are available in Additional file 6.3.

Results and Discussion

Simulation 1: individual samples

microDecon reduced or eliminated the contamination in 98.1% of simulated samples (out of 100,000, each with a different starting community and different contaminant community). As expected, the BC between the uncontaminated and decontaminated samples was consistently lower than the BC between the uncontaminated and contaminated samples, with the effect becoming exaggerated as the amount of contamination increased relative to the amount of DNA in the sample (Figure 6.2). This indicates that microDecon was accurately removing contamination and restoring samples to their proper OTU distributions.

Nevertheless, because my simulations included heterogeneity from extraction and sequencing, as would occur in actual studies, I did not expect decontaminated samples to perfectly match their uncontaminated counterparts, even if they were fully decontaminated. To assess this background heterogeneity, for each decontaminated sample, I used "simulation controls" by subsetting the sample to only the OTUs that did not amplify in the blank and comparing that subset community with the corresponding OTUs in the uncontaminated sample. Because microDecon only affects the OTUs that amplified in the blank (i.e., contaminant OTUs), the OTUs that did not amplify in the blank would have been unaffected by microDecon but would have been affected by stochasticity in the simulation. Therefore, they could be used to measure the background heterogeneity.

I compared the BC frequency distribution between the simulation controls, decontaminated samples, and contaminated samples, with the expectation that the simulation controls and decontaminated samples should have similar distributions, while the contaminated samples should be shifted towards high BC. The results largely matched my predictions, suggesting that microDecon was successfully removing contamination

(Figure 6.3A). The decontaminated distribution was shifted slightly from the simulation control distribution, but this was not unexpected, because BC increased as the number of OTUs increased (Figure 6.3B), and the control communities consisted of a subset of the OTUs in the decontaminated communities. Thus, the decontaminated communities always contained more OTUs and, therefore, I expected them to always have slightly higher BC.

To examine the failure rate of microDecon, I examined the number of iterations in which the decontaminated sample versus the uncontaminated sample had a higher BC than the contaminated sample versus the uncontaminated sample (i.e., cases where microDecon shifted the community further from the uncontaminated community). If microDecon was effective, then I expected that there would be few of these cases, the increases in BC should be small, and most "failures" should occur when then contamination levels were extremely low (in terms of DNA yield), thus making them indistinguishable from stochastic fluctuations in the simulation (Figure 6.3). These expectations were met. Out of the 100,000 iterations, only 1,885 (1.9%) were "failures," and those samples were characterized by low levels of contamination, resulting in low BC when either the contaminated or decontaminated samples were compared to the uncontaminated samples (Additional file 6.3). Additionally, the shifts in BC were generally small. For 1,019 of these samples (54.1%) the decontaminated BC were less than 0.005 BC units higher than the contaminated BC, for 1,463 (77.6%) the BC were less than 0.01 higher, and for 1,720 (91.2%) the BC were less than 0.02 higher. Only 20 iterations were off by more than 0.05.

Nevertheless, a few of the iterations with higher BC do appear to be true microDecon failures and merit further discussion. These generally occurred when samples had very few OTUs that were entirely contamination (Additional file 6.3). Indeed 84 of the "failures" (including the worst one) had no OTUs that were entirely contamination. Given that microDecon operates by finding an OTU that is entirely contamination (the constant), it makes sense that it would struggle in situations where no OTUs are entirely contamination. Nevertheless, in the entire data set (all 100,000 iterations), there were 605 cases with no OTUs that were entirely contamination, and in every case except for these 84, microDecon still improved the results, which can be viewed as an 86.1% success rate even under the worst situation for this method. Additionally, in real microbiome studies, it is unlikely that all of the contaminant OTUs would overlap with the sample's natural (non-contaminant) OTUs. Also, it should be stressed that these results are for individual samples. Thus, the net effect

on a group may still be positive, even if one particular sample was negatively affected. Finally, these samples all used two runs of the decon() function (default), but for samples with very low contamination, the results can be improved by only using one run (see microDecon User's Guide).

Finally, my comparison of microDecon versus the method of simply removing contaminant OTUs showed that microDecon produced more accurate results (Figure 6.4). As expected, the problems with simply removing contaminant OTUs became exaggerated as the proportion of OTUs that were contaminants increased, and when over roughly 20% of the OTUs were contaminants, removing them was actually worse than making no correction at all (Additional file 6.3). However, even when fewer than 5% of the OTUs were contaminants, applying microDecon was superior (mean BC = 0.054: SD = 0.01) to removing the contaminant OTUs (mean = 0.06; SD 0.02).

Simulation 2: groups of samples

If microDecon was effective, then I expected the mean BC per group to be lower for decontaminated versus uncontaminated samples than for contaminated versus uncontaminated samples (Figure 6.5). This prediction was met for both groups in all 300 iterations, once again demonstrating that microDecon restores samples to their correct distributions. This was particularly true for group 2, which had less than half the sample DNA of group 1 (on average).

The benefits of decontamination could also be seen when the two groups were compared within an iteration (Figure 6.6 Because contamination affected all samples in an extraction/sequencing run (iteration), I expected it to make samples more similar to each other, and that is what I observed. Further, the decontamination procedure corrected this, and returned the groups to approximately the correct level of difference (Figure 6.6). I also visualized this using PCoAs (I used the cmdscale() function in the package vegan) (Figure 6.7A–C). Although the decontamination procedure clearly improved the samples, it did not produce BC that were quite as low as the simulation controls. As explained in the Simulation 1 section, this is at least partially an artefact cause by more OTUs being present in the decontaminated samples.

As a final means of assessing the accuracy of microDecon, I examined bar plots showing the proportions for each OTUs in the uncontaminated, decontaminated, and

contaminated samples (Figure 6.8). For simplicity, I have only illustrated the results from the iterations with five samples per group, but to avoid showing cherry-picked results, I have presented the best, median, and worst iteration. The improvements are obvious in the best and median panels, and although they are less obvious for the worst panels, the decontaminated samples still had lower BC than the contaminated samples.

Sequencing experiment

The sequencing experiment provided powerful evidence that microDecon performs well under experimental conditions and accurately removes contaminant reads while retaining the reads from the actual sample. It also demonstrated the validity of my assumption that each sample would receive roughly equal ratios of contaminants.

Sequencing produced a total of 1,598 OTUs; however, the majority of OTUs were not present in most samples, and on average, the uncontaminated samples contained only 361 OTUs (range = 183–511). There were 74 OTUs in the contaminated blanks (when all four blanks were averaged), 47 of which overlapped with the uncontaminated samples in group 1, and 48 of which overlapped with the uncontaminated samples in group 2. Additionally, the second most common OTU in the blank (*S. cerevisiae*; mean = 31.6% of reads in the blank) was also highly abundant in the uncontaminated samples (mean = 44.4%; range = 25.6–69.4%), and the most abundant OTU in the blank (an unidentified fungus; mean = 33.6% of reads in the blank) was present in the uncontaminated samples at low levels (mean = 0.1%, range = 0.03–0.38%). Finally, to obtain a proxy for contamination level, for each sample I divided the number of reads that were removed by microDecon by the number of reads in the decontaminated sample, which resulted in a mean contamination level of 0.31 (range = 0.14–0.63). This combination of high levels of contamination, and lots of OTUs that overlapped between the blank and the sample (including overlap with one of the most numerous members of each community) produced a situation approaching a worst-case scenario for microDecon. Therefore, this experiment should provide a useful test of the method's effectiveness.

Several tests confirmed the utility of microDecon. First, at the broadest scale, and as I would expect given that microDecon should be decontaminating samples and making them more similar to uncontaminated samples, there was no significant difference between the uncontaminated and decontaminated samples (PERMANOVA; pseudo-F =0.66, P = 0.620),

whereas there was a significant difference between the uncontaminated and contaminated samples (pseudo-F = 52.24, P = 0.002). At an alpha of 0.05, the groups were significantly different in both tests, but at a more stringent alpha of 0.01, they were significantly different for the uncontaminated versus decontaminated test (pseudo-F = 5.43, P = 0.002) but not the uncontaminated versus contaminated test (pseudo-F = 4.99; P = 0.026). The interaction term was not significant in either test (pseudo-F < 0.35, P > 0.720). All these results demonstrate that contamination caused the communities to shift away from their true values, and microDecon restored them to approximately their proper (uncontaminated) distributions. Similarly, the difference between the two groups was easier to detect for the decontaminated samples than it was for the contaminated samples. For these tests, all four blanks were used, however, there was little heterogeneity among the blanks and the choice of blank had little impact on the results, thus supporting the assumption that the contamination ratios would be similar across samples (Additional file 6.1).

The utility of microDecon was also supported by the BC. For all eight samples, the BC was lower for the uncontaminated versus decontaminated sample than it was for the uncontaminated versus contaminated sample. This is also reflected in the PCoAs (Figure 6.7D) and stacked bar plots (Figure 6.9). Because heterogeneity in the OTUs that were not in the blank partially obscured the effects of both contamination and decontamination, subsetting the data allowed the trends to be seen more clearly, so I subset the data to just the contaminant OTUs for both visualizations. In Figure 6.7D, it is clear that contamination made the two groups more similar to each other and resulted in greater overlap between them, while the decontaminated results align closely with the uncontaminated results. Similarly, in Figure 6.9, there are several prominent OTUs in the contaminated samples that were completely or largely removed in the decontaminated samples, while the proportions for the OTUs that were retained in the decontaminated samples closely match the proportions for the OTUs in the uncontaminated samples. They do not match perfectly, but that is to be expected because background heterogeneity causes small variations among groups, illustrated by the differences between the replicate uncontaminated samples.

Conclusion and Recommendations

I have demonstrated the usefulness of the microDecon package for decontaminating samples *via* both computer simulations and a sequencing experiment, and I believe that this package will be broadly applicable across the microbiome research community. My tests covered a wide range of situations, including low-yield samples and samples with high levels of contamination, and my method is robust to these situations. Indeed, my sequencing experiment included high contamination levels and a large overlap between the contaminant community and real community, but microDecon was still able to closely recover the real community. Therefore, I recommend that researchers use the following steps in their research.

1. Collect several blank samples at the same time and in the same manner as the actual samples are collected. These should be carried through the entire extraction process, rather than simply using no template PCR controls.
2. If possible, do all DNA extractions using a single kit and single batch of reagents. If this is not possible, then use several blanks (at least 3–4) per kit and per batch of reagents. Treat these statistically as blocks and randomize your samples across the blocks.
3. Sequence the samples and blanks including several blanks per block. If a study involves many blocks and has insufficient sequencing depth for all of the blanks, then pool the blanks per block prior to indexing. If multiple blanks are included within a block in the final analysis, microDecon converts them to proportions and uses the mean of those proportions (see User's Guide for details).
4. Use standard filtering and bioinformatic processing steps to produce an OTU table, but do not transform, normalize, rarefy, or otherwise modify the read counts prior to using microDecon. Do not remove OTUs that are suspected to be entirely from contamination prior to running microDecon.
5. Carefully examine the blanks to ensure that they are reasonably consistent (e.g., *via* stacked bar plots and ordination plots). microDecon inherently assumes a common source of contamination. Therefore, if the contamination was from poor laboratory practices (e.g., cross-contamination among samples), the method will not be effective. If substantial differences among blanks occur only across experimental

blocks, such as extraction kits (suggesting consistent contamination within a block), then use microDecon separately for each block. If, however, there is substantial variability among blanks within blocks (suggesting contamination from poor laboratory techniques), microDecon will not be effective.

Run microDecon (I recommend the decon() function on default settings).

6. Examine the OTUs in the blank and compare the contaminated and decontaminated samples to ensure that the results are reasonable for the given study system (the decon() and decon.diff() functions provide useful outputs for making these comparisons).

Figures

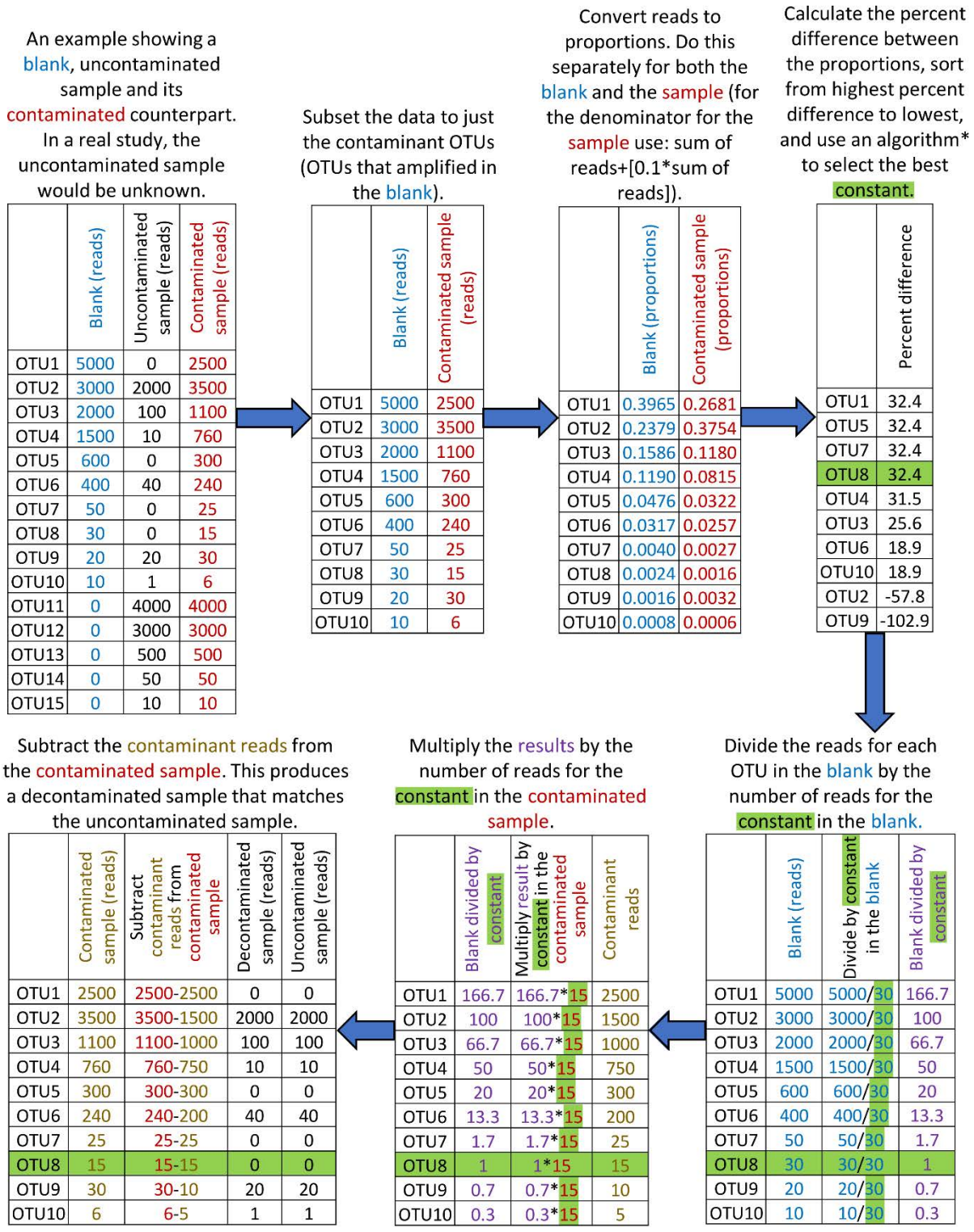

	Blank (reads)	Uncontaminated sample (reads)	Contaminated sample (reads)
OTU1	5000	0	2500
OTU2	3000	2000	3500
OTU3	2000	100	1100
OTU4	1500	10	760
OTU5	600	0	300
OTU6	400	40	240
OTU7	50	0	25
OTU8	30	0	15
OTU9	20	20	30
OTU10	10	1	6
OTU11	0	4000	4000
OTU12	0	3000	3000
OTU13	0	500	500
OTU14	0	50	50
OTU15	0	10	10

	Blank (reads)	Contaminated sample (reads)
OTU1	5000	2500
OTU2	3000	3500
OTU3	2000	1100
OTU4	1500	760
OTU5	600	300
OTU6	400	240
OTU7	50	25
OTU8	30	15
OTU9	20	30
OTU10	10	6

	Blank (proportions)	Contaminated sample (proportions)
OTU1	0.3965	0.2681
OTU2	0.2379	0.3754
OTU3	0.1586	0.1180
OTU4	0.1190	0.0815
OTU5	0.0476	0.0322
OTU6	0.0317	0.0257
OTU7	0.0040	0.0027
OTU8	0.0024	0.0016
OTU9	0.0016	0.0032
OTU10	0.0008	0.0006

	Percent difference
OTU1	32.4
OTU5	32.4
OTU7	32.4
OTU8	32.4
OTU4	31.5
OTU3	25.6
OTU6	18.9
OTU10	18.9
OTU2	-57.8
OTU9	-102.9

	Blank (reads)	Divide by constant in the blank	Blank divided by constant
OTU1	5000	5000/30	166.7
OTU2	3000	3000/30	100
OTU3	2000	2000/30	66.7
OTU4	1500	1500/30	50
OTU5	600	600/30	20
OTU6	400	400/30	13.3
OTU7	50	50/30	1.7
OTU8	30	30/30	1
OTU9	20	20/30	0.7
OTU10	10	10/30	0.3

	Blank divided by constant	Multiply result by constant in the contaminated sample	Contaminant reads
OTU1	166.7	166.7*15	2500
OTU2	100	100*15	1500
OTU3	66.7	66.7*15	1000
OTU4	50	50*15	750
OTU5	20	20*15	300
OTU6	13.3	13.3*15	200
OTU7	1.7	1.7*15	25
OTU8	1	1*15	15
OTU9	0.7	0.7*15	10
OTU10	0.3	0.3*15	5

	Contaminated sample (reads)	Subtract contaminant reads from contaminated sample	Decontaminated sample (reads)	Uncontaminated sample (reads)
OTU1	2500	2500-2500	0	0
OTU2	3500	3500-1500	2000	2000
OTU3	1100	1100-1000	100	100
OTU4	760	760-750	10	10
OTU5	300	300-300	0	0
OTU6	240	240-200	40	40
OTU7	25	25-25	0	0
OTU8	15	15-15	0	0
OTU9	30	30-10	20	20
OTU10	6	6-5	1	1

Figure 6.1 — The basic steps used by microDecon to decontaminate samples. The process is iterative, and each sample is treated completely independently. The constant is an OTU that is entirely contamination (i.e., should not be present in an uncontaminated sample). Because the constant is entirely contamination, it can be used as a point of comparison to

determine how many reads in the sample are from contamination. Percent differences are calculated as: ([blank proportion – sample proportion]/ blank proportion) *100. Some numbers reported in the 4th table appear to be slight deviations of the expected values based on the 3rd table. This is simply an artefact of rounding the values in the 3rd table to four decimal places. *Full details on the algorithms are available in the microDecon user's guide.

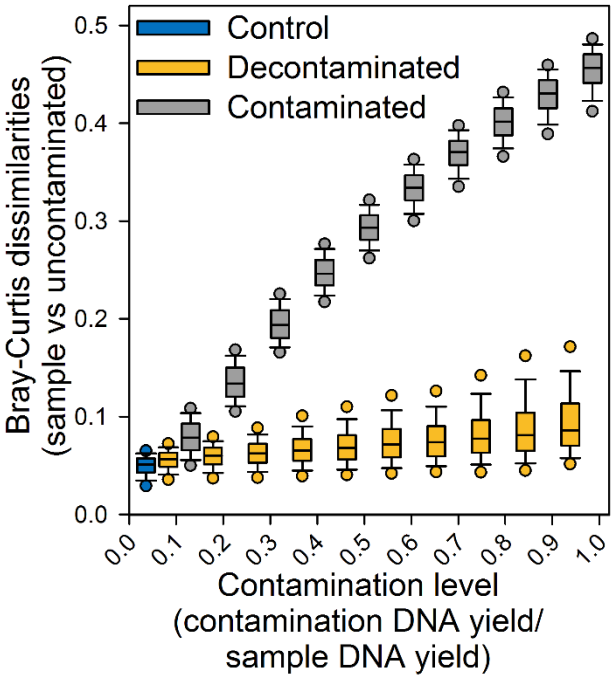

Figure 6.2 — Simulation 1 results showing the ability of microDecon ("Decontaminated") to corrected contaminated samples. Data (Bray-Curtis dissimilarity between the sample and uncontaminated copy of the sample) were grouped based on the proportion of contamination. The simulation control box is based on subsetting the data to only the OTUs that did not amplify in the blank. Whiskers represent the 90th and 10th percentile. For readability, outliers represent the 95th and 5th percentile. A total of 100,000 iterations were run, but 2,395 had contamination levels higher than 1 and are excluded (all iterations and outliers are visible in Additional file 6.3).

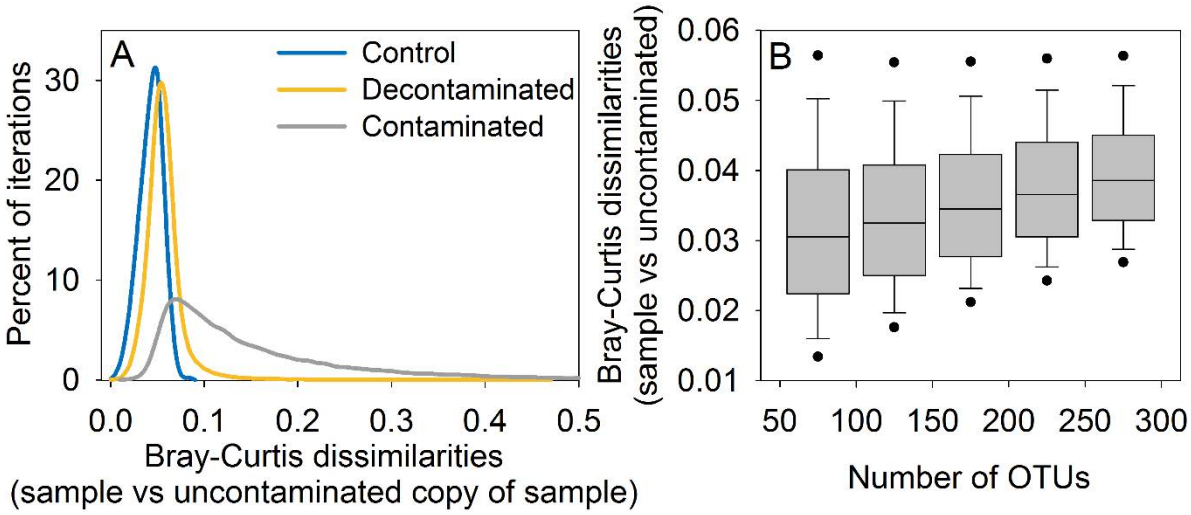

Figure 6.3 — A). Distributions of Bray-Curtis dissimilarities (BC) from 100,000 iterations of simulating individual samples. For readability, the X axis stops at 0.5, but there were 1,756 contaminated points and 20 decontaminated points greater than that (max = 0.906 and 0.712 respectively). The simulation control distribution is from the OTUs in the decontaminated sample that did not amplify in the blank. B). Relationship between the number OTUs and the BC for the simulation controls (i.e., stochastic variation). Increasing numbers of OTUs resulted in greater dissimilarities, which were partially responsible for the slight shift in the decontaminated distribution in Figure 6.3A. Whiskers represent the 90th and 10th percentile, and outliers are shown as the 95th and 5th percentile.

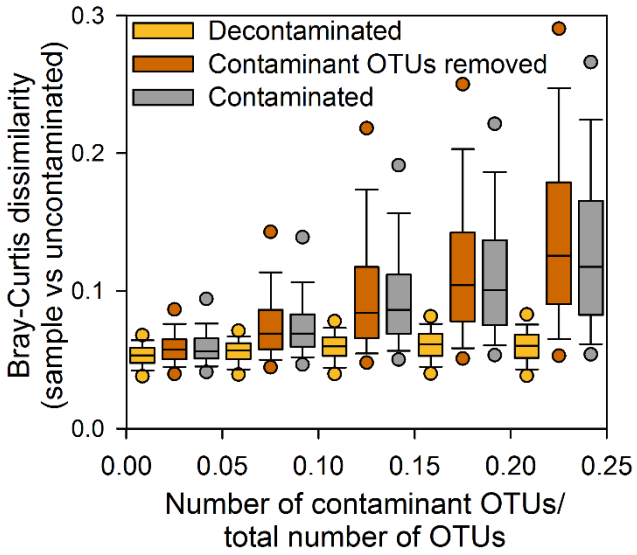

Figure 6.4 — A comparison of the effectiveness of microDecon versus removing all contaminant OTUs for simulated data. Using microDecon ("Decontaminated") was superior to either removing contaminant OTUs ("Contaminated OTUs removed") or making no adjustments for contamination ("contamination"). Whiskers represent the 90th and 10th percentile. For readability, outliers are shown as the 95th and 5th percentile (full data in Additional file 6.3).

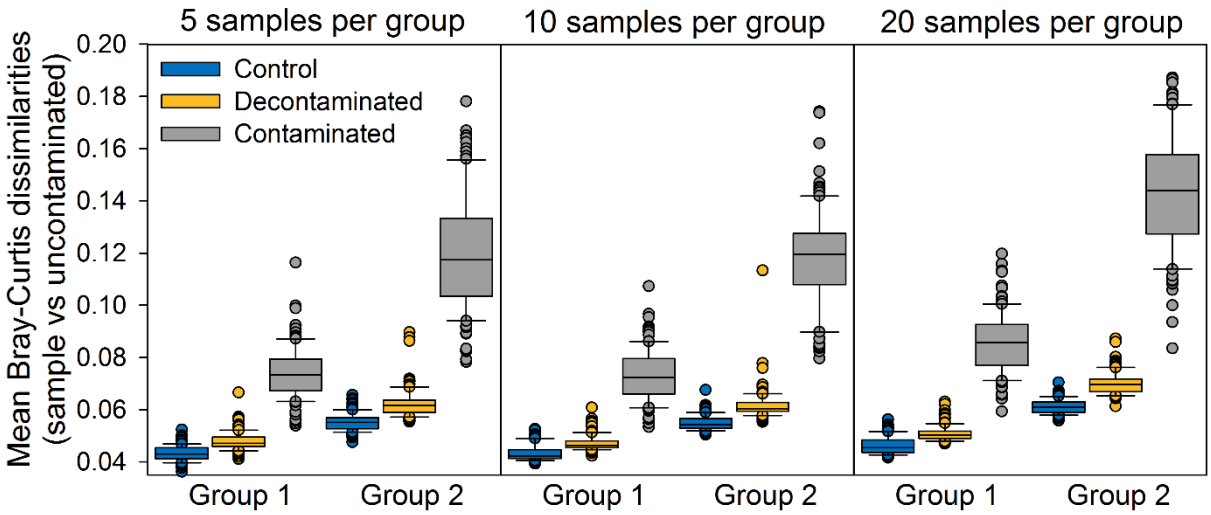

Figure 6.5 — Results of simulations on entire groups (Simulation 2), showing the ability of microDecon ("Decontaminated") to correct contaminated samples. Means are per group per iteration. For the simulation controls, comparisons were made between the decontaminated and uncontaminated samples using only the OTUs that were not in the blank (i.e., the ones unaffected by contamination and decontamination). Controls were expected to be slightly lower than decontaminated samples because they contained fewer OTUs (see Figure 6.3). Whiskers represent the 90th and 10th percentile, and all outliers are shown.

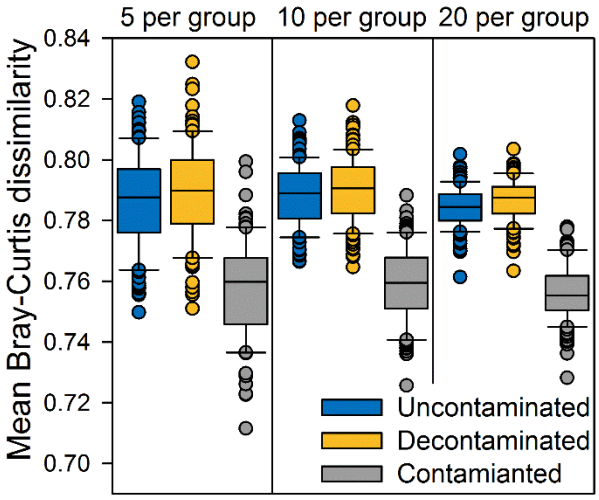

Figure 6.6 — Mean Bray-Curtis dissimilarities for comparisons between groups (groups consisted of 5, 10, or 20 samples). For each iteration (100 per panel), comparisons were made between groups for the uncontaminated, decontaminated (with microDecon), and contaminated samples. Whiskers represent the 90th and 10th percentile, and all outliers are shown.

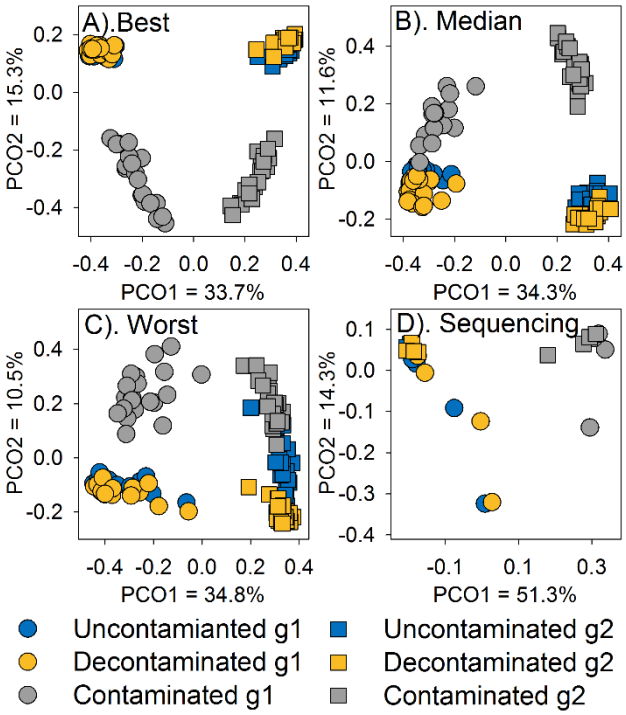

Figure 6.7 — PCoAs (based on square root transformed Bray-Curtis dissimilarities [BC]) comparing groups ("g1" and "g2") for uncontaminated, decontaminated, and contaminated samples. The data were subset to the OTUs that amplified in the blank so that the effects of contamination and microDecon ("Decontaminated") could be seen more clearly. A–C). Best, median, and worst results out of 100 iterations (judged based on mean BC between the uncontaminated and decontaminated samples for group 2). Group 2 had lower DNA yield and, therefore, was more affected by contamination. D). Results from the sequencing experiment, showing that microDecon effectively removed the contamination.

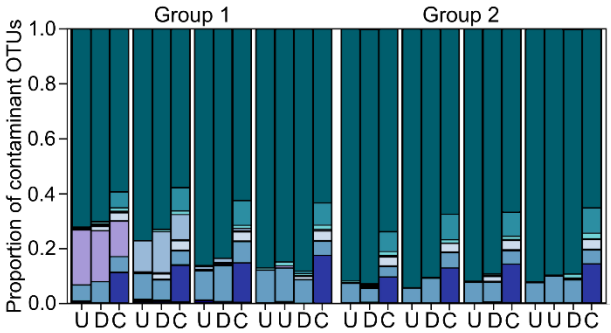

Figure 6.8 — Results from simulation 1, showing the best, median, and worst iteration (out of 100 iterations). The stacked bars show the percent of each sample that was comprised by each OTU (each color/section is an OTU). Each cluster of three samples is a sample. The best, median, and worst were determined by mean Bray-Curtis dissimilarities between the decontaminated and uncontaminated samples, and they were extracted separately per group (e.g., the best for group 1 and for group 2 are not from the same iteration).

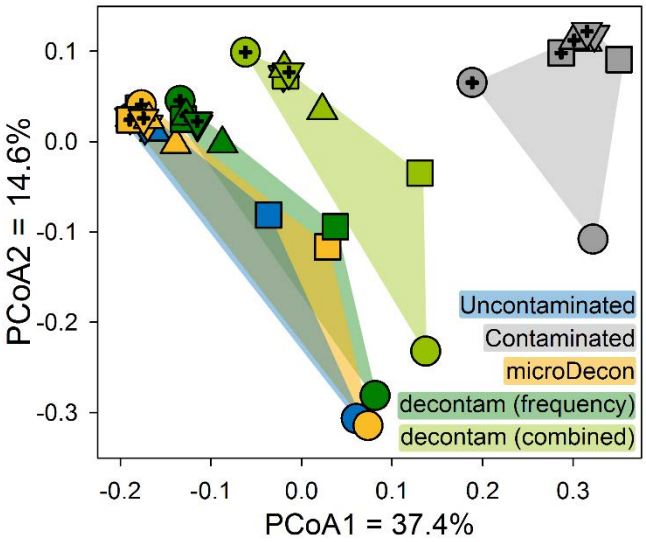

Figure 6.9 — Comparison of uncontaminated (U), decontaminated (D), and contaminated (C) samples for the sequencing test. Stacked bars show the percent of each sample that was comprised by each OTU (each color/section is an OTU). Each group of 3–4 bars is a sample. The last sample in each group has a replicate uncontaminated sample. Data were subset to the OTUs that amplified in the blank (contaminant OTUs) so that trends could easily be seen. There were several prominent OTUs in the contaminated samples that were removed or greatly reduced by microDecon.

CHAPTER 7: MORE IS BETTER: MICROBIOME RICHNESS IS ASSOCIATED WITH FROG POPULATION RECOVERY FOLLOWING A DISEASE OUTBREAK

In preparation as: McKnight, DT, R Huerlimann, DS Bower, L Schwarzkopf, RA Alford, KR Zenger. More is better: Microbiome richness is associated with frog population recovery following a disease outbreak. *Microbial Ecology*

Abstract

Host microbiomes play important roles in infection dynamics, and there is growing evidence that they can both protect hosts from emerging infectious diseases and facilitate population persistence and recoveries. To further our understanding of the interactions between host microbiomes and the amphibian fungal disease chytridiomycosis, I examined the skin microbiomes of four species of frogs in the Australian Wet Tropics, each of which has a different history with chytridiomycosis (extirpation without recolonization - *Litoria dayi*, extirpation with recolonization - *Litoria nannotis*, decline with recovery - *Litoria serrata*, and no decline - *Litoria wilcoxii*). I predicted that both bacterial richness and the relative abundance of inhibitory bacteria would reflect the frogs' patterns of declines and recoveries. Bacterial richness largely matched the historical patterns. The frog species that never declined (*L. wilcoxii*) had high bacterial species richness, while the most sensitive species, which has not shown signs of population recovery (*L. dayi*), had the lowest bacterial richness. Additionally, in the species that had declined and recovered (*L. nannotis* and *L. serrata*), bacterial richness was higher at sites where recoveries took place. In *L. dayi*, there was also a negative correlation between bacterial richness and the infection intensity of *Batrachochytrium dendrobatidis* (*Bd*; the pathogen that causes chytridiomycosis). In contrast, the relative abundances of inhibitory bacteria did not match patterns of declines and recoveries. *Litoria dayi* had the highest relative abundance of inhibitory bacteria, including the highest proportions of *Pseudomonas*, a bacterial genus that is well-known for its anti-*Bd* activity. The prevalence and intensity of *Bd* infections were not significantly associated with the frogs' microbial community composition (beta diversity), and consistent patterns of association between particular bacteria and *Bd* were not observed. These results

suggest that simply having a large relative abundance of inhibitory bacteria may not be sufficient for coexisting with *Bd*, and that bacterial richness plays an important role in infection dynamics.

Introduction

Emerging infectious diseases are a serious threat to wildlife populations, and there is a great need to understand the factors that cause some populations to experience epizootic outbreaks, while allowing others to coexist with pathogens in an enzootic state (Daszak et al. 2000; Smith et al. 2006). It is well established that microbiomes play important roles in the ecology and biology of multicellular organisms, including mitigating diseases (Harris et al. 2009a; Mao-Jones et al. 2010; Mattoso et al. 2011). Therefore, investigations of the relationships between pathogens and host bacterial microbiomes can help in understanding the emergence of diseases and managing the threats they pose (i.e., *via* bioaugmentation using probiotics).

The amphibian fungal disease chytridiomycosis is an ideal candidate for understanding how microbiomes interact with emerging infectious diseases. Chytridiomycosis is caused primarily by the pathogen *Batrachochytrium dendrobatidis* (*Bd*) and has caused declines or extinctions in over 500 species of amphibians worldwide (Berger et al. 1998; Lips et al. 2006; Skerratt et al. 2007; Scheele et al. 2019). However, not all amphibian species are susceptible to chytridiomycosis, and some species and populations that underwent initial declines have transitioned to an enzootic state and are currently persisting despite the continued presence of the pathogen (McKnight et al. 2017a; Scheele et al. 2017). The reasons for these differences among species and populations are not entirely clear, but variations in host microbiomes may play a key role.

Some bacteria in amphibians' skin microbiomes are capable of inhibiting the growth of *Bd in vitro* (Harris et al. 2006; Lauer et al. 2007, 2008; Becker and Harris 2010; Bell et al. 2013), and supplementing amphibians' microbiomes with inhibitory bacteria can increase survival in laboratory trials (Becker et al. 2009; Harris et al. 2009b, a; Muletz et al. 2012). Additionally, some field studies found correlations between the composition of frogs' bacterial communities and host population persistence (Woodhams et al. 2007; Lam et al. 2010; Flechas et al. 2012; Kueneman et al. 2016; Burkart et al. 2017; Jani et al. 2017; Bates et al. 2018; Bell et al. 2018; Catenazzi et al. 2018). Given the increasing interest in using bioaugmentation as a management tool, it is important to identify the relative effects of factors that influence population persistence and recovery.

The frog fauna of the Wet Tropics of Queensland, Australia provides a useful study system for examining this issue. This fauna includes four sympatric, stream-dwelling species of frogs, each of which responded differently to a *Bd* outbreak in the late 1980s and early 1990s. During the outbreak, the Australian lace-lid frog (*Litoria dayi*) was extirpated from upland sites (>300–400 m elevation), but persisted in the warmer low elevation sites (McDonald and Alford 1999). Its populations have never recovered, and it continues to be restricted to sites below 300–400 m in elevation (McKnight et al. 2017a). The waterfall frog (*Litoria nannotis*) experienced the same pattern of declines (Richards et al. 1993; Laurance et al. 1996; McDonald and Alford 1999), but, starting in the early 2000s, it began recolonizing upland sites, and stable, breeding populations are now present at many locations from which it had been extirpated (McKnight et al. 2017a). The green-eyed treefrog (*Litoria serrata* [formerly *genimaculata*]) went through a similar pattern of declines and recovery, but it never fully disappeared from upland locations (McDonald and Alford 1999; Richards and Alford 2005). Finally, the stony creek frog (*Litoria wilcoxii*) never declined at any elevation.

This system allows us to compare sympatric species that have experienced different effects from and responses to *Bd*. Additionally, I can compare low elevations where *L. nannotis* and *L. serrata* persisted and high elevations where they were extirpated or declined, respectively (Richards et al. 1993; Laurance et al. 1996; McDonald and Alford 1999). This system also allows us to compare geographically distant populations within each species to test for consistent patterns. Therefore, I collected and sequenced skin swabs from all four species at several sites and elevations, and I predicted that both the relative abundances of bacteria that are known to inhibit *Bd* and the richness of the communities would correlate with the patterns of declines and recoveries.

Methods

Study sites and sampling

Frogs were sampled from three national parks in the Wet Tropics of Queensland, Australia: Paluma Range National Park, Kirrama Range National Park, and Tully Gorge National Park (the lower section of Kirrama is now part of Girramay National Park, but I will refer to the entire area simply as Kirrama). At Paluma and Kirrama, upland and lowland sites

were sampled, but at Tully, only a single lowland site was available (I will use "site" to refer to a specific sampling location, rather than a park). I defined lowland as < 300 to 400 m elevation, because that is the threshold above which declines and disappearances occurred (McDonald and Alford 1999). To reduce habitat effects within sites, when possible all species were sampled from the same stretch of stream, and the upland and lowland portions of the same stream were sampled. However, species were not distributed uniformly. *Litoria dayi* is no longer found at high elevations and has been extirpated from Paluma, and *Litoria serrata* was not found at the Tully lowland site. Additionally, at both Paluma and Kirrama, *L. nannotis*, *L. serrata*, and *L. wilcoxii* were found together at a lowland stream, but only *L. nannotis* and *L. serrata* were found at the upland portions of those streams. Therefore, at both parks, two nearby upland streams were sampled (one contained *L. nannotis* and *L. serrata* and the other contained *L. serrata* and *L. wilcoxii*) and all of the data were combined into the upland elevation category. Sample sizes and elevations for my sampling design are presented in Table 7.1 (total N = 168).

Throughout this study, I refer to *L. wilcoxii*, however, there is a wide zone of hybridization between *L. wilcoxii* and the morphologically indistinguishable *L. jungguy* (the two species were recently split), and either species, or hybrids of both, could have been present at some of my sites (Donnellan and Mahony 2004). Neither species declined during chytridiomycosis outbreaks, and, given that they do not differ noticeably in ecology or morphology, I will treat them as if they were a single species for the purposes of my study.

Frogs were located by spotlighting along streams at night. Each frog was captured and handled with new nitrile gloves, rinsed with sterile water to remove transient bacteria (Lauer et al. 2007), and swabbed with a sterile, rayon-tipped swab (Medical Wire, MW113), using a total of 25 strokes: five on the stomach, five on the underside of each thigh, and five on the underside of each rear foot. After swabbing, swabs were immediately placed on dry ice, where they remained until they were transferred to a -80°C freezer. All frogs were released at their collection sites shortly after capture. For consistency, the same researcher (DTM) swabbed all frogs. To minimize potential effects of season and weather, at each sampling location, all individuals of all species were sampled within a single night (with a few exceptions at the lower portion of Little Crystal Creek), and all sites were sampled over an 11-night period. Because bacterial contamination is a ubiquitous and often overlooked

problem in microbiome studies (Salter et al. 2014), on each night of sampling, a blank swab was collected to quantify any contaminants present from sampling or laboratory methods.

Laboratory methods

A modified version of the CTAB protocol (Doyle and Doyle 1987) was used to extract both fungal and bacterial DNA from the swabs. Briefly, a bead-beating step was added to lyse fungal cells, followed by a lysozyme incubation to lyse gram positive bacteria and an overnight digestion with proteinase K to lyse any remaining cells. Following lysis, a standard CTAB extraction protocol (with chloroform) was used. Full details of my extraction protocol are available in Appendix 2.

To determine the infection status and *Bd* load of each sample, extracted DNA was sent to a commercial laboratory (Cesar, Melbourne, Australia). They performed triplicate qPCR following the standard protocol in (Boyle et al. 2004). A frog was considered infected if all three replicates were positive, and *Bd* load was calculated by averaging the replicates.

To sequence the bacterial community, samples were prepared following the Illumina 16S Metagenomics Sequencing Library Preparation guide (Illumina 2017) with a few modifications. First, for the amplification PCR, 30 cycles and triplicate 10 µL reactions with KAPA HiFi DNA Polymerase were used. The PCR products were pooled following confirmation of amplification via gel electrophoresis. Second, 40 µL reactions were used for the indexing PCR. Third, Sera-mag SpeedBeads were used for the clean-up steps. Finally, an Illumina MiSeq (Reagent kit V3 600 cycles PE, Illumina, USA) was used to sequence the samples (PhiX = 10%).

Bioinformatics and quality control

MiSeq control software (MCR/RTA; Illumina, CA, USA), FASTX- trimmer (Hannon 2010), Sickle (Joshi and Fass 2011), and PANDAseq (Masella et al. 2012) were used to demultiplex samples, perform quality control filtering, remove 5'- and 3'-ends (16 and 21 bp, respectively), perform paired-end quality trimming (Phred score = 20, amplicon length > 150 bp), and merge the forward and reverse reads. The split_libraries_fastq.py script in QIIME 1.9 was used to combine samples (Caporaso et al. 2010), and USEARCH 6.1 and the filter_fasta.py script were used for chimera checking (Edgar et al. 2011). Operational taxonomic units (OTUs) were assigned with 97% identity using the pick_de_novo_otus.py

script (on default settings) and the SILVA database release 128 (Quast et al. 2013). The filter_otus_from_otu_table.py script in QIIME was utilised to remove any OTUs that comprised less than 0.01% of the data. This resulted in a total of 776 OTUs and a median read depth of 19,922 (range = 4,564–117,495). Adequacy of read depths was confirmed by examining rarefaction curves of OTU richness (i.e., number of OTUs) against read depth, and by checking for a linear correlation between read depth and species richness (t = -0.354, P = 0.724). Bacterial contamination was present in the blanks. Therefore, the recently developed R package microDecon was utilized, on default settings, to identify and remove the contaminant reads from the samples (McKnight et al. 2019c).

Statistical analyses: model structure

My analyses were designed to examine bacterial OTU richness, the composition of bacterial communities, and the relative abundance of known inhibitory bacterial OTUs. First, the models looked for differences among species and between elevations that corresponded with historical patterns of declines and recovery. Second, they examined associations with infection prevalence by comparing infected (*Bd*+) and uninfected (*Bd*-) individuals. Third, they examined associations with infection intensity by looking for associations with *Bd* load (log10 of the qPCR results) among infected individuals.

Because of the complexity of the data, lack of orthogonal structure, specific hypotheses of interest, and large number of potential interactions, the following hierarchical approach was used to develop statistical analyses for each response variable. I started with a model that included data from all individuals, with species, park, and elevation (upland or lowland) as the explanatory variables, but without any interactions or information on *Bd*. Then, to examine potential interactions, a subset of the data that included Paluma and Kirrama, but not *L. dayi* was examined. This allowed us to fit all interactions among species, park, and elevation for *L. nannotis, L. serrata,* and *L. wilcoxii*. To construct a similar model that included *L. dayi*, a subset of the data that only included Tully and the Kirrama lowlands was examined (*L. serrata* was not included because *L. serrata* was not sampled at Tully). Because neither of the previous models allowed for a *L. dayi* x *L. serrata* comparison, an additional model was constructed using just the Kirrama lowlands (this was used strictly for comparing *L. dayi* and *L. serrata* and the significance of any other terms was not assessed). Because of the complexity of the data, post hoc tests were

performed for a factor of interest if the factor was significant in the main model ($P < 0.05$) or if an interaction involving that factor approached significance ($P < 0.1$). Additionally, if an interaction approached significance, the post hoc comparisons were constrained to each level of the interacting factor (e.g., if elevation and species interacted, then a post hoc test was conducted on species in the lowlands and a separate post hoc test on species in the uplands).

A similar approach was used for models examining effects of *Bd* prevalence and intensity. The initial model included the main effects of species, park, elevation, and *Bd* prevalence or intensity, but no interactions other than an interaction between species and *Bd.* Subsequent models on each species included all possible interactions. For *L. nannotis* models, Tully was not included so that an elevation interaction could be included. Post hoc comparisons were made as before. For these tests, only the significance of the *Bd* term and its interactions were examined.

For all general and generalized linear models, significance was assessed via the Anova function in the car package (Fox and Weisberg 2011). For each model, a type II sum of squares was used initially, but if a nearly significant interaction ($P < 0.1$) was present, a type III sum of squares (with contrasts set to sum) was used instead. Tukey's post hoc comparisons were run via the emmeans package (Lenth 2018). For linear models, residual plots and quartile-quartile plots were used to evaluate model assumptions. When a method other than a linear model was used, the standard post hoc method for controlling type I error rates for that method was applied.

Relative abundance of inhibitory bacteria

To identify bacteria in my samples that were known to be inhibitory to *Bd* (hereafter "inhibitory OTUs"), a BLAST search was used to identify OTUs in my data set that were listed as inhibitory towards *Bd* in the anti-fungal isolates database (Woodhams et al. 2015). This allowed us to calculate the relative abundance of inhibitory bacterial by calculating the proportion of reads per sample that belonged to inhibitory OTUs (I will use the term "relative abundance" to refer to the proportion of reads, rather than the proportion of OTUs). To compare the relative abundance of inhibitory bacteria among species, parks, and elevations, and look for associations with *Bd* infection prevalence and intensity, negative binomial models in R (via the glm.nb function) were applied to the hierarchy of models

described previously. The number of inhibitory reads was the response variable and the total number of reads was included as an offset in all models.

Additionally, because bacteria in the genus *Pseudomonas* are highly inhibitory towards *Bd*, additional models were used to examine the relative abundance of *Pseudomonas* specifically. These data did not fit the assumptions of any attempted models, even after transformations; therefore, non-parametric statistics were used, which prevented the application of my usual hierarchical approach. Instead, within each park, the relative abundance of *Pseudomonas* was compared among species using a Kruskal-Wallace test followed by post hoc Dunn's tests via the FSA package (Ogle 2018). Additionally, all species were compared in a test using all data points. Finally, Spearman rank correlations were used to look for associations between *Bd* and *Pseudomonas* among *Bd*+ individuals within each species (Hothorn et al. 2006).

OTU richness

To examine OTU richness (defined as the number of unique OTUs in a given sample) linear models were constructed *via* the lm function in R following my hierarchy of models. Both the total richness of the bacterial communities and the richness of just the inhibitory portion of the community (i.e., the number of inhibitory OTUs per sample) were examined.

Communities and OTUs

To examine beta diversity patterns, community composition was compared among communities using PERMANOVAs (calculated via the adonis2 function in the vegan package in R)(Oksanen et al. 2017). The data were prepared for PERMANOVAs by transforming the data to proportions of reads per sample to account for differences in read depth (McKnight et al. 2019a) followed by calculating Bray-Curtis dissimilarities (an abundance-based β index). PERMANOVAs were also conducted using just the inhibitory OTUs (the data were normalized after being restricted to just inhibitory OTUs). For both sets of PERMANOVAs, the following order of terms was used: species, park, elevation, and (when applicable) *Bd* prevenance or intensity. Post hoc tests were performed by constructing models that had only two levels of a factor of interest (but all other factors remained unchanged) such that there was a model for each pair-wise comparison. Sequential Bonferroni corrections were used to control the family-wise type I error rate.

Several analyses were used to examine possible associations between particular OTUs and *Bd*. First, the R package phylofactor (Washburne et al. 2017) was used to look for possible phylogenetic splits in the microbial communities of infected and uninfected frogs. It was set to return only the 100 most significant splits, and the P values were adjusted to a false discovery rate (FDR) of 0.01. Additionally, DESeq2 (Love et al. 2014) was used to look for OTUs that were differentially abundant between infected and uninfected individuals (FDR = 0.01). For these tests, each species was examined separately, OTUs that did not occur within a given species were removed, and park and elevation were included as factors.

Finally, for infected individuals, linear models were used to look for associations between *Bd* infection intensity and the relative abundance of each OTU (calculated as the proportion of reads). This test was done separately for each species of frog, and within each species, only OTUs that were present in at least 20% of samples were tested. For each OTU, models were constructed that included all possible combinations of main effects and interactions for OTU relative abundance, park, and elevation, including models that excluded park, elevation, or both. The model with the best fit (based on AIC values) was used to assess the association between *Bd* and that OTU. P values were adjusted to an FDR of 0.01.

Results

OTU richness

There was a significant main effect of frog species ($P < 0.001$), park ($P = 0.006$), and elevation ($P = 0.046$) in the linear model for bacterial OTU richness (i.e., number of OTUs) that included all data but no interactions. This model suggested that *L. dayi* had lower richness than the other species (Figure 7.1; Appendix 2 Table 1), Paluma had lower richness than the other parks, and lowlands had lower richness than uplands. Subsequent tests found many significant interactions (Appendix 2 Tables 2–3), therefore post hoc tests were conducted on subsets of the data (Figure 7.2). These tests suggested that *L. dayi* had significantly lower species richness than *L. nannotis* ($P = 0.004$) and *L. wilcoxii* ($P = 0.002$) and marginally lower richness than *L. serrata* ($P = 0.062$). Patterns for the other species varied by park, but, with the exception of *L. dayi*, all significant differences among species

only occurred for comparisons within upland locations. At the Paluma uplands, both *L. nannotis* and *L. serrata* had significantly higher richness than *L. wilcoxii* ($P < 0.001$ and $P = 0.006$, respectively), but they did not differ significantly from each other ($P = 0.275$). In contrast, at the Kirrama uplands, *L. nannotis* had significantly higher richness than *L. serrata* ($P = 0.043$), but the difference between *L. nannotis* and *L. wilcoxii* was not significant ($P = 0.629$), and *L. serrata* had significantly lower richness than *L. wilcoxii* ($P = 0.006$). Most species did not differ significantly between parks, but *L. wilcoxii* had significantly higher richness at the Kirrama uplands than at the Paluma uplands ($P < 0.001$). Bacterial richness was significantly higher at upland sites for *L. nannotis* at Kirrama ($P = 0.005$) and for *L. wilcoxii* at both Paluma ($P = 0.009$) and Kirrama ($P = 0.002$).

Comparisons that only looked at the richness of inhibitory bacteria revealed similar patterns with some important differences (Figures 7.1 and 7.2). First, the richness on *L. serrata* was generally reduced. As a result, *L. dayi* and *L. serrata* generally had a lower inhibitory OTU richness than either *L. nannotis* or *L. wilcoxii*, but there were no significant differences within either pair of species. Second, there were no significant differences among species within Paluma. Third, at Kirrama, significant differences occurred in both the uplands and lowlands. Also, for *L. serrata*, inhibitory richness was significantly higher at Paluma than at Kirrama ($P < 0.001$), and for lowland *L. nannotis* inhibitory richness was significantly higher at Tully than at Paluma ($P = 0.028$). There were no significant differences between elevations, but *L. nannotis* had a marginally higher inhibitory richness in the uplands than in the lowlands ($P = 0.053$).

Associations between richness and Bd

Models that looked for associations between total OTU richness and *Bd* found mixed results. First, the model with all infected individuals (but only including a species x *Bd* interaction) comparing richness and *Bd* intensity (log transformed *Bd* qPCR results) did not find a significant association with *Bd* ($P = 0.841$). Subsequent models on each species (with all interactions; Figure 7.4) found a significant negative association between *Bd* and total richness for *L. dayi* ($P = 0.007$), but not for *L. nannotis* or *L. wilcoxii* ($P = 0.713$ and 0.954, respectively). For *L. serrata*, there was a nearly significant positive association between *Bd* and bacterial richness ($P = 0.053$) and a nearly significant interaction between *Bd* and park

(P = 0.056). Splitting the data by park revealed a significant positive association at Paluma (P = 0.011) but not at Kirrama (P = 0.967).

In contrast, my model examining possible associations between inhibitory OTU richness and *Bd* infection intensity across all species showed there was a slightly significant positive association (P = 0.031), but subsequent models on each species that included interactions did not find any significant associations between individual species and *Bd* intensity (all P > 0.188); however, trendlines were negative for *L. dayi*, positive for *L. nannotis* and *L. serrata*, and flat for *L. wilcoxii* (Figure 7.4). There were no significant interactions (all P > 0.121).

Tests comparing the OTU richness (both total and inhibitory) of infected and uninfected individuals (all individuals; only a species x *Bd* interaction) suggested that infected individuals generally had a higher total richness (P = 0.040) and higher inhibitory richness (P = 0.034; Figure 7.5). Subsequent tests on each species (with full interactions) were generally non-significant (all P > 0.160) with the exceptions of a nearly significant difference in total richness for *L. serrata* (P = 0.050) and a slightly significant difference in inhibitory richness for *L. nannotis* (P = 0.046). However, given the consistency of the pattern across species (with the exception of total richness in *L. dayi*; Figure 7.5), these negative results likely reflect small sample sizes, rather than a true lack of difference. Further, there were no significant interactions for the inhibitory richness models and only one significant interaction for the total richness models (*L. wilcoxii* elevation:park interaction P < 0.001), suggesting that the models with all species and only a species x *Bd* interaction are valid.

Relative abundance of inhibitory bacteria

The models examining the relative abundance of inhibitory bacteria (i.e., the proportion of reads that were assigned to known inhibitory OTUs) revealed significant differences among species and parks (Figure 7.3). The model that included all individuals, but no interactions, found a significant main effect of species (P < 0.001) and park (P = 0.026) but not elevation (0.234). Post hoc tests suggested that *L. dayi* and *L. serrata* had high relative abundance of inhibitory bacteria compared to *L. nannotis* and *L. wilcoxii* (Figure 7.3), but additional tests revealed many interactions (Appendix 2 Tables 2–3). Therefore, post hoc comparisons among species were conducted within parks, and post hoc comparisons among parks were conducted within species. The patterns of differences for

species were generally similar to the results of the model with no interactions (i.e., *L. dayi* and *L. serrata* had high relative abundances of inhibitory bacteria compared to *L. nannotis* and *L. serrata*); however, *L. wilcoxii* had a significantly higher relative abundance of inhibitory bacteria than did *L. nannotis* at Paluma ($P = 0.005$), but not at Kirrama ($P = 0.331$) or Tully ($P = 0.110$), and *L. serrata* had a significantly higher relative abundance of inhibitory bacteria than *L. wilcoxii* at Kirrama ($P < 0.001$), but not at Paluma ($P = 0.701$). The only significant difference among parks was that *L. wilcoxii* had a significantly higher relative abundance of inhibitory bacteria at Paluma than at Kirrama ($P < 0.001$) or Tully ($P = 0.008$). There were no significant main effects or interactions for elevation in any tests (all $P > 0.175$); however, the mean relative abundance of inhibitory bacteria was higher in the lowlands for every species at every park, except for *L. wilcoxii* at Paluma.

A total of 19 OTUs in the genus *Pseudomonas* were identified. Ten of those OTUs matched OTUs in the inhibitory database, and the remaining nine were not common, comprising only 0.006% of the frogs' microbiomes on average (range = 0–0.055%). All individuals except for two *L. serrata* had at least one *Pseudomonas* OTU. Kruskal-Wallace tests found a significant difference among species at Paluma ($P = 0.016$) and Kirrama ($P = 0.001$) but not Tully ($P = 0.688$). Dunn's tests found that at Paluma, *L. nannotis* had a significantly higher relative abundance of *Pseudomonas* than did *L. serrata* ($P = 0.020$), but no other comparisons were significant (all $P > 0.101$). At Kirrama, *L. dayi* had a significantly higher relative abundance of *Pseudomonas* than *L. nannotis* ($P = 0.015$) or *L. serrata* ($P < 0.001$), but no other comparisons were significant (all $P > 0.151$). There was a significant positive correlation between *Bd* intensity and the relative abundance of *Pseudomonas* for *L. wilcoxii* ($P = 0.030$), but not for any of the other species (all $P > 0.160$). Another genus known for being highly inhibitory, *Janthinobacterium* (Harris et al. 2009b; Muletz et al. 2012; Bletz et al. 2013), was not present in any of my samples.

Associations between inhibitory relative abundance and Bd

Examining possible relationships between the relative abundance of inhibitory OTUs and infection intensity demonstrated a significant positive relationship between inhibitory relative abundance and *Bd* in the model with all individuals ($P = 0.002$), as well as a significant interaction between species and *Bd* intensity ($P = 0.006$; Figure 7.4). Subsequent models examining each species found a significant positive association for *L. wilcoxii* ($P =$

0.038) and *L. dayi* (P = 0.005), but not *L. nannotis* (P = 0.539) or *L. serrata* (P = 0.630). There were no significant interactions with *Bd* and either park or elevation in any of these tests (all P > 0.164).

Tests comparing the relative abundance of inhibitory bacteria between infected and uninfected individuals found few significant patterns. The model with all individuals (but only a relative abundance x *Bd* interaction) failed to find a significant difference between infected and uninfected individuals (P = 0.561). Subsequent models on each species that included all interactions failed to find any significant interactions (all P > 0.191) or differences between infected and uninfected individuals for any species (all P > 0.213) except *L. nannotis*. For *L. nannotis*, I examined the data in subsets by each park and elevation because of interactions. Tests on these subsets found that infected individuals had a higher relative abundance of inhibitory OTUs at Paluma's uplands (P < 0.001), but a lower abundance at Paluma's lowlands (P = 0.010). No other comparisons were significant for *L. nannotis* (all P > 0.154).

Communities and OTUs

Comparisons of beta diversity found that communities differed significantly among species, parks, and elevations (Figure 7.6). The PERMANOVA that included all individuals (but no interactions) found significant effects of species, elevation, and park (all P < 0.001), and all pairwise post hoc comparisons for species and park were significant (all P < 0.01). Similarly, for all tests involving reduced data sets (with interactions), all main effects, interactions, and pairwise post hoc comparisons were significant (all P < 0.05). The results of PERMANOVAs using only the inhibitory portion of the bacterial microbiome showed the same patterns. Prevalence and intensity of *Bd* infection were not significant in any tests, including tests that only used the inhibitory communities (all P > 0.150; Figure 7.6).

Within the inhibitory portion of the community, bacteria in the order Burkholderiales were the most abundant bacteria for every frog species at every elevation of every park (Figure 7.7A). Pseudomonadales was generally the second most common order within the inhibitory community, but sometimes Flavobacteriales was more common. At the family level, the inhibitory communities of *L. dayi*, *L. serrata*, and *L. wilcoxii* were generally dominated by members of Alcaligenaceae; however, members of Pseudomonadaceae were sometimes abundant. In contrast, *L. nannotis* inhibitory

communities had few Alcaligenaceae and were dominated by members of Comamonadaceae, which were uncommon in the other frog species (Figure 7.7B).

There was little evidence of associations between *Bd* and particular OTUs. Linear models on infected individuals detected one OTU (genus *Gemmata*) that was significantly associated with the intensity of *Bd* infection for *L. nannotis*, and no significant associations for the other frog species. Similarly, comparisons between infected and uninfected frogs with phylofactor did not reveal any significant phylogenetic splits within the bacterial communities for any of the frog species (after adjusting for multiple comparisons). Comparisons via DESeq2 identified 18 OTUs that were differentially abundant between infected and uninfected frogs, but none of those OTUs were significant in more than one species. Two OTUs were significant in *L. dayi,* five in *L. nannotis*, five in *L. serrata*, and six in *L. wilcoxii* (Appendix 2 Table 4). Eight of the 18 OTUs were negatively associated with *Bd*, and the other ten were positively associated. Only three of the OTUs had previously been identified as inhibitory, and all three of those were more common in infected frogs.

Discussion

Patterns of bacterial OTU richness were largely consistent with the historical patterns of declines and recoveries, and my results add to a growing body of literature suggesting that the richness of amphibians' microbial communities may be a critical factor for protecting amphibians against *Bd* (Jani et al. 2017; Piovia-Scott et al. 2017; Antwis and Harrison 2018; Bates et al. 2018; Bell et al. 2018). At the broadest level, my alpha-diversity patterns across species matched the historical patterns. *Litoria dayi*, which has never been able to recover from the outbreak, had the lowest bacterial richness, whereas *L. nannotis*, *L. serrata*, and *L. wilcoxii*, which either recovered from the outbreak or never declined, all had higher levels of richness. I found similar results for the richness of only the inhibitory portion of the bacterial community. This is consistent with a protective effect of species richness, and it is possible that the population recoveries in *L. nannotis* and *L. serrata* were facilitated by a shift towards microbiomes with increased richness.

This hypothesis is also supported by elevational patterns. At Kirrama, the recovered upland population of *L. nannotis* had higher species richness than the lowland population that did not experience a decline. This is consistent with a previous culture-based study on

this species at this park (Bell et al. 2018), and it may indicate that *L. nannotis* at this park recovered in the uplands because its microbiome shifted to include more bacterial species. Additionally, it is interesting that differences in richness among *L. nannotis*, *L. serrata*, and *L. wilcoxii* only occurred at upland locations (where declines and recoveries occurred). Thus, higher bacterial species richness may not be necessary for survival in the lowlands (where declines did not occur), but higher species richness may have been beneficial as frogs recolonized the upland locations.

The negative correlation between richness and *Bd* infection intensity among infected *L. dayi* provides more evidence that species richness is important for this species. However, there was no negative correlation of this nature in the other species, and, with the exception of *L. dayi*, infected frogs tended to have higher total bacterial richness than did uninfected frogs. Although these results initially seem contradictory, they make sense if frogs with very high levels of richness are able to co-exist with the pathogen without succumbing to the disease, while individuals with low levels of richness tend to quickly die from the infection. This would result in a survivorship bias, wherein the infected frogs that I sampled were more likely to have a high richness simply because the infected frogs with a low richness had died and were not available for sampling. Thus, the higher observed richness in infected frogs for *L. nannotis*, *L. serrata*, and *L. wilcoxii* may simply have occurred because many of the infected frogs with a low richness had already died. I would not, however, expect this bias to be present in *L. dayi*, because it generally had low species richness, and the bias would occur as a result of high richness. A lack of survivorship bias in *L. dayi* would also explain why it had a negative correlation between total richness and infection intensity that was not present in the other species. This explanation is particularly germane to my study, because frogs were sampled late in winter (September) when many mortalities would already have taken place (Woodhams and Alford 2005). Nevertheless, this explanation is admittedly correlative and somewhat speculative, and carefully controlled trials are needed to better understand how richness influences infection dynamics; however, a protective effect of richness has been suggested by multiple studies (Jani et al. 2017; Piovia-Scott et al. 2017; Antwis and Harrison 2018; Bates et al. 2018; Bell et al. 2018).

In contrast to my results for species richness, I failed to find evidence that either community composition or the relative abundance of inhibitory OTUs explained the patterns of decline and recovery in this Wet Tropics' frog assemblage. Although I did find

strong differences in the community composition, with distinct communities for every species, park, and elevation, neither the compositions of the entire communities nor the compositions of the inhibitory portions of the communities were significantly associated with either *Bd* prevalence or infection intensity (tested via PERMANOVAs). This result is similar to results from frog species in Panama (Belden et al. 2015). Further, I was not able to detect consistent, significant subsets of OTUs that were associated with *Bd* via DESeq2, phylofactor, or linear models. I did detect differences between infected and uninfected individuals in the relative abundance of 18 bacterial OTUs, but these differences were not consistent across species, and it is not clear what role, if any, they are playing in infection dynamics.

The relative abundances of inhibitory bacteria were the opposite of what I predicted based on patterns of species declines and recoveries. The most sensitive species (*L. dayi*) had the highest relative abundance of inhibitory bacteria, while the least sensitive species (*L. wilcoxii*) had a low relative abundance. Indeed, the relative abundance of inhibitory bacteria was significantly greater in *L dayi* than it was in either *L. nannotis* or *L. wilcoxii*, despite the fact that *L. dayi* populations have not recovered from the outbreak, whereas *L. nannotis* populations have largely recovered, and *L. wilcoxii* never declined (McKnight et al. 2017a). Similarly, at Kirrama, *Pseudomonas*, which is known to be highly inhibitory towards *Bd* (Harris et al. 2006, 2009b; Lam et al. 2010; Rebollar et al. 2016a), was relatively more abundant in *L. dayi* than in either *L. nannotis* or *L. serrata*. Additionally, the relative abundance of inhibitory bacteria correlated positively with *Bd* infection intensity. These results strongly suggest that simply having a high relative abundance of inhibitory bacteria is insufficient for fighting *Bd* infections. Indeed, the positive associations between *Bd* and the relative abundance of inhibitory bacteria suggest that either *Bd* creates conditions in which those bacteria thrive, or some aspect of the frogs' microhabitats or even skin results in conditions that are favourable for both inhibitory bacteria and *Bd*.

Nevertheless, it should be acknowledged that I was only able to measure relative abundance of inhibitory bacteria, rather than total abundance. Thus, if *L. dayi* harbors fewer bacteria per unit area than the other frog species harbor, it would have few inhibitory bacteria (in terms of actual abundance) even though inhibitory bacteria constitute a large portion of its microbiome. There is, however, no *a priori* reason to expect *L. dayi* to have low bacterial loads. I was not able to directly test this possibility, but I examined the QuantiFluor

DNA quantification data that were obtained prior to sequencing as an admittedly crude proxy for total bacterial abundance, and those data suggested that *L. dayi* did not have low bacterial loads and did have a high true abundance of inhibitory bacteria (Appendix 2).

One potential weakness of my result is that my definition of inhibitory bacteria was necessarily restricted to bacteria that had been identified as inhibitory in previous studies. Thus, frogs in my study may have possessed inhibitory bacteria that were not identified as such because they were not cultured in previous studies. However, the dominant members of amphibian bacterial microbiomes are culturable (Walke et al. 2015), and the inhibitory bacterial database I used (Woodhams et al. 2015) was constructed from the results of multiple studies, including studies that examined some of the same species of frogs and study sites that I used in this study (Bell 2012; Bell et al. 2013). Further, large portions of my communities were inhibitory and my results agreed with a previous culture-based study in my system (Bell et al. 2018). Therefore, I do not think that unidentified inhibitory bacteria are likely to have substantially influenced my results.

My results have mixed agreement with other studies. Research on other disease systems has established that microbial communities with high bacterial species richness are often more resistant to pathogens, which is consistent with my results (Dillon et al. 2005; Matos et al. 2005; Eisenhauer et al. 2013; Fraune et al. 2015; Harrison et al. 2017). Additionally, laboratory trials found that multi-species cultures are more effective at inhibiting *Bd* than are single isolates (Piovia-Scott et al. 2017; Antwis and Harrison 2018), and, in some cases, co-culturing bacteria greatly increased metabolite production (Jousset et al. 2014) and resulted in synergistic inhibitory effects (Loudon et al. 2014a). Further, field-based studies in both North America (Jani et al. 2017) and Europe (Bates et al. 2018) found that populations that have shifted to an enzootic state and are coexisting with *Bd* have high bacterial diversity compared to populations that are still experiencing epidemics. My study builds on this by providing a large, sequence-based comparison of Australian species.

Some studies have, however, failed to find associations between alpha diversity and *Bd* (Belden et al. 2015), and, unlike my study, some have found evidence that either inhibitory bacteria or the overall OTU composition of the bacterial community is important. In Panamanian golden frogs (*Atelopus zeteki*), for example, individuals that were able to clear *Bd* infections had significantly different communities (beta diversity) than individuals that did not clear infections, but the alpha diversity did not differ between the two groups

(Becker et al. 2015). Similarly, a comparison of susceptible and non-susceptible frog species in South America found that the community structures differed between each group, but alpha diversity patterns did not match the pattern of susceptibility (Rebollar et al. 2016a). Further, in Sierra Nevada mountain yellow-legged frogs (*Rana sierrae*), the structure of the microbial communities, but not the alpha diversity, correlated with *Bd* (Jani and Briggs 2014). Some studies have also found differences between the community structure of populations that are co-existing with *Bd* and populations that are experiencing epizootics (Jani et al. 2017; Bates et al. 2018). Additionally, other studies have found significant associations between the inhibitory bacteria and infection status (Kueneman et al. 2016) or population persistence (Woodhams et al. 2007; Lam et al. 2010; Flechas et al. 2012; Kueneman et al. 2016; Burkart et al. 2017; Bell et al. 2018; Catenazzi et al. 2018).

There are several possible explanations for these discrepancies among studies. First, many different methodologies have been employed, including field-based surveys, laboratory infection trials, culture-dependant approaches, and next generation sequencing of entire communities. Therefore, some differences may be methodological artefacts. Second, as my study demonstrates, microbiomes and their interactions with the environment are exquisitely complex, and we have only scratched the surface of that complexity. Thus, the effects of microbiomes on *Bd* are likely determined by a complex series of interactions involving characteristics of the habitats, hosts, and the microbiomes. Indeed, in my study, even within a species, different patterns were observed at different parks and even between elevations within a park. Other studies have, similarly, found that amphibian microbiomes are strongly affected by factors like habitat, season, and study site (Longo et al. 2015; Longo and Zamudio 2016; Bletz et al. 2017; Medina et al. 2017; Bird et al. 2018). Therefore, different populations may be persisting or recovering *via* different mechanisms, and, in some populations, OTU richness may be very important, while in others, having a high abundance of inhibitory bacteria may be more important. Additionally, there are other possible explanations for population recoveries, such as changes in habitat, behaviour, or immune system function, which may be interacting with microbiomes or acting independently (Scheele et al. 2015, 2017; McKnight et al. 2017a).

A final possible explanation, and additional difficulty in interpreting microbiome studies, is the entanglement of cause and effect. Microbiomes can co-evolve with hosts, resulting in increased benefits for the host (Ford and King 2016). Additionally, several

studies have suggested that infection by *Bd* can shift host microbiomes (Jani and Briggs 2014; Longo and Zamudio 2016; Jani et al. 2017). This makes it difficult to determine which features of the microbiome played a causal role in the patterns of decline and recovery and which features were caused by the outbreak. The positive correlation that I observed between inhibitory bacteria and *Bd* infection intensity, for example, could be caused by *Bd* creating an environment on the frogs in which those bacteria thrive. More laboratory trials are needed to elucidate this further. It would also be invaluable for researchers to collect and archive samples from sites that are not currently infected but are likely to become infected (e.g., Papua New Guinea) so that cause and effect can be disentangled in the future (Bower et al. 2017).

Conclusion and management implications

My results showed that patterns of OTU richness largely matched historical patterns of declines and recoveries, which suggests that OTU richness may be a critical factor in *Bd* infection dynamics. In contrast, the relative abundance of inhibitory bacteria did not match historical patterns, and was actually the opposite of what I predicted, with the species that has never recovered from declines (*L. dayi*) having the highest relative abundance of inhibitory bacteria. These results have important implications for management efforts.

In laboratory trials, seeding amphibians with inhibitory bacteria (probiotics) often reduces mortality and allows hosts to clear infections or reduce infection intensity (Becker et al. 2009; Harris et al. 2009b, a; Muletz et al. 2012). As a result, bioaugmentation is widely considered a promising strategy for mitigating *Bd* in wild populations and assisting population recoveries (Woodhams et al. 2011, 2012; Bletz et al. 2013; Ysumiba et al. 2016). My results, coupled with the results of other studies that found strong associations with diversity (Jani et al. 2017; Bates et al. 2018), demonstrate the complexity of microbiomes and highlight the need to better understand the role of microbiomes in protecting amphibians from chytrids. *Litoria dayi,* for example, had a high relative abundance of inhibitory bacteria, comprising 38.9% of their communities on average, and had significantly higher levels of *Pseudomonas* than either *L. nannotis* or *L. serrata* at Kirrama. Nevertheless, *L. dayi* is still restricted to low elevations and, unlike *L. nannotis* or *L. serrata,* has not recolonized upland sites (McKnight et al. 2017a). Therefore, at least for this species, simply

having a high relative abundance of inhibitory bacteria is not sufficient for population recovery and increasing the relative abundance of an inhibitory bacterial species is unlikely to make a substantial difference. A better approach may be to use a diverse consortium of bacteria, with the goal of increasing the richness of the inhibitory community, rather than its abundance (Loudon et al. 2014a; Piovia-Scott et al. 2017; Antwis and Harrison 2018); however, it may be difficult to get a diverse assemblage to establish on the hosts. Additionally, bioaugmentation proposals often suggest increasing the abundance of bacteria that are already present, whereas increasing OTU richness inherently requires seeding hosts with novel bacteria. The potential risks of this approach may be limited by using bacteria from related, sympatric species that are either resistant to *Bd* or have recovered from it (e.g. *L. nannotis* and *L. wilcoxii,* in the case of *L. dayi*), but there are still many unknowns. More research on these specific aspects of bioaugmentation would be valuable to amphibian conservation.

Tables

Table 7.1 — Summary of sample data. Elevation (m) is the mean elevation for a given species at a given site. N *Bd*+ = the number of *Bd* positive (infected) individuals.

Species	Park	Elevation (m)	N	N *Bd+*
L. dayi	Kirrama	Lowland (288)	10	8
	Tully	Lowland (213)	10	5
L. nannotis	Paluma	Lowland (304)	10	7
		Upland (571)	10	8
	Kirrama	Lowland (288)	11	3
		Upland (720)	10	7
	Tully	Lowland (213)	8	5
L. serrata	Paluma	Lowland (351)	10	5
		Upland (679)	19	10
	Kirrama	Lowland (291)	10	6
		Upland (650)	16	9
L. wilcoxii	Paluma	Lowland (345)	8	5
		Upland (781)	10	4
	Kirrama	Lowland (272)	10	6
		Upland (594)	7	2
	Tully	Lowland (213)	9	4

Figures

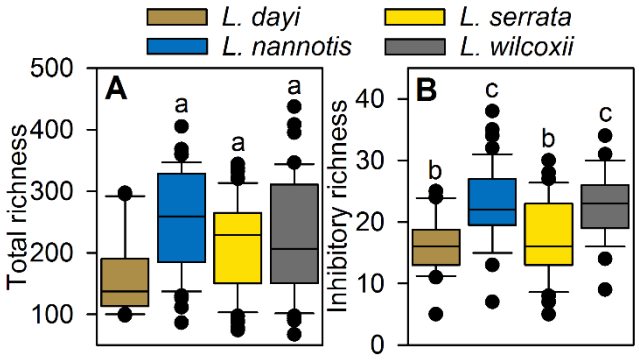

Figure 7.1 — OTU richness for all individuals, regardless of park or elevation. (A) Richness of entire community. (B) Richness of inhibitory bacteria. Letters indicate species that were not significantly different from each other. Whiskers represent the 10th and 90th percentile (calculated via the "standard" formula in SigmaPlot 11.0) and all outliers are shown.

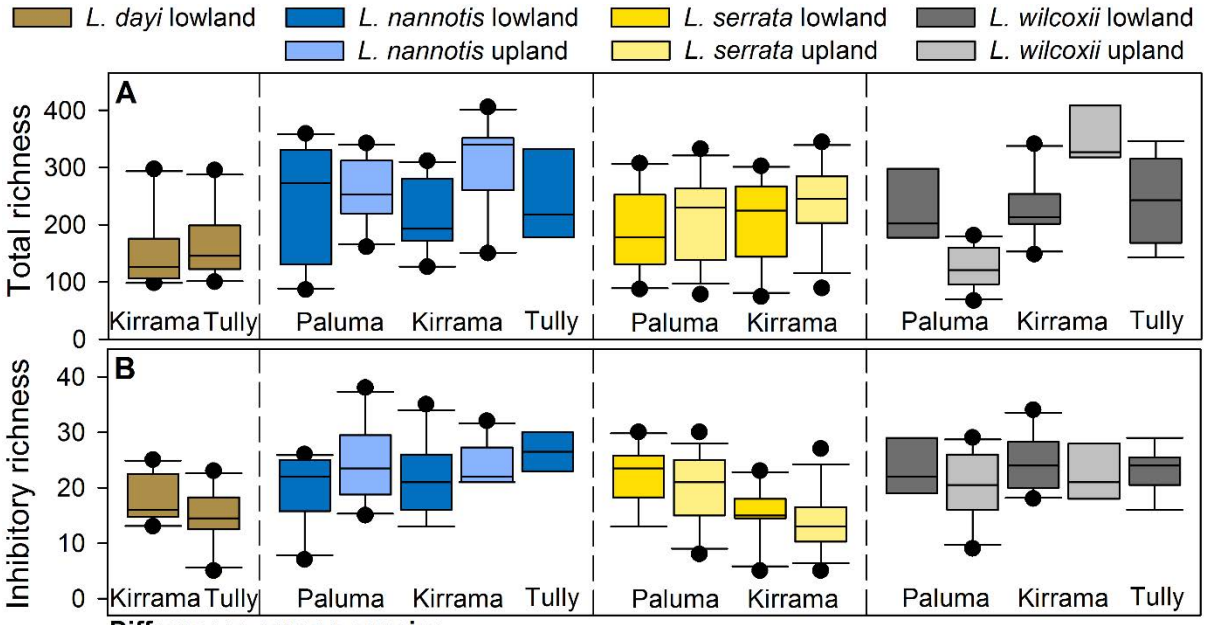

Differences among species

A PU *L. wilcoxii* < PU *L. nannotis* P < 0.001
A PU *L. wilcoxii* < PU *L. serrata* P = 0.006
A K-TL *L. dayi* < K-TL *L. nannotis* P = 0.004
A KL *L. dayi* < KL *L. serrata* P = 0.062
A K-TL *L. dayi* < K-TL *L. wilcoxii* P = 0.002
A KU *L. serrata* < KU *L. nannotis* P = 0.043
A KU *L. serrata* < KU *L. wilcoxii* P = 0.006
B KL *L. dayi* < KL *L. wilcoxii* P = 0.016
B KL *L. serrata* < KL *L. nannotis* P = 0.052
B KU *L. serrata* < KU *L. nannotis* P < 0.001
B KL *L. serrata* < KL *L. wilcoxii* P = 0.003
B KU *L. serrata* < KU *L. wilcoxii* P = 0.007
B KL *L. serrata* < KL *L. wilcoxii* P = 0.003
B KU *L. serrata* < KU *L. wilcoxii* P = 0.007

Differences among parks

A PU *L. wilcoxii* < KU *L. wilcoxii* P < 0.001
B KL *L. nannotis* < TL *L. nannotis* P = 0.028
B K *L. serrata* < P *L. serrata* P < 0.001

Differences between elevations

A PU *L. wilcoxii* < PL *L. wilcoxii* P = 0.009
A KL *L. nannotis* < KU *L. nannotis* P = 0.005
A KL *L. wilcoxii* < KU *L. wilcoxii* P = 0.002
B L *L. nannotis* < U *L. nannotis* P = 0.053

Figure 7.2 — OTU richness split by species, park, and elevation. (A) Richness of entire community (B) Richness of inhibitory bacteria. P values for tests are shown below, with "A" and "B" corresponding to the panels. Results are shown for the post hoc tests on data that were subset based on interactions. Some comparisons were made without subsetting by park or elevation if no relevant interactions were present. Capital letters before species names indicate park (P = Paluma, K = Kirrama, T = Tully, K-T = Kirrama and Tully [when no interaction was present]) and elevation (L = lowland, U = upland). Only significant and nearly significant (P < 0.1) results are shown, but full results are presented in Appendix 2 Tables 1–3. Results for evenness are shown in Appendix 2. Whiskers represent the 10th and 90th percentile (calculated via the "standard" formula in SigmaPlot 11.0) and all outliers are shown.

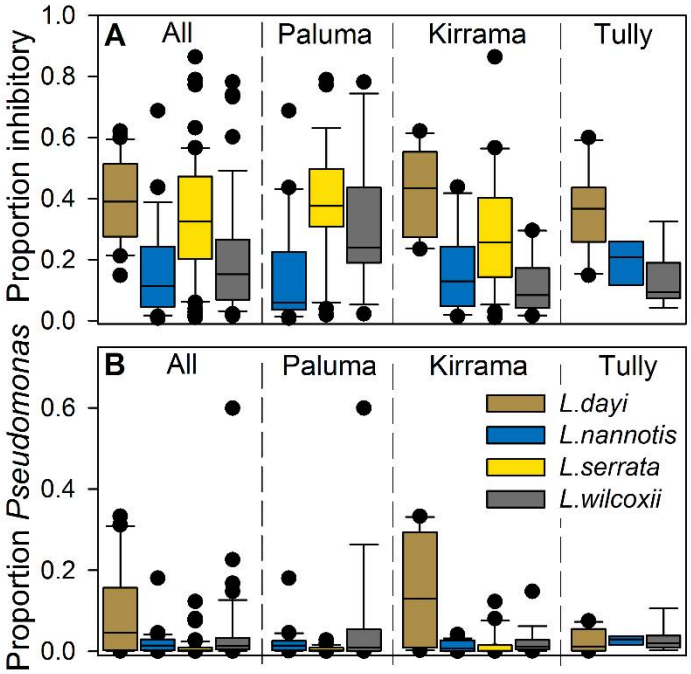

Differences among species (prop. inhib.)

	All	P	K	T
L. dayi > *L. nannotis*	<0.001	-	0.002	
L. dayi > *L. wilcoxii*	0.003	-	<0.001	
L. serrata > *L. nannotis*	<0.001	<0.001	0.036	-
L. serrata > *L. wilcoxii*	0.008	NS	<0.001	-
L. wilcoxii > *L. nannotis*	NS	0.005	NS	-

Differences among parks (prop. inihb.)

P *L. wilcoxii* > K *L. wilcoxii* P < 0.001

P *L. wilcoxii* > T *L. wilcoxii* P = 0.008

Differences among species (prop. *Pseudo*.)

	All	P	K
L. dayi > *L. nannotis*	NS	-	0.015
L. dayi > *L. serrata*	<0.001	-	0.001
L. nannotis > *L. serrata*	0.005	0.020	NS
L. wilcoxii > *L. serrata*	0.002	NS	NS

Figure 7.3 — Relative abundance (proportion) of inhibitory bacteria. (A) All inhibitory bacteria ("prop. Inhib."). (B) Members of the genus *Pseudomonas* ("prop. *Pseudo*"). Dashed horizontal lines separate parks (data for both elevations are included in each box). Tables to the right show the P values for statistical comparisons. For readability, only comparisons that were significant in at least one park are shown (- = no test conducted, NS = not significant). Full results of all statistical tests are available in Appendix 2 Tables 1–3. Whiskers represent the 10th and 90th percentile (calculated via the "standard" formula in SigmaPlot 11.0) and all outliers are shown.

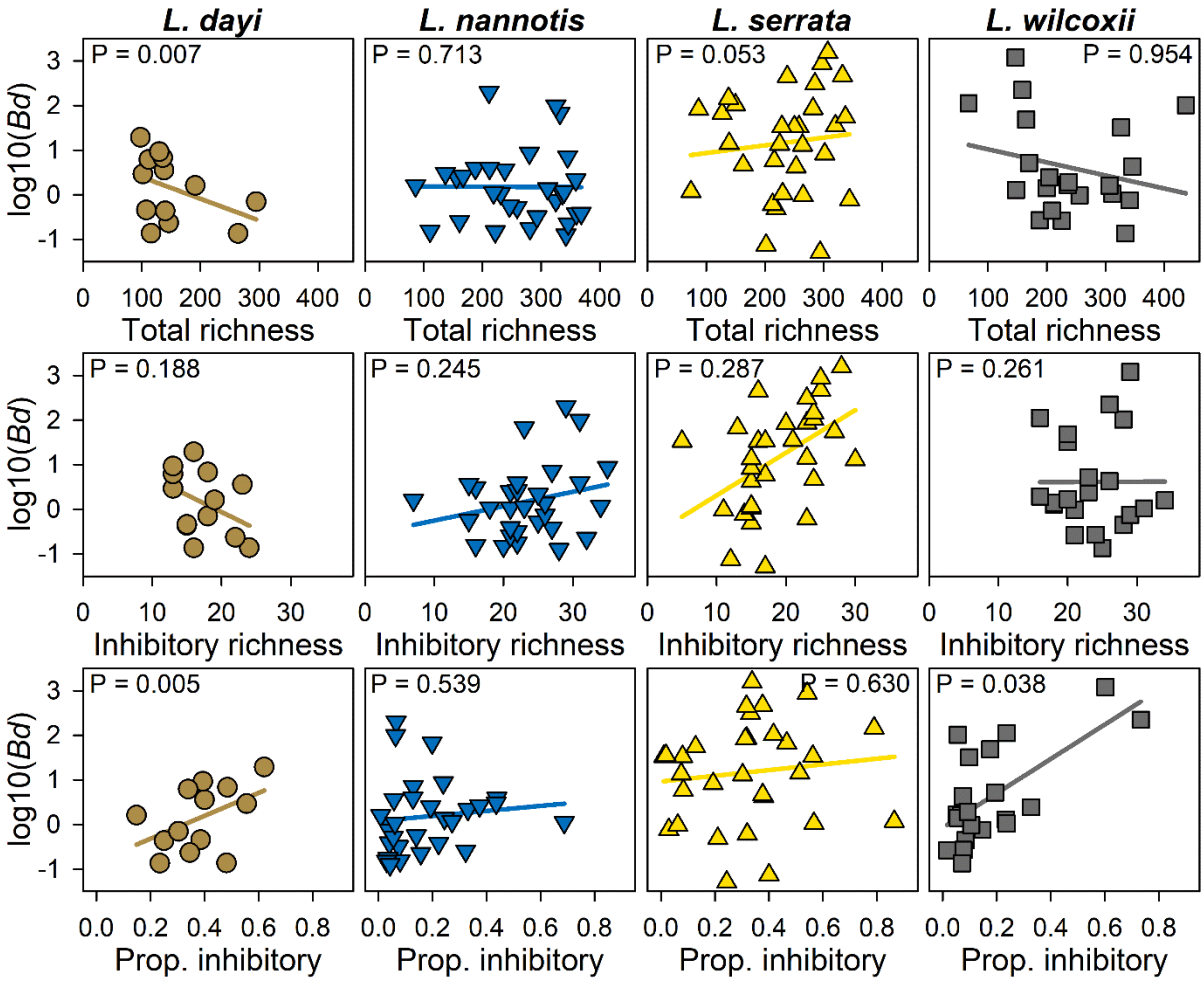

Figure 7.4 — Association between *Bd* infection intensity (for *Bd*+ individuals) and richness. Total OTU richness (row 1), inhibitory richness (row 2), and the relative abundance of inhibitory bacteria (Prop. inhibitory; row 3) are shown. Some *Bd* values are negative because I did not use a pseudocount for the log transformation. The positive trend for *L. serrata* inhibitory richness is largely driven by park effects, and the result is not significant when park is taken into account.

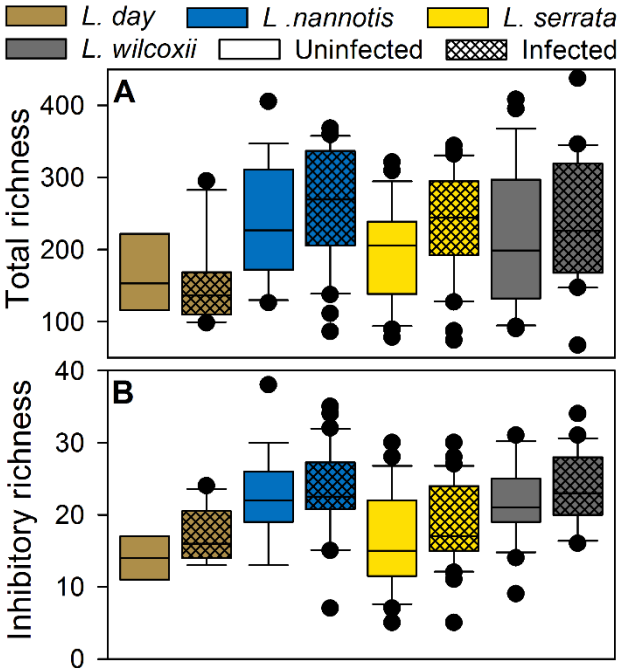

Figure 7.5 — Richness for infected and uninfected frogs. (A) Total OTU richness. (B) Richness of inhibitory OTUs (B) for uninfected and infected frogs. Whiskers represent the 10th and 90th percentile (calculated via the "standard" formula in SigmaPlot 11.0) and all outliers are shown.

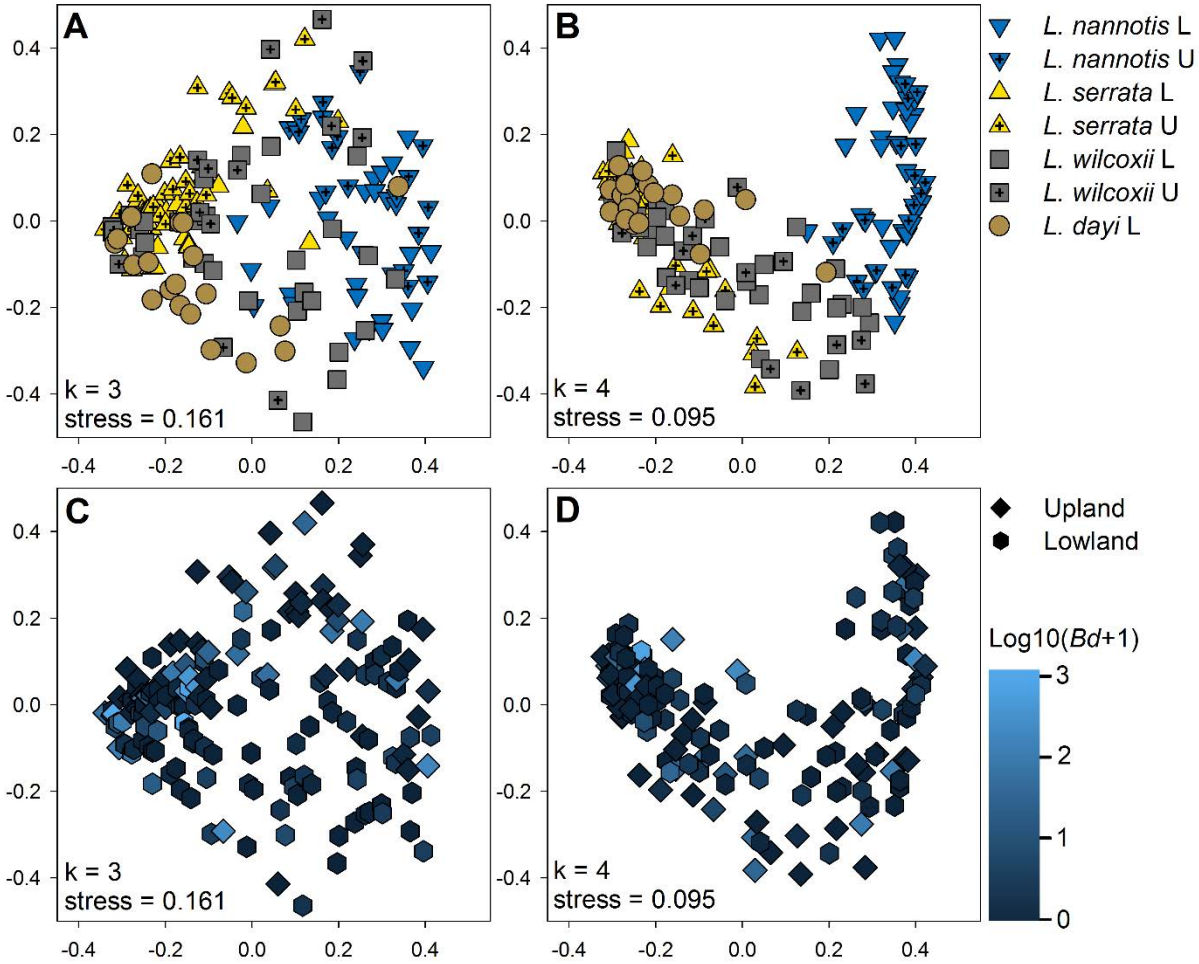

Figure 7.6 — NMDS plots based on Bray-Curtis dissimilarities for frog species, elevation, and infection intensity. A and C show the results for the entire community, and B and D are for just the inhibitory portion of the community. The shading on plots C and D shows the infection intensity based on a log10 transformation of the qPCR results (I added a pseudocount of one to avoid negative values for this visualization). The partial association with *Bd* is driven largely by elevational differences in bacterial communities (*Bd* is more abundant in the uplands), and the patterns are not significant after accounting for elevation. Data were normalized to proportions prior to calculations (B and D, they were normalized after restricting the data to the inhibitory community). The horseshoe affect in B and D is a result of having few overlapping OTUs for many individuals (Morton et al. 2017).

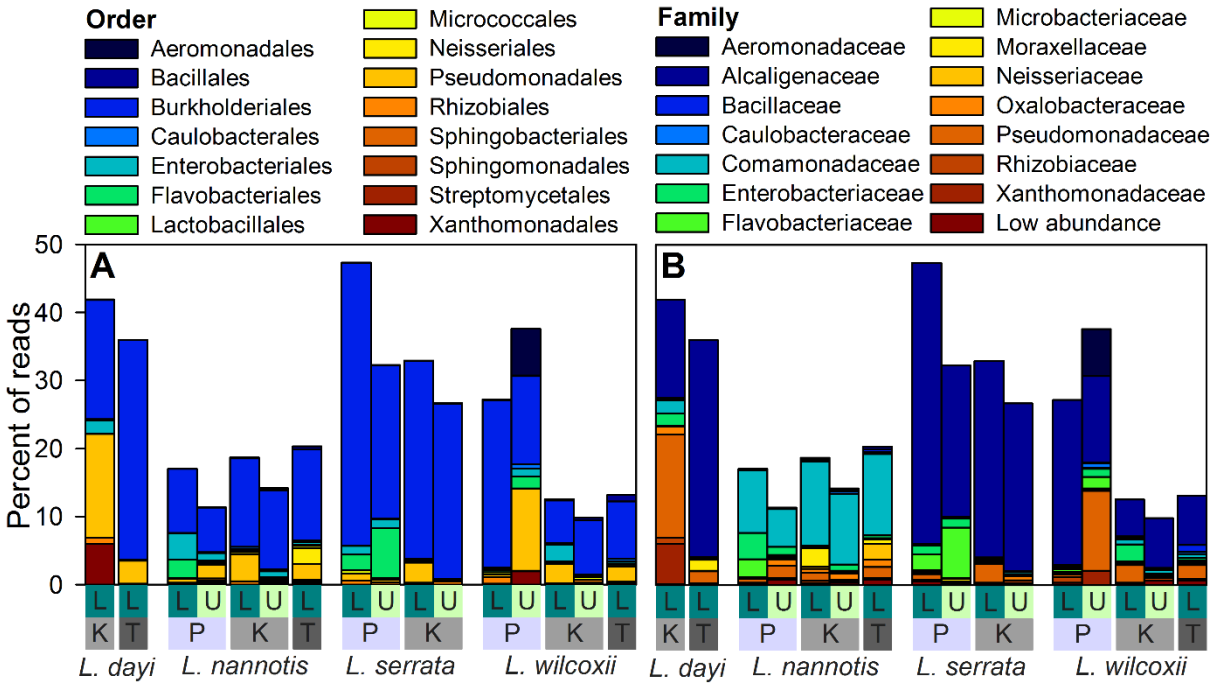

Figure 7.7 — Composition of the inhibitory portion of the bacterial community. (A) Order. (B) Family. Each bar is the mean per collection site. L = lowland, U = upland, T = Tully Gorge National Park. P = Paluma Range National Park, K = Kirrama Range National Park. The "low abundance" category in plot B is the sum of seven families that each comprised an average of less than 0.1% of the communities (Streptococcaceae, Sphingomonadaceae, Sphingobacteriaceae, Burkholderiaceae, Bradyrhizobiaceae, Streptomycetaceae, Micrococcaceae).

CHAPTER 8: THE INTERPLAY OF FUNGAL AND BACTERIAL MICROBIOMES IN RAINFOREST FROGS FOLLOWING A DISEASE OUTBREAK

In preparation for submission as: McKnight, DT, R Huerlimann, DS Bower, L Schwarzkopf, RA Alford, KR Zenger. The interplay of fungal and bacterial microbiomes in rainforest frogs following a disease outbreak. *Science.*

Abstract

Emerging infectious diseases present a serious threat to wildlife populations, and there is growing evidence that host microbiomes play important roles in infection dynamics, possibly even mitigating diseases. Nevertheless, most research on this topic has focused on bacterial microbiomes rather than fungal microbiomes. To help fill this gap in our knowledge, I examined both the bacterial and fungal microbiomes of four sympatric Australian frog species, each of which responded differently to an outbreak of chytridiomycosis. I sequenced 765 bacterial operational taxonomic units (OTUs) and 1122 fungal OTUs. Bacterial communities were more consistent across individuals within a species than were fungal communities (i.e., fungal communities tended to be more variable). Nevertheless, both communities were correlated both for OTU richness and total composition (i.e., pairs of frogs that had similar bacterial microbiomes tended to have similar fungal microbiomes as well). This suggests that either one microbial community was driving the other, or they were both being driven by similar environmental factors. I found little evidence of associations between particular OTUs and chytridiomycosis or between beta-diversity and the disease. However, there was evidence of associations between richness and the disease, with high OTU richness potentially providing a protective effect. This study presents some of the first data on wildlife fungal microbiomes and found evidence that they may be important in infection dynamics.

Introduction

Advances in next generation sequencing technology have rapidly revolutionized the field of microbiology and advanced our understanding of host microbiomes. Studies utilizing these technologies have shown that organisms are hosts to a diverse array of microscopic organisms and these organisms play important roles in host health and ecology, including mitigating diseases (Woodhams et al. 2007; Lam et al. 2010; Flechas et al. 2012; Kueneman et al. 2016; Burkart et al. 2017; Bell et al. 2018; Catenazzi et al. 2018). These discoveries have important implications for managing emerging infectious diseases in wildlife populations, but research on this topic has largely overlooked fungal microbiomes and focused primarily on bacteria. While many papers have been published on the roles played by bacterial communities in wildlife health and ecology, most studies on fungal microbiomes were conducted on mycorrhizal fungi specifically, or soil fungi more generally (Bonfante and Anca 2009; Ma et al. 2016), and within vertebrates, the studies are largely restricted to the fungal microbiomes of humans (Wargo and Hogan 2006; Findley et al. 2013; Hoffmann et al. 2013; Huffnagle and Noverr 2013), domesticated animals (Kittelmann et al. 2013; Chermprapai et al. 2019), and laboratory rodents (Scupham et al. 2006). Few studies have examined fungal microbiomes of vertebrate wildlife (Kueneman et al. 2016, 2017; Kearns et al. 2017; Allender et al. 2018; Chen et al. 2018; Medina et al. 2019). These studies provide valuable starting points, but often had limitations in that they were either conducted in captivity (Kearns et al. 2017; Chen et al. 2018), which causes shifts in microbiomes (Becker et al. 2014; Loudon et al. 2014b), or used 18S primers (Kueneman et al. 2016, 2017), which do not provide as much information about fungal microbiomes as do ITS primers (Schoch et al. 2012).

The shortage of studies on the fungal microbiomes of wildlife is particularly troubling because fungal diseases are among the most widespread and virulent emerging infectious diseases in wildlife (Fisher et al. 2012), with prominent examples, such as chytridiomycosis and white-nose syndrome, causing dramatic declines in numerous species, even dooming some species to extinction (Skerratt et al. 2007). The fungal microbiome is, therefore, an obvious candidate for interacting with and potentially even mitigating these diseases. Indeed, one of the few studies on this topic, which was conducted on captive poison dart frog species (Dendrobates spp.; Kearns et al. 2017) , identified both fungi that enhanced and

fungi that inhibited the growth of *Batrachochytrium dendrobatidis* (*Bd*; the primary pathogen that causes amphibian chytridiomycosis). This is an intriguing and promising result which makes it clear that more studies are needed, particularly studies that use fungi-specific ITS primers to study wild populations.

To explore the potential interactions between fungal microbiomes and *Bd*, as well as comparing fungal and bacterial microbiomes, I used ITS2 and 16S primers to examine the fungal and bacterial microbiomes of frogs in northern Queensland, an area that was heavily impacted by a *Bd* outbreak in the late 1980s and early 1990s. The fungal microbiomes of frogs in this area are particularly interesting, because sympatric frog species exhibited a range of responses to the disease outbreak, including recovery from declines for some species. During the outbreak, all these species persisted at low elevation sites (< 400 m elevation), but the responses of species differed in the uplands (McDonald and Alford 1999). Australian lace-lid frogs (*Litoria dayi*) were extirpated from upland sites and have not recovered (McDonald and Alford 1999; McKnight et al. 2017a), waterfall frogs (*Litoria nannotis*) were extirpated from upland sites and have subsequently recolonized them (McDonald and Alford 1999; McKnight et al. 2017a), green-eyed treefrogs (*Litoria serrata*) declined at upland sites and have recovered (McDonald and Alford 1999; McKnight et al. 2017a), and Stony Creek frogs (*Litoria wilcoxii*) did not decline at any elevation (McKnight et al. 2017a). This range of responses offered an excellent opportunity to determine how host fungal microbiomes interacted with *Bd* infection dynamics and bacterial microbiomes. I examined populations of these species at upland and lowland sites in three separate national parks. My goals were A) Describe the fungal microbiomes of wild frogs and compare them to the frogs' bacterial microbiomes and B) Examine interactions between *Bd* (quantified via qPCR) and the fungal microbiome. I predicted that frogs would have diverse fungal microbiomes, that there would be associations between the fungal and bacterial microbiomes, and that there would be interactions between the fungal microbiome and *Bd*.

Methods

Field sampling

The samples used in this study are the same samples for which the bacterial microbiome was described in Chapter 7. The collection methods, laboratory techniques, and

bioinformatics are described in detail therein. Briefly, I sampled frogs from Paluma Range National Park, Kirrama Range National Park, Girramay National Park, and Tully Gorge National Park. Kirrama and Girramay are adjacent with contiguous streams flowing through them, therefore they will be treated as a single park referred to as "Kirrama." At Paluma and Kirrama, I sampled frogs at upland sites (> 400 m elevation) and lowland sites (< 400 m elevation). When possible, at each elevation, I sampled all frog species from a single section of stream (< 500 m long). At Tully, I only sampled a lowland site. *Litoria dayi* was not present at Paluma and *L. serrata* was not present at the Tully lowland site.

I located frogs by walking along the streams at night and spotlighting them. I captured each individual in a new plastic bag and handled it with a new pair of nitrile gloves. I rinsed each frog in sterile water to remove transient bacteria (Lauer et al. 2007) then used a sterile, rayon-tipped swab (Medical Wire, MW113) to swab it five times along the stomach, five times on each thigh, and five times on the underside of each rear foot. I placed the swabs on dry ice before transferring them to a -80°C freezer. I sampled all frogs (N = 169) within a 11-day period to minimize effects of season and weather (details are provided in the Chapter 7 Table 7.1). During each night of sampling, I also collected blank swabs to account for bacterial contamination.

Laboratory methods

I extracted fungal and bacterial DNA from the samples using a modified version of the CTAB protocol (Doyle and Doyle 1987). It was modified by adding a bead-beating step and a lysozyme incubation step to lyse fungal cells and gram-positive bacteria. I also used an overnight proteinase K digestion.

The *Bd* load on each sample was quantified using triplicate qPCR following the standard protocol for *Bd* (Boyle et al. 2004). I only scored a frog as *Bd+* if all three replicates were positive. The qPCRs were performed by a commercial laboratory (Cesar, Melbourne, Australia).

I prepared samples for sequencing following the Illumina 16S Metagenomics Sequencing Library Preparation guide (Illumina 2017), with a few modifications. I amplified the bacterial DNA using the S-D-Bact-0341-b-S-17/S-D-Bact-0785-a-A-21 primer pair recommended by Illumina, and I amplified the ITS2 region of the fungal genome using the ITS3_KY02/ITS4 primer pair (Toju et al. 2012). For each set of primers (bacterial and fungal) I

used KAPA HiFi DNA Polymerase and triplicate 10 µL PCR reactions to amplify the DNA. I visually inspected for amplification with gel electrophoresis and pooled the triplicates for each sample. I cleaned the pooled samples with Sera-mag SpeedBeads followed by a 40 µL indexing PCR. I used gel electrophoresis to check the results for consistent amplification, cleaned the samples again, and quantified the DNA with a QuantiFluor. I standardized the DNA concentrations and pooled all of the fungal samples into a library and all of the bacterial samples into a library. I sequenced each library on separate runs of an Illumina MiSeq (reagent kit V3 600 cycles PE, Illumina, USA). I included 10% and 20% of PhiX in the bacterial and fungal sequencing runs, respectively.

Bioinformatics and quality control

The bioinformatics methods used are described in Chapter 7 for bacteria and McKnight et al. (2019c) for fungi. Briefly, for bacteria, I used FASTX- trimmer (Hannon 2010), Sickle (Joshi and Fass 2011), PANDAseq (Masella et al. 2012), QIIME 1.9 (Caporaso et al. 2010), and USEARCH (Edgar et al. 2011) to demultiplex the samples, filter the reads and perform quality control, and assign OTUs with 97% identity (using the SILVA database, release 128 (Quast et al. 2013)). For fungi, I used PIPITS (v1.4.5; Gweon et al. 2015), PEAR (Edgar et al. 2011; Zhang et al. 2013), QIIME, and USEARCH for filtering and quality control, and I assigned OTUs with 97% similarity using the UNITE database (12_11, alpha release; Abarenkov et al. 2010). For fungi, this returned 1,335 OTUs, 617 of which were taxonomically "unassigned." Those OTUs were then compared to the NCBI database (accessed 21 January 2018) using BLAST. Following BLAST, any OTUs that were still unassigned or that were assigned to a taxon other than the kingdom fungi were removed. The remaining OTUs were assigned specific taxonomies if both the query coverage and identity score were > 80%, otherwise, they were labeled simply as "Fungi." This resulted in a total of 1,122 OTUs. I used the blank samples to apply the R package microDecon (McKnight et al. 2019c) to both the fungal and bacterial communities and remove contaminant reads. Finally, within both taxa, I examined rarefaction curves and looked for correlations between the read depth and OUT richness of a sample to confirm that I had achieved a sufficient read depth (correlations were calculated based on the read depth and richness of the fully filtered, decontaminated samples). Read depth and OUT richness were not correlated for either taxa (bacteria: $R^2 < 0.001$, $P = 0.896$; fungi: $R^2 = 0.131$, $P = 0.140$).

Statistical analyses

Because *Bd* is an invading pathogen that often a dominated the fungal communities, for most analyses, I thought that it was appropriate to remove it prior to normalizing the data or applying statistical tests. Therefore, unless otherwise specified, results for the fungal communities are results with *Bd* removed. Nevertheless, in some cases, I included *Bd* so that its effects could be seen, and I could compare the communities with and without *Bd*.

To examine alpha-diversity patterns, I calculated richness as the number of unique OTUs present per individual, and I calculated evenness via Pielou's formula, where 1= a totally even community, and 0 = a totally dominant community. For each frog species, I used paired T-tests to compare fungal richness with bacterial richness and fungal evenness with bacterial evenness (paired by frog ID). Additionally, for each frog species, I used general linear models to look for relationships between fungal richness and bacterial richness, fungal evenness and bacterial evenness, bacterial richness and bacterial evenness, and fungal richness and bacterial evenness. I also included park and elevation (as a binary predictor: upland or lowland) in each model (elevation was not included for *L. dayi* because it currently occurs only in the lowlands). I constructed the models *via* the lm function in R (Team 2017b), checked their assumptions via QQ plots and residual plots, and used the car package(Fox and Weisberg 2011) to run ANOVAs. For each model, I initially used a type II sum of squares, but if significant or nearly significant ($P < 0.1$) interactions were present, I switched to a type III sum of squares.

To examine beta-diversity patterns, I normalized the data via proportions (McKnight et al. 2019a) and calculated Bray-Curtis dissimilarities and Jaccard distances via the R package vegan (Oksanen et al. 2017). I used the Bray-Curtis dissimilarities to look at the effects of species, elevation, and park on the fungal and bacterial communities. Initially, to examine elevation and park, I ran PERMANOVAs (via the adonis2 function in vegan) on the entire data sets, with frog species, park, and elevation as predictor variables. Then, because of suspected interactions, I ran separate PERMANOVAs to compare frog species at each elevation of each park. These were followed by post hoc tests comparing each pair of species at a given elevation and park. To conduct those tests, I ran PERMANOVAs on each pair of species and used the sequential Bonferroni method to control the type-1 error rate within each set of comparisons (i.e., each elevation/park for each taxa). For the fungal

communities, I ran this set of tests both with *Bd* included as part of the community and with it removed. Additionally, for both fungi and bacteria, I also ran the species level comparisons using the Jaccard distances. Finally, I used a partial Mantel test (with geographic distance as the z matrix) to look for associations between the Bray-Curtis dissimilarities for the fungal and bacterial communities across all frogs and species. Then, I used partial Mantel tests to look for associations within each species.

I used several methods to look for associations between *Bd* and the fungal community. First, to look for associations with the entire community, I ran a PERMANOVA that included all individuals and *Bd* infection intensity (based on qPCR results) as a predictor variable. It also included frog species, elevation, and park as predictors. Additionally, to examine infection prevalence, I ran a PERMANOVA that was structured identically, but included infection intensity as a binary variable (*Bd*+ or *Bd*- based on qPCR results). I ran both models both with *Bd* included as part of the community and with it removed prior to normalizations and calculations. If *Bd* was having an effect on the community composition other than simply being highly abundant, then I expected to find a significant effect of *Bd* in both sets of tests. In contrast, if *Bd* was dominant but not otherwise influencing community composition, then I expected it only have significant effects when it was included as part of the community.

To look for associations between particular fungal OTUs and *Bd*, first, I used DESeq2 (Love et al. 2014) to look for OTUs that were differentially abundant between *Bd+* and *Bd-* individuals. I did this separately for each species and included elevation and park as factors. Finally, to examine prevalence, I ran linear models comparing the relative abundance of each OTU (data were transformed to proportions) to the infection intensity of *Bd* (based on qPCR results). For these linear models, I only included infected frogs, I only tested OTUs that were present in at least 20% of the individuals in a test, and I ran the tests separately for each species. Additionally, for each OTU I ran several models that included all possible combinations of main effects and interactions for the following predictor variables: OTU abundance, elevation, and park (the included models that excluded some variables). I then selected the best model based on AIC values and only considered its P value. Within each frog species, I controlled the type-1 error rate to an FDR of 0.01.

I did not include a co-occurrence network between fungi and bacteria because my data contained many zeros and rare OTUs, and simulations suggested that none of the

recommended network methods would produce a reliable network for my data. Therefore, I did not feel justified including one.

Results and discussion

Comparing fungal and bacterial microbiomes

In contrast to microbiome research that used 18S (Kueneman et al. 2016, 2017), I found that frog skin contained a large number of fungi. The fungal data clustered into 1122 OTUs, representing five phyla, 19 classes, 57 orders, 132 families, and 262 genera. Most OTUs were in the phyla Ascomycota (482 OTUs) and Basidiomycota (223 OTUs), while Zygomycota (14 OTUs), Chytridiomycota (2 OTUs), and Mucoromycota (2 OTUs) were poorly represented. Finally, 399 OTUs could not be identified beyond Kingdom. Fungal relative abundance (based on proportion of reads) followed a largely similar taxonomic pattern, with Ascomycota (35.4% of reads) being the most abundant phylum, followed by Chytridiomycota (23.9%; 99.89% of Chytridiomycota reads were assigned to *Bd*), Basidiomycota (14.7%), Zygomycota (3.1%), and Mucoromycota (<0.1%). Many reads (22.8%) were not identifiable beyond the kingdom Fungi. The result that Ascomycota and Basidiomycota were the most common phyla (excluding Chytridiomycota) is consistent with a previous study on amphibian microbiomes(Medina et al. 2019). At lower taxonomic levels, most taxa were not abundant, and there was little evidence of dominance (other than *Bd*). Only four classes comprised more than 10% of the reads: Chytridiomycetes (23.9%; mostly *Bd*), Sordariomycetes (14.5%), Agaricomycetes (12.4%), and Dothideomycetes (11.1%). With the exception of Rhizophydiales (23.9%; mostly *Bd*), the most abundant orders were Polyporales (7.2%), Capnodiales (7.2%), and Xylariales (6.0%).

In contrast to the fungal microbiomes, the bacterial microbiomes tended to be dominated by a few taxa. In total, the bacterial microbiomes clustered into 765 OTUs, representing 16 phyla, 39 classes, 70 orders, 129 families, and 207 genera. However, 47.0% of all reads belonged to just two orders: Burkholderiales (29.6%) and Sphingobacteriales (17.4%), which is a large contrast to fungi, in which the two most abundant orders (excluding *Bd*) only comprised 14.4% of the community. Even at the genus level, 24.2% of reads (seven OTUs) were from Achromobacter, and 16.5% of reads (seven OTUs) were from

Sphingobacterium. The next most abundant genus (Chryseobacterium) only contained 2.1% of the reads.

For each frog species, the fungal microbiomes had significantly fewer OTUs per frog (i.e., lower species richness) than did the bacterial microbiomes (all $P < 0.001$), but fungal evenness was higher than bacteria evenness for *L. dayi* ($P < 0.001$) *L. serrata* ($P < 0.001$), and *L. wilcoxii* ($P = 0.020$), but not *L. nannotis* ($P = 0.348$; Figure 8.1). These results are consistent with studies on humans and ruminants which found that humans have fewer fungi than bacteria (Qin et al. 2010) and the fungal microbiome is less diverse than the bacterial microbiome (Kittelmann et al. 2012).

Additionally, the fungal microbiomes were more variable, with many OTUs only occurring on a few individuals. Indeed, when all individuals were included, only 40.1% of fungal OTUs were present in all four species, compared to 72.2% of bacterial OTUs (Figure 8.2). Patterns were similar when looking only at individuals at the Kirrama lowlands (to control for sample sizes as well as park and elevation effects), with only 21.2% of fungal OTUs present in all four species, compared to 54.3% of bacterial OTUs. Further, at the Kirrama lowlands, 33.5% of fungal OTUs were present in only one species, compared to 11.6% of bacterial OTUs.

Beta-diversity patterns were similar. Both taxa generally had high Bray-Curtis dissimilarity values among individuals, but the fungal communities often had higher dissimilarities than the bacterial communities, indicating less stability of the microbiomes across individuals (Figure 8.3). For fungi, 82.9% of comparisons had a Bray-Curtis dissimilarity greater than 0.9 (i.e., over 90% of reads differed between a given pair of frogs). In contrast, only 47.5% of bacterial comparisons had a Bray-Curtis dissimilarity > 0.9. Additionally, the patterns were less consistent among the fungal communities. As a result, in ordination plots, frog species did not cluster as distinctly for the fungal communities as they did for the bacterial communities (Figure 8.4). Similarly, PERMANOVAs on the fungal communities (based on Bray-Curtis distances) revealed significant differences among parks and elevations (all $P < 0.001$), but the differences among species were more limited, and many comparisons were not significant (Table 8.1). In contrast, all comparisons were statistically significant ($P < 0.05$) for the bacterial communities (Table 8.1). PERMANOVAs based on Jaccard distances (which only take presence and absence into account) revealed more fungal differences among species than did the Bray-Curtis comparisons, but these

differences were still more limited for fungi than for bacteria (Table 8.1). Taken together, these results suggest that, when looking at abundance, frog fungal microbiomes were highly variable, resulting in few consistent differences among species, but some fungi are more prevalent on particular frog species, resulting in more consistent differences when looking only at presence/absence. These results are also consistent with results from humans and ruminants which show more variation among samples and less stability for fungal communities than for bacterial communities (Kittelmann et al. 2013; Underhill and Iliev 2014).

Despite these differences, there were some similarities among communities. First, a mantel test that included all individuals found a significant association between the Bray-Curtis dissimilarities of bacterial and fungal communities ($P < 0.001$), and subsequent tests on each species found significant associations for *L. nannotis* ($P = 0.031$), *L. serrata* ($P = 0.003$), and *L. wilcoxii* ($P = 0.009$), but not for *L. dayi* ($P = 0.170$). Second, fungal and bacterial OTU richness were positively correlated for all frog species (all $P < 0.001$), and the patterns among species were similar, with *L. dayi* (the species that has not recovered from the *Bd* outbreak) having the lowest richness for both taxa. In contrast, bacterial evenness and fungal evenness were only positively correlated for *L. dayi* ($P = 0.004$) and showed a slightly negative, non-significant trend for all other species (all $P > 0.150$; Appendix 3). Within fungi, OTU richness and evenness were not significantly correlated for any species (all $P > 0.5$), but within bacteria, they were positively correlated for *L. nannotis*, *L. serrata*, and *L. wilcoxii* (all $P < 0.01$) but not for *L. dayi* ($P = 0.327$).

The result that fungal and bacterial communities were correlated for both community composition (beta-diversity) and richness is interesting. It is consistent with a previous study on amphibians (Medina et al. 2019), but it conflicts with the results of a study on human skin microbiomes (Findley et al. 2013). In humans, bacterial and fungal microbiomes were associated by region (e.g., different areas of the feet clustered together), but there was no general association between the richness of the two communities across body sites (Findley et al. 2013) suggesting that different processes were driving the communities. Correlations can occur, however, when the bacterial and fungal microbiomes are not independent, and one is influencing the other (Wargo and Hogan 2006), a process that is well established in mycorrhizal systems, where the fungal community often dictates the bacterial community (Bonfante and Anca 2009). Conversely, in boreal toads, inhibitory

bacteria strongly influenced the fungal community (Kueneman et al. 2016). Nevertheless, while inter-taxa effects could explain the correlations I observed between Bray-Curtis dissimilarities in my study, they do not provide a satisfactory explanation for the strong correlations between the OTU richness of both communities. An alternative explanation is that both communities are being influenced by the same processes. Thus, a frog that is suitable for hosting a rich assemblage of bacteria may also be suitable for hosting a rich assemblage of fungi. This explanation is reasonable given that, on a particular frog, both communities will be exposed to the same anti-microbial peptides and experience the same environments and climate.

Fungal microbiome and Bd *infection*

There was little evidence of direct associations between particular fungal OTUs and *Bd* infection (*Bd* presence and abundance was assessed by qPCR in addition to sequencing it as part of the community). Based on qPCR, a total of 93 out of 169 frogs were infected with *Bd*, but linear regression models did not detect statistically significant associations between *Bd* infection intensity and the relative abundance of any OTUs (FDR = 0.01). DESeq2 identified 131 OTUs that were differentially abundant between infected and uninfected frogs, but only 13 of those OTUs were differentially abundant in more than one species, and none of them were differentially abundant in more than two species. Additionally, of those 13 OTUs, three were negatively associated with *Bd* in both species, two were positively associated in both species, and the remaining eight were negative in one species and positive in the other. It is, nevertheless, possible that different fungal OTUs are acting differently in each frog species, resulting in little consistency among species.

Examining relationships between community composition and *Bd* revealed a similar lack of significant interactions. When *Bd* was present, it often dominated the fungal microbiome and was frequently the most common fungal OTU, comprising up to 98.9% of fungal reads on a frog (Supplemental information). Thus, including it as part of the community resulted in lower species evenness (Figure 8.1) and lower dissimilarities between samples (Supplemental Information). As a result, including *Bd* often masked trends that were otherwise present (Table 8.1). Indeed, when it was included, it was the primary factor that explained the clustering of individuals in nMDS plots (Figure 8.5). Similarly, PERMANOVAs (based on Bray-Curtis dissimilarities) that included *Bd* as part of the

community found significant effects for both *Bd* infection intensity (based on qPCR results; $P < 0.001$) and prevalence (*Bd+* vs *Bd-*; $P < 0.001$). In contrast, when *Bd* was removed from the community prior to normalization and calculating Bray-Curtis dissimilarities, but its intensity or prevalence (based on qPCR results) was included in the statistical models, there was no significant effect of *Bd* intensity ($P = 0.298$), nor was there a significant difference between *Bd*+ and *Bd*- individuals ($P = 0.578$). Thus, although *Bd* dominated the fungal community in sheer numbers (resulting in a strong influence on Bray-Curtis dissimilarities), the rest of the community did not appear to be strongly influenced by its presence or relative abundance (Figure 8.5). It is, however, possible that the total abundance of fungi was affected, but I was unable to test that.

These results suggest that neither particular fungal OTUs nor the general composition of the fungal communities are important for mitigating *Bd* infections. However, there may be important interactions with groups of OTUs that I was unable to detect by examining each OTU separately. Additionally, it is interesting that *L. dayi* (the species that has not recovered from the *Bd* outbreak) had the lowest levels of species richness for both bacteria and fungi. Multiple studies of the interactions between bacterial microbiomes and pathogens suggest that high levels of richness can provide a protective effect against the disease (Dillon et al. 2005; Matos et al. 2005; Eisenhauer et al. 2013; Fraune et al. 2015; Harrison et al. 2017). Based on my results, this may be occurring in the fungal microbiomes as well. This also raises the possibility that studies that make inferences based on the richness of only on part of microbial community may reach false conclusions (i.e., the combined richness of the fungal and bacterial communities may be more important than the richness of either community by itself).

Conclusion

This study is among the first to explore *in situ* fungal microbiomes in amphibians, and it reveals several important findings. First, it documented a large community of fungi that was not previously known to occur on amphibians. Second, the compositions of the fungal and bacterial microbiomes were fundamentally different. The bacterial communities tended to have many members, with a few dominant OTUs, while the fungal communities had fewer members and little dominance. The fungal microbiome was more variable than

the bacterial microbiome, with higher dissimilarity values and fewer OTUs detected on multiple species. Despite these differences, both the species richness and dissimilarities of the two communities were positively correlated. Particular fungal OTUs or the fungal community composition did not appear to be important for *Bd* infection dynamics, but species richness may be important.

Tables

Table 8.1 — PERMANOVA results comparing species at each elevation of each park. Results are P values after correcting for multiple comparisons within each set of comparisons. Grey cells were statistically significant (adjusted P < 0.05). "Fungi (with *Bd*)" = the entire fungal community was used. "Fungi (no *Bd*)" = *Bd* was removed prior to normalization and analysis. Bray-Curtis dissimilarities take into account abundance, while Jaccard distances look only at presence/absence.

			Bray-Curtis dissimilarity			Jaccard distance	
Park	Elevation	Species comparison	Bacteria	Fungi (with *Bd*)	Fungi (no *Bd*)	Bacteria	Fungi (no *Bd*)
Paluma	Lowland	*L. nannotis - L. serrata*	<0.001	0.037	0.005	0.002	<0.001
		L. nannotis - L. wilcoxii	0.001	0.004	0.002	<0.001	0.002
		L. serrata - L. wilcoxii	0.046	0.107	0.585	0.194	0.304
	Upland	*L. nannotis - L. serrata*	<0.001	0.570	0.106	<0.001	0.002
		L. nannotis - L. wilcoxii	<0.001	0.389	<0.001	<0.001	<0.001
		L. serrata - L. wilcoxii	0.008	0.583	<0.001	<0.001	<0.001
Kirrama	Lowland	*L. dayi - L. nannotis*	0.001	1.000	1.000	0.001	0.041
		L. dayi - L. serrata	0.020	0.419	0.005	0.005	0.010
		L. dayi - L. wilcoxii	0.001	0.010	0.004	0.002	0.006
		L. nannotis - L. serrata	0.001	1.000	0.353	0.002	0.062
		L. nannotis - L. wilcoxii	0.001	0.224	0.383	0.001	0.308
		L. serrata - L. wilcoxii	0.002	0.014	0.025	0.004	0.024
	Upland	*L. nannotis - L. serrata*	<0.001	1.000	0.713	<0.001	0.005
		L. nannotis - L. wilcoxii	<0.001	0.470	0.084	<0.001	0.001
		L. serrata - L. wilcoxii	0.019	0.304	<0.001	0.001	0.012
Tully	Lowland	*L. dayi - L. nannotis*	<0.001	1.000	1.000	0.002	0.404
		L. dayi - L. wilcoxii	0.003	0.570	0.442	0.013	0.199
		L. nannotis - L. wilcoxii	0.011	0.451	1.000	0.002	0.381

Figures

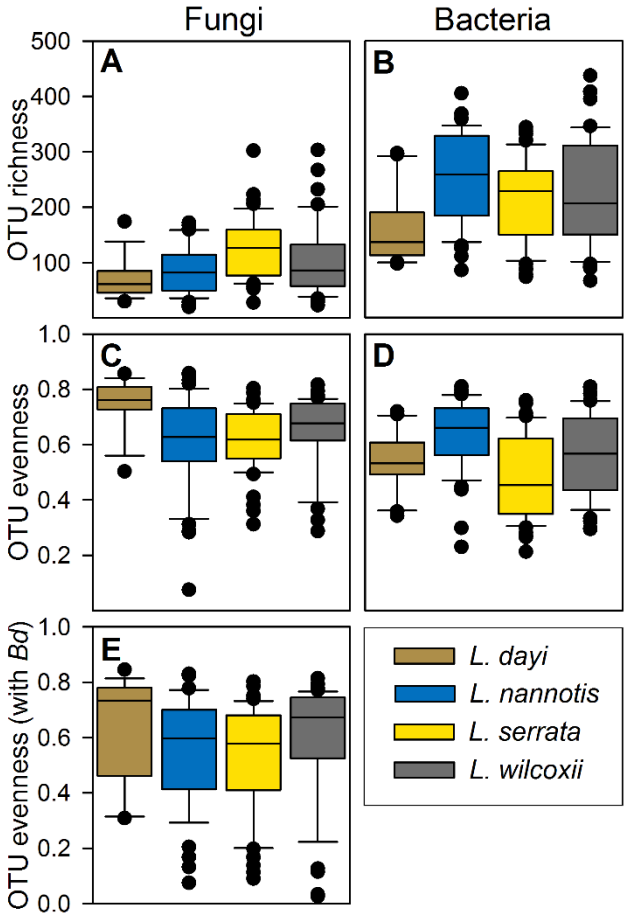

Figure 8.1 — Richness and evenness of the fungal and bacterial communities. Letters indicated groups (within panels) that were not significantly different form each other. For panel C, *Bd* was removed from the community prior to calculations. For panels C–E, 1 = a totally even community. All data per species were combined (data split by park and elevation are available in Appendix 3). Whiskers represent the 10th and 90th percentile and all outliers are shown.

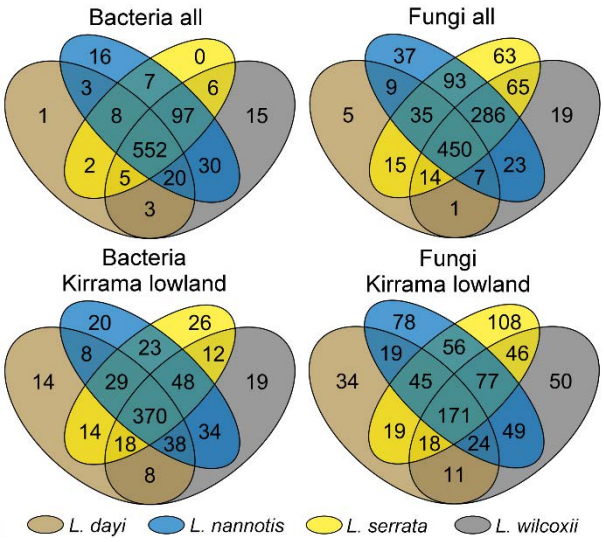

Figure 8.2 — Distributions of OTUs across species. The first row shows the results from all samples, and the second row shows the results for frogs at the Kirrama lowlands only, to control the number of samples per species and park and elevation effects (ten samples per species; one sample was randomly removed for *L. nannotis*).

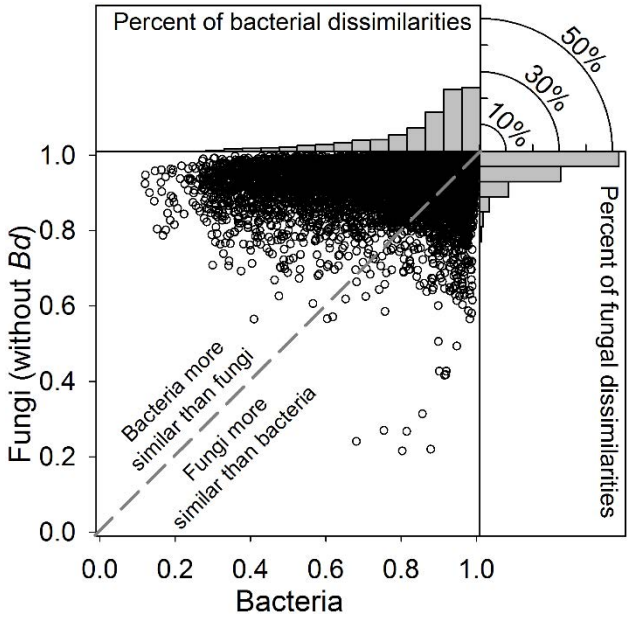

Figure 8.3 — Bray-Curtis dissimilarities for all comparisons (1 = totally dissimilar, 0 = identical). The scatterplot shows the relationship between the bacterial and fungal dissimilarities, with points falling above the line indicating that the bacterial communities were more similar (less dissimilar) than the fungal communities. The histograms show the distribution of dissimilarities for bacteria and fungi. Fungal communities tended to be more dissimilar than bacterial communities.

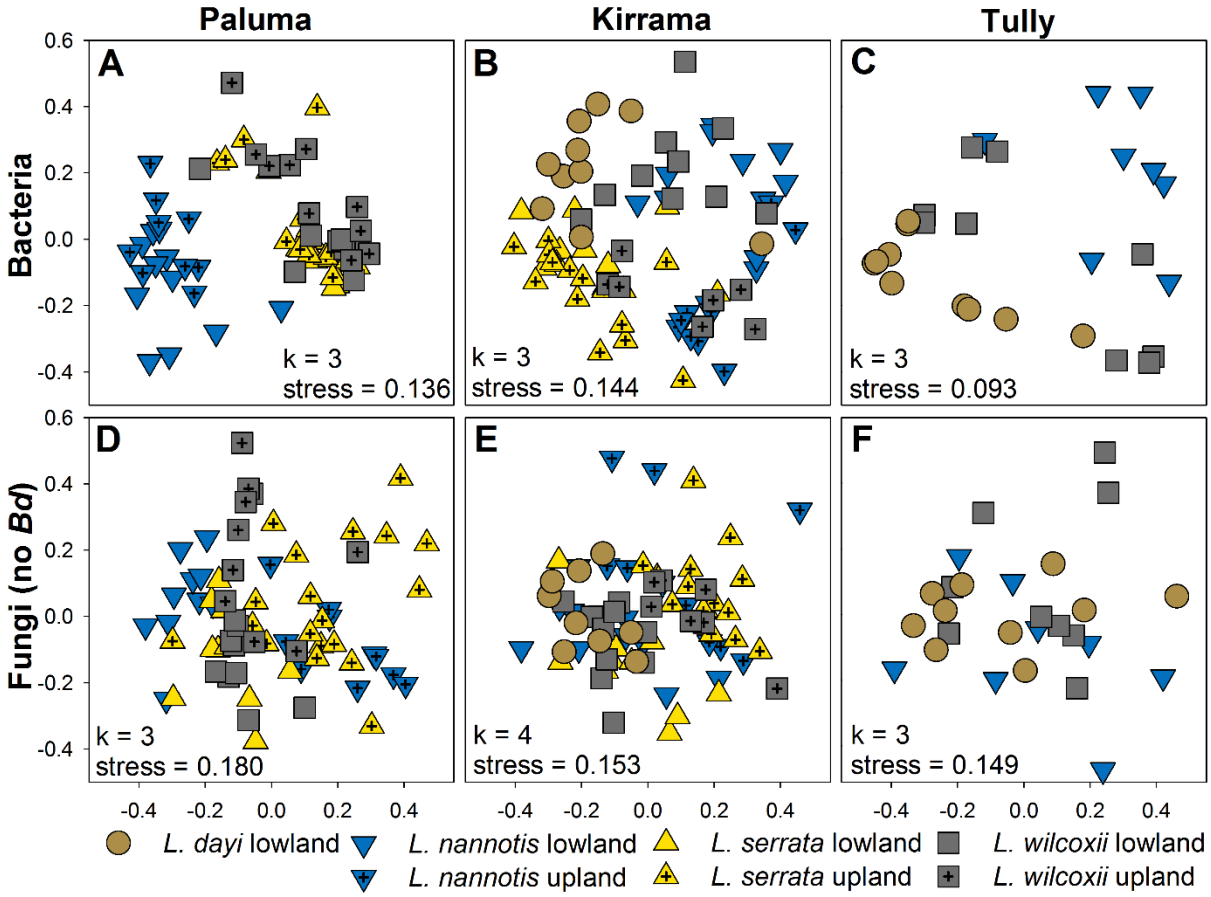

Figure 8.4 — nMDS plots (based on Bray-Curtis dissimilarities) of fungal and bacterial communities split by park and showing clustering of elevations and species. Both fungi and bacteria clustered by elevation, but the clustering by species was not as strong for fungi as it was for bacteria. *Bd* was removed from the fungal community prior to normalizing and calculations.

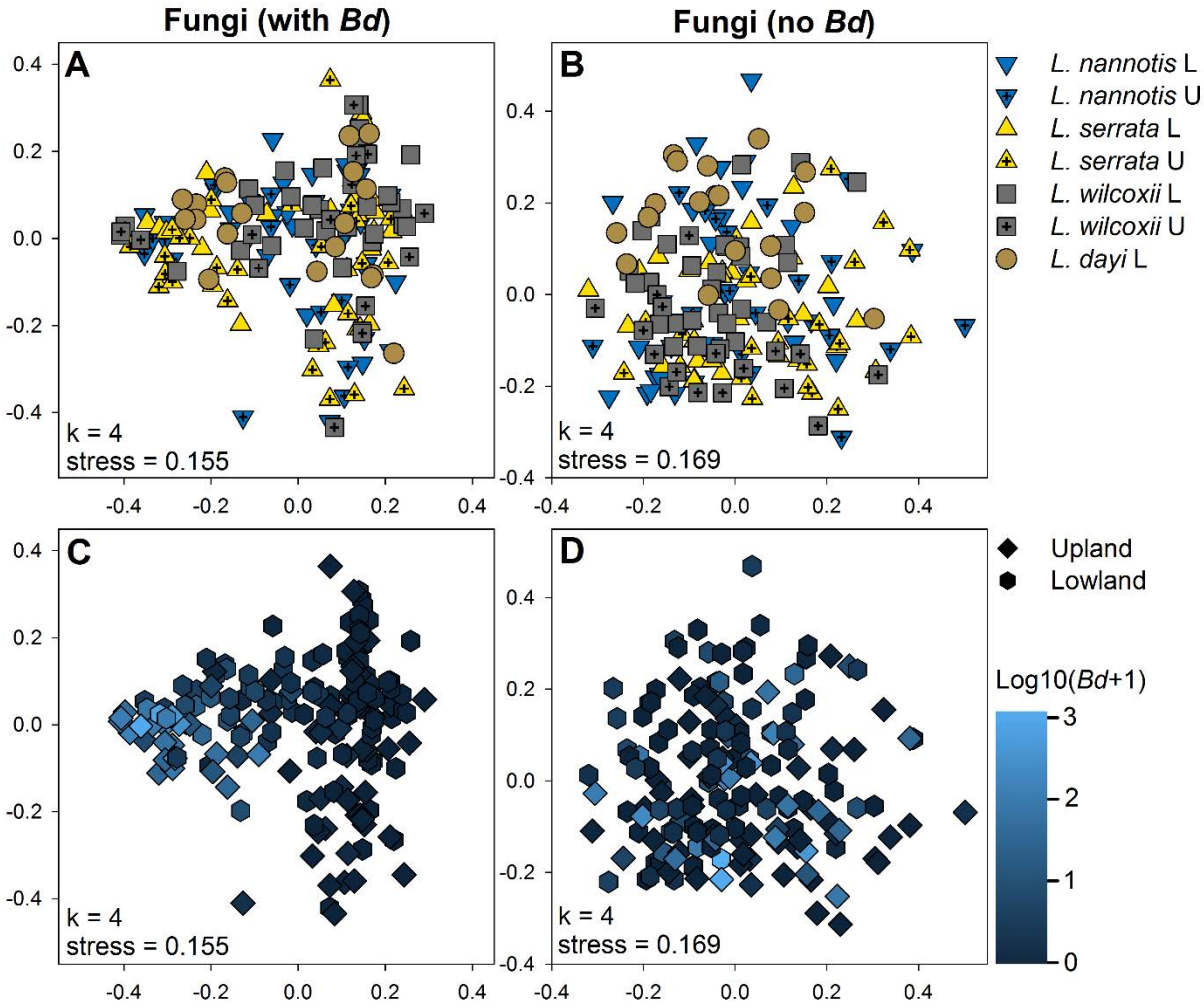

Figure 8.5 — nMDS plots (based on Bray-Curtis dissimilarities) for the fungal communities with and without *Bd* (i.e., for panels B and D, *Bd* was removed from the community prior to normalization and calculations). Panels C and D are shaded by *Bd* infection intensity based on qPCR results. When *Bd* was included in the community, it was the dominant factor explaining the ordination (C) because it was often highly abundant; however, it had no discernible impact on the rest of the community (B and D).

CHAPTER 9: CONCLUDING REMARKS AND SYNTHESIS

Emerging infectious diseases present a serious threat to many species of wildlife, and there is a great need to understand both their long-term consequences and the factors that allow populations to persist with them and even recover from declines (Daszak et al. 2000; Smith et al. 2006). My thesis expands our knowledge of these topics by examining the population genetics (Chapters 3 and 4) and microbiomes (Chapters 7 and 8) of frog species in Australia's Wet Tropics. It produced several novel results that provide important information for managing populations and understanding disease dynamics. It also resulted in the testing and development of improved bioinformatics methods for microbiome data sets (Chapters 5 and 6).

Population genetics

My literature review (Chapter 2) illustrated that not all populations lose diversity during a decline, but the mechanisms allowing diversity to be retained were not entirely clear. The genetic studies I conducted during my thesis helped to fill this knowledge gap. The population genetics data on *L. dayi, L. nannotis*, and *L. serrata* suggested that conserving large areas of habitat refugia are important for maintaining genetic diversity during disease outbreaks (Chapters 3 and 4). It has long been known that habitat refugia are important for surviving environmental disturbances (Puschendorf et al. 2011), but my results build on that by demonstrating associations between the extend and quality of habitat and the amount of genetic diversity that was retained during an outbreak. This pattern was clearest in *L. nannotis*, which had substantially higher genetic diversity at Girramay-Kirrama (which has a larger section of lowland rainforest) than at Paluma (which is drier and has less lowland rainforest) after recovering from a disease outbreak. Similarly, within Paluma, genetic diversity was highest at the streams with the largest sections of lowland rainforest. Comparable patterns were observed for *L. serrata*, though they were less pronounced, probably as a result of its higher dispersal ability (Rowley and Alford 2007b) and the fact that it only declined during the outbreak rather than disappearing from the uplands (McDonald and Alford 1999; Richards and Alford 2005). Quantifying the extent of lowland habitat for *L. dayi* is more difficult, but the lowest diversity levels were at

Girramay-Kirrama which, although wetter than Paluma, is drier than Tully and Wooroonooran further north, and it has less extensive rainforest.

These results are in good agreement with population genetic theory which predicts that populations can endure declines without losing diversity if they can maintain large enough population sizes to avoid inbreeding and genetic drift (Chapter 2; Nei et al. 1975; Allendorf 1986; Zenger et al. 2003). Several other studies have cited large numbers of surviving individuals as the reason that populations experience disease-induced declines without losing substantial amounts of genetic diversity, but the importance of habitat refugia in facilitating that retention of diversity is a novel result of my research (Queney et al. 2000; Lachish et al. 2011; Longo et al. 2015). Interestingly, a recent global analysis of factors affecting the severity of *Bd*-induced declines (Scheele et al. 2019) found that having a large elevational range was a good predictor of both reduced severity of the declines and eventual recovery from the declines. The authors did not directly test the quality or quantity of lowland habitat, but their result is consistent with my findings.

Although a loss of diversity can be detrimental to populations and rob them of the diversity necessary to respond to diseases and other threats (Hedrick and Kalinowski 2000; Keller and Waller 2002; Reed and Frankham 2003; Spielman et al. 2004; Whiteman et al. 2006; Hughes et al. 2008), in my study, low diversity levels did not explain the differences in species' repossesses to *Bd*. The populations of *L. nannotis* at Paluma recovered from the outbreak despite an apparent loss of genetic diversity (Chapter 3), whereas, *L. dayi* populations have not been able to recolonize upland sites despite having high genetic diversity and large lowland populations (Chapter 4). Similarly, *L. dayi*, *L. nannotis*, and *L. serrata* all had high levels of connectivity and gene flow among populations. These high gene flow levels will likely be important for restoring diversity in the populations where it was reduced (Chapter 2; Wright 1931; Slatkin 1985, 1987; Whiteley et al. 2015). However, the fact that *L. dayi* had high levels of connectivity suggests that it has good dispersal abilities, thus falsifying the hypothesis that a lack of dispersal ability has prevented it from recolonizing upland sites.

An additional possibility for the differences in recovery patterns is the hypothesis that some populations have adapted to become tolerant of the pathogen, while others (such as *L. dayi*) have not. Previous work has shown that differences in *Bd* susceptibility are heritable (Palomar et al. 2016), and adaptation to *Bd* has been found in other species

(Grogan et al. 2018; Voyles et al. 2018; Kosch et al. 2019). My tests of this hypothesis were mixed. I did not find compelling evidence of adaptation in *L. nannotis*, however, given the high levels of connectivity among sites, the signature of selection may have been diluted by gene flow, making it difficult to detect (Chapter 2). The influence of gene flow is particularly relevant for this system, because, although lowland frogs do not experience epizootics, they do become infected, and sub-lethal *Bd* infections likely affect fitness (Chatfield et al. 2013; Campbell et al. 2019). Therefore, although the selection pressure for alleles for tolerating *Bd* infections would be strongest at the upper elevation extreme of *L. nannotis*, I would still expect there to be a selection pressure at low elevation sites. Thus, alleles which rose to prominence at high elevation sites would still accumulate at low elevation sites due to a combination of gene flow and a weak or moderate selection pressure (relative to the pressure at high elevation sites). If correct, this situation would result in a limited time window for detecting selection, and I may have simply sampled the populations after beneficial alleles had become common at both elevations.

In contrast to *L. nannotis*, *L. dayi* did show some evidence of adaptation, with different tests agreeing that selection was occurring at the species' current elevation extremes. Unfortunately, the short DNA sequences I was using (~69 base pairs) and lack of genetic resources for the Hylidae family prevented me from reliably identify the regions of the genome that were under selection, so future research is needed to determine if this is actually adaptation to *Bd*. This would be an excellent topic for a future study to try to capture adaptation in action.

Microbiome methods

To examine the potential role of microbial communities in population recoveries, I first had to test and develop two bioinformatics methods. The technology for sequencing entire microbial communities is still relatively new, and adequate bioinformatics methods have necessarily lagged behind the technological advances.

The first major hurdle was normalizing my data (Chapter 5). Microbiome sequencing technologies produced different numbers of reads for each sample, and normalizing those difference is important for accurate analyses. However, most studies on this topic have focused on normalizing samples for differential abundance testing of particular OTUs and largely ignored the community-level effects (i.e., beta-diversity; Bullard et al. 2009; Dillies et

al. 2013; Paulson et al. 2013; McMurdie and Holmes 2014; Lin et al. 2016; Weiss et al. 2017). Comparisons among communities were a critical part of my analysis plan (Chapters 7 and 8); therefore, in Chapter 5, I tested several common normalization methods, specifically examining how they affected community-level comparisons. My results demonstrated that the most common normalization methods (upper quartile, CSS, edgeR-TMM, and DESeq-VS) ignored the importance of species evenness (Stirling and Wilsey 2001; Hillebrand and Cardinale 2004; Wilsey et al. 2005; Ghazoul 2006; Hillebrand et al. 2008; Wittebolle et al. 2009) and, as a result, distorted communities and skewed analyses. In contrast, rarefying or normalizing to proportions produced accurate community comparisons, despite the fact that these methods are not suitable for differential abundance testing. This result was crucial for my ability to accurately compare the communities of my frog samples, and it is broadly applicable to other microbiome studies.

The second challenge was dealing with contamination (Chapter 6). Microbial contamination is a ubiquitous problem in microbiome research (Corless et al. 2000; Kulakov et al. 2002; Peters et al. 2004; Shen et al. 2006; Hang et al. 2014; Weiss et al. 2014), and blank (control) samples revealed that it was present in my samples as well. This contamination could have distorted the communities and made it difficult to discern the true patterns, but no adequate methods for dealing with contamination in sequencing data currently exist. Therefore, I developed and tested the R package microDecon for identifying and removing contaminant reads. Tests using both in silico data and a sequencing experiment showed that microDecon is very accurate at identifying and removing contaminant reads. Thus, I was able to apply it to my frog datasets (Chapters 7 and 8). This method will also be useful for a broad range of studies.

Microbiomes and *Bd*

The methods developed in Chapters 5 and 6 allowed me to examine the potential role of microbiomes played in frog recoveries and test the possibility that differences in microbial communities explain the differential pattern of recoveries. While most studies of microbiomes in wildlife have focused only on the bacterial communities, I examined both the bacterial (Chapter 7) and fungal (Chapter 8) communities. This is a useful approach that

has is not often utilized (Deveau et al. 2018), and it gave my research additional power to detect meaningful patterns.

Results of the fungal and bacterial communities were largely similar, and both species richness and community composition were correlated between the communities. This is interesting because, although bacteria and fungi are known to interact (Wargo and Hogan 2006; Bonfante and Anca 2009; Kueneman et al. 2016), a study on human skin microbiomes found that the fungal and bacterial communities were not correlated (Findley et al. 2013). A recent study on amphibian microbiomes did, however, find correlations between the communities that were similar to the patterns I observed (Medina et al. 2019). My results suggest that either the communities are shaping each other, or some environmental factor is shaping both communities. For example, frogs produce many anti-microbial peptides (AMPs) on their skin (Woodhams et al. 2010), and it is possible that peptides that allow a rich bacterial community to thrive also allow a rich fungal community to thrive. However, given the chemical differences between bacteria and fungi (e.g., cell walls made of peptidoglycan vs chitin) it would be somewhat unexpected if both communities responded to similar environments in the same way, and more research on this is needed. Nevertheless, because of the associations between these communities, it is clear that examining both bacteria and fungi is important for understanding interactions between hosts and their microbiomes (Deveau et al. 2018).

Both communities displayed similar patterns in relation to *Bd,* and those patterns suggest that community richness may be more important than community composition or inhibitory bacteria in protecting hosts against *Bd.* First, in both communities, *L. dayi* had the lowest richness. This is potentially important because it is the only species that I studied that has not recovered from the *Bd* outbreak. Additionally, within *Bd* infected frogs, there was a negative correlation between richness and *Bd* infection intensity. Furthermore, at Girramay-Kirrama, recovered upland populations of *L. nannotis* had higher richness than the lowland populations that did not decline.

Despite the associations with richness, I was unable to detect associations between *Bd* and the composition of either community (beta-diversity), nor did I find consistent evidence of associations between particular OTUs (bacterial or fungal) and *Bd.* Additionally, the relative abundance of known inhibitory bacteria was actually positively associated with

Bd (i.e., heavily infected frogs has high proportions of inhibitory bacteria), and *L. dayi* had the highest proportions of inhibitory bacteria.

Taken together, these results are consistent with a protective effect of richness, but not with a protective effect of either community composition or a relative abundance of inhibitory bacteria. These results are also bolstered by the consistency between the fungal and bacterial communities. Moreover, the hypothesis that species richness plays a beneficial role in infection dynamics is supported by other studies that found associations between richness and *Bd* (Jani et al. 2017; Piovia-Scott et al. 2017; Antwis and Harrison 2018; Bates et al. 2018), as well as studies on other disease systems that found that communities with higher richness were more resistant to invading pathogens (Dillon et al. 2005; Matos et al. 2005; Eisenhauer et al. 2013; Fraune et al. 2015; Harrison et al. 2017). However, there are also studies that have suggested that community composition (Jani and Briggs 2014; Becker et al. 2015; Rebollar et al. 2016b) or an abundance of inhibitory bacteria (Woodhams et al. 2007; Lam et al. 2010; Flechas et al. 2012; Kueneman et al. 2016; Burkart et al. 2017; Bell et al. 2018; Catenazzi et al. 2018) are key factors in *Bd* infection dynamics. These disparate results may be partially artifacts from different methodologies, but, as my results demonstrate, microbiomes are extremely complex, and different species or even the same species at different sites may respond differently. Thus, richness may be important in some cases, while community composition and inhibitory bacteria may be critical in others.

Unfortunately, co-occurrence networks did not provide an appropriate technique to clarify my results. This could have been a useful addition, because co-occurrence networks can, in concept, show relationships and interactions among different members of the microbial communities, as well as revealing how robust the communities are to disturbances (Iyer et al. 2013; Layeghifard et al. 2017). However, the current methods for constructing these networks have limitations and often produce inconsistent results (Weiss et al. 2016). Different methods often disagree with each other widely, as was the case for my data (Faust et al. 2012; Friedman and Alm 2012; Ban et al. 2015; Kurtz et al. 2015; Weiss et al. 2016; Siska and Kechris 2017). Further, simulations modeled on my data sets (following the protocol in Kurtz et al. [2015]) suggested that my data were not producing reliable networks, even when following the recommended guidelines for selecting the best network method (Weiss et al. 2016). Therefore, I have not included any co-occurrence networks in my thesis, but it would be useful to revisit this topic as methodologies improve.

Conclusions, management implications, and future directions

The results of my research have several important implications for management and conservation efforts, as well as future research projects. First, my results have highlighted the importance of both habitat refugia and gene flow in preserving genetic diversity during an outbreak and facilitating population recoveries following an outbreak. Therefore, management efforts should ensure that both habitat refugia and corridors are maintained. Second, given the apparent diversity loses that were observed for *L. nannotis* at Paluma, it will be important to continue to monitor these populations. It would be particularly interesting to resample my sites in a decade or two and re-assess their diversity. If my conclusions are correct, and the current diversity patterns are a result of only a few individuals surviving the outbreak at streams that lacked large sections of lowland habitat, then the current pattern should only persist for a few generations before being homogenized by gene flow from populations that retained more diversity. Thus, repeating part of my study in several years would provide an additional test of my conclusions, as well as providing both more long-term data on population recoveries and a follow-up assessment of the populations' health and diversity.

My tests for adaptation to *Bd* showed potential ongoing adaptation in *L. dayi*, but the results were not conclusive and merit further study. Although I used the best methods available, these still have serious limitations (Hoban et al. 2016; Lowry et al. 2016), and future methodological developments and genetic resources (e.g., a Hylidae genome) may allow a re-analysis of my data using more robust methods. It would also be useful to conduct quantitative breeding experiments to determine the heritability of susceptibility in this species and look for genes controlling tolerance to the disease.

Additionally, transcriptomics may be a useful approach (Rosenblum et al. 2009; Savage et al. 2014; Price et al. 2015). For example, researchers could compare gene expression between upland and lowland frogs when exposed to *Bd*, as well as making comparisons among species. This may allow the elucidation of genes that are mediating recoveries from *Bd*.

My microbiome results are among the first to examine both bacteria and fungi in wildlife, and this is an approach that future studies should implement, because focusing

exclusively on the bacterial community ignores important components of the microbiome. My results from both communities suggest that richness may be playing an important role in population recoveries, and a lack of microbial richness in *L. dayi* may at least partially explain why it has not recovered. In contrast, I did not find evidence that having a high relative abundance of inhibitory bacteria facilitates recoveries. Indeed, *L. dayi* generally had high levels of inhibitory bacteria, including high levels of *Pseudomonas,* a genus that is often targeted because it is highly inhibitory towards *Bd*. These results are important, because there is widespread interest in using bacteria as probiotics to aid recoveries in wild populations (Woodhams et al. 2011, 2012; Bletz et al. 2013; Ysumiba et al. 2016). However, my results do not suggest that this strategy would be viable, since *L. dayi* already has a high proportion of inhibitory bacteria. A more useful approach may be to inoculate frogs with a diverse consortium of bacteria (Loudon et al. 2014a; Piovia-Scott et al. 2017; Antwis and Harrison 2018), however this approach is potentially problematic because it may be difficult to get a diverse community to establish on a host. Additionally, great care is needed to avoid introducing non-native bacteria into an environment or shifting the hosts' microbiomes in ways that are disadvantageous for situations other than *Bd* infections.

Although I tested several possible causes of recoveries, there are others that were beyond the scope of my thesis and would be useful topics for future research (McKnight et al. 2017a). For example, some populations of alpine tree frog (*Litoria verreauxii alpina*) have recovered from a *Bd* outbreak by shifting their reproductive effort earlier in life (Scheele et al. 2015). Thus, they still experience mass adult mortalities, but they produce enough offspring early in life for the populations to persist. Other shifts in behavior (e.g., increased thermoregulatory behavior or reduced contact with conspecifics) could also potentially help frogs to clear infections or avoid becoming infected (Rowley and Alford 2007a, 2013; Daskin et al. 2011). Additionally, attenuation of *Bd* virulence has been overserved in laboratory cultures (Refsnider et al. 2015), leading to the possibility of attenuation as a mechanism of recovery; however, research from Panama suggests that *Bd* is still virulent and attenuation does not explain population recoveries (Voyles et al. 2018). Anti-microbial peptides (AMPs) have also been implicated in some systems (Woodhams et al. 2011). Indeed, one study found that lowland *L. serrata* populations that did not experience *Bd* induced declines had AMPs that were more effective at fighting *Bd* than the AMPs at populations that did decline,

possibly suggesting that AMPs played a role in protecting lowland populations during the outbreak (Woodhams et al. 2010).

These additional possibilities should be investigated, but it is worth mentioning that they are not mutually exclusive with the possibilities that I examined. Different species may be recovering via different mechanism, and several mechanisms may be occurring simultaneously or interacting with each other. To give one hypothetical example, there could be selection for AMPs that result in a rich microbiome which, in turn, defends against *Bd* infections. In this situation, adaptation, shifts in AMP production, and shifts in microbiomes would all be occurring. Although that situation is entirely hypothetical, interactions of that nature are possible, and studies of recoveries should incorporate information on multiple mechanisms. My research has added to our knowledge of recoveries by examining population genetics, bacterial microbiomes, and fungal microbiomes, but there is still more work to be done, as well as ample opportunity to build on my research and incorporate my results into future studies.

LITERATURE CITED

Abarenkov K, Nilsson RH, Larsson K-H, et al (2010) The UNITE database for molecular identification of fungi–recent updates and future perspectives. New Phytol 186:281–285

Acevedo-Whitehouse K, Gullans F, Greig D, Amos W (2003) Inbreeding: Disease susceptibility in California sea lions. Nature 422:6927

Addison JA, Hart MW (2004) Analysis of population genetic structure of the green sea urchin (*Strongylocentrotus droebachiensis*) using microsatellites. Mar Biol 144:243–251. doi: 10.1007/s00227-003-1193-6

Albert EM, Fernández-Beaskoetxea S, Godoy JA, et al (2014) Genetic management of an amphibian population after a chytridiomycosis outbreak. Conserv Genet 16:103–111. doi: 10.1007/s10592-014-0644-6

Alford RA (2010) Declines and the Global Status of Amphibians. In: Sparling DW, Linder G, Bishop CA, Krest SK (eds) Ecotoxicology of Amphibians and Reptiles, 2nd edn. SETAC Press, Pensacola, Florida, pp 13–45

Alford RA, Bradfield KS, Richards SJ (2007) Global warming and amphibian losses. Nature 447:E3–E4. doi: 10.1038/nature05940

Allender MC, Baker S, Britton M, Kent AD (2018) Snake fungal disease alters skin bacterial and fungal diversity in an endangered rattlesnake. Sci Rep 8:12147. doi: 10.1038/s41598-018-30709-x

Allendorf FW (1986) Genetic drift and the loss of alleles versus heterozygosity. Zoo Biol 5:181–190

Allentoft ME, O'Brien J (2010) Global amphibian declines, loss of genetic diversity and fitness: A review. Diversity 2:47–71. doi: 10.3390/d2010047

Altschul SF, Madden TL, Shaffer AA, et al (1997) Gapped BLAST and PSI-BLAST: a new generation of protein database search programs. Nucleic Acids Res 25:3389–3402

Anderson PK, Cunningham AA, Patel NG, et al (2004) Emerging infectious disease of plants: pathogen pollution, climate change and agrotechnology drivers. Trends Ecol Evol 19:535–544

Antao T, Lopes A, Lopes RJ, et al (2008) LOSITAN: A workbench to detect molecular

adaptation based on a Fst-outlier method. BMC Bioinformatics 9:323

Antwis RE, Harrison XA (2018) Probiotic consortia are not uniformly effective against different amphibian chytrid pathogen isolates. Mol Ecol 27:577–589. doi: 10.1111/mec.14456

Archie EA, Luikart G, Ezenwa VO (2009) Infecting epidemiology with genetics: A new frontier in disease ecology. Trends Ecol Evol 24:21–30

Atkinson CT, Dusek RJ, Woods KL, Iko WM (2000) Pathogenicity of avian malaria in experimentally-infected Hawaii amakihi. J Wildl Dis 36:197–201

Atkinson CT, Saili KS, Utzurrum RB, Jarvi SI (2013) Experimental evidence for evolved tolerance to avian malaria in a wild population of low elevation Hawai'i 'amakihi (Hemignathus virens). Ecohealth 10:366–375

Atkinson CT, Woods KL, Dusek RJ, et al (1995) Wildlife disease and conservation in Hawaii: pathogenicity of avian malaria (Plasmodium relictum) in experimentally infected iiwi (Vestiaria coccinea). Parasitology 111:S59–S69

Ban Y, An L, Jiang H (2015) Investigating microbial co-occurrence patterns based on metagenomic compositional data. Bioinformatics 31:3322–3329. doi: 10.1093/bioinformatics/btv364

Barton HA, Taylor NM, Lubbers BR, Pemberton AC (2006) DNA extraction from low-biomass carbonate rock: An improved method with reduced contamination and the low-biomass contaminant database. J Microbiol Methods 66:21–31

Bataille A, Cashins SD, Grogan L, et al (2015) Susceptibility of amphibians to chytridiomycosis is associated with MHC class II conformation. Proc R Soc B Biol Sci 282:20143127–20143127. doi: 10.1098/rspb.2014.3127

Bates KA, Clare FC, O'Hanlon S, et al (2018) Amphibian chytridiomycosis outbreak dynamics are linked with host skin bacterial community structure. Nat Commun 9:1–11. doi: 10.1038/s41467-018-02967-w

Becker CG, Zamudio KR (2011) Tropical amphibian populations experience higher disease risk in natural habitats. Proc Natl Acad Sci 108:9893–9898. doi: 10.1073/pnas.1014497108

Becker MH, Brucker RM, Schwantes CR, et al (2009) The bacterially produced metabolite violacein is associated with survival of amphibians infected with a lethal fungus. Appl Environ Microbiol 75:6635–6638. doi: 10.1128/AEM.01294-09

Becker MH, Harris RN (2010) Cutaneous bacteria of the redback salamander prevent morbidity associated with a lethal disease. PLoS One 5:1–6. doi: 10.1371/journal.pone.0010957

Becker MH, Richards-Zawacki CL, Gratwicke B, Belden LK (2014) The effect of captivity on the cutaneous bacterial community of the critically endangered Panamanian golden frog (*Atelopus zeteki*). Biol Conserv 176:199–206. doi: 10.1016/j.biocon.2014.05.029

Becker MH, Walke JB, Cikanek S, et al (2015) Composition of symbiotic bacteria predicts survival in Panamanian golden frogs infected with a lethal fungus. Proc R Acad Sci B 282:20142881

Belden LK, Hughey MC, Rebollar EA, et al (2015) Panamanian frog species host unique skin bacterial communities. Front Microbiol 6:1–21. doi: 10.3389/fmicb.2015.01171

Belkhir K (2004) Genetix 4.05.2. Univ Montpellier II, Lab Génome Popul Montpellier, Fr

Bell SC (2012) The role of cutaneous bacteria in resistance of Australian tropical rainforest frogs to the amphibian chytrid fungus *Batrachochytrium dendrobatidis*

Bell SC, Alford RA, Garland S, et al (2013) Screening bacterial metabolites for inhibitory effects against *Batrachochytrium dendrobatidis* using a spectrophotometric assay. Dis Aquat Organ 103:77–85. doi: 10.3354/dao02560

Bell SC, Garland S, Alford RA (2018) Increased numbers of culturable inhibitory bacterial taxa may mitigate the effects of *Batrachochytrium dendrobatidis* in Australian Wet Tropics frogs. Front Microbiol 9:1–14. doi: 10.3389/fmicb.2018.01604

Bengis RG, Kock RA, Fischer J (2002) Infectious animal diseases: the wildlife/livestock interface. Rev Sci Tech Int des épizooties 21:53–66

Bennett AF (1998) Linkages in the landscape: The role of corridors and connectivity in wildlife conservation. World Conservation Union, Gland, Switzerland

Benning TL, LaPointe D, Atkinson CT, Vitousek PM (2002) Interactions of climate change with biological invasions and land use in the Hawaiian islands: Modeling the fate of endemic birds using a geographic information system. Proc Natl Acad Sci 99:14246–14249

Berger L, Speare R, Daszak P, et al (1998) Chytridiomycosis causes amphibian mortality associated with population declines in the rain forests of Australia and Central America. Proc Natl Acad Sci U S A 95:9031–9036. doi: 10.1073/pnas.95.15.9031

Biek R, Real LA (2010) The landscape genetics of infectious disease emergence and spread. Mol Ecol 19:3515–3531. doi: 10.1111/j.1365-294X.2010.04679.x

Bird AK, Prado-Irwin SR, Vredenburg VT, Zink AG (2018) Skin microbiomes of California terrestrial salamanders are influenced by habitat more than host phylogeny. Front Microbiol 9:1–14. doi: 10.3389/fmicb.2018.00442

Blanchong JA, Robinson SJ, Samuel MD, Foster JT (2016) Application of genetics and genomics to wildlife epidemiology. J Wildl Manage in press. doi: 10.1002/jwmg.1064

Bletz MC, Archer H, Harris RN, et al (2017) Host ecology rather than host phylogeny drives amphibian skin microbial community structure in the biodiversity hotspot of Madagascar. Front Microbiol 8:1–14. doi: 10.3389/fmicb.2017.01530

Bletz MC, Loudon AH, Becker MH, et al (2013) Mitigating amphibian chytridiomycosis with bioaugmentation: Characteristics of effective probiotics and strategies for their selection and use. Ecol Lett 16:807–820. doi: 10.1111/ele.12099

Bolnick D, Caldera E, Matthews B (2008) Evidence for asymmetric migration load in a pair of ecologically divergent stickleback populations. Biol J Linn … 94:273–287

Bonfante P, Anca I (2009) Plants, mycorrhizal fungi, and bacteria: A network of interactions. Annu Rev Ecol Evol Syst 63:363–383. doi: 10.1146/annurev.micro.091208.073504

Bonneaud C, Balenger SL, Russell AF, et al (2011) Rapid evolution of disease resistance is accompanied by functional changes in gene expression in a wild bird. Proc Natl Acad Sci 108:7866–7871. doi: 10.1073/pnas.1018580108

Bonneaud C, Balenger SL, Zhang J, et al (2012) Innate immunity and the evolution of resistance to an emerging infectious disease in a wild bird. Mol Ecol 21:2628–2639. doi: 10.1111/j.1365-294X.2012.05551.x

Bonneaud C, Pérez-Tris J, Federici P, et al (2006) Major histocompatibility alleles associated with local resistance to malaria in a passerine. Evolution (N Y) 60:383–389

Boots M, Best A, Miller MR, White A (2009) The role of ecological feedbacks in the evolution of host defence: what does theory tell us? Philos Trans R Soc London B Biol Sci 364:27–36. doi: 10.1098/rstb.2008.0160

Boots M, Hudson PJ, Sasaki A (2004) Large shifts in pathogen virulence related to host population structure. Science (80-) 303:824–844

Bower DS, Lips KR, Schwarzkopf L, et al (2017) Amphibians on the brink: Preemptive policies can protect amphibians from devastating fungal diseases. Science (80-) 357:454–456

Bowne DR, Bowers M a (2004) Interpatch movements in spatially structured population: a literature review. Landsc Ecol 19:1–20. doi: 10.1023/B:LAND.0000018357.45262.b9

Boyle DG, Boyle DB, Olsen V, et al (2004) Rapid quantitative detection of chytridiomycosis (*Batrachochytrium dendrobatidis*) in amphibian samples using real-time Taqman PCR assayo Title. Dis Aquat Organ 60:141–148

Briggs CJ, Knapp RA, Vredenburg VT (2010) Enzootic and epizootic dynamics of the chytrid fungal pathogen of amphibians. Proc Natl Acad Sci 107:9695–9700. doi: 10.1073/pnas.0912886107

Brooks JP (2016) Challenges for case-control studies with microbiome data. Ann Epidemiol 26:336–341. doi: 10.1016/j.annepidem.2016.03.009

Brüniche-Olsen A, Austin JJ, Jones ME, et al (2016) Detecting selection on temporal and spatial scales: A genomic time-series assessment of selective responses to devil facial tumor disease. PLoS One 11:1–15. doi: 10.1371/journal.pone.0147875

Brüniche-Olsen A, Burridge CP, Austin JJ, Jones ME (2013) Disease induced changes in gene flow patterns among Tasmanian devil populations. Biol Conserv 165:69–78. doi: 10.1016/j.biocon.2013.05.014

Bullard JH, Purdom E, Hansen KD, Dudoit S (2009) Evaluation of statistical methods for normalization and differential expression in mRNA-Seq experiments. BMC Bioinformatics 11:94. doi: 10.1186/1471-2105-11-94

Burkart D, Flechas S V, Vredenburg VT, Catenazzi A (2017) Cutaneous bacteria , but not peptide, are associated with chytridiomycosis resistance in Peruvian marsupial frogs. Anim Conserv 20:483–491. doi: 10.1111/acv.12352

Campbell L, Bower DS, Clulow S, et al (2019) Interaction between temperature and sublethal infection with the amphibian chytrid fungus impacts a susceptible frog species. Sci Rep 9:83. doi: 10.1038/s41598-018-35874-7

Caporaso JG, Kuczynski J, Stombaugh J, et al (2010) QIIME allows analysis of high-throughput community sequencing data. Nat Methods 7:335–336

Carvajal-Rodriguez A (2017) HacDivSel: Two new methods (haplotype-based and outlier-based) for the detection of divergent selection in pairs of populations. PLoS One 12:e0175944

Catenazzi A, Flechas S V., Burkart D, et al (2018) Widespread elevational occurrence of antifungal bacteria in Andean Amphibians decimated by disease: A complex role for skin symbionts in defense against chytridiomycosis. Front Microbiol 9:1–14. doi: 10.3389/fmicb.2018.00465

Catenazzi A, Swei A, Finkle J, et al (2017) Epizootic to enzootic transition of a fungal disease in tropical Andean frogs: Are surviving species still susceptible? PLoS One 12:1–17. doi: 10.1371/journal.pone.0186478

Champlot S, Berthelot C, Pruvost M, et al (2010) An efficient multistrategy DNA decontamination procedure of PCR reagents for hypersensitive PCR applications. PLoS One 5:e13042. doi: 10.1371/journal.pone.0013042

Chatfield MWH, Brannelly LA, Robak MJ, et al (2013) Fitness consequences of cnfection by Batrachochytrium dendrobatidis in northern leopard frogs *Lithobates pipens*. Ecohealth 10:90–98. doi: 10.1007/s10393-013-0833-7

Chen D, Li C, Feng L, et al (2018) Analysis of the influence of living environment and age on vaginal fungal microbiome in giant pandas (Ailuropoda melanoleuca) by high throughput sequencing. Microb Pathog 115:280–286. doi: 10.1016/j.micpath.2017.12.067

Chermprapai S, Ederveen THA, Broere F, et al (2019) The bacterial and fungal microbiome of the skin of healthy dogs and dogs with atopic dermatitis and the impact of topical antimicrobial therapy, an exploratory study. Vet Microbiol 229:90–99. doi: 10.1016/j.vetmic.2018.12.022

Coltman DW, Pilkington JG, Smith JA, Pemberton JM (1999) Parasite-mediated selection against inbred Soay sheep in a free-living, island population. Evolution (N Y) 53:1259–1267

Corless CE, Guiver M, Borrow R, et al (2000) Contamination and sensitivity issues with a real-time universal 16S rRNA PCR. J Clin Microbiol 38:1747–1752

Costea PI, Zeller G, Sunagawa S, Bork P (2014) A fair comparison. Nat Methods 11:359. doi: 10.1038/nmeth.2898

Cottrell MT, Kirchman DL (2003) Contribution of major bacterial groups to bacterial biomass production (thymidine and leucine incorporation) in the Delaware estuary. Limnol Oceanogr 48:168–178

Couvet D (2002) Deleterious effects of restricted gene flow in fragmented populations. Conserv Biol 16:369–376. doi: 10.1046/j.1523-1739.2002.99518.x

Crooks KR, Sanjayan M (eds) (2006) Connectivity conservation. Conservation Biology 14. Cambridge University Press

Crow JF, Kimura M (1970) An introduction to population genetics theory. Harper and Row,

New York

Cunningham M (2001) Vicariance, speciation, and diversity in Australopapuan rainforest frogs

Daskin JH, Alford RA, Puschendorf R (2011) Short-term exposure to warm microhabitats could explain amphibian persistence with *Batrachochytrium dendrobatidis*. PLoS One 6:e26215. doi: 10.1371/journal.pone.0026215

Daszak P, Berger L, Cunningham AA, et al (1999) Emerging infectious diseases and amphibian population declines. Emerg Infect Dis 5:735–48. doi: 10.3201/eid0506.990601

Daszak P, Cunningham AA, Hyatt AD (2001) Anthropogenic environmental change and the emergence of infectious diseases in wildlife. Acta Trop 78:103–116

Daszak P, Cunningham AA, Hyatt AD (2000) Emerging infectious diseases of wildlife--threats to biodiversity and human health. Science (80-) 287:443–449

Davies M, Richards SJ (1990) Developmental biology of the Australian hylid frog Nyctimystes dayi (Gunther). Trans R Soc South Aust 114:207–211

De Castro F, Bolker B (2005) Mechanisms of disease-induced extinction. Ecol Lett 8:117–126. doi: 10.1111/j.1461-0248.2004.00693.x

Deveau A, Bonito G, Uehling J, et al (2018) Bacterial-fungal interactions: Ecology, mechanisms and challenges. FEMS Microbiol Rev 42:335–352. doi: 10.1093/femsre/fuy008

Dillies MA, Rau A, Aubert J, et al (2013) A comprehensive evaluation of normalization methods for Illumina high-throughput RNA sequencing data analysis. Brief Bioinform 14:671–683. doi: 10.1093/bib/bbs046

Dillon RJ, Vennard CT, Buckling A, Charnley AK (2005) Diversity of locust gut bacteria protects against pathogen invasion. Ecol Lett 8:1291–1298. doi: 10.1111/j.1461-0248.2005.00828.x

Do C, Waples RS, Peel D, et al (2014) NeEstimator V2: re-implementation of software for the estimation of contemporary effective population size (Ne) from genetic data. Mol Ecol Resour 14:209–214

Donnellan SC, Mahony MJ (2004) Allozyme, chromosmal and morphological variability in the *Litoria lesueuri* species group (Anura: Hylidae), including a description of a new species. Aust J Zool 52:1–28

Doyle JJ, Doyle JL (1987) A rapid procedure for DNA purification from small quantities of fresh leaf tissue. Phytochem Bull 19:11–15

Dybdahl MF, Lively CM (1998) Host-parasite coevolution: evidence for rare advantage and time-lagged selection in a natural population. Evolution (N Y) 52:1057–1066. doi: 10.2307/2411236

Edgar RC, Haas BJ, Clemente JC, et al (2011) UCHIME improves sensitivity and speed of chimera detection. Bioinformatics 27:2197–2200

Eggert LS, Terwilliger LA, Woodworth BL, et al (2008) Genetic structure along an elevational gradient in Hawaiian honeycreepers reveals contrasting evolutionary responses to avian malaria. BMC Evol Biol 8:315. doi: 10.1186/1471-2148-8-315

Eisenhauer N, Schulz W, Scheu S, Jousset A (2013) Niche dimensionality links biodiversity and invasibility of microbial communities. Funct Ecol 27:282–288. doi: 10.1111/j.1365-2435.2012.02060.x

Elderd BD, Dushoff J, Dwyer G (2008) Host-pathogen interactions, insect outbreaks, and natural selection for disease resistance. Am Nat 172:829–842

Epstein B, Jones M, Hamede R, et al (2016) Rapid evolutionary response to a transmissible cancer in Tasmanian devils. Nat Commun 7:1–7. doi: 10.1038/ncomms12684

Excoffier L, Laval G, Schneider S (2005) Arlequin (version 3.0): An integrated software package for population genetics data analysis. Evol Bioinform Online 1:47–50

Faust K, Sathirapongsasuti JF, Izard J, et al (2012) Microbial co-occurrence relationships in the human microbiome. PLoS Comput Biol 8:e1002606

Fèvre EM, Bronsvoort BM de C, Hamilton KA, Cleaveland S (2006) Animal movements and the spread of infectious diseases. Trends Microbiol 14:125–131

Findley K, Oh J, Yang J, et al (2013) Topographic diversity of fungal and bacterial communities in human skin. Nature 498:367–370. doi: 10.1038/nature12171

Fisher MC, Garner TWJ (2007) *Batrachochytrium dendrobatidis*, the international trade in amphibians and introduced amphibian species. Fungal Biol Rev 21:2–9

Fisher MC, Garner TWJ, Walker SF (2009) Global emergence of *Batrachochytrium dendrobatidis* and amphibian chytridiomycosis in space, time, and host. Annu Rev Microbiol 63:291–310. doi: 10.1146/annurev.micro.091208.073435

Fisher MC, Henk DA, Briggs CJ, et al (2012) Emerging fungal threats to animal, plant and ecosystem health. Nature 484:186–194. doi: 10.1038/nature10947

Fisher MC, Henk DA, Briggs CJ, et al (2013) Emergining fungal threats to animal, plant and ecosystem health. Nature 484:1–18. doi: 10.1038/nature10947.Emerging

Flanagan SP, Jones AG (2017) Constraints on the FST-heterozygosity outlier approach. J Hered 108:561–573. doi: 10.1093/jhered/esx048

Flechas S V, Sarmiento C, Cardenas ME, et al (2012) Surviving Chytridiomycosis: Differential Anti-Batrachochytrium dendrobatidis activity in bacterial isolates from three lowland species of Atelopus. PLoS One 7:e44832. doi: 10.1371/journal.pone.0044832

Foll M (2012) BayeScan v2.1 User Manual. Ecology 20:1450–1462

Foll M, Gaggiotti O (2008) A genome-scan method to identify selected loci appropriate for both dominant and codominant markers: A bayesian perspective. Genetics 180:977–993

Ford SA, King KC (2016) Harnessing the power of defensive microbes: Evolutionary implications in nature and disease control. PLoS Pathog 12:1–12. doi: 10.1371/journal.ppat.1005465

Forrest MJ, Schlaepfer MA (2011) Nothing a hot bath won't cure: infection rates of amphibian chytrid fungus correlate negatively with water temperature under natural field settings. PLoS One 6:e28444. doi: 10.1371/journal.pone.0028444

Foster JT, Woodworth BL, Eggert LE, et al (2007) Genetic structure and evolved malaria resistance in Hawaiian honeycreepers. Mol Ecol 16:4738–4746. doi: 10.1111/j.1365-294X.2007.03550.x

Fox J, Weisberg S (2011) An R Companion to Applied Regression, 2nd edn. Sage, CA

Frankham R (2015) Genetic rescue of small inbred populations: meta-analysis reveals large and consistent benefits of gene flow. Mol Ecol 24:2610–2618. doi: 10.1111/mec.13139

Frankham R, Ballou JD, Eldridge MDB, et al (2011) Predicting the probability of outbreeding depression. Conserv Biol 25:465–475. doi: 10.1111/j.1523-1739.2011.01662.x

Fraune S, Anton-erxleben F, Knop M, et al (2015) Bacteria – bacteria interactions within the microbiota of the ancestral metazoan Hydra contribute to fungal resistance. ISME J 9:1543–1556. doi: 10.1038/ismej.2014.239

Frick WF, Pollock JF, Hicks AC, et al (2010) An emerging disease causes regional population collapse of a common North American bat species. Science (80-) 329:679–682

Friedman J, Alm EJ (2012) Inferring correlation networks from genomic survey data. PLoS Comput Biol 8:1–11. doi: 10.1371/journal.pcbi.1002687

Fuhrman JA (2009) Microbial community structure and its functional implications. Nature 459:193–199. doi: 10.1038/nature08058

Funk WC, McKay JK, Hohenlohe PA, Allendorf FW (2012) Harnessing genomics for delineating conservation units. Trends Ecol Evol 27:489–496. doi: 10.1016/j.tree.2012.05.012

Gandon S, Capowiez Y, Dubois Y, et al (1996) Local adaptation and gene-for-gene coevolution in a metapopulation model. Proc R Soc London B Biol Sci 263:1003–1009

Gandon S, Michalakis Y (2002) Local adaptation, evolutionary potential and host-parasite coevolution: Interactions between migration, mutation, population size and generation time. J Evol Biol 15:451–462. doi: 10.1046/j.1420-9101.2002.00402.x

García-Ramos G, Kirkpatrick M (1997) Genetic models of adaptation and gene flow in peripheral populations. Evolution (N Y) 51:21–28. doi: 10.1017/CBO9781107415324.004

Ghazoul J (2006) Floral diversity and the facilitation of pollination. J Ecol 94:295–304

Gilpin ME, Soule ME (1986) Minimum viable populations: processes of species extinction. In: Soule ME (ed) Conservation Biology: The Science of Scarcity and Diversity. Sinauer Associates, Sunderland, Massachusetts, pp 19–34

Gortazar C, Ferroglio E, Höfle U, et al (2007) Diseases shared between wildlife and livestock: a European perspective. Eur J Wildl Res 53:241–256

Green D, Converse KA, Schrader AK (2002) Epizootiology of sixty-four amphibian morbidity and mortality events in the USA, 1996-2001. Ann N Y Acad Sci 969:323–339

Grisnik M, Leys JE, Bryan D, et al (2018) Host and geographic range of snake fungal disease in Tennessee, USA. Herpetol Rev 49:682–690

Grogan LF, Robert J, Berger L, et al (2018) Review of the amphibian immune response to chytridiomycosis, and future directions. Front Immunol 9:1–20. doi: 10.3389/fimmu.2018.02536

Guarnizo CE, Cannatella DC (2013) Geographic determinants of gene flow in two sister species of tropical Andean frogs. J Hered 105:216–225

Gweon HS, Oliver A, Taylor J, et al (2015) PIPITS: an automated pipeline for analyses of fungal internal transcribed spacer sequences from the Illumina sequencing platform. Methods Ecol Evol 6:973–980

Hale KA, Briskie J V (2007) Decreased immunocompetence in a severely bottlenecked

population of an endemic New Zealand bird. Anim Conserv 10:2–10

Hang J, Desai V, Zavaljevski N, et al (2014) 16S rRNA gene pyrosequencing of reference and clinical samples and investigation of the temperature stability of microbiome profiles. Microbiome 2:31. doi: 10.1186/2049-2618-2-31

Hanlon SJO, Rieux A, Farrer RA, et al (2018) Recent Asian origin of chytrid fungi causing global amphibian declines. Science (80-) 627:621–627

Hannon L (2010) FASTX-Toolkit. FASTQ/A short-reads pre-processing tools

Harding KC, Harkonene T, Caswell H (2002) The 2002 European seal plague: epidemiology and population consequences. Ecol Lett 727–732

Harris RN, Brucker RM, Walke JB, et al (2009a) Skin microbes on frogs prevent morbidity and mortality caused by a lethal skin fungus. ISME J 3:818–24. doi: 10.1038/ismej.2009.27

Harris RN, James TY, Lauer A, et al (2006) Amphibian pathogen *Batrachochytrium dendrobatidis* is inhibited by the cutaneous bacteria of amphibian species. Ecohealth 3:53–56

Harris RN, Lauer A, Simon MA, et al (2009b) Addition of antifungal skin bacteria to salamanders ameliorates the effects of chytridiomycosis. Dis Aquat Organ 83:11–16

Harrison S, Bruna E (1999) Habitat fragmentation and large-scale conservation: What do we know for sure? Ecography (Cop) 22:225–232

Harrison XA, Price SJ, Hopkins K, et al (2017) Host microbiome richness predicts resistance to disturbance by pathogenic infection in a vertebrate host. 44:

Harvell CD, E MC, Ward JR, et al (2002) Climate warming and disease risks for terrestrial and marine biota. Science (80-) 296:2158–2162

Harvell CD, Kim K, Burkholder JM, et al (1999) Emerging marine diseases-climate links and anthropogenic factors. Science (80-) 285:1505–1510

Hawkins CE, Baars C, Hesterman H, et al (2006) Emerging disease and population decline of an island endemic, the Tasmanian devil Sarcophilus harrisii. Biol Conserv 131:307–324

Hedrick PW, Kalinowski ST (2000) Inbreeding depression in conservation biology. Annu Rev Ecol Syst 31:139–162

Hillebrand H, Bennett DM, Cadotte MW (2008) Consequences of dominance: A review of evenness effects on local and regional ecosystem processes. Ecology 89:1510–1520

Hillebrand H, Cardinale BJ (2004) Consumer effects decline with prey diversity. Ecol Lett 7:192–201

Hillebrand H, Gruner DS, Borer ET, et al (2007) Consumer versus resource control of producer diversity depends on ecosystem type and producer community structure. Proc Natl Acad Sci 104:10904–10909. doi: 10.1073/pnas.0701918104

Hitchings SP, Beebee TJC (1997) Genetic substructuring as a result of barriers to gene flow in urban Rana temporaria (common frog) populations: implications for biodiversity conservation. Heredity (Edinb) 79:117–127

Hoban S, Gaggiotti O, Consortium C, Bertorelle G (2013a) Sample planning optimization tool for conservation and population genetics (SPOTG): a software for choosing the appropriate number of markers and samples. Methods Ecol Evol 4:299–303

Hoban S, Kelley JL, Lotterhos KE, et al (2016) Finding the genomic basis of local adaptation: Pitfalls, practical solutions, and future directions. Am Nat 188:000–000. doi: 10.1086/688018

Hoban SM, Gaggiotti OE, Bertorelle G (2013b) The number of markers and samples needed for detecting bottlenecks under realistic scenarios, with and without recovery: A simulation-based study. Mol Ecol 22:3444–3450. doi: 10.1111/mec.12258

Hodgkison SC, Hero J-M (1999) Seasonal behaviour of *Litoria nannotis*, *Litoria rheocola* and *Nyctimystes dayi* in Tully Gorge, North Queensland, Australia. In: Frogs in the Community: Proceedings of the Brisbane Symposium. http://www.qldfrogs.asn.au/, pp 29–39

Hoffmann C, Dollive S, Grunberg S, et al (2013) Archaea and fungi of the human gut microbiome: Correlations with diet and bacterial residents. PLoS One 8:. doi: 10.1371/journal.pone.0066019

Hogg JT, Forbes SH, Steele BM, Luikart G (2006) Genetic rescue of an insular population of large mammals. Proc R Soc London B Biol Sci 273:1491–1499

Holderegger R, Giulio MD (2010) The genetic effects of roads: A review of empirical evidence. Basic Appl Ecol 11:522–531. doi: 10.1016/j.baae.2010.06.006

Hothorn T, Hornik K, van de Wiel MA, Zeileis A (2006) A lego system for conditional inference. Am Stat 60:257–263

Hudson MA, Young RP, D'Urban Jackson J, et al (2016) Dynamics and genetics of a disease-driven species decline to near extinction: lessons for conservation. Sci Rep 6:30772. doi: 10.1038/srep30772

Huffnagle GB, Noverr MC (2013) The emerging world of the fungal microbiome. Trends

Microbiol 21:334–341. doi: 10.1016/j.tim.2013.04.002

Hughes AR, Inouye BD, Johnson MTJ, et al (2008) Ecological consequences of genetic diversity. Ecol Lett 11:609–623

Hurtado P (2008) The potential impact of disease on the migratory structure of a partially migratory passerine population. Bull Math Biol 70:2264–2282

Illumina (2017) 16S Metagenomic Sequencing Library Preparation. In: Illumina

Ingram GJ, McDonald KR (1993) An update on the decline of Queensland's frogs. In: Lunney D, Ayers D (eds) Herpetology in Australia: A Diverse Discipline. Zoological Society of New South Whales, Mosman, NSW, pp 297–303

Iyer S, Killingback T, Sundaram B, Wang Z (2013) Attack robustness and centrality of complex networks. PLoS One 8:. doi: 10.1371/journal.pone.0059613

Jackson DA (1997) Compositional data in community ecology: The paradigm or peril of proportions. Ecology 78:929–940

Jani AJ, Briggs CJ (2014) The pathogen *Batrachochytrium dendrobatidis* disturbs the frog skin microbiome during a natural epidemic and experimental infection. Proc Natl Acad Sci 111:E5049–E5058. doi: 10.1073/pnas.1412752111

Jani AJ, Knapp RA, Briggs CJ (2017) Epidemic and endemic pathogen dynamics correspond to distinct host population microbiomes at a landscape scale. Proc R Soc B Biol Sci 284:20170944. doi: 10.1098/rspb.2017.0944

Jeffery KJM, Bangham CRM (2000) Do infectious diseases drive MHC diversity? Microbes Infect 2:133–1341

Jervis-Bardy J, Leong LEX, Marri S, et al (2015) Deriving accurate microbiota profiles from human samples with low bacterial content through post-sequencing processing of Illumina MiSeq data. Microbiome 3:19. doi: 10.1186/s40168-015-0083-8

Johnson AJ, Pessier AP, Wellehan JFX, et al (2008) Ranavirus infection of free-ranging and captive box turtles and tortoises in the United States. J Wildl Dis 44:851–863

Johnson C, Johnson J, Vanderloo JP, et al (2006) Prion protein polymorphisms in white-tailed deer influence susceptibility to chronic wasting disease. J Gen Virol 87:2109–2114

Jombart T (2008) adegenet: a R package for the multivariate analysis of genetic markers. Bioinformatics 24:1403–1405. doi: 10.1093/bioinformatics/btn129

Jones ME, Cockburn A, Hamede R, et al (2008) Life-histroy change in disease-ravaged Tasmanian devil popualtions. Proc Natl Acad Sci U S A 105:10023–10027

Jones OR, Wang J (2010) COLONY: a program for parentage and sibship inference from multilocus genotype data. Mol Ecol Resour 10:551–555

Joshi NA, Fass JN (2011) Sickle. A sliding-window, adaptive, quality-based trimming tool for FastQ files

Jousset A, Becker J, Chatterjee S, et al (2014) Biodiversity and species identity shape the antifungal activity of bacterial communities. Ecology 95:1184–1190. doi: 10.1890/13-1215.1

Karesh WB, Cook RA, Bennett EL, Newcomb J (2005) Wildlife trade and global disease emergence. Emerg Infect Dis 11:1000–1002

Karlsson EK, Kwiatkowski DP, Sabeti PC (2014) Natural selection and infectious disease in human populations. Nat Rev Genet 15:379–393

Kawecki TJ, Ebert D (2004) Conceptual issues in local adaptation. Ecol Lett 7:1225–1241. doi: 10.1111/j.1461-0248.2004.00684.x

Keane DP, Barr DJ, Bochsler PN, et al (2008) Chronic wasting disease in a Wisconsin white-tailed deer farm. J Vet Diagnostic Investig 20:698–703

Kearns PJ, Fischer S, Fernández-Beaskoetxea S, et al (2017) Fight fungi with fungi: Antifungal properties of the amphibian mycobiome. Front Microbiol 8:1–12. doi: 10.3389/fmicb.2017.02494

Keenan K, McGinnity P, Cross TF, et al (2013) diveRsity: An R package for the estimation and exploration of population genetics parameters and their associated errors. Methods Ecol Evol 4:782–788

Keller I, Largiader CR (2003) Recent habitat fragmentation caused by major roads leads to reduction of gene flow and loss of genetic variability in ground beetles. Proc R Soc London B Biol Sci 270:417–423

Keller LF, Jeffery KJ, Arcese P, et al (2001) Immigration and the ephemerality of a natural population bottleneck: evidence from molecular markers. Proc R Soc London B Biol Sci 268:1387–1394

Keller LF, Waller DM (2002) Inbreeding effects in wild populations. Trends Ecol Evol 17:230–241. doi: 10.1016/S0169-5347(02)02489-8

Kelly E, Phillips BL (2015) Targeted gene flow for conservation. Conserv Biol 30:259–267. doi: 10.1111/cobi.12623

Kennedy S, Kuiken T, Jepson PD, et al (2000) Mass die-off of Caspian seals caused by canine

distemper virus. Emerg Infect Dis 6:637–639

Kilian A, Wenzl P, Huttner E, et al (2012) Diversity Arrays Technology: A generic genome profiling technology on open platforms. Methods Mol Biol 888:67–89

King KC, Lively CM (2012) Does genetic diversity limit disease spread in natural host populations. Heredity (Edinb) 190:199–203

Kittelmann S, Naylor GE, Koolaard JP, Janssen PH (2012) A proposed taxonomy of anaerobic fungi (Class Neocallimastigomycetes) suitable for large-scale sequence-based community structure analysis. PLoS One 7:e36866

Kittelmann S, Seedorf H, Walters WA, et al (2013) Simultaneous amplicon sequencing to explore co-occurrence patterns of bacterial, archaeal and Eukaryotic microorganisms in rumen microbial communities. PLoS One 8:. doi: 10.1371/journal.pone.0047879

Kosch TA, Silva CNS, Brannelly LA, et al (2019) Genetic potential for disease resistance in critically endangered amphibians decimated by chytridiomycosis. Anim Conserv 22:238–250. doi: 10.1111/acv.12459

Kueneman JG, Weiss S, McKenzie VJ (2017) Composition of micro-eukaryotes on the skin of the cascades frog (Rana cascadae) and patterns of correlation between skin microbes and *Batrachochytrium dendrobatidis*. Front Microbiol 8:1–10. doi: 10.3389/fmicb.2017.02350

Kueneman JG, Woodhams DC, Treuren W Van, et al (2016) Inhibitory bacteria reduce fungi on early life stages of endangered Colorado boreal toads (*Anaxyrus boreas*). ISME J 10:934–944. doi: 10.1038/ismej.2015.168

Kulakov LA, McAlister MB, Ogden KL, et al (2002) Analysis of bacteria contaminating ultrapure water in industrial systems. Appl Environ Microbiol 68:1548–1555

Kurtz ZD, Müller CL, Miraldi ER, et al (2015) Sparse and compositionally robust inference of microbial ecological networks. PLoS Comput Biol 11:1–25. doi: 10.1371/journal.pcbi.1004226

Lachish S, McCallum H, Jones M (2008) Demography, disease and the devil: life-history changes in a disease-affected population of Tasmanian devils (Sarcophilus harrisii). J Anim Ecol 78:427–436

Lachish S, Miller KJ, Storfer A, et al (2011) Evidence that disease-induced population decline changes genetic structure and alters dispersal patterns in the Tasmanian devil. Heredity (Edinb) 106:172–182. doi: 10.1038/hdy.2010.17

Lacy RC (1987) Loss of genetic diversity from managed populations: interacting effects of drift, mutation, immigration, selection, and population subdivision. Conserv Biol 1:143–158

Lal MM, Southgate PC, Jerry DR, et al (2017) Swept away: ocean currents and seascape features influence genetic structure across the 18,000 Km Indo-Pacific distribution of a marine invertebrate, the black-lip pearl oyster *Pinctada margaritifera*. BMC Genomics 18:66. doi: 10.1186/s12864-016-3410-y

Lam BA, Walke JB, Vredenburg VT, Harris RN (2010) Proportion of individuals with anti-*Batrachochytrium dendrobatidis* skin bacteria is associated with population persistence in the frog *Rana muscosa*. Biol Conserv 143:529–531. doi: 10.1016/j.biocon.2009.11.015

Langdon JS, Humphrey JD (1987) Epizootic haematopoietic necrosis, a new viral disease in redfin perch, Perca fluviatilis L., in Australia. J Fish Dis 10:289–297

Lauer A, Simon MA, Banning JL, et al (2008) Diversity of cutaneous bacteria with antifungal activity isolated from female four-toed salamanders. ISME J 2:145–157. doi: 10.1038/ismej.2007.110

Lauer A, Simon MA, Banning JL, et al (2007) Common cutaneous bacteria from the eastern red-backed salamander can inhibit pathogenic fungi. Copeia 2007:630–640

Laurance WF (2008) Global warming and amphibian extinctions in eastern Australia. Austral Ecol 33:1–9

Laurance WF, McDonald KR, Speare R (1996) Epidemic disease and the catastrophic decline of Australian rain forest frogs. Conserv Biol 10:406–413. doi: 10.1046/j.1523-1739.1996.10020406.x

Layeghifard M, Hwang DM, Guttman DS (2017) Disentangling interactions in the microbiome: A network perspective. Trends Microbiol 25:217–228. doi: 10.1016/j.tim.2016.11.008

le Gouar PJ, Vallet D, David L, et al (2009) How Ebola impacts genetics of western lowland gorilla populations. PLoS One 4:. doi: 10.1371/journal.pone.0008375

Lenormand T (2002) Gene flow and the limits to natural selection. Trends Ecol Evol 17:183–189

Lenth R (2018) emmeans: estimated marginal means, aka least-squares means

Lesbarrères D, Primmer CR, Lodé T, Merilä J (2006) The effects of 20 years of highway

presence on the genetic structure of Rana dalmatina populations. Ecoscience 13:531–538

Limborg NT, Helyar SJ, de Bruyn M, et al (2012) Environmental selection on transcriptome-derived SNPs in a high gene flow marine fish, the Atlantic herring (*Clupea harengus*). Mol Ecol 21:3686–3703

Lin Y, Golovnina K, Chen Z-X, et al (2016) Comparison of normalization and differential expression analyses using RNA-Seq data from 726 individual Drosophila melanogaster. BMC Genomics 17:28. doi: 10.1186/s12864-015-2353-z

Lips KR, Brem F, Brenes R, et al (2006) Emerging infectious disease and the loss of biodiversity in a Neotropical amphibian community. Proc Natl Acad Sci 103:3165–3170

Lips KR, Diffendorfer J, Mendelson JR, Sears MW (2008) Riding the wave: Reconciling the roles of disease and climate change in amphibian declines. PLoS Biol 6:441–454. doi: 10.1371/journal.pbio.0060072

Lipscomb TP, Scott DP, Garber RL, et al (2000) Common metastatic carcinoma of California sea lions (Zalophus californianus): evidence of genital origin and association with novel gammaherpesvirus. Vet Pathol Online 37:609–617

Longo A V, Savage AE, Hewson I, Zamudio KR (2015) Seasonal and ontogenetic variation of skin microbial communities and relationships to natural disease dynamics in declining amphibians. R Soc Open Sci 2:140377

Longo A V, Zamudio KR (2016) Environmental fluctuations and host skin bacteria shift survival advantage between frogs and their fungal pathogen. ISME J 11:1–13. doi: 10.1038/ismej.2016.138

Loudon AH, Holland JA, Umile TP, et al (2014a) Interactions between amphibians' symbiotic bacteria cause the production of emergent anti-fungal metabolites. Front Microbiol 5:1–8. doi: 10.3389/fmicb.2014.00441

Loudon AH, Woodhams DC, Parfrey LW, et al (2014b) Microbial community dynamics and effect of environmental microbial reservoirs on red-backed salamanders (*Plethodon cinereus*). ISME J 8:830–40. doi: 10.1038/ismej.2013.200

Love MI, Huber W, Anders S (2014) Moderated estimation of fold change and dispersion for RNA-seq data with DESeq2. Genome Biol 15:550. doi: 10.1186/s13059-014-0550-8

Lowry DB, Hoban S, Kelley JL, et al (2016) Breaking RAD: An evaluation of the utility of restriction site associated DNA sequencing for genome scans of adaptation. Mol Ecol

Resour 108:7866–7871. doi: 10.1111/1755-0998.12596

Ma B, Wang H, Dsouza M, et al (2016) Geographic patterns of co-occurrence network topological features for soil microbiota at continental scale in eastern China. ISME J 10:1891–1901. doi: 10.1038/ismej.2015.261

Mamaev L V., Denikina NN, Belikov SI, et al (1995) Characterization of morbilliviruses isolated from Lake Baikal seals (Phoca sibirica). Vet Microbiol 44:349–379

Mao-Jones J, Ritchie KB, Jones LE, Ellner SP (2010) How microbial community composition regulates coral disease development. PLoS Biol 8:e1000345

Masella AP, Bartram AK, Truszkowski JM, et al (2012) PANDAseq: paired-end assembler for illumina sequences. BMC Bioinformatics 13:31

Matos A, Kerkhof L, Garland JL (2005) Effects of microbial community diversity on the survival of *Pseudomonas aeruginosa* in the wheat rhizosphere. Microb Ecol 49:257–264. doi: 10.1007/s00248-004-0179-3

Mattoso TC, Moreira DDO, Samuels RI (2011) Symbiotic bacteria on the cuticle of the leaf-cutting ant Acromyrmex subterraneus subterraneus protect workers from attack by entomopathogenic fungi. Biol Lett 8:461–464

May RM, Anderson RM (1983) Epidemiology and genetics in the coevolution of parasites and hosts. Proc R Soc London B Biol Sci 219:281–313

McCarthy DJ, Chen Y, Smyth GK (2012) Differential expression analysis of multifactor RNA-Seq experiments with respect to biological variation. Nucleic Acids Res 40:4288–4297

McDonald BA, Linde C (2002) Pathogen population genetics, evolutionary potential, and durable resistance. Annu Rev Phytopathol 40:349–379

McDonald KR, Alford RA (1999) A review of declining frogs in northern Queensland. In: Campbell A (ed) Declines and Disappearances of Australian Frogs. Envrionment Australia, pp 14–22

McKnight DT, Alford RA, Hoskin CJ, et al (2017a) Fighting an uphill battle: the recovery of frogs in Australia's Wet Tropics. Ecology 98:3221–3223. doi: 10.1002/ecy.2019

McKnight DT, Huerlimann R, Bower DS, et al (2019a) Methods for normalizing microbiome data: An ecological perspective. Methods Ecol Evol 10:389–400. doi: 10.1111/2041-210X.13115

McKnight DT, Lal MM, Bower DS, et al (2019b) The return of the frogs: The importance of habitat refugia in maintaining diversity during a disease outbreak. Mol Ecol 28:2731–

2745. doi: 10.1111/mec.15108

McKnight DT, Schwarzkopf L, Alford RA, et al (2017b) Effects of emerging infectious diseases on host population genetics: a review. Conserv Genet 18:1235–1245. doi: 10.1007/s10592-017-0974-2

McKnight DT, Schwarzkopf L, Huerlimann R, et al (2019c) microDecon: A highly accurate read-subtraction tool for the post-sequencing removal of contamination in metabarcoding studies. Environ DNA 1:14–25. doi: 10.1002/edn3.11

McMurdie PJ, Holmes S (2014) Waste not, want not: Why rarefying microbiome data is inadmissible. PLoS Comput Biol 10:e1003531. doi: 10.1371/journal.pcbi.1003531

McMurdie PJ, Holmes S (2013) phyloseq: an R package for peproducible interactive analysis and graphics of microbiome census data. PLoS One 8:e61217

Meagher S (1999) Genetic diversity and *Capillaria hepatica* (nematode) prevalence in Michigan deer mouse populations. Evolution (N Y) 53:1318–1324

Medina D, Hughey MC, Becker MH, et al (2017) Variation in metabolite profiles of amphibian skin bacterial communities across elevations in the neotropics. Microb Ecol. doi: 10.1007/s00248-017-0933-y

Medina D, Hughey MC, Walke JB, et al (2019) Amphibian skin fungal communities vary across host species and do not correlate with infection by a pathogenic fungus. Environ Microbiol 00: doi: 10.1111/1462-2920.14682

Melbourne BA, Hastings A (2008) Extinction risk depends strongly on factors contributing to stochasticity. Nature 454:100–103

Miller MW, Williams ES, McCarty CW, et al (2000) Epizootiology of chronic wasting disease in free-ranging cervids in Colorado and Wyoming. J Wildl Dis 36:676–690

Minor ES, Urban DL (2008) A graph-theory framework for evaluating landscape connectivity and conservation planning. Conserv Biol 22:297–307

Mohammadi T, Reesink HW, Vandenbroucke-Grauls CMJE, Savelkoul PHM (2005) Removal of contaminating DNA from commercial nucleic acid extraction kit reagents. J Microbiol Methods 61:285–288. doi: 10.1016/j.mimet.2004.11.018

Morgan AD, Gandon S, Buckling A (2005) The effect of migration on local adaptation in a coevolving host–parasite system. Nature 437:253–256. doi: 10.1038/nature03913

Morgan MJ, Hunter D, Pietsch R, et al (2008) Assessment of genetic diversity in the critically endangered Australian corroboree frogs, *Pseudophryne corroboree* and *Pseudophryne*

pengilleyi, identifies four evolutionarily significant units for conservation. Mol Ecol 17:3448–3463. doi: 10.1111/j.1365-294X.2008.03841.x

Moritz C (1999) Conservation units and translocations: evolutionary processes. Hereditas 130:217–228

Morton JT, Toran L, Edlund A, et al (2017) Uncovering the horseshoe effect in microbial analyses. Ecol Evol Sci 2:1–8

Muletz CR, Myers JM, Domangue RJ, et al (2012) Soil bioaugmentation with amphibian cutaneous bacteria protects amphibian hosts from infection by *Batrachochytrium dendrobatidis*. Biol Conserv 152:119–126. doi: 10.1016/j.biocon.2012.03.022

Murphy MA, Dezzani R, Pilliod DS, Storfer A (2010) Landscape genetics of high mountain frog metapopulations. Mol Ecol 19:3634–3649. doi: 10.1111/j.1365-294X.2010.04723.x

Nayfa MG, Zenger KR (2016) Unravelling the effects of gene flow and selection in highly connected populations of the silver-lip pearl oyster (*Pinctada maxima*). Mar Genomics in press: doi: 10.1016/j.margen.2016.02.005

Nei M, Maruyama T, Chakraborty R (1975) The bottleneck effect and genetic variability in populations. Evolution (N Y) 29:1–10

O'Brien SJ, Everamnn JF (1988) Interactive influence of infectious disease and genetic diversity in natural populations. Trends Ecol Evol 10:254–259

Ogle DH (2018) FSA: Fisheries stock analysis. R package version 0.8.20.

Oksanen JF, Blanchet FG, Friendly M, et al (2017) vegan: Community ecology package

Painter I, Washington U of (2013) GWASExactHW: Exact Hardy-Weinburg testing for Genome Wide Association Studies. R package version 1.01.

Palomar G, Bosch J, Cano JM (2016) Heritability of *Batrachochytrium dendrobatidis* burden and its genetic correlation with development time in a population of common toad (*Bufo spinosus*). Evolution (N Y) 70:2346–2356. doi: 10.1111/evo.13029

Paulson JN, Stine OC, Bravo HC, Pop M (2013) Robust methods for differential abundance analysis in marker gene surveys. Nat Methods 10:1200–1202. doi: 10.1038/nmeth.2658.Robust

Peakall R, Smouse P (2012) GenAlEx 6.5: genetic analysis in Excel. Population genetic software for teaching and research-an update. Bioinformatics 28:2537–2539

Pearman PB, Garner TWJ (2005) Susceptibility of Italian agile frog populations to an emerging strain of ranavirus parallels population genetic diversity. Ecol Lettes 8:401–

408

Pedrós-Alió C (2006) Marine microbial diversity: can it be determined? Trends Microbiol 14:257–263

Peery MZ, Kirby R, Reid BN, et al (2012) Reliability of genetic bottleneck tests for detecting recent population declines. Mol Ecol 21:3403–3418. doi: 10.1111/j.1365-294X.2012.05635.x

Peters RPH, Mohammadi T, Vandenbroucke-Grauls CMJE, et al (2004) Detection of bacterial DNA in blood samples from febrile patients: underestimated infection or emerging contamination? FEMS Pathog Dis 42:249–253

Pew J, Wang J, Muir P, Frasier T (2015) related: an R package for analyzing pairwise relatedness data based on codominant molecular markers. R package version 1.0.

Phillips BL, Puschendorf R (2013) Do pathogens become more virulent as they spread? Evidence from the amphibian declines in Central America. Proc Biol Sci 280:20131290. doi: 10.1098/rspb.2013.1290

Piotrowski JS, Annis SL, Longcore JE (2004) Physiology of *Batrachochytrium dendrobatidis*, a chytrid pathogen of amphibians. Mycologia 96:9–15. doi: 10.2307/3761981

Piovia-Scott J, Rejmanek D, Woodhams DC, et al (2017) Greater species richness of bacterial skin symbionts better suppresses the amphibian fungal pathogen *Batrachochytrium dendrobatidis*. Microb Ecol 74:217–226. doi: 10.1007/s00248-016-0916-4

Pounds JA, Bustamante MR, Coloma LA, et al (2006) Widespread amphibian extinctions from epidemic disease driven by global warming. Nature 439:161–167. doi: 10.1038/nature04246

Price SJ, Garner TWJ, Balloux F, et al (2015) A de novo assembly of the common frog (*Rana temporaria*) transcriptome and comparison of transcription following exposure to ranavirus and Batrachochytrium dendrobatidis. PLoS One 10:e0130500. doi: 10.1371/journal.pone.0130500

Purcell S, Neale B, Todd-Brown K, et al (2007) PLINK: a toolset for whole-genome association and population-based linkage analysis. Am J Hum Genet 81:559–575

Puschendorf R, Hoskin CJ, Cashins SD, et al (2011) Environmental refuge from disease-driven amphibian extinction. Conserv Biol 25:956–964. doi: 10.1111/j.1523-1739.2011.01728.x

Qin J, Li R, Raes J, et al (2010) A human gut microbial gene catalogue established by

metagenomic sequencing. Nature 464:59–65. doi: 10.1038/nature08821

Quast C, Pruesse E, Yilmaz P, et al (2013) The SILVA ribosomal RNA gene database project: improved data processing and web-based tools. Nucleic Acids Res 41:D590–D596

Queller DC, Goodnight KF (1989) Estimating relatedness using molecular markers. Evolution (N Y) 43:258–275

Queney G, Ferrand N, Marchandeau S, et al (2000) Absence of a genetic bottleneck in a wild rabbit (*Oryctolagus cuniculus*) population exposed to a severe viral epizootic. Mol Ecol 9:1253–1264. doi: 10.1046/j.1365-294X.2000.01003.x

Rachowicz LJ, Hero JM, Alford RA, et al (2005) The novel and endemic pathogen hypotheses: Competing explanations for the origin of emerging infectious diseases of wildlife. Conserv Biol 19:1441–1448. doi: 10.1111/j.1523-1739.2005.00255.x

Rachowicz LJ, Knapp RA, Morgan JAT, et al (2006) Emerging infectious disease as a proximate cause of amphibian mass mortality. Ecology 87:1671–1683

Radwan J, Biedrzycka A, Babik W (2010) Does reduced MHC diversity decrease viability of vertebrate populations? Biol Conserv 143:537–544

Rebollar EA, Hughey MC, Medina D, et al (2016a) Skin bacterial diversity of Panamanian frogs is associated with host susceptibility and presence of *Batrachochytrium dendrobatidis*. ISME J 1–14. doi: 10.1038/ismej.2015.234

Rebollar EA, Hughey MC, Medina D, et al (2016b) Skin bacterial diversity of Panamanian frogs is associated with host susceptibility and presence of *Batrachochytrium dendrobatidis*. ISME J 10:1682–1695. doi: 10.1038/ismej.2015.234

Reed DH, Frankham R (2003) Correlation between fitness and genetic diversity. Conserv Biol 17:230–237

Refsnider JM, Poorten TJ, Langhammer PF, et al (2015) Genomic correlates of virulence attenuation in the deadly amphibian chytrid fungus, *Batrachochytrium dendrobatidis*. G3 5:2291–2298. doi: 10.1534/g3.115.021808

Retallick RWR (2002) Using experimental translocations to learn about declines in Queensland's frog populations. Implement Queensland's Threat frog Recover plans - Exp Ecol Project 64:

Richards-Zawacki CL (2010) Thermoregulatory behaviour affects prevalence of chytrid fungal infection in a wild population of Panamanian golden frogs. Proc Biol Sci 277:519–528. doi: 10.1098/rspb.2009.1656

Richards SJ, Alford RA (2005) Structure and dynamics of a rainforest frog (*Litoria genimaculata*) population in northern Queensland. Aust J Zool 53:229–236. doi: 10.1071/ZO03036

Richards SJ, McDonald KR, Alford RA (1993) Declines in populations of Australia's endemic tropical rainforest frogs. Pacific Conserv Biol 1:66–77

Robinson KM, Crabtree J, Mattick JSA, et al (2017) Distinguishing potential bacteria-tumor associations from contamination in a secondary data analysis of public cancer genome sequence data. Microbiome 5:9. doi: 10.1186/s40168-016-0224-8

Robinson MD, McCarthy DJ, Smyth GK (2010) edgeR: a Bioconductor package for differential expression analysis of digital gene expression data. Bioinformatics 26:139–140

Robinson SJ, Samuel MD, Johnson CJ, et al (2012) Emerging prion disease drives host selection in a wildlife population. Ecol Appl 22:1050–1059

Rohr JR, Raffel TR (2010) Linking global climate and temperature variability to widespread amphibian declines putatively caused by disease. Proc Natl Acad Sci U S A 107:8269–74. doi: 10.1073/pnas.0912883107

Rosenblum EB, Fisher MC, James TY, et al (2010) A molecular perspective: Biology of the emerging pathogen *Batrachochytrium dendrobatidis*. Dis Aquat Organ 92:131–147. doi: 10.3354/dao02179

Rosenblum EB, Poorten TJ, Settles M, et al (2009) Genome-wide transcriptional response of Silurana (*Xenopus*) tropicalis to infection with the deadly chytrid fungus. PLoS One 4:e6494. doi: 10.1371/journal.pone.0006494

Rowley JJL, Alford RA (2007a) Behaviour of Australian rainforest stream frogs may affect the transmission of chytridiomycosis. Dis Aquat Organ 77:1–9. doi: 10.3354/dao01830

Rowley JJL, Alford RA (2007b) Movement patterns and habitat use of rainforest stream frogs in northern Queensland, Australia: Implications for extinction vulnerability. Wildl Res 34:371–378. doi: 10.1071/WR07014

Rowley JJL, Alford RA (2013) Hot bodies protect amphibians against chytrid infection in nature. Sci Rep 3:1515. doi: 10.1038/srep01515

Rueckert A, Morgan HW (2007) Removal of contaminating DNA from polymerase chain reaction using ethidium monoazide. J Microbiol Methods 68:596–600

Salter SJ, Cox MJ, Turek EM, et al (2014) Reagent and laboratory contamination can critically impact sequence-based microbiome analyses. BMC Biol 12:87. doi: 10.1186/s12915-

014-0087-z

Sansaloni C, Petroli C, Jaccoud D, et al (2011) Diversity Arrays Technology (DArT) and next-generation sequencing combined: genome-wide, high throughput, highly informative genotyping for molecular breeding of Eucalyptus. BMC Proc 5:P54. doi: 10.1186/1753-6561-5-S7-P54

Sapsford SJ, Alford RA, Schwarzkopf L (2013) Elevation, temperature, and aquatic connectivity all influence the infection dynamics of the amphibian chytrid fungus in adult frogs. PLoS One 8:e82425. doi: 10.1371/journal.pone.0082425

Savage AE, Becker CG, Zamudio KR (2015) Linking genetic and environmental factors in amphibian disease risk. Evol Appl 8:560–572. doi: 10.1111/eva.12264

Savage AE, Kiemnec-Tyburczy KM, Ellison AR, et al (2014) Conservation and divergence in the frog immunome: Pyrosequencing and de novo assembly of immune tissue transcriptomes. Gene 542:98–108. doi: 10.1016/j.gene.2014.03.051

Savage AE, Zamudio KR (2011) MHC genotypes associate with resistance to a frog-killing fungus. Proc Natl Acad Sci 108:16705–16710

Savage AE, Zamudio KR (2016) Adaptive tolerance to a pathogenic fungus drives major histocompatibility complex evolution in natural amphibian populations. Proc R Soc B 283:20153115. doi: 10.1098/rspb.2015.3115

Scheele BC, Hunter DA, Skerratt LF, et al (2015) Low impact of chytridiomycosis on frog recruitment enables persistence in refuges despite high adult mortality. Biol Conserv 182:36–43. doi: 10.1016/j.biocon.2014.11.032

Scheele BC, Pasmans F, Skerratt LF, et al (2019) Amphibian fungal panzootic causes catastrophic and ongoing loss of biodiversity. Science (80-) 363:1459 LP – 1463. doi: 10.1126/science.aav0379

Scheele BC, Skerratt LF, Grogan LF, et al (2017) After the epidemic: Ongoing declines, stabilizations and recoveries in amphibians afflicted by chytridiomycosis. Biol Conserv 206:37–46. doi: 10.1016/j.biocon.2016.12.010

Schneider C, Cunningham M, Moritz C (1998) Comparative phylogeography and the history of endemic vertebrates in the Wet Tropics rainforests of Australia. Mol Ecol 7:487–498

Schoch CL, Seifert KA, Huhndorf S, et al (2012) Nuclear ribosomal internal transcribed spacer (ITS) region as a universal DNA barcode marker for fungi. Proc Natl Acad Sci 109:6241–6246. doi: 10.1073/pnas.1117018109

Schoville SD, Tustall TS, Vredenburg VT, et al (2011) Conservation genetics of evolutionary lineages of the endangered mountain yellow-legged frog, *Rana muscosa* (Amphibia: Ranidae), in southern California. Biol Conserv 144:2031–2040. doi: 10.1016/j.biocon.2011.04.025

Scott ME (1988) The impact of infection and disease on animal populations: implications for conservation biology. Conserv Biol 40–56

Scupham AJ, Presley LL, Wei B, et al (2006) Abundant and diverse fungal microbiota in the murine intestine. Appl Environ Microbiol 72:793–801. doi: 10.1128/AEM.72.1.793-801.2006

Segal LN, Alekseyenko A V, Clement JC, et al (2013) Enrichment of lung microbiome with supraglottic taxa is associated with increased pulmonary inflammation. Microbiome 1:19

Seitz WRA (1990) The influence of land use on the genetic structure of populations of the common frog Rana temporaria. Biol Conserv 54:23–249

Serieys LEK, Lea A, Pollinger JP, et al (2015) Disease and freeways drive genetic change in urban bobcat populations. Evol Appl 8:75–92. doi: 10.1111/eva.12226

Shaffer ML (1981) Minimum population sizes for species conservation. Bioscience 31:131–134

Shen H, Rogelj S, Kieft TL (2006) Sensitive, real-time PCR detects low-levels of contamination by Legionella pneumophila in commercial reagents. Mol Cell Probes 20:147–153

Shultz AJ, Baker AJ, Hill GE, et al (2016) SNPs across time and space: population genomic signatures of founder events and epizootics in the house finch (*Haemorhous mexicanus*). Ecol Evol 6:7475–7489. doi: 10.1002/ece3.2444

Siska C, Kechris K (2017) Differential correlation for sequencing data. BMC Res Notes 10:1–9. doi: 10.1186/s13104-016-2331-9

Skerratt LF, Berger L, Speare R, et al (2007) Spread of chytridiomycosis has caused the rapid global decline and extinction of frogs. Ecohealth 4:125–134. doi: 10.1007/s10393-007-0093-5

Slatkin M (1985) Gene flow in natural populations. Annu Rev Ecol Syst 16:393–430

Slatkin M (1987) Gene flow and the geographic structure of natural populations. Science (80-) 236:787–792

Slatkin M, Barton NH (1989) A comparison of three indirect methods for estimating average

levels of gene flow. Evolution (N Y) 43:1349–1368. doi: 10.2307/2409452

Smith KF, Sax DF, Lafferty KD (2006) Evidence for the role of infectious disease in species extinction and endangerment. Conserv Biol 20:1349–57. doi: 10.1111/j.1523-1739.2006.00524.x

Spiegel CS, Hart PJ, Woodworth BL, et al (2006) Distribution and abundance of forest birds in low-altitude habitat on Hawai'i Island: Evidence for range expansion of native species. Bird Conserv Int 16:175–185

Spielman D, Brook BW, Briscoe DA, Frankham R (2004) Does inbreeding and loss of genetic diversity decrease disease resistance? Conserv Genet 5:439–448

Spurgin LG, Richardson DS (2010) How pathogens drive genetic diversity: MHC, mechanisms and misunderstandings. Proc R Soc London B Biol Sci 277:979–988

Stanton JP, Stanton D (2005) Vegetation of the Wet Tropics bioregion of Queensland. Wet Trop Manag Authority, Cairns

Steinig EJ, Neuditschko M, Khatkar MS, et al (2015) NetView P: A network visualization tool to unravel complex population structure using genome-wide SNPs. Mol Ecol Resour 16:216–227. doi: 10.1111/1755-0998.12442

Stevenson LA, Alford RA, Bell SC, et al (2013) Variation in thermal performance of a widespread pathogen, the amphibian chytrid fungus *Batrachochytrium dendrobatidis*. PLoS One 8:e73830. doi: 10.1371/journal.pone.0073830

Stevenson LA, Roznik EA, Alford RA, Pike DA (2014) Host-specific thermal profiles affect fitness of a widespread pathogen. Ecol Evol 4:4053–4064. doi: 10.1002/ece3.1271

Stirling G, Wilsey B (2001) Empirical relationships between species richness, evenness, and proportional diversity. Am Nat 158:286–299

Storfer (1999) Gene flow and endangered species translocations: a topic revisited. Biol Conserv 87:173–180

Strand TM, Segelbacher G, Quintela M, et al (2012) Can balancing selection on MHC loci counteract genetic drift in fragmented populations of black grouse. Ecol Evol 2:314–353

Talbi C, Lemey P, Suchard MA, et al (2010) Phylodynamics and human-mediated dispersal of a zoonotic virus. PLoS Pathog 6:e1001166

Tallmon DA, Luikart G, Waples RS (2004) The alluring simplicity and complex reality of genetic rescue. Trends Ecol Evol 19:489–496

Teacher AGF, Garner TWJ, Nichols RA (2009a) Evidence for directional selection at a novel major histocompatibility class I marker in wild common frogs (Rana temporaria) exposed to a viral pathogen (Ranavirus). PLoS One 4:e4616

Teacher AGF, Garner TWJ, Nichols RA (2009b) Population genetic patterns suggest a behavioural change in wild common frogs (*Rana temporaria*) following disease outbreaks (Ranavirus). Mol Ecol 18:3163–3172. doi: 10.1111/j.1365-294X.2009.04263.x

Team RC (2017a) R: A language and environment for statistical computing.

Team RC (2017b) R: A language and environment for statistical computing

Toju H, Tanabe AS, Yamamoto S, Sato H (2012) High-coverage ITS primers for the DNA-based identification of ascomycetes and basidiomycetes in environmental samples. PLoS One 7:e40863. doi: 10.1371/journal.pone.0040863

Tompkins DM, Carver S, Jones ME, et al (2015) Emerging infectious diseases of wildlife: a critical perspective. Trends Parasitol 31:149–159

Traill LW, Brook BW, Frankham RR, Bradshaw CJA (2010) Pragmatic population viability targets in a rapidly changing world. Biol Conserv 143:28–34. doi: 10.1016/j.biocon.2009.09.001

Trenerry MP, Laurance WF, McDonald KR (1994) Further evidence for the precipitous decline of endemic rainforest frogs in tropical Australia. Pacific Conserv Biol 1:150–153

Trudeau KM, Britten HB, Restani M (2004) Sylvatic plague reduces genetic variability in black-tailed prairie dogs. J Wildl Dis 40:205–211. doi: 10.7589/0090-3558-40.2.205

Tschirren B (2015) Borrelia burgdorferi sensu lato infection pressure shapes innate immune gene evolution in natural rodent populations across Europe. Biol Lett 11:20150263. doi: 10.1098/rsbl.2015.0263

Tschirren B, Andersson A, Scherman K, et al (2013) Polymorphisms at the innate immune receptor TLR2 are associated with Borrelia infection in a wild rodent population. Proc R Acad Sci B 280:20130364

Turnbaugh PJ, Ridaura VK, Faith JJ, et al (2009) The effect of diet on the human gut microbiome: A metagenomic analysis in humanized gnotobiotic mice. Sci Transl Med 1:1–19. doi: 10.1126/scitranslmed.3000322.The

Underhill DM, Iliev ID (2014) The mycobiota: interactions between commensal fungi and the host immune system. Nat Rev 14:405–416. doi: 10.1038/nri3684

Valsecchi E, Amos W, Raga J a, et al (2004) The effects of inbreeding on moratlity during a

morbillivirus outbreak in the Mediterranean striped dolphin (*Stenella coeruleoalba*). Anim Conserv 7:139–146

van Riper III C, van Riper SG, Goff ML, Laird. M (1986) The epizootiology and ecological significance of malaria in Hawaiian land birds. Ecol Monogr 56:327–344

Vitalis R, Gautier M, Dawson KJ, Beaumont MA (2014) Detecting and measuring selection from gene frequency data. Genetics 196:799–817

Voyles J, Berger L, Young S, et al (2007) Electrolyte depletion and osmotic imbalance in amphibians with chytridiomycosis. Dis Aquat Organ 77:113–118

Voyles J, Rosenblum EB, Berger L (2011) Interactions between *Batrachochytrium dendrobatidis* and its amphibian hosts: a review of pathogenesis and immunity. Microbes Infect Inst Pasteur 13:25–32. doi: 10.1016/j.micinf.2010.09.015

Voyles J, Woodhams DC, Saenz V, et al (2018) Shifts in disease dynamics in a tropical amphibian assemblage are not due to pathogen attenuation. Sceince 359:1517–1519

Voyles J, Young S, Berger L, et al (2009) Pathogenesis of chytridiomycosis, a cause of catastrophic amphibian declines. Science (80-) 326:582–585

Walke JB, Becker MH, Hughey MC, et al (2015) Most of the dominant members of amphibian skin bacterial communities can be readily cultured. Appl Environ Microbiol 81:6589–6600. doi: 10.1128/AEM.01486-15

Wargo MJ, Hogan DA (2006) Fungal-bacterial interactions: a mixed bag of mingling microbes. Curr Opin Microbiol 9:359–364. doi: 10.1016/j.mib.2006.06.001

Warner RE (1968) The role of introduced diseases in the extinction of the endemic Hawaiian avifauna. Condor 70:101–120

Washburne AD, Silverman JD, Leff JW, et al (2017) Phylogenetic factorization of compositional data yields lineage-level associations in microbiome datasets. PeerJ 5:e2969. doi: 10.7717/peerj.2969

Weiss S, Amir A, Hyde ER, et al (2014) Tracking down the sources of experimental contamination in microbiome studies. Genome Biol 15:564. doi: 10.1186/s13059-014-0564-2

Weiss S, Treuren W Van, Lozupone C, et al (2016) Correlation detection strategies in microbial data sets vary widely in sensitivity and precision. ISME J 10:1669–1681. doi: 10.1038/ismej.2015.235

Weiss S, Xu ZZ, Peddada S, et al (2017) Normalization and microbial differential abundance

strategies depend upon data characteristics. Microbiome 5:27. doi: 10.1186/s40168-017-0237-y

Whiteley AR, Fitzpatrick SW, Funk WC, Tallmon DA (2015) Genetic rescue to the rescue. Trends Ecol Evol 30:42–49. doi: 10.1016/j.tree.2014.10.009

Whiteman NK, Matson KD, Bollmer JL, Parker PG (2006) Disease ecology in the Galapagos hawk (*Buteo galapagoensis*): host genetic diversity, parasite load and natural antibodies. Proc R Soc London B Biol Sci 273:797–804

Whitlock MC (2000) Fixation of new alleles and the extinction of small populations: drift load, beneficial alleles, and sexual selection. Evolution (N Y) 54:1855–1861

Whittington RJ, Jones JB, Hine PM, Hyatt AD (1997) Epizootic mortality in the pilchard Sardinops sagax neopilchardus in Australia and New Zealand in 1995. I. Pathology and epizootiology. Dis Aquat Organ 28:1–16

Wilner D, Daly J, Whiley D, et al (2013) Comparison of DNA extraction methods for microbial community profiling with an application to pediatric bronchoalveolar lavage samples. PLoS One 7:e34605

Wilsey BJ, Chalcraft DR, Bowles CM, Willig MR (2005) Relationships among indices suggest that richness is an incomplete surrogate for grassland biodiversity. Ecology 86:1178–1184

Wilsey BJ, Polley HW (2002) Reductions in grassland species evenness increase dicot seedling invasion and spittle bug infestation. Ecol Lett 5:676–684

Wittebolle L, Marzorati M, Clement L, et al (2009) Initial community evenness favours functionality under selective stress. Nature 458:623–626. doi: 10.1038/nature07840

Woodhams DC, Alford RA (2005) Ecology of chytridiomycosis in rainforest stream frog assemblages of tropical Queensland. Conserv Biol 19:815–825. doi: 10.1111/j.1523-1739.2005.00236.x

Woodhams DC, Alford RA, Antwis RE, et al (2015) Antifungal isolates database of amphibian skin-associated bacteria and function against emerging fungal pathogens. Ecology 96:595–595. doi: 10.1890/14-1837.1

Woodhams DC, Alford RA, Marantelli G (2003) Emerging disease of amphibians cured by elevated body temperature. Dis Aquat Organ 55:65–67. doi: 10.3354/dao055065

Woodhams DC, Bosch J, Briggs CJ, et al (2011) Mitigating amphibian disease: strategies to maintain wild populations and control chytridiomycosis. Front Zool 8:8

Woodhams DC, Geiger CC, Reinert LK, et al (2012) Treatment of amphibians infected with chytrid fungus: Learning from failed trials with itraconazole, antimicrobial peptides, bacteria, and heat therapy. Dis Aquat Organ 98:11–25. doi: 10.3354/dao02429

Woodhams DC, Kenyon N, Bell SC, et al (2010) Adaptations of skin peptide defences and possible response to the amphibian chytrid fungus in populations of Australian green-eyed treefrogs, *Litoria genimaculata*. Divers Distrib 703–712

Woodhams DC, Vredenburg VT, Simon MA, et al (2007) Symbiotic bacteria contribute to innate immune defenses of the threatened mountain yellow-legged frog, *Rana muscosa*. Biol Conserv 138:390–398

Woodworth BL, Atkinson CT, LaPointe DA, et al (2005) Host population persistence in the face of introduced vector-borne diseases: Hawaii amakihi and avian malaria. Proc Natl Acad Sci U S A 102:1531–1536

Wright S (1931) Evolution in Mendelian populations. Genetics 16:97–159

Ysumiba K, Bell S, Alford RA (2016) Cell density effects of frog skin bacteria on their capacity to inhibit growth of the chytrid fungus, *Batrachochytrium dendrobatidis*. Microb Ecol 71:124–130

Yuan ML, Dean SH, Longo A V., et al (2015) Kinship, inbreeding and fine-scale spatial structure influence gut microbiota in a hindgut-fermenting tortoise. Mol Ecol 24:2521–2536. doi: 10.1111/mec.13169

Zeisset I, Beebee TJC (2014) Drift rather than selection dominates MHC class II allelic diversity patterns at the biogeographical range scale in natterjack toads Bufo calamita. PLoS One 9:1–12. doi: 10.1371/journal.pone.0100176

Zellmer a. J, Knowles LL (2009) Disentangling the effects of historic vs. contemporary landscape structure on population genetic divergence. Mol Ecol 18:3593–3602. doi: 10.1111/j.1365-294X.2009.04305.x

Zenger KR, Richardson BJ, Vachot-Griffin AM (2003) A rapid population expansion retains genetic diversity within European rabbits in Australia. Mol Ecol 12:789–794. doi: 10.1046/j.1365-294X.2003.01759.x

Zhang J, Kassian K, Flouri T, Stamatakis A (2013) PEAR: a fast and accurate Illumina paired-end read merger. Bioinformatics 30:614–620

Zhang Y, Jiao N, Cottrell MT, Kirchman DL (2006) Contribution of major bacterial groups to bacterial biomass production along a salinity gradient in the South China Sea. Aquat

Microb Ecol 43:233–241

APPENDICES

Appendix 1: Fighting an uphill battle: The recovery of frogs in Australia's Wet Tropics

Published as: McKnight, DT, RA Alford, CJ Hoskin, L Schwarzkopf, SA Greenspan, KR Zenger, DS Bower. 2017. Fighting an uphill battle: The recovery of frogs in Australia's Wet Tropics. *Ecology* 98:3221–3223

In the 1980s and early 1990s, an outbreak of the fungal disease chytridiomycosis caused multiple species of frog to decline or disappear throughout the Wet Tropics of northern Queensland, Australia (Richards et al. 1993; McDonald and Alford 1999). This disease is caused by the pathogen *Batrachochytrium dendrobatidis* (*Bd*; Berger et al. 1998), which is temperature sensitive and does not grow well at warm temperatures (Piotrowski et al. 2004). As a result, the declines often followed elevational gradients, with the most severe declines occurring at cool, high-elevation sites. For example, throughout the Wet Tropics, populations of the waterfall frog (*Litoria nannotis*), common mist frog (*Litoria rheocola*), and Australian lace-lid frog (*Litoria* [*Nyctimystes*] *dayi*) disappeared above 300–400 m, but these species did not decline noticeably in the lowlands (Richards *et al*. 1993; Laurance *et al*. 1996; McDonald and Alford 1999). The green-eyed tree frog (*Litoria serrata*; formerly *L. genimaculata*) also declined sharply above 300–400 m, but it did not completely disappear from those sites (Richards and Alford 2005).

Although these declines and disappearances are well documented, much less attention has been given to the fact that many of the upland populations have recovered to varying degrees, even though *Bd* persists at a relatively high prevalence at upland sites. Our research groups have been working with these species since before the outbreak occurred and have surveyed them repeatedly throughout the intervening years. Herein, I describe the recovery of some populations and discuss hypotheses regarding the nature of the recoveries.

Population recovery has been most widespread and pronounced in green-eyed tree frogs and waterfall frogs. Upland populations of green-eyed tree frogs recovered rapidly from the decline, and at many sites they are currently at or close to their pre-decline abundances (Richards and Alford 2005). Similarly, despite being apparently extirpated from

upland rainforest sites, high-elevation populations of waterfall frogs are now found in many parts of their former range, and at sites that I have surveyed intensively, they are present in most of the upland streams from which they had disappeared (Appendix 1 Figure 1). However, at some sites that I have surveyed, they do not appear to have returned to pre-decline abundances. Common mist frogs have also made strong recoveries at some upland sites. Nevertheless, their pattern of recovery is not as consistent, and there are many sites at which they have not recovered. Finally, lace-lids do not appear to have recovered at any sites and may have been extirpated entirely from the southern extreme of their range (e.g., Paluma Range National Park).

Frog abundances in Girringun (now part of Girramay) and Kirrama Range National Parks (S18.20445°, E145.81259°) illustrate the pattern of recoveries well. I have been surveying localities within this area for many years (from 1988 to as recently as 2017), and green-eyed tree frogs and waterfall frogs are presently abundant at high-elevation sites where they had previously declined or disappeared, respectively. Indeed, a recent survey (May 2017; Appendix 1 Figure 1 site 9) documented 33 green-eyed tree frogs and 64 waterfall frogs along a 200 m transect at 725 m elevation. Nevertheless, I have yet to document lace-lids or mist frogs at these high-elevation sites, even though they are abundant at low-elevation sites. Mist frog populations do not occur above roughly 400 m elevation at Girringun and Kirrama Range National Parks, and established lace-lid populations do not occur above 330 m (although a few scattered individuals were documented as high as 400 m). Four hundred meters is the highest elevation at which these species survived during the initial outbreak, so in this region, it does not appear that they have recovered from that initial decline.

Four major hypotheses may explain the recovery of upland populations of green-eyed tree frogs, waterfall frogs, and some populations of mist frogs, as well as their current coexistence with *Bd*. In any population, more than one of these mechanisms may be occurring and interacting with each other.

- Hypothesis 1: There has been a change in the host species' behaviour, demography, physiology, microbiota, or some combination of these.
- Hypothesis 2: The fungus (*Bd*) has become less virulent.
- Hypothesis 3: The environment has changed to be more favourable for the frogs or less favourable for the fungus.

- Hypothesis 4: Major chytridiomycosis outbreaks occur only when there is a precise combination of environmental conditions, and those conditions have not been replicated since the initial outbreak.

Hypothesis 1

This hypothesis includes several mechanisms that could have facilitated population recovery. First, diseases can act as strong selective pressures, so chytridiomycosis may have driven some populations to adapt to tolerate *Bd* infections, for example by changing their behaviour (e.g., choosing to thermoregulate at increased temperatures) or increasing the effectiveness of their immune responses. Second, the species may have undergone demographic shifts. For example, alpine tree frogs (*Litoria verreauxii alpina*) recovered from a *Bd* outbreak by shifting reproductive effort earlier in life (Scheele *et al*. 2015). Thus, although adults continue to have high mortality rates, populations are persisting because of high reproductive rates during the first breeding season. Third, the frogs' microbiomes may have shifted. It is well established that some genera of bacteria are effective at combatting *Bd* (Harris et al. 2009, Woodhams et al. 2012), and those bacteria may have played a role in recoveries. This mechanism is supported by research showing that the microbiota of upland waterfall frogs and green-eyed tree frogs at Kirrama have a significantly greater proportion of anti-microbial isolates than their lowland counterparts (Bell 2012). As in the first two options, changes in the microbiomes could have involved selection that acted directly on the frogs (i.e., selection for peptides, behaviour, etc. that favour anti-fungal bacteria), however selection may also have acted directly on the microbiome itself.

Hypothesis 2

Reduced pathogen virulence may have played a role in population recoveries (Phillips and Puschendorf 2013). This would, however, have presented all of the species with opportunities for recovery, yet it is clear that not all species (or populations) have recovered. Therefore, if this mechanism is occurring, it must be interacting with other mechanisms or factors. For example, if different species and populations had pre-existing differences in their susceptibility to the fungus, then a slight decrease in virulence could allow some species or populations (or both) to recover, while still precluding recovery in others, such as lace-lids. Similarly, frogs may be adapting simultaneously (hypothesis 1), but

some species may adapt more quickly than others, thus allowing them to quickly take advantage of reduced virulence and recolonize upland sites more rapidly.

Hypothesis 3

Changed environmental conditions may be contributing to recoveries, but similar to hypothesis 2, it is unclear why these broad scale changes would have acted differently among species. If environmental changes are involved in the recoveries, they either must be interacting with the mechanisms posited for the other hypotheses, or the environment must have dramatic interspecific effects on the host-pathogen dynamics. Although there are many potential differences among the species that could account for varying responses to changes in the environment (e.g., demography, life history, or behaviour), differences in dispersal abilities are unlikely to be a key factor, because mist frog populations have recovered at some sites in the northern extent of their range, which suggests that they can disperse into the uplands. Also, at Girringun and Kirrama Range National Parks, mist frogs and lace-lids still appear to be fully restricted to the low-elevation sections, rather than slowly dispersing upstream.

Hypothesis 4

The idea that chytridiomycosis outbreaks are triggered by a precise combination of environmental variables has been proposed as an explanation for the timing of outbreaks (Pounds et al. 2006), and subsequent recoveries may indicate that those conditions have not been replicated since the initial outbreak. Examinations of weather and climate data near the dates and places of known outbreaks have produced equivocal results (Laurance 2008); however, analysis of larger datasets lends some support to the hypothesis that the timing of initial chytridiomycosis outbreaks may be driven to some extent by weather patterns (Rohr and Raffel 2010). Although weather patterns may be important in determining the timing of initial lethal outbreaks, it is likely that the necessary conditions would recur following those outbreaks, making it unlikely that this hypothesis provides the explanation for long-term recovery.

Conclusion

In conclusion, this system has the potential to present fascinating insights into how populations recover from disease outbreaks. Emerging infectious diseases are complex, and the recovery of host species and persistence with pathogens may result from multiple factors. I have presented four major hypotheses, but there is not yet enough information to determine which of their mechanisms have occurred, and a combination of them is likely at play. Future research should carefully examine these hypotheses, because understanding the factors influencing the recovery of these populations could have wide-reaching implications not only for the conservation of amphibians, but for disease-afflicted populations more generally.

Figures

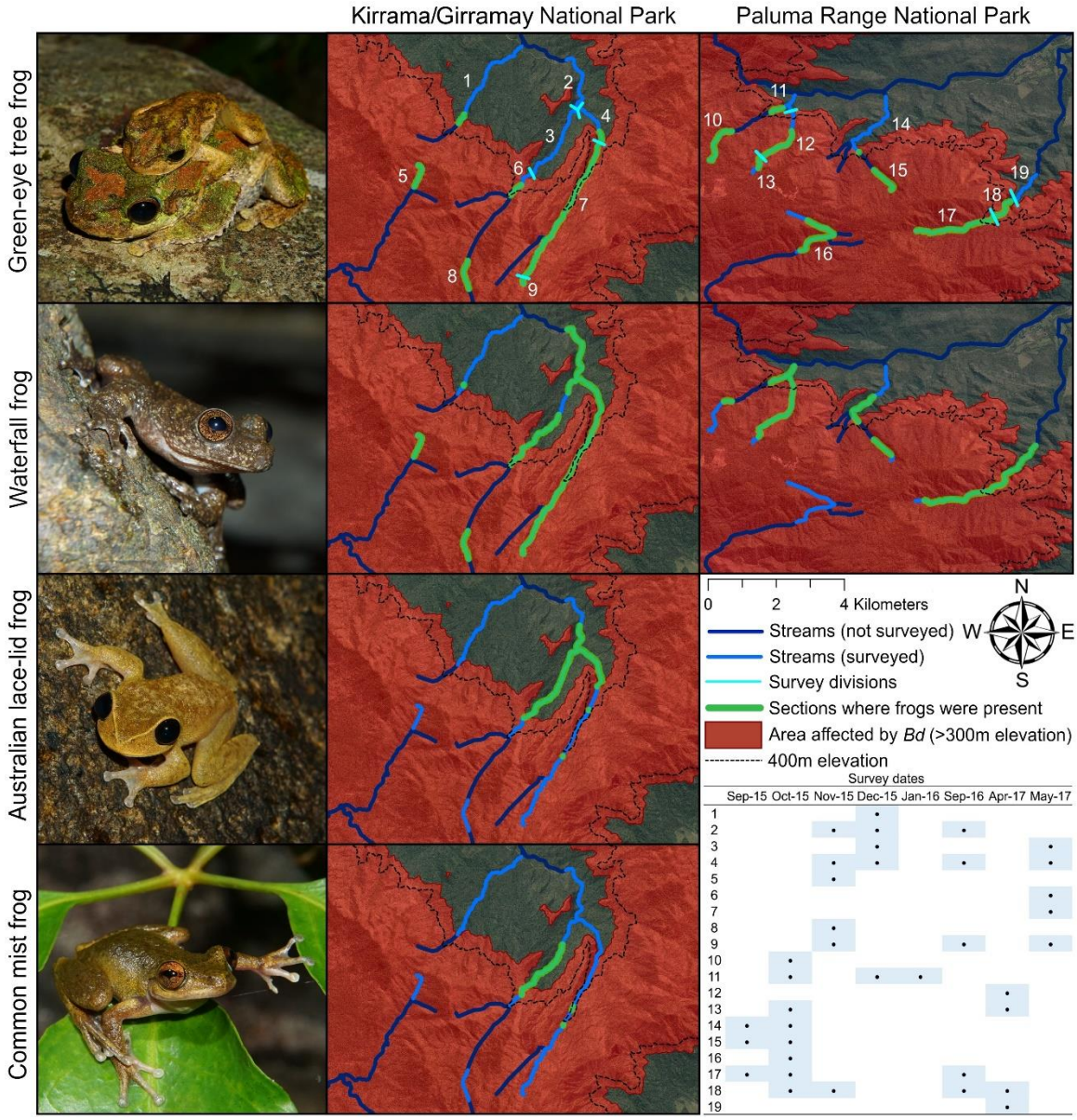

Appendix 1 Figure 1 — Recent survey data for four species of Australian frog that were affected by an amphibian chytridiomycosis outbreak. Frogs were present in the bright green highlighted sections at each survey date, and they were never present in the non-highlighted sections. Waterfall frogs and green-eyed tree frogs have recovered at upland locations (photographed at recovered upland sites at Paluma Range National Park, 2015). Mist frogs and lace-lids are no longer present at Paluma (photographed at lowland sites at Girringun [now Girramay] Range National Park, 2015). At Kirrama/Girringun, lace-lids are essentially restricted to low elevation sites (≤330 m elevation; the highlights at 350 m and 410 m represent one frog each). Mist frogs have established slightly further up the streams,

but they are still not found above roughly 400 m elevation (the two points on survey site seven represented fewer than 10 recorded individuals each).

Appendix 2: Additional methods, tables, and figures from Chapter 7

Detailed DNA extraction protocol

I took several steps to minimize batch effects. First, I prepared all reagents ahead of time so that I could use a single batch for all extractions. Second, I used the same batch of tubes for all extractions. Third, I grouped my samples into blocks of 48, such that each block contained roughly equal numbers of samples from each species at each collection site (thus samples were fully crossed with blocks). I extracted all samples in each block simultaneously. Fourth, I carefully standardized the times for each step of the extraction process to ensure consistency.

I developed a modified version of the CTAB protocol to extract fungal and bacterial DNA simultaneously. I also trialled variations of Qiagen Powersoil kit, Qaigen DNeasy Blood and Tissue kit, and the Prepman ultra kit, but after extensive testing, I concluded that the modification of CTAB method was the best method for consistently getting high yields out of both taxa.

My modifications to the CTAB protocol include the addition of a bead beating step (to lyse fungal cells), the addition of a lysozyme step (to lyse gram positive bacteria), and modifications to the standard times. The protocol is outlined below.

1. Remove samples from freezer and let sit for 10 minutes
2. Pour 0.45g of beads from Bioline DNA Isolate II into tube with swab
3. Add 70µL of a freshly made lysozyme solution (20mM Tris-HCL, 2mM EDTA, 1.2% Tween, 20mg/mL Lysozyme powder; the actual solution can be made ahead of time, but add the powder right before use, keep lysozyme frozen until use).
4. Bead beat for 45s
5. Briefly centrifuge at 16,000g. Make sure that swab tip is at the bottom of the tube after centrifuging. If it is not, use a clean pipet tip to push it down.
6. Incubate on the heat-block at 37ºC for 30 min
7. Centrifuge briefly to remove droplets
8. Add 650µL CTAB and 10uL Proteinase K
9. Incubate overnight (14 hours) at 56C (place on oscillating stand).
10. Centrifuge briefly to remove droplets

*If doing two batches of 24 simultaneously, then before starting step 11 pre-make tubes with 600uL Chloroform:*Isoamyl Alcohol* and a second set with 600uL Isopropanol. Label both sets. (place the isopropanol ones in the freezer). If doing just one batch, make these during the first 10-minute spin (step 11)

11. Add 700uL Chloroform:*Isoamyl Alcohol* (24:1), invert several times to mix, then centrifuge at 16,000g for 10 minutes (pipet chloroform in and out a few times before beginning, otherwise the pipet tip will leak)

    *if doing two sets of 24, wait a few minutes before actually starting the centrifuge while you begin taking care of the next batch of vials. This way, the centrifuge finishes just as you are ready to load the next batch. This makes it easier to remove the supernatant.
12. Carefully remove the supernatant and add it to the vials with 600uL Chloroform:*Isoamyl Alcohol*, invert several times to mix, and centrifuge at 16,000g for 10 minutes (the plastic swab stick will have dissolved, and there will be a thick layer of white junk in the middle, try to avoid this layer, but if you get a tiny bit it will be cleaned up in the next step)

    *Again, for multiple batches, stagger things so that the centrifuge finishes just as you are ready for it
13. Carefully remove supernatant and add to the cold isopropanol vials
14. Invert several times to mix
15. Place in -20 freezer for 4.5 hours
16. Remove from freezer and centrifuge at 16,000g for 45 minutes
17. Carefully pour off fluid
18. Add 1mL of cold 70% EtOH (pre-make the EtOH and place in freezer to chill)
19. Centrifuge for 10 minutes at 16,000g
20. Carefully pour off EtOH, use a pipet to remove the rest (do not lose the pellet).
21. Leave lids open and place in fume cabinet to air dry for 15 minutes.
22. Resuspend in 10mM Tris-HCL pH8

DNA yield analyses

I used QuantiFluor DNA quantification data to examine the possibility that *Litoria dayi* had a low bacterial load, resulting in a low total abundance of inhibitory bacteria. These data were collected as part of the process of preparing samples for sequencing. They were collected following both rounds of PCR and clean-up steps. As such, they are a crude proxy for the original DNA quantities on each swab. Nevertheless, given the high relative abundance of inhibitory bacteria in *L. dayi*, the total abundance of all bacteria on *L. dayi* would have to have been substantially lower than on other species for the total abundance of inhibitory bacteria to be lower, and such a substantial difference should have been detectable, even in the QuantiFluor data. If *L. dayi* had substantially lower bacterial loads than the other species, I would expect *L. dayi* swabs to have less bacteria, which should have resulted in less DNA being extracted, and substantially lower DNA yields following PCR. Thus, although this method is crude, I do think that it is useful.

I used several steps to assess the data. First, because contamination was present in my data, I took the proportion of reads that were not from contamination (calculated via microDecon) and multiplied that by the QuantiFluor data, resulting in the DNA yield from the frogs, rather than from the frogs and contamination. Then, to obtain the quantity of inhibitory bacteria, I took the proportion of reads (for decontaminated data) that were from inhibitory bacteria and multiplied that by the quantification data (with contamination removed). Finally, for both sets of yields (total and inhibitory), I divided by the frogs' snout-urostyle length (SUL) to obtain quantity per unit area. Although surface area is a squared value rather than a linear value, I chose SUL because the swab strokes were all made lengthwise down the frogs. Therefore, SUL should appropriately correct for the total area of each frog that was swabbed. The results of these data are presented in Appendix 2 Figure 1. Although total yield was slightly lower for *L. dayi* than it was for *L. nannotis* and *L. serrata*, the difference was not substantial. Further, the inhibitory DNA yield for *L. dayi* was much higher than the yield for *L. nannotis* or *L. wilcoxii*, strongly suggesting that *L. dayi* did not have a lower actual abundance of inhibitory bacteria than the other species.

Tables

Appendix 2 Table 1 — P values for the tests examining total bacterial richness, richness of the inhibitory community, and the relative abundance of the inhibitory community. Comparisons were made among species, elevations, and parks. This table shows the results for the full models that included all data but no interactions. Grey shading = significant at α = 0.05.

Test	Comparison	P value		
		Total richness	Inhibitory richness	Inhibitory relative abundance
Full linear model: lm(~Species+ Elevation+Park)	Species	<0.0001	<0.0001	<0.0001
	Elevation	0.0455	0.4560	0.2337
	Park	0.0060	0.1855	0.0263
Post hoc test comparing species	*L. dayi* - *L. nannotis*	<0.0001	0.0003	0.0002
	L. dayi - *L. serrata*	0.0368	0.7800	0.6862
	L. dayi - *L. wilcoxii*	0.0065	0.0013	0.0028
	L. nannotis - *L. serrata*	0.0648	0.0001	0.0001
	L. nannotis - *L. wilcoxii*	0.2738	0.9659	0.7771
	L. serrata - *L. wilcoxii*	0.9277	0.0013	0.0084
Post hoc test comparing parks	Kirrama - Paluma	0.0068	-	0.0217
	Kirrama - TullyGorge	0.9627	-	0.9916
	Paluma - TullyGorge	0.0647	-	0.1538

Appendix 2 Table 2 — P values for the tests examining total bacterial richness, richness of the inhibitory community, and the relative abundance of inhibitory community. Comparisons were made among species, elevations, and parks. This table shows the results from a data set containing only Paluma and Kirrama and no *L. dayi*. This was done to allow all interactions (*) between species, park, and elevation. The interactions and main effects in the full models determined how post hoc comparisons were conducted (e.g., the *L. nannotis – L. serrata* relative abundance comparison at Kirrama was not subset by elevation due to a lack of significance in the main model). Grey shading = significant at α = 0.05.

Data (subset)	Comparison	P value		
		Total richness	Inhibitory richness	Inhibitory relative abundance
All data (Full linear model: lm(~Species* Elevation*Park))	Species	0.0182	0.0001	<0.0001
	Elevation	0.0284	0.7524	0.1752
	Park	0.0003	0.1414	0.0080
	Species*Elevation	0.4243	0.0360	0.5486
	Species*Park	0.0053	0.0034	0.0061
	Elevation*Park	0.0005	0.7841	0.7609
	Species*Elevation*Park	0.0077	0.8270	0.5435
Post hoc tests comparing species given park and elevation				
Kirrama lowland	*L. nannotis - L. serrata*	0.9887	0.0515	0.0358
Kirrama upland		0.0430	0.0001	
Paluma lowland		0.2072	0.6470	0.0001
Paluma upland		0.2754	0.1067	
Kirrama lowland	*L. nannotis - L. wilcoxii*	0.9137	0.4987	0.3306
Kirrama upland		0.6288	0.7738	
Paluma lowland		0.7294	0.447	0.0050
Paluma upland		0.0002	0.2717	
Kirrama lowland	*L. serrata - L. wilcoxii*	0.8538	0.0025	0.0005
Kirrama upland		0.0055	0.0068	
Paluma lowland		0.6725	0.9257	0.7014
Paluma upland		0.0064	0.9611	
Post hoc tests comparing parks given species and elevation				
L. nannotis lowlands	Kirrama - Paluma	0.3765	0.7919	0.5395
L. nannotis uplands		0.1337		
L. serrata lowlands		0.4864	0.0001	0.2266
L. serrata uplands		0.3846		
L. wilcoxii lowlands		0.7546	0.5225	0.0002
L. wilcoxii uplands		<0.0001		
Post hoc tests comparing elevations given species and park				
L. nannotis Kirrama	Lowland - Upland	0.0048	0.0533	-
L. nannotis Paluma		0.6667		-
L. serrata Kirrama		0.404	0.2246	-
L. serrata Paluma		0.367		-
L. wilcoxii Kirrama		0.0023	0.2018	-
L. wilcoxii Paluma		0.0085		-

Appendix 2 Table 3 — P values for the tests examining total bacterial richness, richness of the inhibitory community, and the relative abundance of inhibitory community. Comparisons were made among species, elevations, and parks. This table shows a data set that only included Tully and Kirrama lowlands, without *L. serrata*. This was done so that *L. dayi* comparisons could be made, as well as comparisons between Tully and Kirrama. The interactions and main effects in the full models determined how post hoc comparisons were conducted (e.g., the *L. dayi* - *L. nannotis* comparison for total richness was not run separately on each park because there was not a significant main effect or interaction for Park in the full model). Grey shading = significant at $\alpha = 0.05$.

Data (subset)	Comparison	P value		
		Total richness	Inhibitory richness	Inhibitory relative abundance
All (model: lm(richness~ Species*Park))	Species	0.0008	0.0209	<0.0001
	Park	0.2619	0.1896	0.9514
	Species*Park	0.9053	0.0361	0.8211
Post hoc tests comparing species given park				
Kirrama	*L. dayi* - *L. nannotis*	0.004	0.2313	0.0020
Tully			<0.0001	
Kirrama	*L. dayi* - *L. wilcoxii*	0.0018	0.0156	<0.0001
Tully			0.0021	
Kirrama	*L. nannotis* - *L. wilcoxii*	0.9676	0.4069	0.1103
Tully			0.3069	
Post hoc tests comparing parks given species				
L. dayi	Kirrama - Tully	-	0.1896	-
L. nannotis	Kirrama - Tully	-	0.0282	-
L. wilcoxii	Kirrama - Tully	-	0.6103	-

Appendix 2 Table 4 — Bacterial OTUs that were differentially abundant between infected and uninfected frogs. Each species was tested separately, and within species, FDR = 0.01 was applied. Numbers are log-fold changes. Only significant results are shown. Yellow (positive) indicates that an OTU was more abundant in infected individuals, and blue (negative) indicates that it was less abundant in infected individuals. The "Inhibitory" shows whether an OTU was inhibitory in the Woodhams et al. 2015 database.

L. nannotis	*L. serrata*	*L. wilcoxii*	*L. dayi*	Inhibitory	Taxonomy
-18.0394				no	*K*_Bacteria; *P*_Cyanobacteria; *C*_Cyanobacteria
-6.9393				no	*K*_Bacteria; *P*_Cyanobacteria; *C*_Cyanobacteria
5.4098				yes	*K*_Bacteria; *P*_Proteobacteria; *C*_Betaproteobacteria; *O*_Neisseriales; *F*_Neisseriaceae; *G*_Iodobacter
21.3795				no	*K*_Bacteria; *P*_Proteobacteria; *C*_Gammaproteobacteria; *O*_Pseudomonadales; *F*_Pseudomonadaceae; *G*_Pseudomonas
25.3529				no	*K*_Bacteria; *P*_Proteobacteria; *C*_Gammaproteobacteria; *O*_X35
	-17.3226			no	*K*_Bacteria; *P*_Bacteroidetes; *C*_Sphingobacteriia; *O*_Sphingobacteriales; *F*_Chitinophagaceae; *G*_Ferruginibacter
	2.8664			no	*K*_Bacteria; *P*_Proteobacteria; *C*_Alphaproteobacteria; *O*_Rhizobiales; *F*_Hyphomicrobiaceae; *G*_Rhodoplanes
	4.5170			no	*K*_Bacteria; *P*_Acidobacteria; *C*_Subgroup 6
	4.8097			yes	*K*_Bacteria; *P*_Bacteroidetes; *C*_Flavobacteriia; *O*_Flavobacteriales; *F*_Flavobacteriaceae; *G*_Chryseobacterium
	4.8601			yes	*K*_Bacteria; *P*_Bacteroidetes; *C*_Flavobacteriia; *O*_Flavobacteriales; *F*_Flavobacteriaceae; *G*_Chryseobacterium
		-18.4996		no	*K*_Bacteria; *P*_Bacteroidetes; *C*_Bacteroidia; *O*_Bacteroidales; *F*_Rikenellaceae; *G*_Alistipes; *S*_ Bacteroidetes bacterium
		-18.1915		no	*K*_Bacteria; *P*_Proteobacteria; *C*_Betaproteobacteria; *O*_Rhodocyclales; *F*_Rhodocyclaceae; *G*_Azoarcus
		-8.9509		no	*K*_Bacteria; *P*_Cyanobacteria; *C*_Cyanobacteria; *O*_SubsectionIV; *F*_FamilyI
		9.9142		no	*K*_Bacteria; *P*_Cyanobacteria; *C*_Chloroplast
		25.0678		no	*K*_Bacteria; *P*_Chloroflexi; *C*_Ktedonobacteria; *O*_Ktedonobacterales; *F*_Thermosporotrichaceae
		30.0000		no	*K*_Bacteria; *P*_Cyanobacteria; *C*_Chloroplast; *O*_Bryum argenteum var. argenteum
			-19.3749	no	*K*_Bacteria; *P*_Cyanobacteria; *C*_Chloroplast
			-18.8647	no	*K*_Bacteria; *P*_Proteobacteria; *C*_Betaproteobacteria; *O*_Neisseriales; *F*_Neisseriaceae; *G*_Andreprevotia

Figures

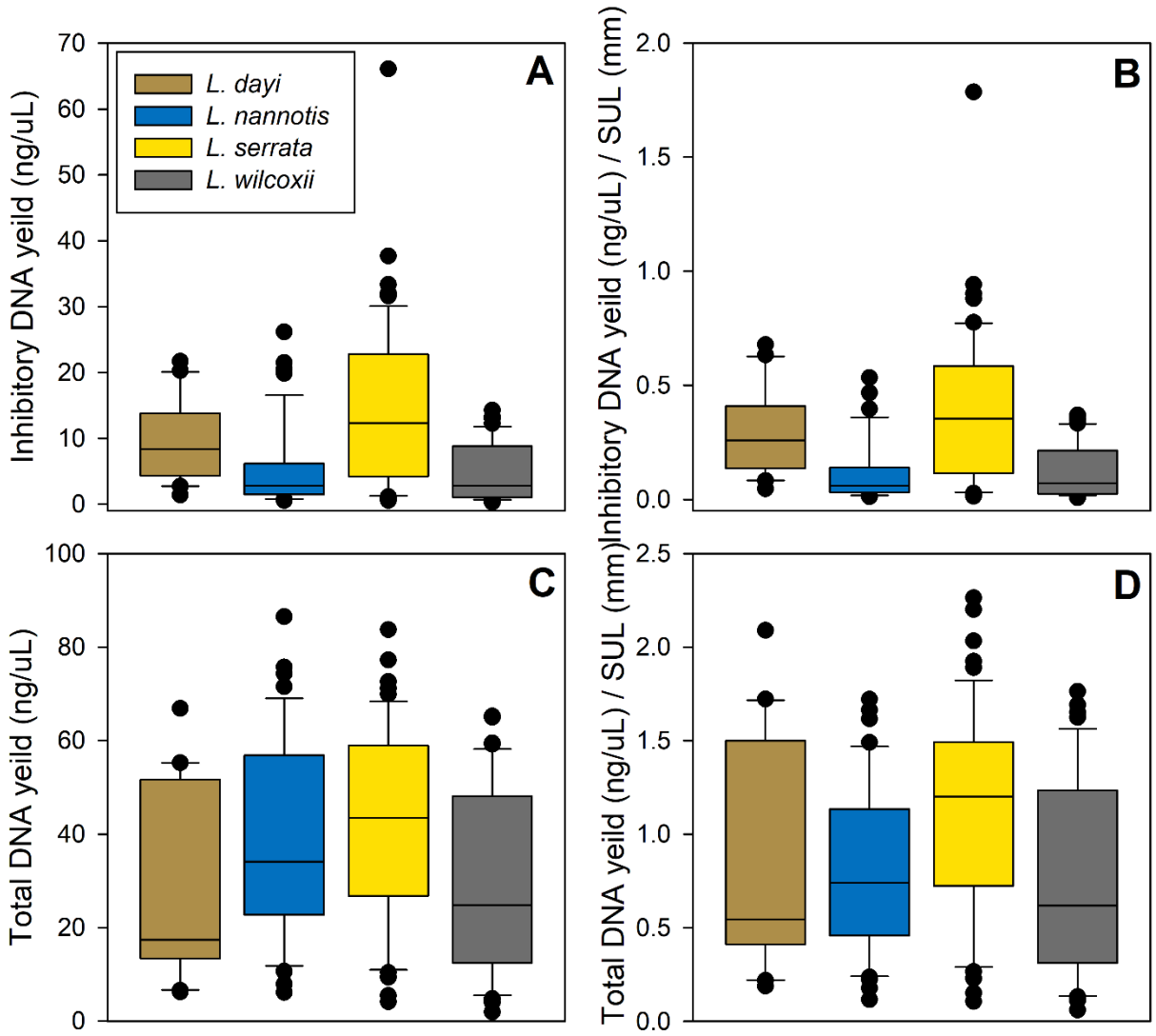

Appendix 2 Figure 1 — A). Calculated yield of inhibitory bacteria. B). Calculated yield of inhibitory bacteria divided by snout-urostyle length (SUL). C). Calculated yield of all bacteria. D). Calculated yield of all bacteria divided by SUL.

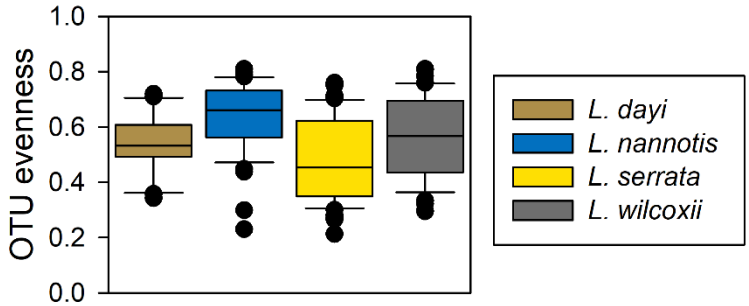

Appendix 2 Figure 2 — Bacterial OTU evenness for all individuals of each species. Whiskers represent the 10th and 90th percentile (calculated via the "standard" formula in SigmaPlot 11.0) and all outliers are shown.

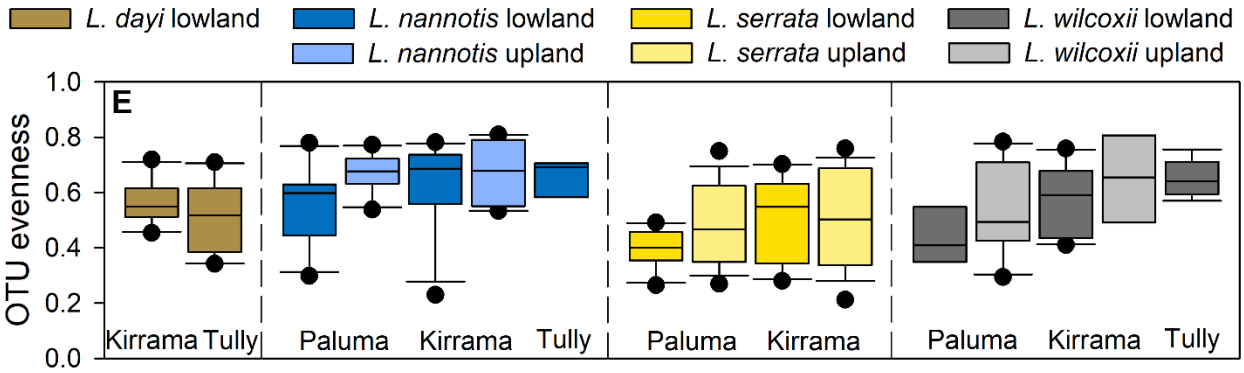

Appendix 2 Figure 3 — Bacterial OTU evenness split by species, parks, and elevations. Whiskers represent the 10th and 90th percentile (calculated via the "standard" formula in SigmaPlot 11.0) and all outliers are shown.

Appendix 3: Additional tables and figures for Chapter 8

Tables

Appendix 3 Table 1 — P values from correlations between richness and evenness. The panel letters correspond to the panels in Appendix 3 Figure 1.

Comparison	Group	P value
Bacterial evenness x bacterial richness (panel A)	All species	<0.001
	L. dayi	0.327
	L. nannotis	<0.001
	L. serrata	<0.001
	L. wilcoxii	0.002
Fungal richness x Bacterial richness (panel B)	All species	<0.001
	L. dayi	<0.001
	L. nannotis	<0.001
	L. serrata	<0.001
	L. wilcoxii	<0.001
Bacterial evenness x fungal evenness (without *Bd*; panel C)	All species	0.492
	L. dayi	0.004
	L. nannotis	0.557
	L. serrata	0.194
	L. wilcoxii	0.156
Fungal richness x fungal evenness (without *Bd*; panel D)	All species	0.299
	L. dayi	0.542
	L. nannotis	0.839
	L. serrata	0.529
	L. wilcoxii	0.730
Bacterial evenness x fungal evenness (with *Bd*; panel E)	All species	0.403
	L. dayi	0.269
	L. nannotis	0.095
	L. serrata	0.623
	L. wilcoxii	0.596
Fungal richness x fungal evenness (without *Bd*; panel F)	All species	0.004
	L. dayi	0.077
	L. nannotis	0.700
	L. serrata	0.299
	L. wilcoxii	0.478

Appendix 3 Table 2 — Fungal OTUs that were differentially abundant between infected and uninfected frogs. Each species was tested separately, and within species, FDR = 0.01 was applied. Numbers are log-fold changes. Only significant results are shown. Yellow (positive) indicates that an OTU was more abundant in infected individuals, and blue (negative) indicates that it was less abundant in infected individuals.

OTU	*L. nannotis*	*L. serrata*	*L. wilcoxii*	*L. dayi*	Taxonomy
denovo14628	-28.0134				k__Fungi; p__Zygomycota; c__Incertae_sedis; o__Entomophthorales; f__Basidiobolaceae; g__Basidiobolus; s__Basidiobolus_meristosporus
denovo6698	-25.1348				k__Fungi
denovo30083	-22.5244				k__Fungi
denovo27647	-22.1037				k__Fungi
denovo39083	-21.1314				k__Fungi; p__Basidiomycota; c__Agaricomycetes
denovo46001	-18.5362				k__Fungi
denovo16277	-17.1317				k__Fungi; p__Ascomycota
denovo1106	-16.9891				k__Fungi; p__Ascomycota; c__Eurotiomycetes
denovo5041	-16.9859				k__Fungi
denovo1879	-16.9267				k__Fungi; p__Basidiomycota; c__Tremellomycetes; o__Filobasidiales; f__Filobasidiaceae; g__Heterocephalacria
denovo14	-16.7203				k__Fungi
denovo434	-16.4972				k__Fungi; p__Ascomycota; c__Sordariomycetes; o__Sordariales; f__Chaetomiaceae; g__Chaetomium
denovo11237	-16.4225				k__Fungi; p__Ascomycota; c__Dothideomycetes
denovo41174	-16.3209				k__Fungi
denovo48754	-16.3066				k__Fungi
denovo39483	-16.3006				k__Fungi; p__Ascomycota; c__Dothideomycetes; o__Pleosporales
denovo5409	-16.1813				k__Fungi; p__Ascomycota
denovo15363	-16.1201				k__Fungi; p__Ascomycota; c__Sordariomycetes; o__Hypocreales; f__Hypocreaceae; g__Hypomyces
denovo10078	-16.0945				k__Fungi
denovo22466	-16.0945				k__Fungi; p__Ascomycota; c__Sordariomycetes; o__Xylariales; f__Amphisphaeriaceae; g__Amphisphaeriaceae_incertae_sedis; s__Adisciso_tricellulare
denovo24452	-16.0234				k__Fungi
denovo30493	-15.9976			-23.8002	k__Fungi
denovo23934	-15.9298				k__Fungi
denovo45323	-15.9170		-18.5174		k__Fungi; p__Ascomycota; c__Leotiomycetes; o__Helotiales
denovo11499	-15.8811				k__Fungi
denovo27522	-15.7581		24.5457		k__Fungi
denovo29042	-15.6971				k__Fungi; p__Ascomycota; c__Dothideomycetes; o__unidentified
denovo48308	-15.2805				k__Fungi; p__Ascomycota; c__Sordariomycetes; o__Xylariales; f__Xylariales_incertae_sedis; g__Phialemoniopsis; s__Phialemoniopsis_curvata
denovo28144	-14.8324				k__Fungi
denovo33088	-14.0827				k__Fungi; p__Ascomycota; c__Dothideomycetes; o__Pleosporales; f__Corynesporascaceae; g__Corynespora; s__Corynespora_olivacea
denovo41401	-13.8161				k__Fungi; p__Ascomycota; c__Sordariomycetes; o__Xylariales; f__Xylariaceae; g__Kretzschmaria; s__Kretzschmaria_deusta
denovo33400	-12.8667				k__Fungi

Appendix 3 Table 2 continued

OTU	*L. nannotis*	*L. serrata*	*L. wilcoxii*	*L. dayi*	Taxonomy
denovo40886	-12.8123				k__Fungi; p__Ascomycota; c__Sordariomycetes; o__Sordariales; f__Incertae_sedis; g__Pleurothecium; s__Pleurothecium_sp_LXS_2012
denovo42260	-12.6216				k__Fungi
denovo29654	-12.4336				k__Fungi; p__Ascomycota; c__Dothideomycetes; o__Capnodiales
denovo32635	-12.0036				k__Fungi
denovo47855	-11.7095				k__Fungi; p__Basidiomycota; c__Agaricomycetes; o__Agaricales; f__Marasmiaceae; g__Moniliophthora; s__Moniliophthora_sp_JFK_2009a
denovo6314	-11.4500				k__Fungi; p__Ascomycota; c__Dothideomycetes; o__Pleosporales; f__Tetraplosphaeriaceae; g__Quadricrura; s__Quadricrura_meridionalis
denovo41603	-11.4354		22.4540		k__Fungi; p__Basidiomycota; c__Agaricomycetes; o__Agaricales; f__Psathyrellaceae; g__Psathyrella
denovo3852	-11.0978				k__Fungi; p__Ascomycota; c__Eurotiomycetes; o__Eurotiales; f__Trichocomaceae; g__Penicillium
denovo13014	11.0152				k__Fungi; p__Ascomycota; c__Leotiomycetes; o__Helotiales
denovo39075	22.0659				k__Fungi; p__Basidiomycota; c__Agaricomycetes; o__Polyporales; f__Phanerochaetaceae; g__Phanerochaete; s__Phanerochaete_chrysosporium
denovo30385	22.2217				k__Fungi; p__Ascomycota; c__Dothideomycetes; o__Pleosporales; f__Pleomassariaceae; g__Helminthosporium
denovo2291	22.5714				k__Fungi; p__Ascomycota; c__Dothideomycetes; o__Capnodiales
denovo17703	22.8568				k__Fungi; p__Ascomycota; c__Sordariomycetes; o__Xylariales; f__Xylariaceae; g__Xylaria; s__Xylaria_grammica
denovo28424	22.9305				k__Fungi
denovo19496	23.2162				k__Fungi
denovo2548	24.0984			-22.9721	k__Fungi; p__Basidiomycota; c__Agaricomycetes; o__Polyporales; f__Polyporaceae
denovo48588	24.3082		-10.7982		k__Fungi; p__Basidiomycota; c__Agaricomycetes; o__Polyporales; f__Ganodermataceae; g__Ganoderma
denovo34384	24.8086				k__Fungi; p__Ascomycota; c__Eurotiomycetes; o__Chaetothyriales; f__Herpotrichiellaceae; g__Exophiala; s__Exophiala_sp_EXP0371F
denovo38736	24.9618		24.8570		k__Fungi
denovo6170	25.3291				k__Fungi; p__Basidiomycota; c__Ustilaginomycetes; o__Ustilaginales; f__Ustilaginaceae; g__Moesziomyces
denovo12199	25.4782			-21.0634	k__Fungi; p__Ascomycota; c__Sordariomycetes; o__Hypocreales; f__Incertae_sedis; g__Emericellopsis; s__Emericellopsis_humicola
denovo42441	26.4835				k__Fungi; p__Zygomycota; c__Incertae_sedis; o__Mucorales; f__Syncephalastraceae; g__Thamnostylum; s__Thamnostylum_piriforme
denovo14425	27.1658		-20.7325		k__Fungi
denovo41063	29.7607				k__Fungi; p__Ascomycota; c__Sordariomycetes; o__Trichosphaeriales; f__Incertae_sedis; g__Khuskia; s__Nigrospora_oryzae
denovo45525		-17.7414			k__Fungi; p__Ascomycota; c__Dothideomycetes; o__Pleosporales
denovo42977		9.8589			k__Fungi
denovo14344		23.6645			k__Fungi
denovo10023		24.2370			k__Fungi
denovo28516		25.8394			k__Fungi

Appendix 3 Table 2 continued

OTU	*L. nannotis*	*L. serrata*	*L. wilcoxii*	*L. dayi*	Taxonomy
denovo45828		25.9696			k__Fungi; p__Ascomycota; c__Dothideomycetes; o__Capnodiales; f__Mycosphaerellaceae; g__Cercosporella; s__Cercosporella_dolichandrae
denovo44964		26.0688			k__Fungi; p__Ascomycota; c__Sordariomycetes; o__Hypocreales; f__Nectriaceae; g__Fusarium
denovo327			-30.0000		k__Fungi; p__Ascomycota; c__Sordariomycetes; o__Xylariales
denovo17857			-22.2427		k__Fungi; p__Ascomycota; c__Sordariomycetes; o__Phyllachorales; f__Phyllachoraceae; g__Colletotrichum
denovo38345			-19.8300		k__Fungi; p__Ascomycota; c__Dothideomycetes; o__Pleosporales; f__Tetraplosphaeriaceae; g__Ernakulamia; s__Ernakulamia_cochinensis
denovo31782			-19.5931	-19.7023	k__Fungi; p__Ascomycota; c__Sordariomycetes
denovo25398			-18.4197		k__Fungi; p__Ascomycota; c__Sordariomycetes
denovo38954			-18.3921		k__Fungi
denovo32209			-18.3665		k__Fungi; p__Basidiomycota; c__Agaricomycetes; o__Polyporales; f__Meruliaceae; g__Resinicium
denovo47621			-18.0720		k__Fungi
denovo1189			-17.9460		k__Fungi; p__Ascomycota; c__Sordariomycetes; o__Hypocreales
denovo27735			-17.8600		k__Fungi
denovo15496			-17.3869		k__Fungi; p__Ascomycota; c__Eurotiomycetes; o__Coryneliales; f__Coryneliaceae; g__Corynelia; s__Corynelia_uberata
denovo25808			-17.3798		k__Fungi; p__Ascomycota; c__Sordariomycetes; o__Sordariomycetidae_incertae_sedis; f__Sordariomycetidae_incertae_sedis; g__Sporidesmium; s__Sporidesmium_tropicale
denovo29668			-17.2619		k__Fungi; p__Ascomycota; c__Eurotiomycetes; o__Chaetothyriales
denovo38830			-11.4645		k__Fungi
denovo39296			8.6014		k__Fungi; p__Basidiomycota; c__Agaricomycetes; o__Polyporales; f__Ganodermataceae; g__Ganoderma
denovo27872			10.2294		k__Fungi
denovo9901			10.2727		k__Fungi; p__Basidiomycota; c__Agaricomycetes; o__Polyporales; f__Hyphodermataceae; g__Hyphoderma; s__Hyphoderma_setigerum
denovo39098			11.7676	-21.6960	k__Fungi
denovo20555			12.1091		k__Fungi; p__Ascomycota; c__Sordariomycetes; o__Hypocreales; f__Nectriaceae
denovo32003			12.2025		k__Fungi; p__Ascomycota; c__Sordariomycetes; o__Hypocreales; f__Incertae_sedis; g__Myrothecium
denovo12847			12.6532		k__Fungi; p__Basidiomycota; c__Agaricomycetes; o__Hymenochaetales; f__Hymenochaetaceae; g__Fuscoporia; s__Fuscoporia_torulosa
denovo36848			12.9080		k__Fungi; p__Ascomycota; c__Dothideomycetes; o__Dothideales
denovo16526			22.0116		k__Fungi; p__Basidiomycota; c__Agaricomycetes; o__Auriculariales; f__Auriculariaceae; g__Auricularia; s__Auricularia_polytricha
denovo7572			22.1486		k__Fungi
denovo24638			22.8540		k__Fungi; p__Ascomycota
denovo24587			23.3072		k__Fungi; p__Ascomycota; c__Sordariomycetes
denovo37505			23.3299		k__Fungi; p__Basidiomycota; c__Agaricomycetes; o__Hymenochaetales; f__Hymenochaetaceae; g__Hymenochaete; s__Hymenochaete_innexa
denovo39936			23.4879	21.7141	k__Fungi

Appendix 3 Table 2 continued

OTU	*L. nannotis*	*L. serrata*	*L. wilcoxii*	*L. dayi*	Taxonomy
denovo11925			23.7035		k__Fungi; p__Basidiomycota; c__Agaricomycetes; o__Polyporales; f__Xenasmataceae
denovo44913			23.7460		k__Fungi
denovo4941			24.0350		k__Fungi
denovo45506			24.3809		k__Fungi; p__Basidiomycota; c__Agaricomycetes; o__Atheliales; f__Atheliaceae; g__Tylospora; s__Tylospora_asterophora
denovo18647			24.9167		k__Fungi; p__Ascomycota; c__Eurotiomycetes; o__Chaetothyriales; f__Herpotrichiellaceae
denovo3979			25.0135		k__Fungi
denovo14512			25.8163		k__Fungi
denovo11751			26.0368	-23.6583	k__Fungi; p__Basidiomycota; c__Microbotryomycetes; o__Sporidiobolales; f__Incertae_sedis; g__Sporobolomyces
denovo8300-denovo9079			26.4225		k__Fungi; p__Ascomycota; c__Eurotiomycetes; o__Chaetothyriales
denovo43266			27.0192		k__Fungi; p__Ascomycota; c__Eurotiomycetes; o__Chaetothyriales
denovo21161				-24.9822	k__Fungi; p__Ascomycota; c__Sordariomycetes; o__Xylariales; f__Amphisphaeriaceae; g__Pestalotiopsis
denovo46996				-24.4272	k__Fungi
denovo32281				-24.1572	k__Fungi; p__Ascomycota; c__Sordariomycetes; o__Diaporthales; f__Schizoparmaceae; g__Pilidiella
denovo42988				-24.1548	k__Fungi; p__Basidiomycota; c__Agaricomycetes; o__Hymenochaetales; f__Schizoporaceae; g__Hyphodontia; s__Hyphodontia_niemelaei
denovo2771				-24.0679	k__Fungi; p__Basidiomycota; c__Agaricomycetes; o__Auriculariales; f__Aporpiaceae; g__Aporpium; s__Aporpium_miniporum
denovo8129				-24.0066	k__Fungi
denovo47432				-23.7424	k__Fungi
denovo28218				-23.6233	k__Fungi; p__Ascomycota; c__Sordariomycetes
denovo38015				-23.0552	k__Fungi; p__Ascomycota; c__Sordariomycetes; o__Xylariales; f__Xylariaceae; g__Nemania; s__Nemania_bipapillata
denovo13392				-22.4613	k__Fungi; p__Basidiomycota; c__Agaricomycetes; o__Hymenochaetales; f__Hymenochaetaceae; g__Fomitiporella
denovo31496				-22.4301	k__Fungi; p__Ascomycota
denovo11618				-22.3480	k__Fungi; p__Ascomycota; c__Sordariomycetes; o__Diaporthales
denovo4907				-22.2461	k__Fungi; p__Basidiomycota
denovo603				-22.2173	k__Fungi; p__Basidiomycota; c__Agaricomycetes; o__Polyporales
denovo35177				-21.9984	k__Fungi; p__Basidiomycota; c__Agaricomycetes; o__Polyporales; f__Steccherinaceae; g__Junghuhnia; s__Junghuhnia_crustacea
denovo8031				-21.7759	k__Fungi
denovo9854				-21.2155	k__Fungi
denovo5031				-21.1709	k__Fungi
denovo37394				-20.7110	k__Fungi; p__Ascomycota; c__Sordariomycetes; o__Chaetosphaeriales; f__Chaetosphaeriaceae
denovo41842				-20.5325	k__Fungi; p__Ascomycota; c__Sordariomycetes; o__Hypocreales; f__Incertae_sedis; g__Myrothecium
denovo42883				-20.3841	k__Fungi; p__Basidiomycota; c__Agaricomycetes; o__Polyporales
denovo1356				-20.2676	k__Fungi; p__Ascomycota; c__Eurotiomycetes; o__Chaetothyriales
denovo22687				-20.2676	k__Fungi

Appendix 3 Table 2 continued

OTU	*L. nannotis*	*L. serrata*	*L. wilcoxii*	*L. dayi*	Taxonomy
denovo14388				-11.1156	k__Fungi; p__Ascomycota; c__Sordariomycetes; o__Xylariales; f__Amphisphaeriaceae; g__Pestalotiopsis; s__Pestalotiopsis_theae
denovo11980				-10.9243	k__Fungi
denovo43942				22.3761	k__Fungi; p__Basidiomycota; c__Agaricomycetes; o__Polyporales
denovo28320				22.7647	k__Fungi; p__Ascomycota
denovo21408				22.7903	k__Fungi; p__Basidiomycota; c__Agaricomycetes; o__Cantharellales; f__Botryobasidiaceae
denovo28236				22.8494	k__Fungi; p__Basidiomycota; c__Agaricomycetes; o__Polyporales; f__Ganodermataceae; g__Ganoderma; s__Ganoderma_sp_E7091
denovo43950				24.0465	k__Fungi; p__Basidiomycota; c__Tremellomycetes

Figures

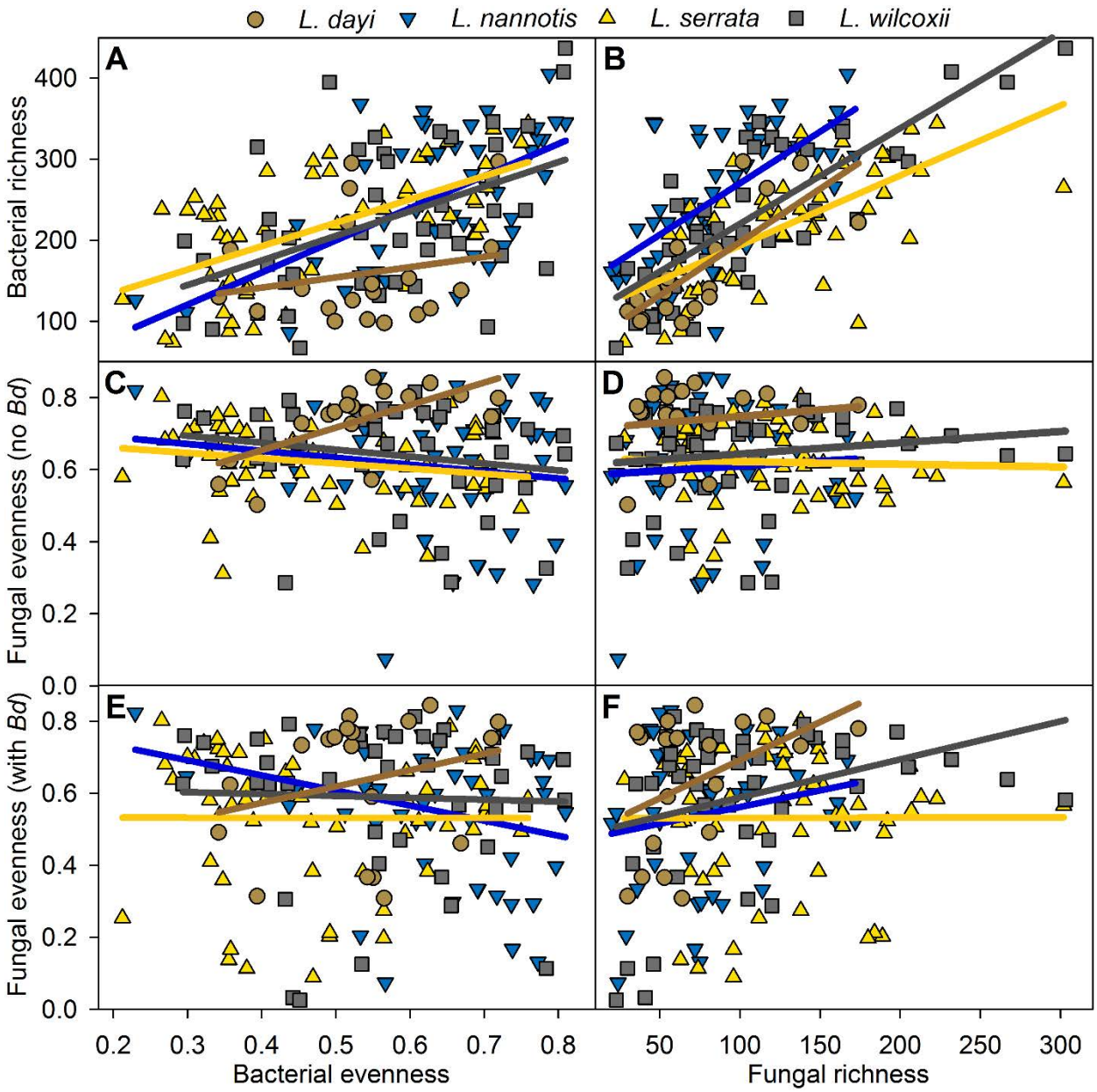

Appendix 3 Figure 1 — Scatter plots comparing richness and evenness within and among bacterial and fungal communities. P values are provided in Appendix 3 Table 1.

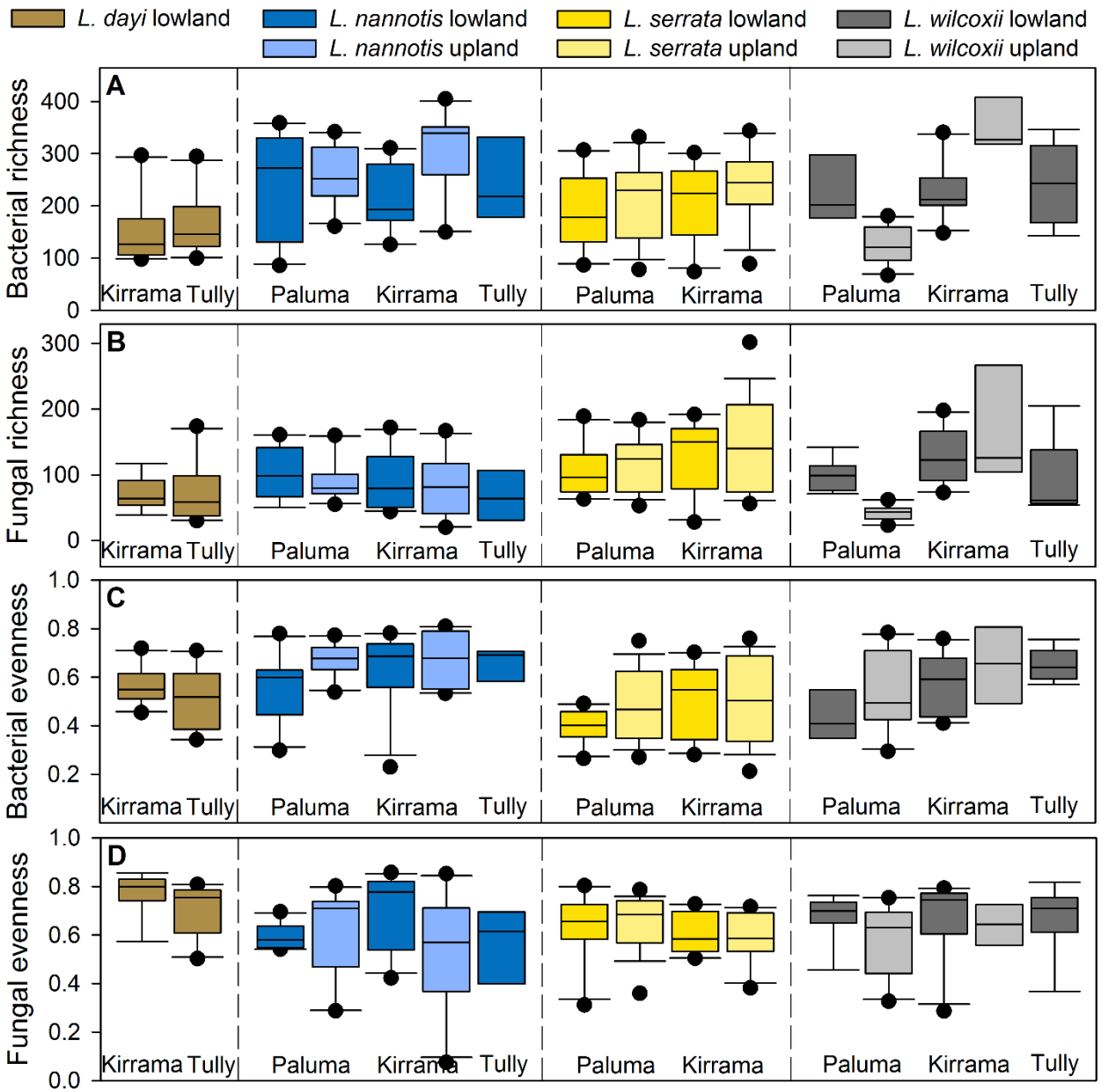

Appendix 3 Figure 2 — Bacterial and fungal richness and evenness split by species, park, and elevation. Fungal results were calculated after removing *Bd*. Bacterial results were previously reported in Chapter 7 and are shown again here for sake of easy comparisons. Whiskers represent the 10th and 90th percentile and all outliers are shown.